THE ROLE OF HAEM IN THE MECHANISM OF ACTION OF ANTIMALARIALS IN PLASMODIUM FALCIPARUM

University of Cape Town

Division of Pharmacology

Department of Medicine

University of Cape Town

This dissertation is submitted for the degree of Doctor of Philosophy

November 2016

For Emma

Plagiarism Declaration

This thesis, **"The Role of Haem in the Mechanism of Action of Antimalarials in Plasmodium falciparum"** has been submitted to the Turnitin module (or equivalent similarity and originality checking software) and I confirm that my supervisor has seen my report and any concerns revealed by such have been resolved with my supervisor.

Name: Jill Michelle Combrinck
Student number: cmbjil001
Signature:

Signed by candidate

Date: 5 September 2016

Abstract

The malaria parasite detoxifies host red blood cell derived haem by conversion into the inert biocrystal haemozoin. Inhibiting this critical pathway is proposed to be the mechanism of action of chloroquine and related antimalarials and several studies have linked inhibition of the formation of synthetic haemozoin, β-haematin, to parasite survival. However, haemozoin inhibition with a dose related increase in "free" haem correlated to decreased survival has not been demonstrated in the parasite. This project investigated the role of haem in the mechanism of action of several clinically relevant and novel antimalarials in the malaria parasite, *Plasmodium falciparum*.

A pyridine-haem cellular fractionation assay was developed to directly determine all major haem species in drug treated chloroquine sensitive *Plasmodium falciparum*. Originally applied to chloroquine treated cells, the percentages of aqueous soluble Hb, "free" haem corresponding to haem that is labile and detergent soluble and finally base soluble Hz was determined through a series of fractionation steps in isolated trophozoites. Based on a method developed by Ncokazi and Egan, each haem species was spectrophotometrically determined as a low spin complex with aqueous pyridine (5% v/v, pH 7.5). Chloroquine inhibited haemozoin formation, causing a dose-dependent increase in toxic cellular "free" haem correlated with decreased parasite survival. The assay was extended to artesunate, amodiaquine, quinine, mefloquine, lumefantrine, and the antifolates pyrimethamine and a pyrimethamine sulfadoxine combination, at a single dose corresponding to 2.5× the parasite growth IC_{50}. Excluding the antifolates, all drugs exhibited inhibition of haemozoin in comparison to the control, but none to the degree which chloroquine inhibited haemozoin formation in *Plasmodium falciparum*. The results suggested that in addition to haemozoin inhibition, some of the antimalarials tested possess an alternative or additional mechanism of action.

A comprehensive haem species dose response profile was required for each compound, however low throughput limited the application of the haem cellular fractionation assay. The method was subsequently modified to a higher throughput process performed in 24-well plates, providing a significant improvement in productivity and reduction in starting material volume. The modified method was validated against the original pyridine-haem fractionation

assay using chloroquine. A fluorescent flow cytometry-based technique was developed for the determination of cell counts of isolated trophozoites, allowing results to be expressed in terms of the amount of each haem species per cell rather than percentages. Flow cytometry of isolated trophozoites also provided information describing the change in morphology of drug treated cells. This modified method was applied to the previously mentioned antimalarials (excluding the pyrimethamine sulfadoxine combination) as well as quinidine, atovaquone and primaquine and an experimental artemisinin, 10-deoxoartimisinin. The results showed that atovaquone, primaquine, artesunate and 10-deoxoartimisinin did not inhibit haemozoin formation. Among the quinolines tested, only amodiaquine displayed direct haemozoin inhibition in a manner which resembled chloroquine. Quinine and quinidine both showed evidence of haemozoin inhibition, however neither to the same degree exhibited by chloroquine and amodiaquine. This was accompanied by a reduction in total haem Fe attributed to interference with haemoglobin uptake. Despite being inhibitors of β-haematin formation, neither mefloquine nor lumefantrine showed evidence of direct haemozoin inhibition. Both compounds showed dose related decreases in total haem Fe attributed to a possible interference with haemoglobin uptake upon drug treatment. Finally, the technique was applied to six novel compounds active against *Plasmodium falciparum*, derived from benzamide and triarylimidazole scaffolds, identified through a high throughput screening campaign to inhibit β-haematin formation twice as effectively as chloroquine. All novel compounds capable of inhibiting β-haematin formation were found to inhibit haemozoin formation. Interestingly, these compounds produced levels of "free" haem higher than any compound previously tested, up to 5.5× greater than the maximum level of "free" haem reached with chloroquine treatment. Transmission electron microscopy images performed on cells treated with one of these compounds revealed a significantly enlarged digestive vacuole containing a large number of vesicles with evidence of disrupted haemozoin formation.

Application of the haem cellular fractionation assay to a diverse group of compounds confirmed or excluded haemozoin inhibition as a mechanism of action. The method identified varying degrees of Hz inhibition, possibly attributed to the attenuated toxicity of "free" haem amongst certain scaffolds, while others exhibited

alternative mechanisms in addition to haemozoin inhibition possibly as a downstream effect of haemozoin inhibition or as a direct effect of the drug itself.

Publications and Conference Proceedings

Parts of this thesis have been published:

1. Wicht, K. J., Combrinck, J. M., Smith, P. J., Hunter, R., and Egan, T. J. (2016) Identification and SAR evaluation of hemozoin-inhibiting benzamides active against *Plasmodium falciparum*. *J. Med. Chem. 59*. 6512.

2. Combrinck, J. M., Fong, K. Y., Gibhard, L., Smith, P. J., Wright, D. W. and Egan, T. J. (2015) Optimization of a multi-well colorimetric assay to determine haem species in *Plasmodium falciparum* in the presence of antimalarials. *Malar. J. 14*. 253.

3. Combrinck, J. M., Mabotha, T. E., Ncokazi, K. K., Ambele, M. A., Taylor, D., Smith, P. J., Hoppe, H. C., and Egan, T. J. (2012) Insights into the role of haem in the mechanism of action of antimalarials. *ACS Chem. Biol. 8*. 153.

Parts of this thesis have been presented at the following conferences:

1. 2015: 17th International Conference on Biological Inorganic Chemistry held at the China National Convention Centre, Beijing, China on 20 – 24 July 2015.
   Poster: A Novel Assay for the Quantification of Haem Species in the Malaria Parasite, *Plasmodium falciparum.*

2. 2013: Inorganic 2013, 16th South African Chemical Institute National Inorganic Chemistry Conference held at the Elangeni Hotel, Durban, KwaZulu-Natal on 30 June – 4 July 2013.
   Poster: The Role of Haem in the Mechanism of Action of Antimalarials in *Plasmodium falciparum.*

3. 2012: 50th Microscopy Society of Southern Africa Annual Conference held at the University of Cape Town on 4 – 7 December 2012.
   Poster: The Effect of Chloroquine and Related Antimalarials on Haem in *Plasmodium falciparum.*

4. 2012: 2012 Gordon Research Conference on "Chemistry and Biology of Tetrapyrroles" held at Salve Regina University, Newport Rhode Island, United States of America on 22 July 2012 to 27 July 2012.
   Poster: The Effect of Chloroquine and Related Antimalarials Compounds on Haem in the Malaria Parasite *Plasmodium falciparum.*
   Conference was attended as a recipient of the Carl Storm Diversity Fellowship.

Acknowledgements

I would like to convey my sincere gratitude to the following people without whom this work would not have been possible:

Prof. Timothy John Egan. Not only for his invaluable and vast knowledge on this topic but also for his mentorship and the opportunities afforded during my studies. Your door was always open. It has been a privilege to learn from you.

Associate Professor Peter Smith as a co-supervisor who was always available to provide support, encouragement and generally anything else required! Thank you for everything.

All members of the **Chemistry Haem Team**: **John Okombo**, **John Woodland**, **Nikki Dare**, **Roxanne Openshaw**, **Fabrizio L'Abatte** and **Stefan Benjamin.** A special mention to **Roxanne Mohunlul** with whom I shared many tissue culture experiences. Even though no longer members of the haem team I would like to thank **Dr Melvin Ambele, Dr Tameryn Stringer, Dr David Kuter, Dr Aneesa Omar** and **Dr Kathryn Wicht.**

My colleagues from the **Division of Pharmacology**. With special mention to the following people who have made the journey easier for me and who have become friends along the way: **Jenna Johnston** for her critical reading of this thesis. **Dr Carmen de Kock** for your input and advice on all things related to tissue culture. I have so enjoyed sharing an office with both of you**. Dr Liezl** (it is what it is) **Gibhard** for your advice regarding flow cytometry and for your encouragement and motivation. **Dr Dale Taylor** for always being able to answer all of my pharmacology related questions, and for your very special sense of humour. **Sumaya Salie** and **Virgil Verhoog** without whom tissue culture would not function, thank you for all the parasite donations.

Mr. Mohamed Jaffer for his expertise and invaluable help in the Electron Microscopy Unit.

Dr Danni Ramduth for her support and technical skill for all things related to flow cytometry. Tree Star Inc. for the donation of a one year subscription to FloJo.

Most of all I would like to thank my family for their unconditional love and support through this journey. My mom, **Beverley Combrinck**, my husband, **Mario Fisher** and my little sunshine, **Emma Hope Fisher**. I could not have done this without you. Thank you.

Lastly, this project would not have been possible without the financial support received from the following organisations for which I am very grateful: **Medical Research Council of South Africa** for providing seed funding, **National Institutes of Health (NIH)** under grant number R01AI110329 for funding the project and providing scholarship support. **National Research Foundation** and the **University of Cape Town** for further scholarship funding.

List of Abbreviations and Acronyms

9-EQN:	9-epiquinine
9-EQD:	9-epiquinidine
10-dO-AMN:	10-deoxoartemisinin
AMN:	artemisinin
APAD:	3-acetyl pyridine dinucleotide
AQ:	amodiaquine
ART:	artesunate
ATV:	atovaquone
βH:	β-haematin
βHIA:	β-haematin inhibitory activity assay
C:	cytostome
CQ:	chloroquine
CQR:	chloroquine resistant
CQS:	chloroquine sensitive
DHA:	dihydroartemisinin
DMSO:	dimethyl sulphoxide
DMT:	Drug/Metabolite Transporter
DNA:	deoxyribonucleic acid
DV:	digestive vacuole
EELS:	electron energy loss spectroscopy
EM:	electron microscopy
ESI:	electron spectroscopic imaging
ER:	endoplasmic reticulum
FACS:	flow assisted cell sorting
Fe(III)PPIX:	ferriprotoporphyrin IX
FSC:	forward scatter
GFP:	green fluorescent protein
HAP:	histoaspartic protease
Hb:	haemoglobin
HDP:	haem detoxification protein
HEPES:	4-(2-Hydroxyethyl)-1-piperazineethanesulfonic acid
HF:	halofantrine

HPE:	"haem polymerase" enzyme
HPIA:	haem polymerisation inhibitory activity
HRP II:	histidine rich protein
HRP III:	histidine rich protein
Hz:	haemozoin
iRBC:	infected red blood cell
LF:	lumefantrine
MQ:	mefloquine
NAD:	nicotinamide adenine dinucleotide
NBT:	nitro blue tetrazolium
NP-40:	nonidet P-40
PABA:	*p*-aminobenzoic acid
PBS:	phosphate buffered saline
PfCRT:	'*Plasmodium falciparum* CQ resistance transporter'
PfMDR1:	Plasmodium falciparum multidrug resistance transporter 1
Phi-β:	pyridine hemichrome inhibition assay
PIs:	protease inhibitors
pLDH:	parasite lactate dehydrogenase
PM I:	plasmepsin I
PM II:	plasmepsin II
PM IV:	plasmepsin IV
PPM:	parasite plasma membrane
PQ:	primaquine
PRBCs:	parasitised red blood cells
PV:	parasitophorous vacuole
PVM:	PV membrane
PYR:	pyrimethamine
QD:	quinidine
QN:	quinine
RBC:	red blood cell
rcf:	relative centrifugal force
Rf:	retention factor
ROS:	reactive oxygen species
rpm:	revolutions per minute

S:	sulfadoxine
SK:	surface knobs
SP:	sulfadoxine- pyrimethamine
SSC:	side scatter
T:	troph
TEM:	transmission electron microscopy
TLC:	thin layer chromatography
VP:	verapamil
WHO:	World Health Organisation

1 LITERATURE REVIEW AND INTRODUCTION

1.1 Malaria in 2016

Malaria continues to be one of the leading causes of death worldwide, despite decades of strategic interventions aimed at reducing the incidence of malaria and malaria related deaths. The disease continues to have a heavy impact on global heath and the economy, most severely in countries with a high incidence of poverty.[1] The most recent World Malaria report published at the end of 2015 coincided with the end of the 15 year period assigned to the Millennium Development Goals. As part of goal number 6 pertaining to malaria, the aim was not only to halt, but reverse the global incidence of malaria by 2015. In keeping with this goal, 57 countries have managed to reduce their malaria burden by more than 75%, with 1 billion fewer cases of malaria and 6.2 million fewer malaria deaths occurring between 2001 and 2015, than if rates had remained unchanged since 2000 (Figure 1-1a, b). [2] One area of notable success during this 15 year period has been the substantial reduction in child mortality, falling by 48% in malaria endemic areas of sub-Saharan Africa. As shown in Figure 1-2, malaria is no longer the leading cause of death among children in sub-Saharan Africa. The disease has largely been eliminated in North America and in 2015, the World Health Organisation (WHO) for the first time reported no new indigenous cases of malaria in the WHO European region. [3] [2] [4] These successes have largely been achieved through an increased use of insecticide-treated mosquito nets and treatment in the form of artemisinin (AMN) based combination therapies. AMN based combination therapies have been shown to effectively reduce malaria mortality in the treatment of uncomplicated malaria in children younger than 2 years by more than 97%.[5]

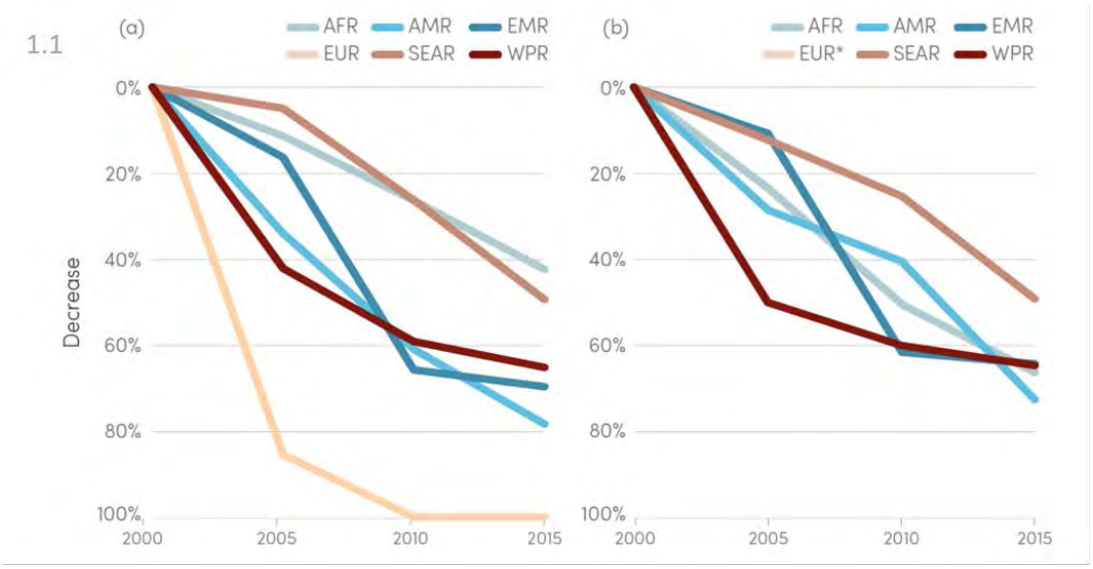

AFR, African Region; AMR, Region of the Americas; EMR, Eastern Mediterranean Region; EUR, European Region; SEAR, South-East Asia Region; WPR, Western Pacific Region

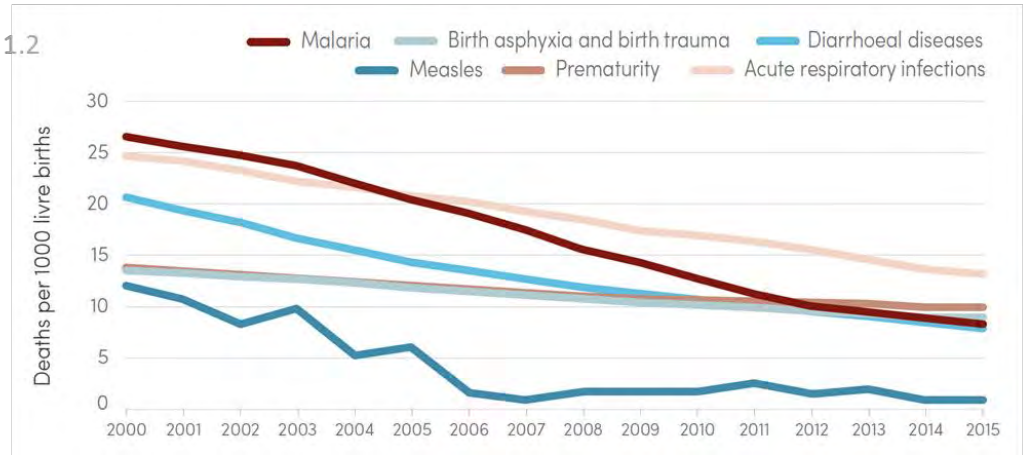

Figure 1-1: The percentage decrease in the estimated number of malaria cases and the malaria death rate are shown in Figures 1-1a and 1-1b respectively for each WHO region from the year 2000 to 2015. Figure 1-2 shows that the number of deaths caused by malaria in children younger than five years of age has decreased over the fifteen year period. Malaria is no longer the leading cause of death among children younger than five years of age in sub-Saharan Africa. All figures reproduced from the WHO World Malaria Report 2015.[2]

However, in the face of these successes, Africa continues to carry the heaviest malaria disease burden. Of the 214 million new cases of malaria and 438 000 deaths reported in 2015, more than 90% of deaths occurred in the WHO African region. It is of critical concern that the rates of decline in malaria related incidence and mortality are the slowest in these higher burden countries which include several African countries. To address this, the WHO has rolled out another fifteen

year plan, "Global Technical Strategy for Malaria 2016 – 2030". The goal of this new strategy is to reduce the global incidence of malaria and mortality by 90% and eventually have a world free of malaria. [2] In addition to vector control measures and improved surveillance, chemoprevention remains an essential tool in the implementation of this new technical strategy. AMN combination therapy is our current first line therapy for the treatment of malaria. However, reduced sensitivity to the AMNs threaten the continued success of this drug class.[6] It is therefore imperative to continue exploring malaria parasite biology to improve our understanding of current drug targets, identify new drug targets and aid in the development of new effective antimalarials to help achieve the goal of a world free of malaria.

1.2 A brief history of the disease

For centuries, the theories regarding the transmission of malaria have been widely debated. From Hippocrates theory in the 5th century BCE of bad air to our current day understanding of insect vectors.[7] During the 1800s malaria was endemic in all parts of Europe with the exception of Lichtenstein. The organs of patients who had succumbed to the disease were characterised by black deposits, originally attributed to bile. In 1846, Adelheid B at the age of 43 and after 24 years of hospitalisation as a mentally ill patient died from malaria, although malaria had not been identified as the cause of death. Her brain was found to be dark brown, her spleen enlarged and dark brown and her capillaries filled with brown particles. Several years later the association between the brown pigment found in her organs and malaria was made by the instructor in pathological anatomy at the University of Berlin, Virchow. Virchow associated the pigment with haematin crystals and today we know its formation is as a result of haemoglobin (Hb) digestion and consequent formation of the malaria pigment, haemozoin (Hz), an essential process in the malaria parasite.[7]

In the 19th century, while on assignment in Secunderabad, India the British army surgeon, Ronald Ross made a Nobel Prize winning discovery when he conclusively identified the mosquito as the vector for malaria.[8] He fed mosquitoes with spotted wings blood containing crescent shaped cells from patient Hussein Khan and

detected brown pigment in the stomach wall of the mosquito, now identified as the *Anopheles* mosquito.[9] Further evidence for the involvement of the mosquito was provided by Patrick Manson in 1900 who allowed *Anopheles* mosquitoes imported from Rome to London to bite the fingers of his healthy 23 year old son who had never previously suffered from malaria and had not been out of the country since the age of three. Approximately fourteen days after being bitten, his son suffered from malaria characteristic intermittent fevers and recovered after being administered quinine (QN).[10]

1.3 The lifecycle of *P. falciparum*

Currently five *Plasmodium* species which commonly infect humans have been identified. *Plasmodium falciparum, P. vivax, P. ovale*, *P. malariae* and more recently *P. knowlesi.*[11] [12] Current information suggests that although *P. knowlesi* malaria infects humans it is largely transmitted through zoonotic transmission, when an anopheles mosquito infected by a macaque monkey bites and infects a human.[13] The malaria parasite, *Plasmodium falciparum* is responsible for the most virulent form of malaria. This species predominates in Africa affecting young children and pregnant women most severely.[2] *P. falciparum* has a complicated lifecycle which can be divided into two parts. The sexual lifecycle within the female *Anopheles* mosquito and the asexual lifecycle in a vertebrate host. The asexual stage can be further subdivided in to two parts during which the parasite resides within hepatocytes and erythrocytes as displayed in Figure 1-2. The latter stage is responsible for most of the clinical symptoms associated with malaria, and is characterised by the adhesion of infected erythrocytes to endothelial cells, reducing the clearance of infected cells by the spleen, resulting in potentially fatal cerebral and placental malaria.[3] [6]

The sexual lifecycle begins when a female *Anopheles* mosquito feeds from a vertebrate host infected with malaria, picking up mature gametocytes circulating in the blood stream of the host. The transition from vertebrate to mosquito host initiates gametogenesis in the stomach of the mosquito. Male and female gametes fuse to form a zygote. Zygotes undergo meiosis and transform into motile ookinetes. The ookinete moves through the mosquito gut wall and matures into an

oocyst and eventually into sporozoites. After a period of 10-22 days, the sporozoites migrate to the lobes of the mosquito salivary glands.[4 8] When an infected female *Anopheles* mosquito bites a vertebrate host, motile sporozoites in the mosquito's saliva enter the host bloodstream via the dermal tissue and then the liver where they invade hepatocytes. This liver stage within the human host is asymptomatic and lasts approximately six days. During this time the parasites flourish and each sporozoite multiplies to produce thousands of merozoites that are released into the blood stream. This signifies the beginning of the asexual lifecycle, when one merozoite invades a host erythrocyte. Within the host red blood cell (RBC) three distinct phases are observed within a single 48 h cycle, the ring stage, trophozoite stage and the schizont stage. Each schizont will give rise to between eight and twenty daughter merozoites in each cycle, which burst from the host RBC and invade new erythrocytes, perpetuating the cycle of infection.[4] After several asexual cycles some parasites develop into gametocyte forms which are taken up by a mosquito with its next blood meal and after approximately 2 weeks the mosquito is infectious to its next host and the cycle of infection is preserved.[3]

Each point in the lifecycle of *P. falciparum* can be seen as a potential drug target. In the past drug discovery focussed on the asexual stage as it presents the most accessible laboratory model to study. Several distinct processes and organelles in the asexual lifecycle of the parasite including Hb degradation, Hz formation, folate synthesis, the mitochondrial electron transport system and the apicoplast have been used as drug targets. [1 14 15] Recently, more reliable and accessible tools for the study of gametocytes and improved gametocyte activity screening assays has resulted in the study and identification of promising chemotherapies which have the added benefit of blocking transmission of malaria. [16-18] This literature review focusses on the asexual blood stage of the parasite lifecycle and the drugs which target this stage of the lifecycle.

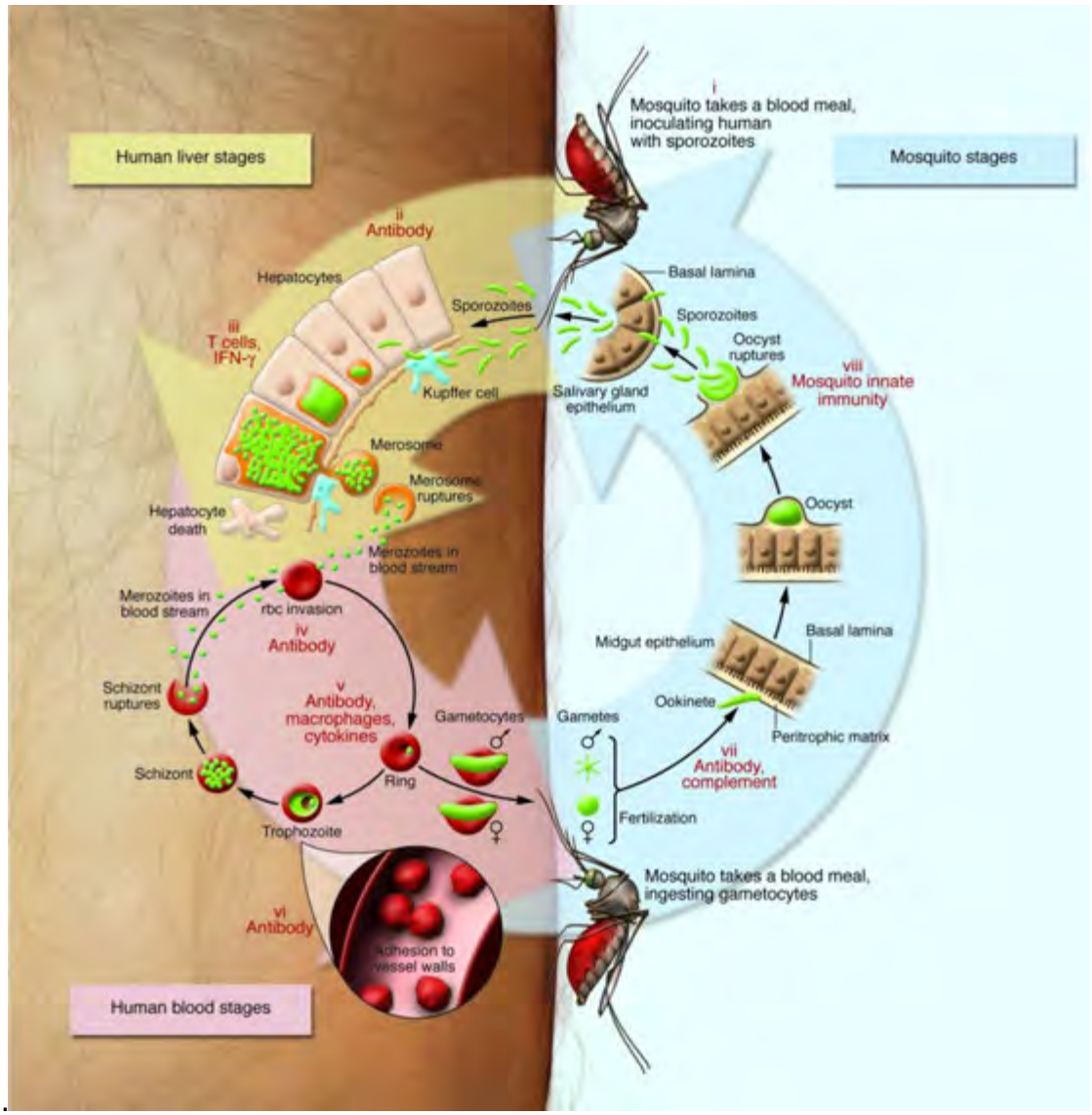

Figure 1-2: The lifecycle of the malaria parasite *Plasmodium falciparum*. The sexual cycle is shown in the female anopheles vector and the asexual cycle within the hepatocytes and erythrocytes of its vertebrate host. This image has been reproduced with permission from the American Society for Clinical Investigation.[3] Republished with permission of American Society for Clinical Investigation, from Greenwood, B. M., Fidock, D. A., Kyle, D. E., Kappe, S. H., Alonso, P. L., Collins, F. H., and Duffy, P. E. (2008) Malaria: progress, perils, and prospects for eradication, *J. Clin. Invest. 118*, 1266.; permission conveyed through Copyright Clearance Center, Inc.

1.4 The asexual blood stages of *Plasmodium falciparum*

The apicomplexan malaria parasite is a unicellular, largely intracellular eukaryote. The merozoite, the ring, the trophozoite and the schizont are identified as four distinct stages in the asexual lifecycle of the parasite.

1.4.1 The Merozoite

The merozoite is the smallest of all *Plasmodium* stages, specialised for its role of capturing and invading a host RBC (Figure 1-3a). This stage represents a moment of vulnerability for the parasite as the merozoite is briefly extracellular between escaping the remnants of its previous host RBC and invading a new host RBC. At its apex, the merozoite has a cluster of several secretory organelles, rhoptries, dense granules, micronemes and mononemes used during invasion of the host RBC.[19] These organelles discharge a mix of proteins and lipids, during invasion and change the shape and composition of the RBC, forming an invagination pit on the surface of the RBC which eventually forms the parasitophorous vacuole (PV). The PV encloses the merozoite within a membrane lined cavity, separating and shielding the parasite from the host RBC cytoplasm cavity where it develops and matures into a ring. [20 21]

1.4.2 Ring

The merozoite matures and flattens into a thin cup shape with a thicker rim identified as the ring-form of a trophozoite (Figure 1-3b). The structure appears as a ring or signet shape when viewed as a Giemsa stained slide under a light microscope as the nucleus, plastids and ribosomes are all housed on the outer rim while very little else exists at its centre. [21] The parasite feeds through its cytostome, a mouth like structure at the parasite surface, pulling through RBC cytosol as well as bits of PV. Host RBC cytosol, composed essentially of Hb is transported in vesicles to the parasite digestive vacuole (DV) where Hb is digested by a series of proteases. Initially several small vacuoles exist and fuse later to form

one large DV. [4 22] The processes of Hb digestion within the parasite DV is discussed in detail in Section 1.5 of this review.

1.4.3 Trophozoite

The trophozoite stage is distinguished from the ring stage by change in shape and size rather than function. This stage is defined by high metabolic activity during which copious amounts of host RBC cytosol are digested within the acidic DV by a series of proteases.[23] A portion of the resulting amino acids are used by the parasite and the rest are exported to the extracellular medium. Toxic haematin (Fe(III)protoporphyrin IX) produced as a consequence of Hb metabolism is transformed into non-toxic crystalline Hz inside the single large parasite DV (Figure 1-3c).[24] [6] The RBC physiology is altered dramatically during the trophozoite stage as a result of large amounts of parasite proteins being exported into the RBC cytoplasm and surface as well as the interaction of specific malarial antigens with the host RBC.[25] [21] Ribosomes, the endoplasmic reticulum (ER) and the Golgi-body increase in number and complexity to meet the increased demand for protein synthesis. The trophozoite establishes an exo-membrane system within its host RBC arising from the PV membrane (PVM) which functions as a highway for the trafficking of proteins. [26] The surface area of the trophozoite becomes considerably larger and several ultrastructural changes at its surface corresponding to irregular bulges and invaginations are identified as surface knobs (SK) and Maurer's clefts in Figure 1-3c. These structures are speculated to be involved in trafficking of substances and are associated with adhesins, proteins which facilitate adhesion of parasitised RBCs (PRBCs) to blood vessel walls. [12] This prevents splenic clearance of PRBCs, as infected cells do not pass through the spleen where they would normally be identified by macrophages which remove any cells with deformations or compromised antigenicity. [25 6 21]

1.4.4 Schizont

The ingestion of host cell cytoplasm and consequent Hz formation in the acidic DV, continues into the schizont stage, virtually depleting the Hb content of the RBC.

Similarly, the formation and export of proteins into the RBC continues, distorting the RBC membrane and cytoskeleton and increasing permeability of the RBC membrane (Figure 1-3d). According to Goldberg and Cowman, the parasite exports more than 400 proteins to the host cell throughout its asexual lifecycle to ensure survival, including kinases, lipases and adhesins. [27] [28] Most notably, the schizont is defined by nuclear division, resulting in the formation of sixteen to twenty nuclei. As schizont development nears the end, individual nuclei formed move towards the surface of the parasite and the daughter merozoites are assembled in specific stages beginning with the apical organelles and ending with the rupture of the PVM and RBC membrane presumably triggered by secretions from the merozoite apical organelles.[21]

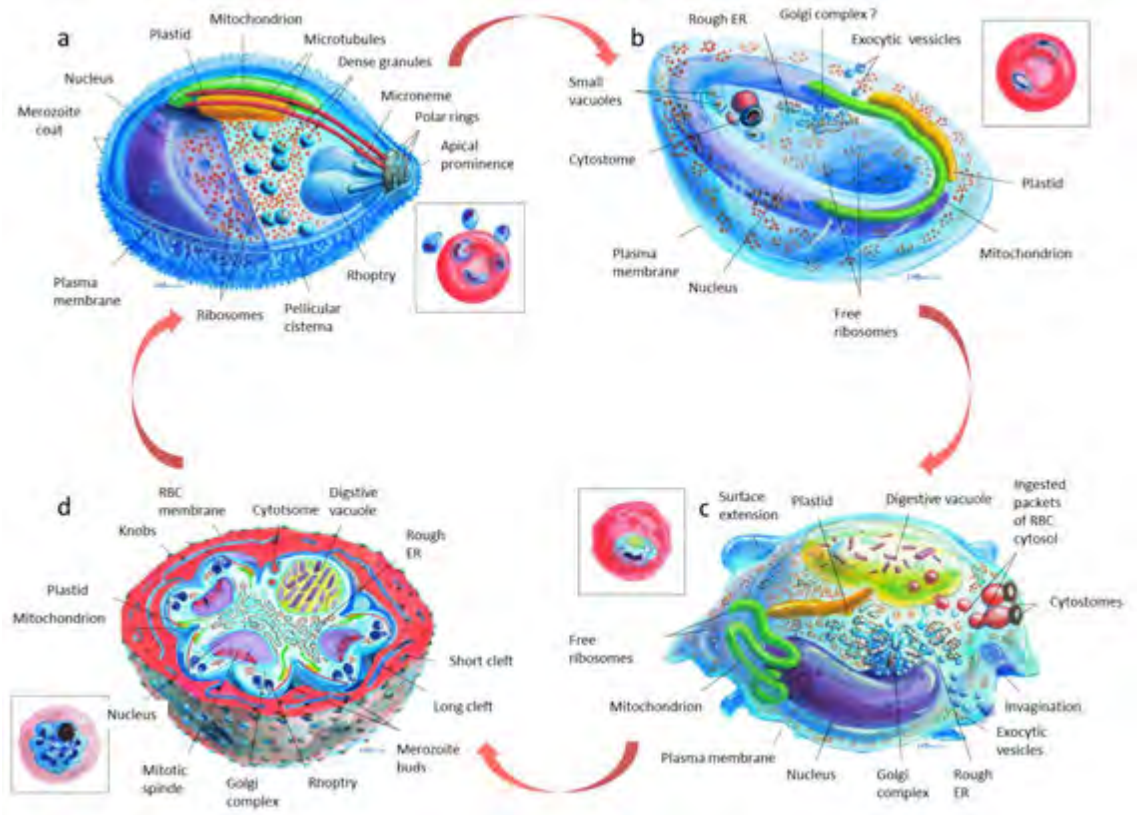

Figure 1-3: The asexual stages of *Plasmodium falciparum*. (a) A lemon shaped merozoite with the secretory organelles specialised for host cell invasion located at its apex. The inset depicts merozoites invading a host RBC. (b) Cup shaped flat ring stage. The RBC and PVM are not shown in this image and the Golgi-body is not conclusively identified. The inset shows a host RBC invaded by 2 ring stage parasites. (c) A trophozoite with increased numbers of free ribosomes, ER and enlarged Golgi-body. Multiple cytostomes and a single large DV for the ingestion and digestion of RBC cytosol are easily identified. The inset shows a trophozoite within an irregularly shaped RBC. (d) The schizont stage of the lifecycle with SK visible on the RBC surface and daughter merozoites budding at the schizont surface. The inset shows a schizont invaded RBC with the schizont occupying the majority of the RBC volume. Reprinted from Parasitology Today, 16(10), Bannister, L.H., Hopkins, J.M., Fowler, R.E., Krishna, S. and Mitchell, G.H, A brief illustrated guide to the ultrastructure of *Plasmodium falciparum* asexual blood stages, 427-433., Copyright (2000), with permission from Elsevier. [21]

1.5 Haemoglobin degradation

Haemoglobin is a major component of RBCs, making up 95% of the cytosolic proteins and reaching concentrations of 5 mM within the RBC.[4] The malaria parasite metabolises Hb in an essential process which dominates a large part of the 48 h asexual parasite lifecycle. Occurring most prolifically during the metabolically active trophozoite stage, approximately 60% of the host RBC Hb is digested. [29] [30] Hb metabolism continues into the schizont stage where the parasite occupies most of the volume of the host RBC and approximately 80% of the host RBC Hb has been digested. [31] The process occurs within the acidic DV, driven by a series of proteases and several peptidases resulting in the formation of amino acids, oxygen radicals and haem (Figure 1-4). Hb metabolism and the formation of Hz is a massive process in the asexual parasite and represents a pathway exclusive to the parasite, differing significantly to its host. Full understanding and consequent manipulation of the processes involved can open doors to the discovery of new effective drug targets. The details of Hb metabolism, eventually leading to the formation of Hz are discussed below.

1.5.1 Hb ingestion

Malaria parasites endocytose large amounts of host cell Hb primarily during the trophozoite stage via a cytostomal system. [32] Several of these double membraned pear shaped cytostomes can be found inside one parasite. The cytostome originates from an invagination of the PVM and parasite plasma membrane (PPM) forming a bridge between the two membranes separating the parasite and host RBC cytoplasm.[33] Although most prolific at the trophozoite stage, recent evidence of an inactive cytostomal ring, indicative of a feeding apparatus, was seen at the periphery of merozoites suggesting that Hb uptake occurs very early in the parasite lifecycle. [34] [33] Host RBC cytosol is ingested by the cytostome and double membrane vesicles budding from the cytostome transport RBC Hb to the acidic DV. [35] [4] Baker et al have shown that the development of the DV and the degradation of Hb start at the ring stage of the *P. falciparum* lifecycle. Using fluorescence and electron tomography, “pre-DV” acidified Hz containing compartments at the

periphery of mid ring stage parasites have been detected.[36] As the parasites mature these peripheral acidic compartments coalesce into a single large DV.[37] Upon reaching the DV the outer membrane of the Hb containing vesicles fuse with the DV membrane. Once within the vacuole the single membrane of the vesicle lyses in a process specific to the vesicle membrane, hypothesized to be governed by phospholipases. Hb digestion ensues after the vesicle membrane has lysed. [36]

1.5.2 Hb metabolism

Within the acidic DV, Hb is degraded in a stepwise manner by a series of proteases, beginning during the ring phase and peaking during the trophozoite stage. [38] [36] In the presence of aspartic acid and cysteine protease inhibitors (Pepstatin and E62 respectively) globin metabolism is completely blocked resulting in osmotic swelling, followed by the disruption of vacuolar processes and consequent parasite death.[39] When administered individually, pepstatin inhibits digestion of Hb, while E-64 a specific cysteine protease inhibitor, has minimal effect on Hb degradation.[40] This suggests Hb metabolism follows a specific order. Cleavage of Hb into peptides is initiated by the aspartic acid proteases plasmepsin I and II (PM I and II), followed by plasmepsin IV (PM IV) and histoaspartic protease (HAP). [40] [41] Peptides are further broken down by a family of cysteine proteases, falcipain II and III and the Zn-metalloprotease, falcilysin. [42] [41] Aminopeptidases degrade short peptides into amino acids (Figure 1-4). [43]

Despite digesting up to 80% of the RBC Hb by the schizont stage, several studies have shown that *P. falciparum* only utilises approximately 16% of the amino acids released from Hb digestion. [31] [29] *P. falciparum* has a limited capacity for the *de novo* synthesis of amino acids. [29] Haemoglobin contains no isoleucine and is lacking in methionine, cysteine, glutamine and glutamate. [44] The parasite therefore relies on exogenous sources as well as Hb digestion to fulfil its amino acid quota. Despite being grown in cultures containing all 20 essential amino acids, parasites will continue to digest Hb. [45] Further studies have shown that parasites grown in the presence of protease inhibitors in medium supplemented with all the essential amino acids resulted in inhibition of parasite growth. [46] [47] [48] Therefore the provision of essential nutrients is not the only motivation behind Hb metabolism. It has been suggested that in addition to providing a protein source, Hb is broken

down to "make room" for parasite growth by digesting RBC cytoplasm to prevent premature host RBC lysis. [49]

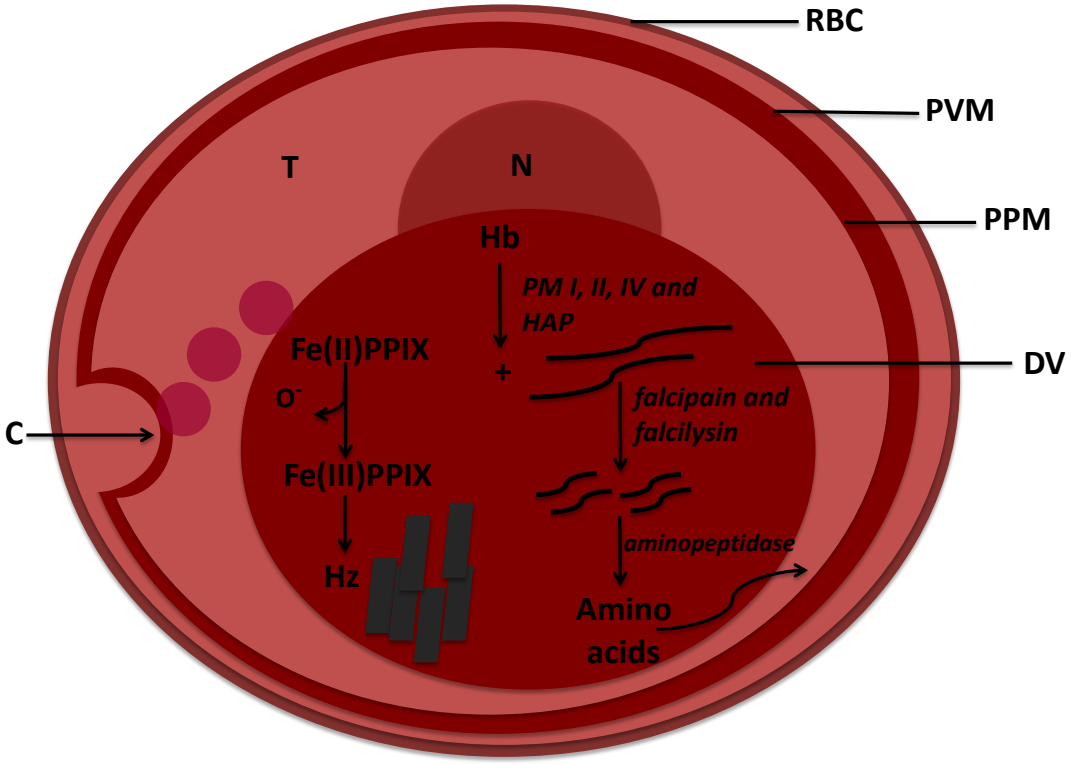

Figure 1-4: The process of Hb degradation and Hz formation with the trophozoite. RBC = red blood cell, PVM = parasitophorous vacuole membrane, PPM = parasite plasma membrane, DV = digestive vacuole, C = cytostome, T = troph, PM I, II, IV = plasmepsin I, II, IV, HAP = histoaspartic protease.

1.6 Haemozoin in *Plasmodium falciparum*

The detoxification of haem to inert Hz crystals is one of the final stages in the process of Hb degradation in the malaria parasite. In addition to providing amino acids as a nutrient source for the parasite, Hb metabolism results in the release of four haem (Fe(II)PPIX) units. Lacking haem oxygenase required for haem catabolism, the parasite sequesters it into inert Hz crystals.[50 51] The activity of several important current antimalarials, including chloroquine (CQ), is attributed to their ability to inhibit the sequestering of toxic haem into inert Hz in the DV.[4 52]

1.6.1 The toxicity of Haem

Haemoglobin degradation is a major source of oxidative stress for the parasite. As a consequence of Hb digestion, haem (Fe(II)PPIX) is released and immediately autooxidised to haematin (Fe(III)PPIX) resulting in the formation of reactive oxygen species (ROS) within the acidic environment of the DV.[53] The terms haem (Fe(II)PPIX) and haematin (Fe(III)PPIX) are used interchangeably, however all haem in the parasite DV is technically in the oxidised form, haematin.

In the 4 fL volume DV, haematin can reach concentrations of up to 0.4 M.[54] Micromolar concentrations of free haem have been shown to be toxic by causing oxidative stress, membrane destabilisation and cell lysis. [40] [51] [55] Although it has been shown that more than 95% of toxic haem is sequestered as inert Hz in the parasite DV, even a small amount of free haem is capable of damaging the parasite. [30] Haem has a lipophilic nature and has been shown to accumulate in membranes. [56] [57] This most likely results in impairment of membrane functioning which possibly manifest as interference with endocytosis and vesicle fusion required for the uptake and degradation of Hb in the parasite. [58] Both haemin (Fe(III)PPIX-Cl) and complexes of CQ-Fe(III)PPIX have been shown to cause swelling and eventual lysis of isolated *P. berghei* trophozoites as shown in Figure 1-5. [55]

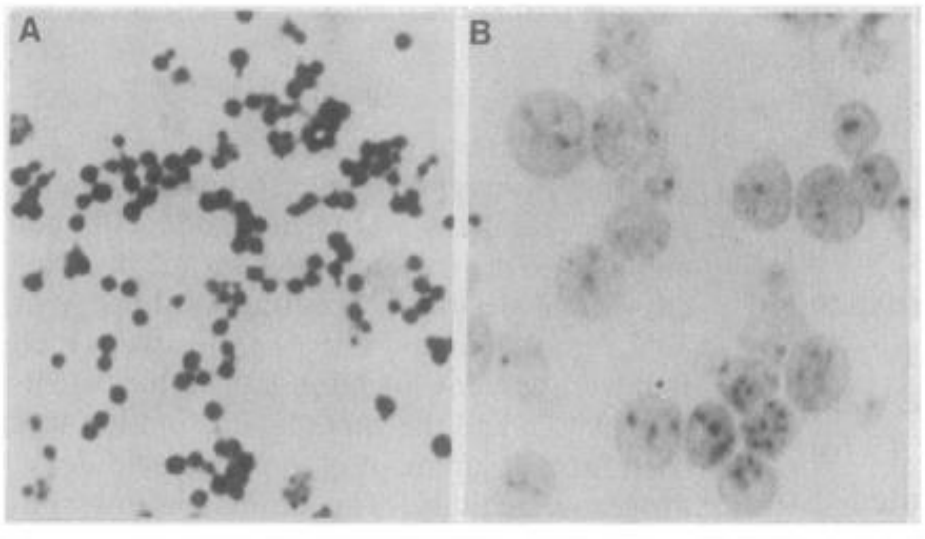

Figure 1-5: Haemin lyses malaria parasite (×1100). Isolated *P. berghei* trophozoites suspended in culture medium as control (A) and incubated in the presence of 20 μM haemin (B). Cells treated with a complex formed from 20 μM haemin and 5 μM CQ produced similar results to B, while cells incubated with CQ alone showed no effect. From: Orjih, A. U., Banyal, H., Chevli, R., and Fitch, C. D. (1981) Hemin lyses malaria parasites, *Science 214*, 667**.** Reprinted with permission from The American Association for the Advancement of Science. [55]

While the toxicity of haem is prevented through Hz formation, auto-oxidation of haem to haematin within the DV liberates electrons which combine with oxygen to form several ROS, including superoxide anions (O_2^-), hydroxyl radicals ($OH\cdot$) and hydrogen peroxide (H_2O_2).[50 59] The presence of ROS is kept to a minimum by the antioxidant and redox systems within the parasite (Figure 1-6). A family of superoxide dismutases catalyse the dismutation of O_2^- to H_2O_2 and O_2, Thioredoxin peroxidases then reduce H_2O_2 to H_2O and O_2.[60] Highly reactive OH^- radicals, known to cause lipid peroxidation are generated through the spontaneous reaction of O_2^- and H_2O_2 or via the Fenton reaction.[60 61]

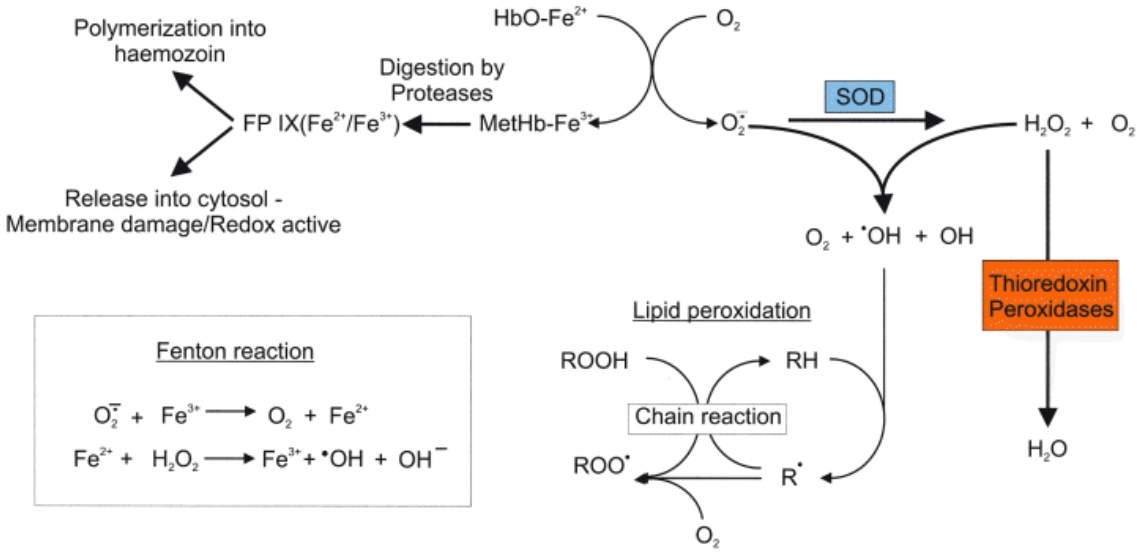

Figure 1-6: The generation of reactive oxygen species in *P. falciparum*. From: Müller, Sylke, 2004. Image reprinted with permission from Wiley Online. Copyright © 2004, John Wiley and Sons Library. [60] FP IX = ferri/ferroprotoporphyrin IX; HbO-Fe2+ = oxy-haemoglobin containing ferriprotoporphyrin IX; MetHb-Fe3+ = methaemoglobin containing ferriprotoporhpyrin IX; SOD = superoxide dismutase.

1.6.2 The structure of haemozoin

As mentioned above, in 1846 dark brown pigment was found in the organs of a mental patient who had succumbed to malaria. The pigment was originally attributed to bile until several years later when the connection between the dark brown malaria pigment we know today as Hz, and malaria was made. [62] The association between malaria and haematin was made by Brown in 1911, when dark brown pigment was identified as a haematin-protein complex. [63] Chemical analysis of purified Hz extracted from *P. falciparum* by Slater et al, showed that Hz was identical to haematin and without a protein component. Further analysis using Fourier-transform IR spectroscopy, extended X-ray absorption fine structure spectroscopy (EXAFS) and X-ray powder diffraction revealed that purified Hz was structurally identical to synthetic Hz, β-haematin (βH). The structure of βH (and hence Hz) was proposed to be a polymer of Fe(III)PPIX units linked by co-ordination of the propionate group of one Fe(III)PPIX molecule to the Fe(III) centre of the next. [64] Hz was referred to as a polymer until 2000 when this model was invalidated by Pagola et al. Having first established that the powder X-ray

diffraction pattern of βH was identical to that of whole dried PRBCs, the crystal structure of βH was determined from the powder diffraction data obtained with synchrotron radiation using Rietveldt refinement (Figure 1-7). Hz was determined to be made up of cyclic dimers of Fe(III)PPIX, with the propionate of one Fe(III)PPIX co-ordinated to the Fe(III) centre of the other. Dimers are linked to each other by hydrogen bonding of propionate groups. [65] [24]

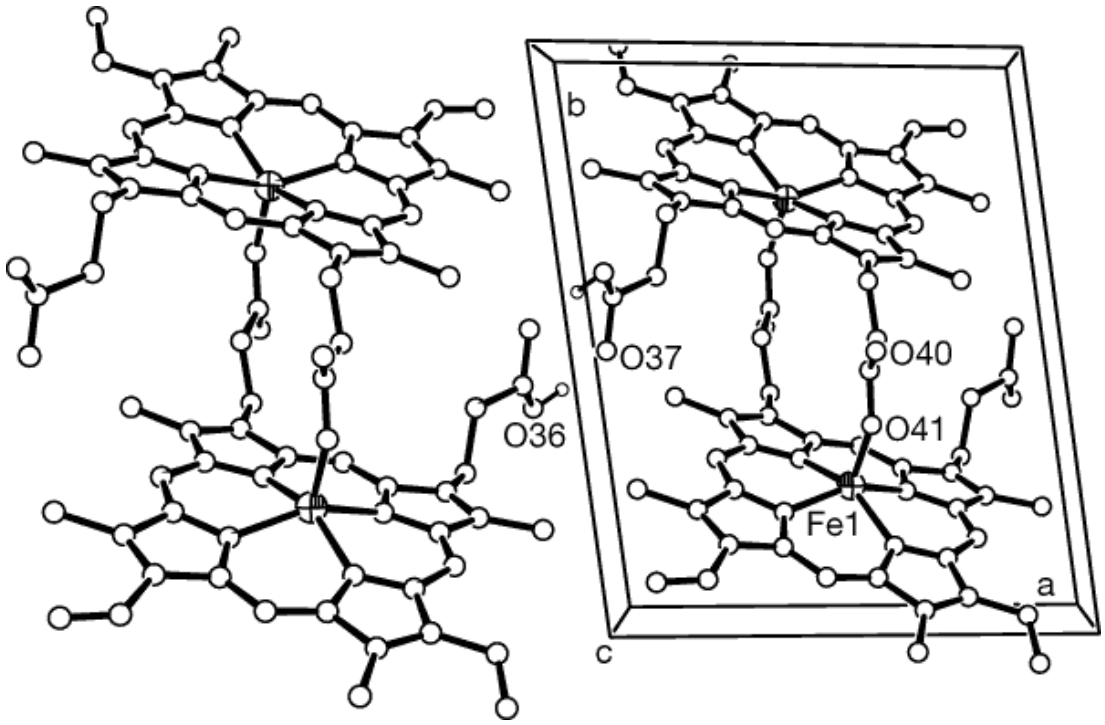

Figure 1-7: Two unit cells of the crystal structure of Hz as determined by Pagola et al. Reprinted by permission from Macmillan Publishers Ltd: [Nature Publishing Proup], Copyright (2000). [24]

1.6.3 Haemozoin formation in *Plasmodium falciparum*

The exact mechanism by which Hz is formed in the acidic DV of the parasite is not conclusively known, however, several theories have been proposed to explain the mechanism.

Slater and Cerami suggested that a "haem polymerase" enzyme (HPE) catalysed Hz formation after showing that βH formation was promoted in the presence of extracts of PRBCs. [66] The theory was discredited when it was shown the "enzyme" remained active after extensive boiling and protease treatment. Hz itself was

proposed to be a nucleation site for further crystal formation when it was shown that both Hz and βH, promoted βH formation. [67] [68] However this theory does not account for the formation of Hz in the absence of pre-existing Hz such as in the ring stage when Hb degradation is only beginning. Egan et al in 1994 showed that βH could be formed spontaneously from haematin in acid acetate solutions (pH 4.2 – 5.0, 6°C – 65°C). [69] The reaction was inhibited in the presence of antimalarials CQ, AQ and QN but not primaquine (PQ), an antimalarial active against hypnozoites in the liver stage in *P. vivax* and also shown to have potent activity against stage V gametocytes in *P. falciparum.* [70] The antimalarially inactive compounds 9-epiquinine and 8-hydroxy quinoline had no effect on βH formation.

In 1996, Sullivan et al associated two histidine rich proteins (HRP II and HRP III) with the initiation of Hz formation. It was found that HRP II was able to bind more than 17 mol equivalents of haem under acidic conditions. Both HRP II and HRP III were shown to accumulate in the DV and bind haem in a process that was inhibited by CQ. [71] However when it was found that a *P. falciparum* clone of the CQ sensitive (CQS) HB3 and CQ resistant (CQR) Dd2 strains lack both HRP II and HRP III but still forms Hz, the significance of the role played by HRP in Hz formation was questioned. [72] Another protein speculated to be involved in Hz formation was identified by Jani et al in 2008. The haem detoxification protein (HDP) was found to rapidly convert haem into Hz within the DV. Unlike HRP II and III, HDP has been found in all species of *Plasmodium.* It is speculated that HDP specifically catalyses the formation of haem dimers and acts as a chaperone of dimers, delivering them to lipid bodies where Hz is assembled. [73]

The theory of lipid mediated Hz formation was popularised in a study by Fitch et al where it was found that lipid extracted from PRBC membranes promoted βH formation from Fe(III)PPIX under conditions mimicking the environment of the DV. [74] In 2007, Pisciotta et al demonstrated the presence of Hz crystals within lipid droplets in transmission electron microscopy (TEM) images of malachite green stained PRBCs, supporting the theory of lipid mediated formation of Hz (Figure 1-8). Isolation and characterisation of the lipid droplets from *P. falciparum* via mass spectrometry found the composition to be a 4:2:1:1:1 ratio of monostearic: monopalmitic: dipalmitic: dioleic and dilinoleic glycerols. The lipid blend was capable of initiating haem crystallisation. [75] Recently, Ambele and Egan demonstrated that the neutral lipids associated with Hz formation mediate the

formation of βH under physiological conditions at rates analogous to the parasite. Confocal microscopy performed on samples of laboratory formed βH, directly demonstrated that βH was formed in close association with the neutral lipid blend. [76]

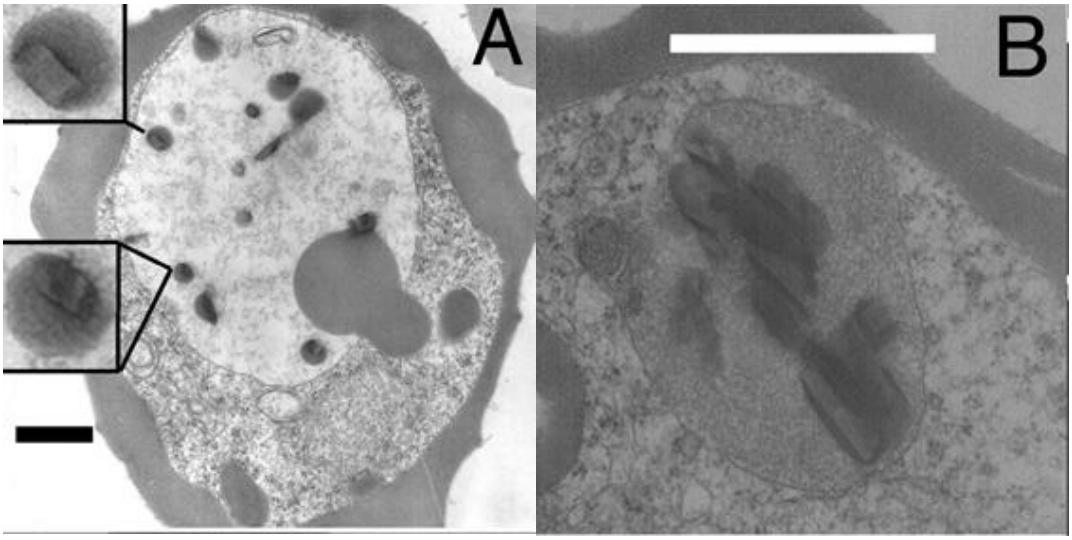

Figure 1-8: TEM of trophozoites stained with malachite green. (A) An early trophozoite with small Hz crystals surrounded by neutral lipid spheres inside the DV. The inset clearly shows the crystals embedded within a lipid droplet and the lack of bilayer membrane at the periphery of lipid sphere. (B) A more mature trophozoite with larger haem crystals within the lipid. This image was originally published in: http://www.biochemj.org/content/402/1/197, Pisciotta, J.M et al, 2007 with permission from the Biochemical Society. [75]

1.7 Chloroquine and related antimalarials

The quinolines represent one of the world's most successful drug classes (Figure 1-9).[77] QN was the first quinoline to be isolated from extracts of the bark of the *Cinchona* tree in 1820 by Pelletier and Caventou. [78] QN was used extensively during WWI and when demand for the drug exceeded supply, research into the production of synthetic alternatives was pursued. This led to the development of CQ and pyrimethamine (PYR).[79] In 1943, CQ was taken into clinical trials and was subsequently widely used due to its effectiveness and low risk side effect profile.[80]

Following the success of CQ, the closely related 4-aminoquinoline, amodiaquine (AQ) was synthesized followed by the 8-aminoquinoline primaquine (PQ). Both were introduced as alternatives to CQ at the end of WWII.[81] However, misuse of CQ led to the development of resistance in the 1960's and although CQ is no longer recommended as a first line therapy for the treatment of malaria, this 4-aminoquinoline still holds the record as the world's most successful antimalarial.[82] In response to CQ resistance, the quinoline methanols, mefloquine (MQ) and the aryl methanol halofantrine (HF) were developed by the Walter Reed Army Institute of Research in 1963.[83]

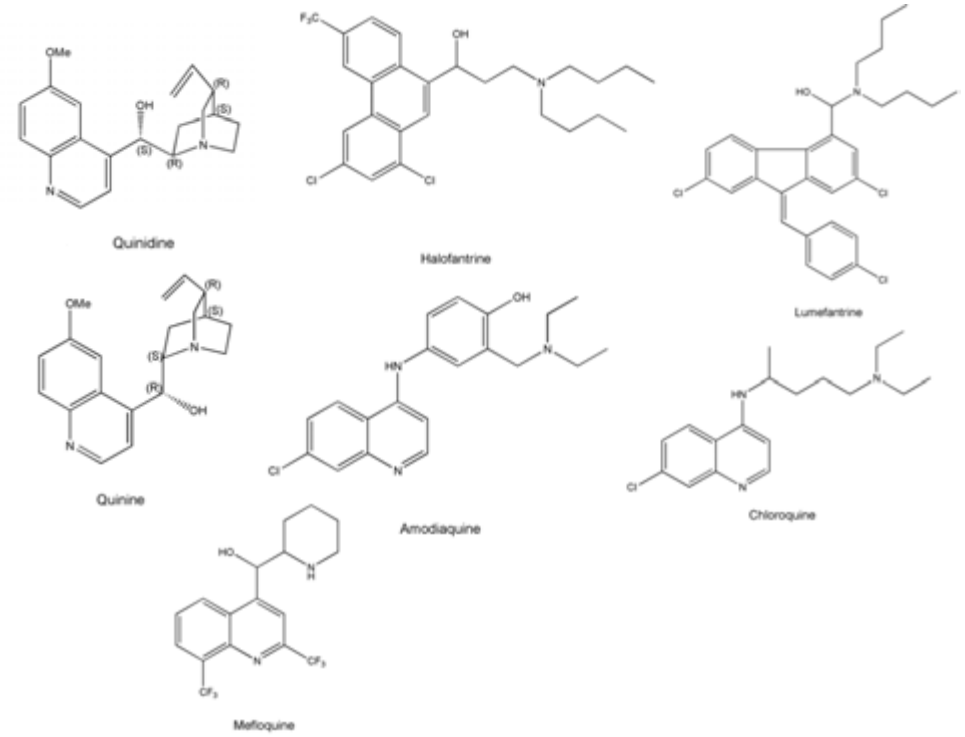

Figure 1-9: Structures of some quinoline and related antimalarials discussed in this literature review.

1.7.1 Mechanism of action of chloroquine and related antimalarials

Chloroquine has been shown to be active only against the intraerythrocytic stage of the parasite lifecycle where Hb is actively degraded, providing the first clue that its mechanism must be related to processes which occur during this stage of the parasite lifecycle. [84] Further clues towards the mechanism of action of CQ were provided when treatment of parasites with pharmacologically relevant

concentrations of CQ, produced swelling of the DV and the accumulation of Hb. [35 85] The evidence above suggested that CQ acts on the Hb degradation pathway. Several theories for the mechanism of action of CQ have been proposed including the inhibition of haemoglobin proteases, inhibition of the peroxidative degradation of haem, inhibition of glutathione dependent degradation of haem in the parasite cytosol and direct inhibition of Hz formation. [40 31 86 66]

1.7.1.1 Accumulation in the digestive vacuole

A weak diprotic base, CQ has been shown to accumulate several thousand fold within the acidic DV of the malaria parasite by ion-trapping. [87 88] In its unprotonated form CQ moves down the pH gradient to the acidic DV, where once protonated becomes trapped as result of its membrane impermeability. [89 90] Chloroquine is thus able to concentrate from nanomolar to almost millimolar concentrations in the DV. The pH gradient is important in determining the level of CQ accumulation and has received significant attention, especially in light of CQ resistance. Decreasing the pH gradient by increasing the pH of the DV would results in decreased CQ accumulation. However there is little evidence of this and indeed, several studies even went so far as to claim that the pH of the DV in CQR strains is more acidic, reducing the solubility of haem in the DV and hence reducing the availability of the prosed drug target for CQ rather than the accumulation of CQ itself. [91 92]

Establishing the exact pH of the DV has been an area of significant debate, with pH values ranging from 4.2 to 5.9. The variation being largely dependent on the method of measurement used. [92 90 93 94 91] Klonis et al measured the DV pH to be 5.4 – 5.5 using a flow cytometry based method based on the pH sensitivity of green fluorescent protein (GFP). Furthermore they found no difference in the pH of between CQS and CQR strains. [95] In addition to pH trapping, CQ has been shown to accumulate in the DV as a result of interaction with free haem in the DV which acts as a CQ receptor. [96] The accumulation of CQ in the DV supports the theory that the mechanism of action of CQ and related antimalarials is related to the process of Hb degradation which occurs in the parasite DV.

1.7.1.2 Measuring inhibition of Hz formation

The determination of the ability of a compound to inhibit Hz formation within the malaria parasite is routinely carried by measuring the formation of synthetic Hz, βH, within a cell-free environment mimicking conditions of Hz formation within the DV. Several methods have been developed to achieve this (Table 1-1).

The evolution of the βH inhibition assay can be traced back to the experiments by Slater and Cerami where it was demonstrated that CQ and QN inhibited the formation of Hz under physiological conditions and in the presence of PRBC extracts. [64] [66] Quantitative spectroscopic measurement was first reported by Basilico et al. Based on the solubility of haem but not βH in aqueous mildly alkali solutions, haem could be measured in mixtures of haem and βH. [97] The method was subsequently modified to a higher throughput 96-well plate method used for screening larger volumes of compounds for βH inhibitory activity. In this method, test compounds were incubated overnight in 4.5 M acetic acid. Unreacted haem solubilised in DMSO was measured spectroscopically. [98] The method, referred to as the haem polymerisation inhibitory activity (HPIA) assay was subsequently modified to eliminate the presence of interference by phosphates and chloride salts. Haemin rather than haematin was used as the starting material and sodium hydroxide as the solvent for unreacted haemin. [99] Ncokazi and Egan introduced further improvements for the measurement of βH inhibition with the development of the ferrihemochrome method, based on the pyridine hemochrome method published by Partos in 1922. [100] This modification improved the detection of the haem species by spectroscopically measuring haem as a low spin haem-pyridine complex. Additionally this method required only 60 min of incubation at 60 °C. [101] Recently the assay has been adapted to a more physiologically relevant one, where inhibition of βH is measured in a lipid environment representing the site of Hz inhibition in the DV. Later, Carter et al reported the lipophilic detergent Nonidet P-40 (NP-40) best mimicked results obtained when compared to the neutral lipid blend identified in the parasite DV (Section 1.6.3). [102] This method has been adapted to a high throughput screening method used to screening libraries of tens of thousands of compounds for the identification of novel βH inhibiting compounds. [103] [104] [105]

Measurement of βH using several of the methods described above has been extensively performed on the quinolines and a strong relationship between the quinolines, βH inhibition and parasite growth inhibition has been demonstrated on several occasions. [106] [107] [52] [69] [101] [72] [108] [109] Although most of the research surrounding Hz inhibition has been carried out in relation to CQ, the findings have been associated with related quinolines. The relationships established by these studies on βH formation supports the view that these quinolines share a mechanism of action involving Hz inhibition with CQ.

Table 1-1: Several methods used to measure βH inhibition

Reference	Assay conditions	Quantification method	CQ	AQ	PQ	QD	QN	MQ	HF	AMN	DHA	PYR	ATV	10-dO-AMN
69	Acetate, pH 4.5, 4.5 M, 60 °C, 30 min incubation	Infrared spectroscopy	+	+	-		+							
98	Acetic acid, pH 3, 37 °C, 24 h incubation	Absorbance of haematin @ 405nm	+	+	+	+				+	+	-	-	
106	Purified Hz extract. Sodium acetate pH 4.8 or sodium phosphate pH 6.5, overnight, 37 C	Scintillation counter	+	+	-		+	+	+					
99	DMS0-acetate buffer, pH 5, 18 h incubation	Absorbance of haematin @ 405nm	+	+	-		+	+						
110	Acetic acid, pH 3, 37 °C, 18 h incubation	Absorbance of haematin @ 405nm									+			-
	DMS0-acetate buffer, pH 5, 18 h incubation	Absorbance of haematin @ 405nm									-			-
52	Acetate, pH 5, 60 °C, 60 min	Aqueous pyridine (5% v/v, pH 7.5) for detection of haem @ 405 nm.	+	+		+	+	+	+					
102	NP-40 mediated. Acetate, pH 4.9, 37 °C, 4-6 h	Aqueous pyridine (5% v/v, pH 7.5) for detection of haem @ 405 nm.	+	+										
105			+	+								-		
103			+									-		

CQ = chloroquine, AQ = amodiaquine, PQ = primaquine, QD = quinidine, QN = quinine, MQ = mefloquine, HF = halofantrine, AMN = artemisinin, DHA = dihydroartemisinin, PYR = pyrimethamine, ATV = atovaquone, 10-dO-AMN = 10-deoxoartemisinin.

While measuring βH inhibition in a non-cellular system has been widely applied, demonstrating the effects of Hz inhibition within the parasite has not been as straight forward. A study by Asawamabasakda et al measured the effects of CQ and AMN on Hz production in three strains of *P. falciparum,* CQR, W2 and FCR3 and CQS, D6. Hz was extracted from drug treated (6 h) isolated trophozoites by filtration and spectrophotometrically quantified as pmol of Hz per 10^6 cells. Interestingly it was found that CQR strains contained more Hz than the CQS strain. The amount of Hz in treated cells was measured in conjunction with hypoxanthine content to determine if Hz formation occurs at or below concentrations which affect parasite viability. Hypoxanthine is known to be taken up by malaria parasites and incorporated into nucleic acids and was used to determine parasite viability. It was found Hz formation was inhibited only in cells treated with CQ concentrations at or greater than the parasite growth $IC_{50.}$ The authors deduced the effect of CQ on Hz formation was small in comparison to parasite survival and therefore a small effect of CQ on Hz formation is required to kill the parasite, or the drug is killing via a secondary mechanism affecting Hz production indirectly. Treatment with AMNs produced no change in Hz levels at any concentration tested. [111] Another study by Burgess et al examined the effects of Hz formation in a CQS strain D6 and CQR strain Dd2 of *P. falciparum* inoculated with 2 novel CQ analogues (compound **1** and **22**) which contained CQ resistance reversal moieties. [112] [113] Both compounds inhibited the formation of βH and were derived from a series which demonstrated a favourable correlation between the parasite growth inhibition and the ability to inhibit the formation of βH. Trophozoites were isolated by saponin lysis 24 h after inoculation and Hz was extracted via centrifugation. The washed Hz was dissolved in 0.2 M sodium hydroxide and the amount of haem was spectroscopically determined. The results were examined in conjunction with microscopy images (Figure 1-10). Haemozoin formation in cells treated with compound **22** was almost completely inhibited at 10 nM in D6 and 100 nM in Dd2. A similar effect was seen in Dd2 treated with CQ at 1000 nM. Results for compound **1** were between compound **22** and CQ. Examination of the Hz crystals within the DV of microscopy slides confirmed the results obtained for measured Hz. The authors deduced that compounds **1** and **22** had a similar mechanism of action to CQ.

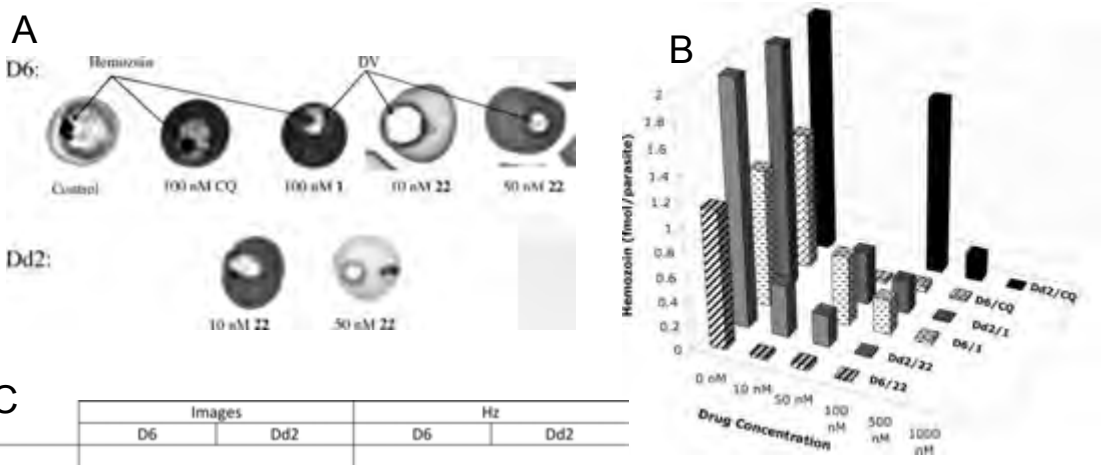

C

	Images		Hz	
	D6	Dd2	D6	Dd2
Control	Small DV with Hz		N/A	
Compound 22	At 10 nM little Hz and enlarged DV		At 10 nM almost complete inhibition of Hz	At 100 nM almost complete inhibition of Hz
Compound 1	At 100 nM very little Hz and enlarged DV		Produced effects between CQ and compound 22	
CQ	At 100 nM enlarged DV and reduced Hz		Similar to compound 22	At 1000 nM same effect as compound 22 @ 100 nM

Figure 1-10: The effect of various concentrations of CQ, compound **1** and **22** on D6 and Dd2 demonstrated via light microscopy images (A) and Hz formation (B). The table (C) summarises the observations made from Figure A and B. Reprinted and adapted with permission Burgess, S.J., Kelly, J.X., Shomloo, S., Wittlin, S., Brun, R., Liebmann, K. and Peyton, D.H., 2010., Synthesis, Structure– Activity Relationship, and Mode-of-Action Studies of Antimalarial Reversed Chloroquine Compounds. J. Med. Chem., 53, 6477-6489 with permission from American Chemical Society (Copyright 2010). *112*

Although both studies were able to measure changes in Hz formation in *P. falciparum* in response to drug treatment, neither study demonstrated the result of Hz inhibition. The level of haem produced, if any, in response to changes in Hz formation was not determined. This is an important determination as this free haem is regarded as the route of toxicity attributed to Hz inhibition resulting in parasite death. Furthermore decreased level of Hz formation could be as a result of secondary unrelated effects in the cell due to reduced Hb uptake, resulting in less Hz formation and interpreted as Hz inhibition. Although providing useful

information neither method is able to directly attribute the mechanism of action of the compounds investigated to direct Hz inhibition.

1.7.1.3 Hz inhibition as a drug target

Evidence that the mechanism of action of several quinoline antimalarials do not directly interfere with Hb degradation was demonstrated using protease inhibitors which block the digestion of Hb. While inhibition of Hb digestion by protease inhibitors was reversed upon removal, this was not true for quinoline antimalarials suggesting a mechanism downstream from the inhibition of Hb degradation is involved. [114] [115] Chou et al in 1980 reported than haematin was the receptor of CQ in *P. falciparum.*[96] Several studies followed implicating Hz inhibition as the mechanism of action either through interaction with haem or with the Hz crystal itself. In 1992 Slater and Cerami showed that both CQ and QN inhibited the formation of Hz under physiological conditions and in the presence of PRBC extracts, suggesting that a subsequent increase in toxic free haem or haem-drug complexes killed the parasite. At the time Hz inhibition was attributed to the ability of CQ and QN to inhibit the functioning of HPE. [66] Sullivan et al demonstrated the association of Hz with quinolines using electron microscopy (EM) autoradiography. Parasites incubated in the presence of [^{3}H] quinidine (QD) and [^{3}H] CQ showed the signal arising from the labelled quinolines was almost exclusively over the Hz in the DV. Furthermore subcellular fractionation of parasites incubated in the presence of [^{3}H] QD and [^{3}H] CQ showed the quinolines were associated with recovered Hz. It was suggested that the quinolines bind haem and form a drug-haem complex which is incorporated into growing Hz, preventing the addition of further haem and terminating growth of Hz (Figure 1-11). The theory explains the hyper-concentration of CQ within the DV which cannot be fully accounted for by the effects of pH trapping alone. [116] Haem in RBC Hb is present at approximately 20 mM. If most of this is digested by the parasite within the 4 fL DV haem concentrations could theoretically reach 0.4 M. If a quinoline molecule were incorporated at every 400th haem, quinoline concentrations would reach 1mM within the DV. [54]

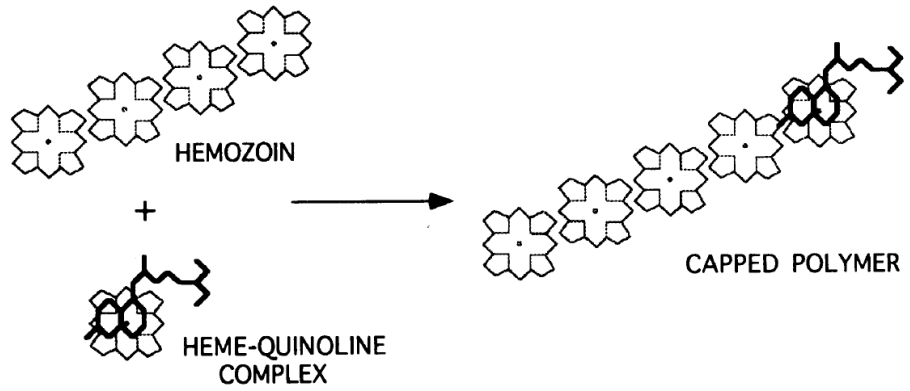

Figure 1-11: Model of quinoline inhibition of Hz formation as proposed by Sullivan et al. Quinolines bind haem forming a drug-haem complex which is incorporated into growing Hz [54]. From: Sullivan, D.J., Gluzman, I.Y., Russell, D.G. and Goldberg, D.E., 1996. On the molecular mechanism of chloroquine's antimalarial action. Proceedings of the National Academy of Sciences, 93(21), 11865-11870. Copyright (1996) National Academy of Sciences.

Despite overwhelming evidence that CQ and related antimalarials inhibit Hz formation, it is not clear whether this is due to direct interaction of the drug with haematin or adsorption of the drug onto the fastest growing face of the Hz. [96] [54] The structures of co-ordination complexes between Fe(III)PPIX and each of HF, QN and QD have previously successfully been determined using single X-ray diffraction, demonstrating direct interaction with Fe(III)PPIX. [117] [118] An unsuccessful attempt to similarly grow and elucidate the crystal structures for the 4-aminoquinolines by Gildenhuys et al led to the discovery that in a lipid water system at low concentrations of CQ the rate of βH formation decreases. This outcome reproduces results obtained by Egan and Ncokazi, where it was shown that the formation of βH (4.5 M acetate, pH 4.5 at 60 °C) in the presence of CQ, AQ, QN and QD is not inhibited, but rather the rate at which βH forms is decreased. [52] Adsorption of the drug to the fastest growing face of the βH crystal, rather than the formation a complex with Fe(III)PPIX was used to explain the behaviour observed at lower, more biologically relevant drug concentrations. Modelling of the results showed that at higher drug concentrations, the βH yield decreased and an insoluble Fe(III)PPIX precipitate was formed.[119]

The recent discovery that Hb metabolism and Hz formation take place in acidified "pre-DV" compartments during the early ring phase of the parasite lifecycle has

implications for antimalarials such as CQ which most likely act on the Hz formation pathway and accumulate in acidic compartments. [36] Ring stage parasites would therefore accumulate CQ and inhibit the early stages of Hz formation resulting in the formation of toxic haem and continue into the trophozoite stage. This would provide a rationale for previous studies have shown that ring stage parasites are more susceptible to CQ treatment. [120]

1.7.1.4 Inhibition of haemoglobin degradation

Several quinolines, including CQ have in the past been shown to interfere with the process of Hb degradation. Treatment with CQ has been shown to increase the amount of undigested Hb in parasites. [121] [122] Ginsburg et al in 1984 showed that increased Hb levels were accompanied by an accumulation of single membrane Hb laden transport vesicles in the DV of CQ treated cells. This was attributed to inhibition of phospholipases responsible for digesting the transport vesicle membranes and releasing the RBC cytosol contents into the DV for digestion of Hb. [123] A subsequent study by Hoppe et al studied the effects of CQ, AMN and MQ on endocytosis in *P. falciparum.* In this study increased levels of Hb in cells treated with CQ at the ring stage for 12 h was accompanied by the presence of double membrane transport vesicles outside the parasite DV (Figure 1-12 A, B). This was attributed to failure to deliver transport vesicles to the DV and the inability to fuse transport vesicles with the DV. Interestingly when cells were treated with CQ for a shorter time period (5 h), later in the lifecycle, an increase in undigested Hb levels was observed but no accumulation of transport vesicles. This observation suggests the parasite is more sensitive to the effects of CQ at the ring stage. [120] The downstream effect of inhibiting Hb degradation whether by preventing fusion of transport vesicles with the DV or inhibiting the lysis of transport vesicle membranes is that the parasite cannot access Hb. Although studies have shown that only a fraction of these amino acids are required, inhibiting the degradation of Hb also prevents parasite growth as Hb degradation will free up space in the cell for expansion and parasite growth. [29] [49] Moderate increases in undigested Hb were also seen in cells treated with AMN, with no accompanying accumulation of transport vesicles. [124] Parasites treated with MQ showed a decrease in parasite Hb levels attributed to the inhibition of the process of endocytosis by the parasite

cytostomal system. [121] As in the case of AMN no accompanying evidence of accumulation of transport vesicles was observed in the MQ treated parasite. [124]

In a subsequent study by Roberts et al the effects of QN, HF and AQ were investigated and compared to CQ. [125] Parasites were inoculated at concentrations corresponding to 5× the parasite growth IC_{50} for 8 h. Cells treated with MQ, QN and HF reduced Hb content by 83%, 64% and 84% respectively and showed no evidence of increased accumulation of transport vesicles (Figure 1-12 C). Cells treated with CQ resulted in a 283% increase in Hb content and an accumulation of Hb transport vesicles as previously shown. [124] [121] [122] It was expected that the 4-aminoquinoline AQ, closely related to CQ, would produce an effect similar to CQ in treated cells. However treatment with AQ produced no increase in levels of undigested Hb, but did show an increase in Hb laden transport vesicles in the parasite. Closer examination revealed that AQ treated cells exhibited a combination of behaviours seen in CQ treated cells and cells treated with MQ, QN and HF. Inhibition of endocytosis accompanied by an accumulation of Hb transport vesicles which caused the net effect to show no change in Hb levels of AQ treated cells.[125] Previous studies have shown that Hb antagonises the action of the quinolines. [126] The addition of protease inhibitors (PIs) increased Hb levels in the control and caused no real change in the Hb levels of both CQ and AQ treated cells. In cells treated with MQ, QN and HF, Hb levels were decreased by 66%, 31% and 30% respectively, in comparison to decreases of 83%, 64% and 84% in the absence of PIs (Figure 1-12 D). This indicates that the presence of undigested Hb in cells treated with MQ, QN and HF in the presence of PIs antagonised the effect the drugs had on the inhibition of endocytosis, agreeing with previous work. [126] [125]

The effects of the above mentioned drugs cannot exclusively be attributed to a direct effect of the drugs themselves, but could be due to a secondary downstream effect of the drug. In the case of CQ, treatment is postulated cause a build-up of toxic haem through inhibition of Hz formation. The increased levels of lipophilic toxic haem could very well interact with membranes and causing membrane damage preventing membrane fusion resulting in an accumulation of transport vesicles in the parasite cytosol as demonstrated by Hoppe et al. [57] [124] However the evidence summarised above suggest the quinoline methanols differ in their mechanism of action in comparison to CQ. Further evidence that the quinoline methanols possess a different drug target is shown in the treatment of *P. berghei*

infected mice with a range of antimalarials. Whereas CQ and 4-aminoquinoline derivatives caused a decrease in the amount of Hz produced, QN, MQ and PQ showed no effect. [127]

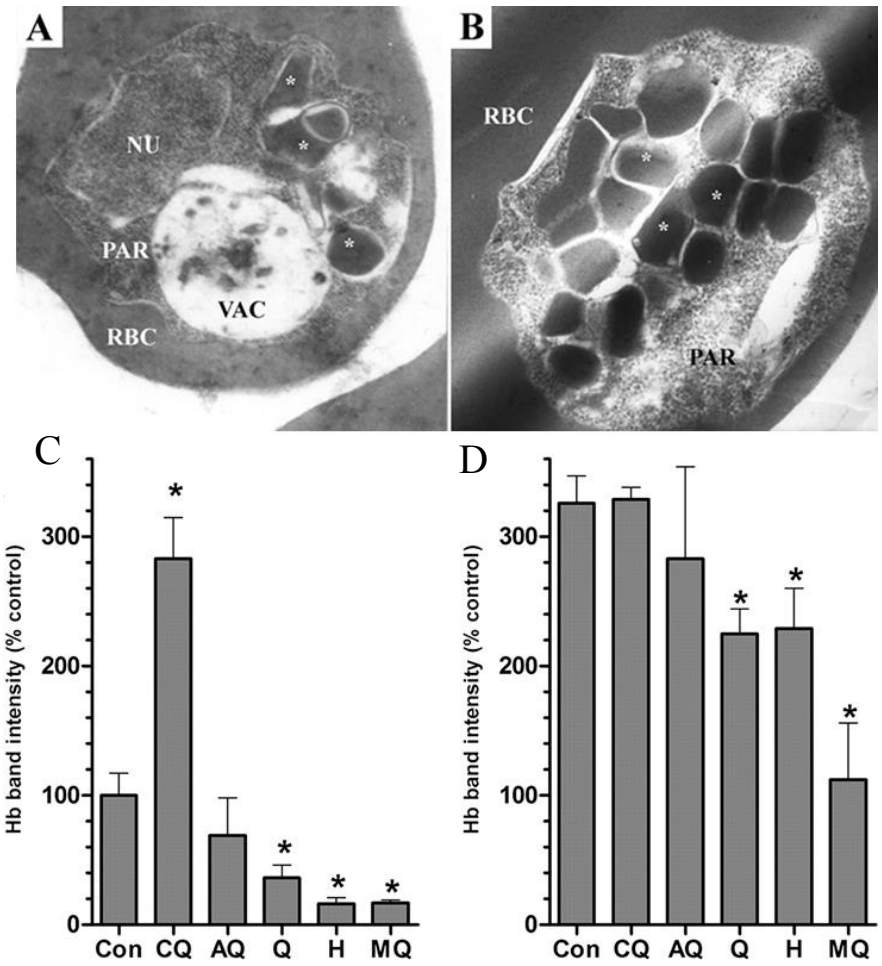

Figure 1-12: TEM of chloroquine-treated parasites in A, B showing accumulation of transport of vesicles outside the DV. infected red blood cell = RBC, parasite = PAR, parasite nucleus = NU, digestive vacuole = VAC, and transport vesicles (asterisks). Hb levels in drug-treated parasites in C, D. (C) Parasite cultures were untreated (control [Con]) or incubated with CQ, AQ, quinine (Q), halofantrine (H) and MQ. (D) In parallel cultures, the quinoline drugs were added in combination with the protease inhibitors. An asterisk (*) indicates a significant change from the results for the controls ($P < 0.05$; 95% confidence interval [CI]). Images A, B from Hoppe et al, 2004 [124] and C, D from Roberts et al, 2008 [125] reproduced with the permission of the American Society for Microbiology Copyright (2004) and (2008).

1.7.2 Resistance to chloroquine and related quinolines

1.7.2.1 Chloroquine resistance

Chloroquine was successfully used for the treatment of malaria throughout the 1940s and 1950s. [128] Resistance to CQ emerged in the 1960s in S.E. Asia and South America and by the 1980s had spread across Africa. [82] The development and spread of resistance to CQ and related antimalarials has significantly increased the global cost of controlling malaria, as new drugs must be continually developed to replace ineffective treatments. [2]

The emergence of CQ resistance is attributed to mutations in the '*Plasmodium falciparum* CQ resistance transporter' (PfCRT) and other DV membrane proteins resulting in reduced CQ accumulation. [129] [130] In comparison to CQS strains, resistant parasites have been shown to accumulate up to ten times less CQ in the DV, falling outside the effective therapeutic range for CQ.[131] PfCRT is a member of the Drug/Metabolite Transporter (DMT) superfamily (Figure 1-12). The 424 amino acid protein, encoded by the *pfcrt* gene on chromosome 7, localises to the parasite DV. [130] PfCRT has been found to be essential to the parasite and is assumed to play a role in the transport of amino acids and peptides out of the DV.[132] Several mutations in PfCRT ($PfCRT^{CQR}$) have been identified in CQR strains, most of which are located on the vacuolar side of the protein (Figure 1-13). However the substitution of positively charged lysine for neutral hydrophobic threonine at position 76 (K76T) has been shown to be essential in conferring resistance. As a consequence of this mutation, protonated CQ (CQH_2^+ or CQH^+) previously trapped in the DV is able to efflux out of the DV. In its protonated state, CQ is unable to interact with the wild type K76 PfCRT, however protonated CQ can interact with $PfCRT^{CQR}$ allowing transport down the electrochemical gradient away from the DV. Resistance arises due to a reduced concentration of CQ at its site of action within the DV.[133] The process has been shown to be saturable and temperature dependent. The effect of $PfCRT^{CQR}$ can therefore be overcome by increasing the dose of CQ administered and in so doing saturate the transport process of CQ out of the DV allowing lethal concentrations of CQ to be reached within the DV.[129] A recent study conducted in Guinea-Bissau on patients infected with CQR malaria

showed that at high doses, CQ treatment was as therapeutically effective as AMN-lumefantrine (LF) combination therapy at curing infection. [134]

Resistance to CQ is reversed in the presence of the calcium channel blocker verapamil (VP) causing a decrease in the parasite growth IC_{50} value and increased accumulation in CQR strains. [135] [136] However, the concentration of VP required to bring about this change is beyond its therapeutic concentrations. [137] It has been suggested that some resistance reversers are themselves substrates for $PfCRT^{CQR}$ and therefore compete with CQ for transport out of DV. [138] These substrates therefore represent a possible class of effective antimalarials which could possibly block functioning of normal PfCRT. Although the K76T mutation is essential for resistance, the mutation alone is not sufficient for resistance. The CQR strain Dd2 for example, contains eight mutations in $PfCRT^{CQR}$ not found in the wild type. [129] This suggests that one or more additional mutations work together to transport CQ out of the DV.

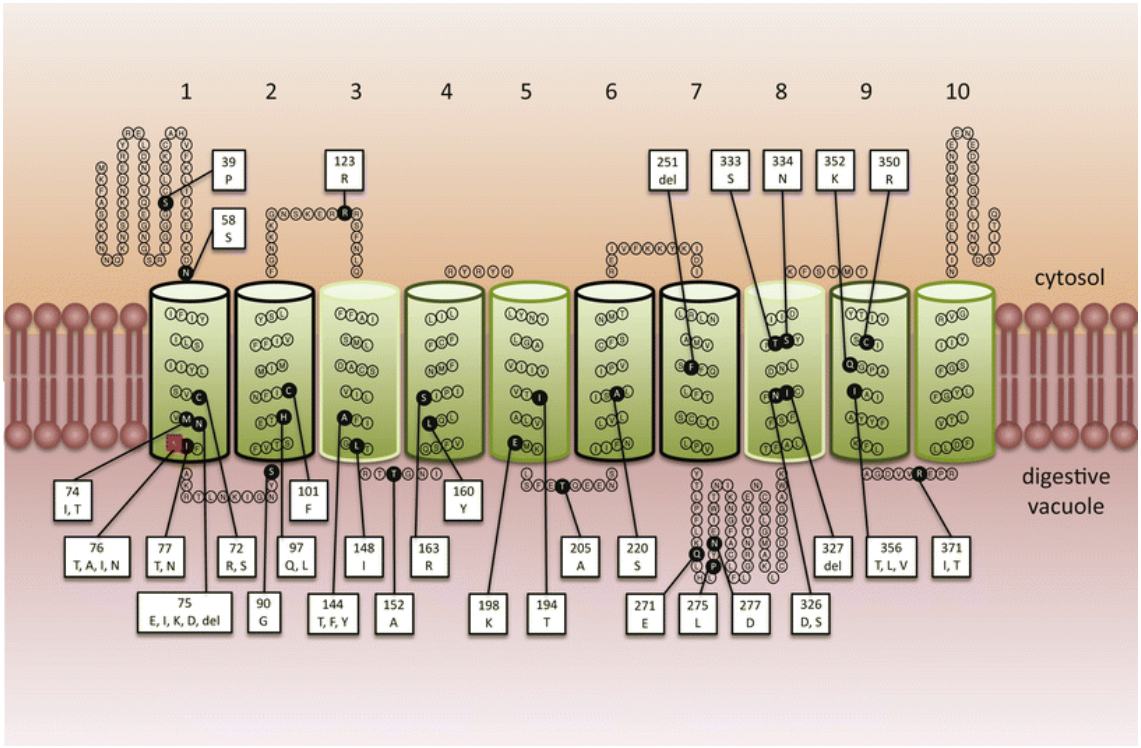

Figure 1-13: Arrangement of known polymorphic residues in PfCRT. PfCRT is predicted to contain 10 α-helical transmembrane domains (TMDs) and to be orientated in the DV membrane with the N- and C-termini extending into the parasite cytosol. The positions of the polymorphic residues are indicated with black circles. The key CQ resistance-associated mutation (K76T) is

represented as a red square. The box attached to each polymorphic residue lists the (non-wild-type) amino acid(s) known to occur at that position. The predicted roles of the TMDs are as follows: 4 and 9 (outlined in dark green) are implicated in the binding and translocation of substrates, TMDs 3 and 8 (boxed in light green) are thought to assist in the binding and translocation of the substrate and may also influence the substrate-specificity of the transporter, TMDs 1, 2, 6, and 7 (boxed in black) are involved in recognising and discriminating between substrates, and TMDs 5 and 10 (outlined in mid-green) play a role in the formation of homo-dimers. [129] Cellular and Molecular Life Sciences, Know your enemy: understanding the role of PfCRT in drug resistance could lead to new antimalarial tactics, 69, 2012, 1967 – 1995, Summers, Robert L., Megan N. Nash, and Rowena E. Martin, (Springer Basel AG 2012). With permission of Springer.

Mutations in proteins other than PfCRT have also been identified in relation to CQ resistance. A homologue of eukaryotic ATP-binding cassette (ABC) protein, the Plasmodium falciparum multidrug resistance transporter 1 (PfMDR1) has been linked to CQ resistance. Expressed at the DV membrane, PfMDR1 is thought to be involved in the transport of substrates from the cytosol into the DV.[139] Indeed it has been shown that wild type PfMDR1 expressed in oocytes mediates CQ transport. [140] Alone, mutations in PfMDR1 do not confer resistance, but can modulate resistance to CQ in parasites with $PfCRT^{CQR}$. Mammalian Chinese hamster ovarian cells modified to express PfMDR1 showed an increase in CQ accumulation and increased sensitivity to CQ toxicity. [141] Therefore it is likely that while in wild type parasites PfMDR1 may transport CQ into the DV, in resistant parasites the ability of PfMDR1 to transport CQ into the DV is compromised. In CQR strains, PfMDR1 works synergistically with $PfCRT^{CQR}$ to reduce the concentration of CQ in the DV. [140]

1.7.2.2 Resistance to other quinolines

Based on their ability to inhibit βH formation, the more hydrophobic aryl methanols including, QN, QD, MF, lumefantrine (LF) and HF are postulated to share the mechanism of Hz inhibition of CQ. However as discussed in Section 1.7.1.4 it is

also possible that QN, Mef and HF have drug targets other than the inhibition of Hz formation. Similarly mechanisms of resistance in these quinolines share similarities, but also differ in several aspects.

Resistance to MQ has been related to increase copies of the pfmdr1 gene resulting in the increased expression of PfMDR1. [142] [143] [144] [145] It has been shown that parasite strains which are resistant to MQ also show reduced susceptibilities to HF, LF as well as QN. [143] [146] [147] However, resistance to MQ has been associated with increased CQ sensitivity. [144] [148] Cowman et al showed that two CQR strains of *P. falciparum* cultured under MQ drug pressure had an amplification of the pfmdr1 gene which resulted in an overexpression of the protein PfMDR1. The strains showed an increase in resistance to MQ, as well as HF and QN and a decrease in resistance to CQ.[143] When the CQR strain K1 was cultured under HF drug pressure, the resulting strain (K1HF) demonstrated increased susceptibility to CQ and reduced susceptibility to HF and MF. Three novel PfCRT mutations were identified in K1HF one of which (S163R) reintroduced a positive charge to $PfCRT^{CQR}$. [132] This novel mutation was postulated to increase sensitivity to CQ by reinstating the ability of CQ to accumulate in the DV. [149] An inverse relationship was established between CQ resistance and MQ resistance, related to the accumulation via PfMDR1. The relationship suggests that as the function of PfMDR1 is to transport substrates into the DV and the amplification of PfMDR1 results in resistance to MQ, HF, LF and QN. These drugs may have targets outside the DV in the parasite cytosol. The reverse is true for CQ. Amplification of PfMDR1 results in increased CQ susceptibility as a result of increased transport into the DV, the site of action of CQ. It has also been postulated $PfCRT^{CQR}$ effluxes MQ out of DV as in the case of CQ and if indeed MQ has a drug target in the cytosol, this explains why $PfCRT^{CQR}$ increases susceptibility to MQ.

Parasites resistant to CQ often share a reduced sensitivity to QN, implicating PfCRT in the mechanism of resistance of QN. [150] [151] It has been shown that CQR parasites efflux QN out of the DV at a rate greater than that of a CQS strain. [152] Additionally QN, like CQ has been shown to induce a proton pump leak from CQR parasites, consistent with the theory that resistance is a result of efflux of drug out of the DV in the presence of $PfCRT^{CQR}$. [138] Evidence that QN, like CQ is effluxed out of the DV, re-affirms Hz inhibition is the likely target for QN. However, parasite strains which are resistant to MQ also show reduced susceptibilities to HF, LF and QN. [143] [146] [147]

The replacement of PfCRT by PfCRT^{CQR} in a CQS strain, GCO3 increased susceptibility to both MQ and QN, suggesting that QN, as in the case of MQ, has a cytosolic target.[153] QN resistance does not seem to arise from a single cause. It is suggested that this is due to a mechanism of action which has more than one target in the cell in the case of QN. [58 125]

Given the structural similarity of AQ to CQ it is expected that the mechanism of resistance would be similar. As is the case for CQ, AQ resistance is associated with changes in both PfCRT and PfMDR1 translating into efflux out of the DV and reduced transport into the DV respectively. [154 129] However the more hydrophobic, AQ retains some activity against CQR parasites.[155] This has been partly attributed to their retention in the hydrophobic lining of CQR-PfCRT channel. [135 156] Furthermore, resistance to AQ has been associated with different haplotypes in PfCRT compared to CQ resistance. [157]

1.8 The Artemisinins

AMNs in combination with a partner drug are currently recommended by the WHO as a first-line treatment of *P. falciparum* malaria.[158] Derived from ancient Chinese herbal medicines, the AMNs are effective against both CQR and multi-drug resistant strains of malaria. They are fast acting and effective against all asexual stages of *P. falciparum*, from recently formed rings to schizonts and possess anti-gametocyte activity imparting the added benefit of transmission prevention. [159 160]

1.8.1 Resistance to the artemisinins

Reports of emerging resistance to the AMNs have been increasing, with cases first recorded in Western Cambodia. [161 162] Resistance is defined as a decline in the efficacy of treatment characterised by slow parasite clearance. Dondorp et al in 2009 conducted a clinical study in Pailin, Western Cambodia and Wang Pha, Thailand where the effects of oral artesunate (ART) and ART-MQ combination therapy were evaluated. Median parasite clearance in Thailand was determined to be 48 h, compared to 84 h in Cambodia. In a subsequent study published by Ashley et al in 2014 it was found that AMN resistance to *P. falciparum* was prevalent

across most of South East Asia (Figure 1-14). The study was conducted on patients with acute, uncomplicated *P. falciparum* malaria, treated with ART from May 2011 to April 2013 at fifteen different sites in ten countries. Parasite clearance half-life at the Thailand-Cambodia border was found to be 7 h, 5 h longer than in the Democratic Republic of Congo, with resistance defined as a parasite clearance with half-life of 5 h or longer. These resistant strains were strongly associated with single point mutations on chromosome 13 (*kelch13* polymorphism), which encodes a kelch protein. The mutation has been detected throughout mainland Southeast Asia where prolonged courses of AMN-based combination therapies are required for effective treatment.[163] Novel antimalarial treatments currently in development will not be available for several years. It is therefore imperative to curb the spread of resistance to AMN combination therapies.

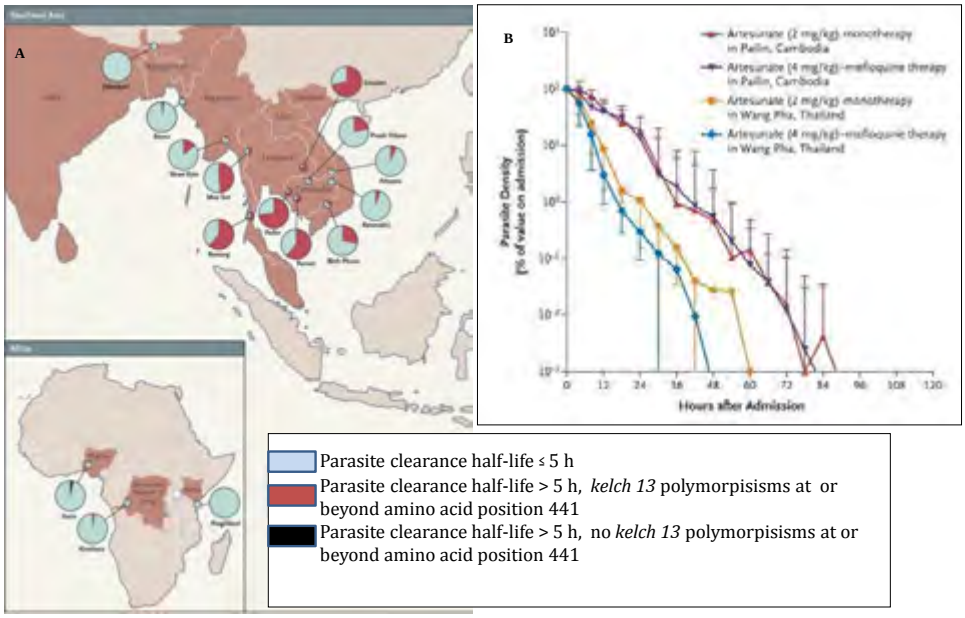

Figure 1-14: The location of patient study sites described by Ashley et al is shown in Figure A with insets indicating the proportions of patients with AMN resistance (parasite clearance half-life > 5 h). Parasite clearance curves for groups of 20 patients from Pailin, Cambodia (red and purple lines) and Wang Pha, Thailand (orange and blue lines) are shown in figure B. Graphs representing ART monotherapy at a dose of 2 mg/ml (red and orange) and ART-MQ combination therapy at 4 mg/kg of ART for 3 days followed by MQ at 15 mg/kg on day 3 and 10 mg/kg on day 4 (purple and blue) are shown. Image A was reproduced with permission from Ashley et al [163], Copyright Massachusetts Medical Society. Image B was reproduced with permission from Dondorp et al [162], Copyright Massachusetts Medical Society.

1.8.2 Mechanism of action of the artemisinins

1.8.2.1 Activation

The AMNs are characterised by a peroxide group in a 1,2,4-trioxane system, proved to be essential for antimalarial activity.[160] These drugs require activation by cleavage of the endoperoxide ring creating reactive intermediates which, through various cellular interactions including interaction with parasite protein nucleophilic groups, result in parasite death.[164] The mechanism of action of AMNs has not been fully elucidated and the role of haem in the mechanism of action of this drug class remains a widely debated topic.[2 110 98] Reduced haem and ferrous iron have been suggested as activators. Ferrous iron derived from a small labile pool of intracellular iron released by haem degradation in the DV and haem as a by-product of Hb digestion occurs most abundantly in the trophozoite phase. [31 36 165 166 167 168] Given the abundance of haem as a consequence of parasite Hb digestion during the trophozoite stage, it seems an obvious choice as a preferred activator. However, the presence of Fe chelators were shown to antagonise the effect of the AMNs, demonstrating that non haem sources of Fe were required for activation.[169] Recently, Xie et al demonstrated that the presence of Fe chelators at the early ring stage attenuated AMN activity, while at the troph stage PIs effectively reduced the activity of the AMNs, proposing that both ferrous haem and Fe^{2+} are involved in activation at different stages of the lifecycle depending on abundance.[170] Since Fe chelators antagonised but did not eliminate AMN activity and haem reacts with AMNs much more efficiently than other Fe containing molecules, haem activation of the AMNs remains a feasible option. However, haem dependent AMN activation conflicts with the fact that AMN maintain activity at all stages of the *P. falciparum* lifecycle, with very high activity against very early ring stages (2 – 4 h post invasion) believed to possess little or no free haem. [171 111] Recent research has shown that down modulating the expression of falcipain II and III rendered early rings resistant to AMNs, implicating Hb derived haem in the activation and activity of AMNs and indirectly demonstrating that Hb degradation does to some degree occur even in early rings.[170] As discussed in Section 1.5.1,

fluorescence and electron tomography of mid ring stage parasites showed a detectable "pre-DV" acidified Hz containing compartment signifying that Hb degradation does occur at the early ring stage.[36] Furthermore an inactive cytostomal ring indicative of feeding apparatus was seen at the periphery of merozoites suggesting that Hb uptake and degradation does occur very early in the parasite lifecycle, making the presence of haem in early ring stages a possibility. [34] [33]

1.8.2.2 Haemozoin inhibition

The AMNs are known to interact with haem and several studies have identified the formation of haem-AMN adducts through the alkylation of ferrous haem by AMNs. Evidence of AMN haem association was found as haem-AMN adducts in the spleen and urine of *Plasmodium vinckei* infected mice treated with AMNs. [172] [173] [174] Although this finding does suggest that AMNs interfere with Hz formation, accumulation of haem in organs could also just be associated with disease progression. The adduct has been isolated and identified in several chemical studies, however the role of these adducts in the mechanism of action of the AMNs is not defined. Nonetheless it has been proposed that formation of this adduct inhibits haemozoin formation causing toxic build up of haem eventually killing the parasite through oxidative stress or inhibition of essential cellular processes. [51] [175] [176] [177] Loup et al showed that haem-AMN adducts were able to inhibit the formation of βH from haemin in acetate at pH 5 (37 °C, 18 h incubation).[178] However evidence against AMN inhibition of haemozoin in the parasites was shown when AMN treatment of PRBCs at both the ring (12 – 16 h into cycle) and troph stage did not diminish Hz content, while treatment with CQ inhibited Hz formation.[111] Further evidence against AMN driven Hz inhibition provided by Eckstein, Ludwig et al, showed AMN in parasites does not accumulate in the DV and Asawamahasakda et al, showed that only 13-15% of radiolabelled AMN was found in the isolated Hz fraction. [179] [111] AMNs are also effective against parasites that do not degrade Hb, such as *Toxoplasma gondii* and *Babesia* spp, while CQ, known to inhibit Hz formation has been shown to be almost 200 fold less potent against *Babesia Gibsoni.* [180] [181] [182] Therefore, although Hz inhibition has been implicated as a target for this drug class, it remains a controversial topic.[98] [111] [183] In

2003, Haynes et al published an article which showed two potent AMN derivatives, 10-deoxoartemisinin (10-dO-AMN) and dihydroartemisinin (DHA) do not inhibit the formation of the synthetic Hz analogue, βH.[110] The drugs were screened for βH inhibition using two alternative methods, the haem polymerisation inhibitory activity assay (HPIA, acetic acid at pH 2.7 for 18 h at 37 °C) and the β-haematin inhibitory activity assay (βHIA, DMSO-acetate buffer at pH 5.0 for 18 h at 37 °C). [98 99] DHA showed a dose dependent inhibition in the HPIA assay only, while no activity was seen with 10-dO-AMN in either assay, contrary to positive results previously obtained for several quinolines, including CQ, AQ, QN and MQ. [105 184 101] In a separate study AMN, like DHA showed activity in the HPIA.[98] The activity of AMN and DHA in the HPIA can be attributed the unstable nature of these compounds under the aqueous conditions used in the HPIA resulting in an opening of the ring and consequent binding to free haem. 10-dO-AMN is more stable than both AMN and DHA under aqueous condition therefore less likely to interact with haem. With no oxygen at C-10, 10-dO-AMN is not prone to ring opening under aqueous condition and therefore cannot bind Fe(III)PPIX. Despite lack of activity in the HPIA and the βHIA, 10-dO-AMN remains a potent antimalarial indicating that βH inhibition and binding to Fe(III)PPIX is not required for antimalarial action.

Several other drug targets of the AMNs, other than Hz inhibition have also been explored; however, a single target resulting in cell death has not yet been identified. Radiolabelled AMN derivatives incubated at physiological drug concentrations with PRBCs at various stages of the parasite lifecycle were found to be covalently bound to six parasite proteins indicating a possible drug target. [185 186] AMNs have also been shown to accumulate in neutral lipids causing membrane damage and have been shown to affect the mitochondrial electron transport chain in yeast. [187 188 189]

1.9 Non-haemozoin inhibiting antimalarials

The structure of the non-βH inhibiting antimalarials PQ, PYR, Sulfadoxine (S) and atovaquone (ATV) are shown in Figure 1-15. The 8-aminoquinoline, PQ is known to have a distinctly different target in *P. falciparum*, acting on the liver stage rather than the asexual stage of the malaria lifecycle.[190 79] PQ has also been shown to have

potent gametocytocidal activity in *P. falciparum.*[191] [70] Methylene blue, was the first synthetic compound to be used for the clinical treatment of malaria in the 19th century, however its toxicity led to the synthesis of PQ.[192] As previously mentioned PQ, like QN and MQ, when used to treat *P. berghei* infected mice showed no effect on Hz formation while CQ treatment showed a decrease in Hz production.[127] PQ has also been shown not to produce any evidence of βH inhibition and unlike CQ, MQ and QN was shown not to complex with haem. [99] [69] [193]

PYR and S are two antifolates most frequently used for the treatment of malaria. Both compounds act on the folate synthesis pathway, required for nucleotide synthesis and amino acid metabolism. PYR inhibits the enzyme dihydrofolate reductase and S interferes with dihydroopteroate synthase.[1] [194] [195] Administered as a combination therapy (SP), the two antifolates have a synergistic effect, however, widespread use of the combination has led to resistance. [196] [197] Neither PYR or S have an effect the formation of βH and are often used as negative controls in assays which screen for βH inhibiting antimalarials.[105]

ATV interferes with the mitochondrial electron transport chain in the malaria parasite through inhibition of the respiratory enzyme complex, cytochrome *bc1*.[198] [199] ATV resistance coincides with mutations in the cytochrome *bc1* gene, confirming the mechanism of action of ATV.[200] The use of ATV as a monotherapy is associated with a high rate of recrudescent parasitemia and high rate of resistance and is limited in developing countries due to the high cost associated with the production of the drug.[29]

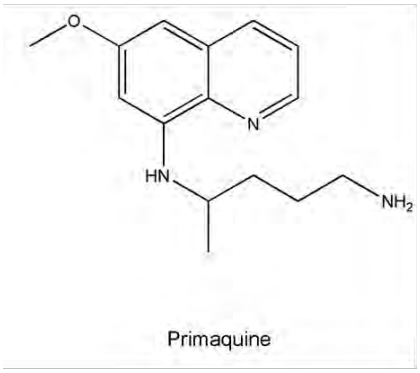

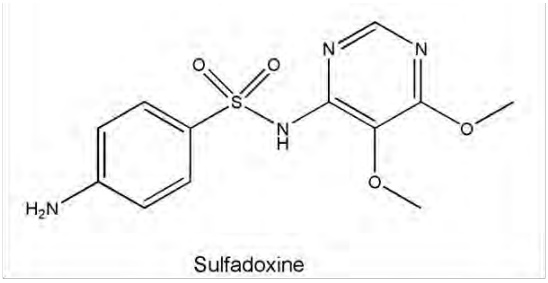

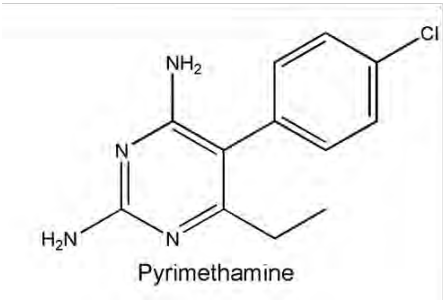

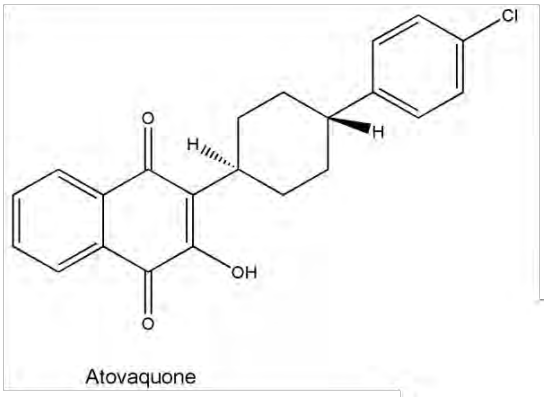

Figure 1-15: Structures of non-βH inhibiting antimalarials discussed in this literature review

1.10 The relevance of investigating the role of haem in the mechanism of action in antimalarials

An effective vaccine is seen by many as the only solution for the elimination of malaria. A malaria vaccine currently in phase 3 clinical trials has been found to reduce clinical malaria by 39% and severe malaria by 31.5% in children aged 5 – 17 months who received four doses of the vaccine. Chemoprophylaxis, certainly for the near future remains our only viable option in combatting malaria and in light of emerging AMN resistance we have a limited supply of effective available antimalarials to choose from. In recent years there has been a marked reduction in the global incidence of malaria. The disease is no longer the leading cause of death in children younger than five. However the rates of decline in Africa have been among the slowest. [2]

An overwhelming amount of evidence suggests that CQ and related antimalarials target Hz formation, resulting in increased levels of toxic haem (or haem-drug

complexes) eventually leading to cell death most likely through inhibition of proteases, oxidative stress and membrane damage. [201] [202] [51] [57] However, prior to this report, a decrease in Hz, accompanied by an increase in free haem, confirming that this is the killing mechanism had never been demonstrated in the malaria parasite. Recently, several HTS campaigns of thousands of compounds to identify βH inhibitors have been carried out. [103] [104] Demonstration of inhibition of Hz would be a valuable validation step. The application of such a method could provide insight into the mechanism of Hz inhibition. Although widely studied, the details behind the mechanism of Hz formation and consequent inhibition of this process remain unclear.

The long running success of CQ as antimalarial and the slow rate at which resistance emerged to this drug warrants further study into the mechanism of action behind this drug and related quinolines.

1.11 Aims and Objectives

1.11.1 Aim

To develop a method to measure whether CQ causes a dose related decrease in Hz and increase in 'free" haem within treated *P. falciparum* that can be correlated to parasite survival and extend this method to other antimalarials.

1.11.2 Objectives:

The aim was accomplished by fulfilling the following objectives:

- Developing a method, the haem cellular fractionation assay, capable of determining the quantities of each of the haem species corresponding to Hb, "free" haem and Hz in CQ treated *P. falciparum*.

- Modifying the haem cellular fractionation assay to a higher throughput technique and validate the new method using CQ.

- Applying the higher throughput method to several clinically relevant antimalarials of various mechanisms of action to confirm or exclude Hz inhibition as the mechanism of action.

- Applying the method to several novel antimalarials which show promising activity to aid in understanding their mechanism of action and the process of Hz inhibition in non-quinoline scaffolds.

2 GENERAL MATERIALS, INSTRUMENTATION AND METHODS

2.1 Materials

All materials used were of AR grade or higher and unless specified used without further purification. The materials are listed according to the methods for which they were needed. Where materials are common to more than one method, they are mentioned where first used unless sourced from a different supplier. All consumables were purchased from Lasec, Millipore, Merck South Africa and Sigma Aldrich. The water used throughout this work was double distilled deionised Millipore® Direct-Q water.

Table 2-1: List of materials used for the tissue culture of *Plasmodium falciparum*

Materials for tissue culture of *Plasmodium falciparum*	**Supplier**
RPMI 1640 with glutamine but without sodium bicarbonate (R6504)	Sigma Life Science
D-(+)-Glucose	Sigma Life Science
(*N*-2-[hydroxyethyl]piperizine-*N*'-2-[ethanesulfonic acid]) HEPES	Sigma Life Science
Hypoxanthine	Sigma Life Science
Albumax II	Gibco
Gentamicin solution	Sigma Life Science
Sodium bicarbonate	Sigma Life Science
Sodium chloride	Sigma Aldrich
Sodium L-lactate	Sigma Life Science
Potassium chloride	Sigma
Sodium dihydrogen phosphate	Merck
Glycerine (1,2,3 – propantriol)	Sigma Aldrich
D- Sorbitol	Sigma Life Science
Oil for immersion lenses	Merck
Giemsa's azur eosin methylene blue solution	Merck
Phosphate buffered saline (PBS) tablet	Sigma Life Science

Table 2-2: List of materials used for the antiplasmodial assays

Materials for antiplasmodial assays	Supplier
Dimethyl sulfoxide (DMSO)	Merck
Triton X 100	Merck
3-Acetylpyridine adenine dinucleotide (APAD)	Sigma Life Sciences
Calcium L-lactate hydrate	Sigma Life Sciences
Trizma base (Tris)	Sigma Life Sciences
Nitro blue tetrazolium salt (NBT)	Sigma Aldrich
Phenazine ethosulphate	Sigma Aldrich
Hydrochloric acid 32%	Sigma Aldrich
SYBR Green I nucleic acid gel stain (10 000 × in DMSO)	Sigma Aldrich
Ethylenediaminetetraacetic acid (EDTA)	BDH
Saponin	Sigma Life Science

Table 2-3: List of materials used for the detergent mediated assay for β-haematin inhibitors

Materials for detergent mediated assay for β-haematin inhibitors	Supplier
Sodium hydroxide	Sigma Aldrich
Sodium acetate trihydrate	Sigma Aldrich
Acetic acid	Sigma Aldrich
Haemin (> 98%)	Fluka
Acetone	Sigma Aldrich
Pyridine	Sigma Aldrich
Nonidet P-40 (NP-40), 305.5 µM	Pierce Biotechnology

Table 2-4: List of materials used for transmission electron microscopy

Materials for transmission electron microscopy (TEM)	Supplier
Percoll®	Sigma Life Science
Gluteraldehyde (50% in H_2O)	Sigma Aldrich
Osmium tetroxide	SPI CHEM
Agarose (low gelling temperature)	Sigma Aldrich
Ethanol	Merck
Acetone	Saarchem
Spurr's epoxy resin	Agar Scientific
Uranyl acetate	BDH
Lead citrate	Merck
DNase I	Sigma

Table 2-5: A List of materials used for the pyridine haem fractionation study and the suppliers they were purchased from. The empirical formula and Mw are listed for antimalarials.

Materials for pyridine haem fractionation assay	**Supplier**
Chloroquine ($C_{18}H_{26}ClN_3.2H_3PO_4$, Mw = 515.87 g/mol)	Sigma Life Sciences
Pyrimethamine ($C_{12}H_{13}ClN_4$, Mw = 248.71 g/mol)	Fluka Analytical
Sulfadoxine ($C_{12}H_{14}N_4O_4S$, Mw = 310.33 g/mol)	Sigma Aldrich
Amodiaquine ($C_{20}H_{22}ClN_3O.2HCl.2H_2O$, Mw = 464.8 g/mol)	Sigma
Quinine ($C_{20}H_{24}N_2O_2.HCl$, Mw = 369.9 g/mol)	Sigma
Mefloquine ($C_{17}H_{16}F_6N_2O.HCl$, Mw = 414.77 g/mol)	Sigma Life Sciences
Artesunate ($C_{19}H_{28}O_8$, Mw = 384.42 g/mol)	Sigma Life Sciences
Lumefantrine ($C_{30}H_{32}Cl_3NO$, Mw = 528.94 g/mol)	Sigma
Saponin	Sigma Life Science
Magnesium sulphate	Merck
Phosphate buffered saline tablet	Sigma Life Science
Sodium Dodecyl Sulfate (SDS)	Sigma Aldrich
Haematin porcine	Sigma Aldrich
Trucount ™ Tubes	Becton, Dickinson and Company

Table 2-6: A List of materials used for the ferrozine assay and the suppliers they were purchased from.

Materials for ferrozine assay	Supplier
Trichloroacetic acid (TCA)	Fluka
30 % Hydrogen peroxide	Sigma Aldrich
Ascorbic acid	Sigma Aldrich
Ammonium acetate	Saarchem
Ferrozine (disodium salt of 3-(2-pyridyl-5, 6-bis-(4-phenyl-sulphonic acid)-1, 2, 4-triazine)	Sigma Aldrich
Ferrous ammonium sulphate hexahydrate	Hopkin and Williams Ltd.
Neocuproine HCl hydrate	Sigma
Sulphuric acid	KIMIX

Table 2-7: A List of materials used for thin layer chromatography (TLC) of haemin and osmium tetroxide fixed haem and the suppliers they were purchased from.

Materials for thin layer chromatography of haem and osmium tetroxide fixed haem	Supplier
Haemin (from porcine)	Sigma

Table 2-8: A list of materials used for the 24 well plate haem fractionation assay and the supplier they were purchased from. The empirical formula and Mw is listed for antimalarials.

Materials for 24 well plate haem fractionation assay	Supplier
Trucount™ beads	Becton Dickonson
Atovaquone ($C_{22}H_{15}ClO_3$, Mw =366.84 g/mol)	Sigma Aldrich
Quinidine ($C_{20}O_{24}.N_2O_2.HCl.H_2O$ Mw = 378.89 g/mol)	Sigma Aldrich
10-deoxoartemisinin ($C_{15}H_{24}O_4$, Mw = 268.3 g/mol)	*Donated by Dr Liezl Gibhard

*Division of Pharmacology, Department of Medicine, University of Cape Town

2.2 General Instrumentation

The instrumentation detailed below refers to general instrumentation used throughout this study. Instrumentation specific to a technique is described where the instrument was used.

2.2.1 Centrifuge

The centrifugation of suspensions was carried out using an Eppendorf Centrifuge 5810R or 5804 in plastic Greiner Falcon tubes (15 and 50 mL). Suspensions in 24 and 96 well assay plates were centrifuged using an Eppendorf deep well plate attachment (A-2-DWP). A Boeco Microspin12 centrifuge was used for the centrifugation of suspensions corresponding to volumes of 5 ml or less in plastic Eppendorf tubes.

2.2.2 Incubator

A Labcon 508IU incubator maintained at 37 °C was used to store all cultures of *Plasmodium falciparum*.

2.2.3 Light microscope

A Laborlux 12 Leitz Light microscope was used to view thin films of malaria parasites on glass microscope slides to determine the integrity of parasites in culture. A Sigma bright-line hemacytometer (Z353, 962-9) was used to determine cell counts.

2.2.4 pH meter

The pH of all solutions was determined and adjusted to the required working pH value using a bench Jenway 3510 pH meter fitted with a 924 007 glass Jenway

electrode or a Crison MicropH 2000 pH meter and Crison 52 03 glass electrode. Both pH meters were calibrated before use with standard solutions at pH 4.00 ± 0.01 (Buffer, reference standard, Sigma B5020) and 7.00 ± 0.01 (Buffer, reference standard, Sigma B4770) at room temperature of ~ 23 °C. Electrodes were stored immersed in a 3 M KCl solution obtained from Sigma Aldrich.

2.2.5 Sonicator

A Bandelin Sonorex RK100H sonicator was used where required to ensure the dissolution of all prepared samples.

2.2.6 Vortex

A Scientific Industries Vortex Genie2 (G560E) was used where required to ensure all suspensions and solutions prepared were homogenous.

2.2.7 Water bath

A GRANT digital Y6 water bath or a YIH DER BL-710 water bath with the temperature of the water maintained at 37 °C and confirmed with an external thermometer was used throughout this study.

2.2.8 Weighing balance

A four decimal place Adventure™ OHAUS weighing balance or five decimal place Sartorius R200D balance was used to weigh out all materials. The balances were regularly calibrated with mass standards.

2.2.9 UV-vis measurements

All single UV-vis spectra were recorded on a Varian Cary 100 or Shimadzu UV1800 UV-visible spectrophotometer. Measurements were conducted using a 1 cm pathlength Hellma® quartz cuvette. A SpectraMax 340PC, 96-well plate reader was

used to measure the UV-vis absorbance of all 96-well plates using SoftMax Pro software.

2.3 Software

GraphPad Prism version 4 (GraphPad Software Inc.) for windows was used to analyse all data and calculate statistical significance. [203] ChemDraw Professional V15.0.0.0.16 (PerkinElmer) was used to generate chemical structures and figures. All flow cytometry data was analysed using FloJo software version 10 for which Tree Star Inc. donated a one year subscription (Tree Star Inc). The bibliography was created using EndNote X7.4 (Thomson Reuters).

2.4 Sample Preparation

2.4.1 Tissue culture of *Plasmodium falciparum*

Incomplete culture medium

Incomplete culture medium was prepared by dissolving 10.4 g RPMI 1640 (with glutamine but without sodium bicarbonate), 4 g D-(+)-glucose, 6 g HEPES, 0.088 g hypoxanthine, 5 g albumax II, and 1.2 ml (0.05 g/L) gentamicin in 1 L of distilled water. The solution was pre-filtered through a 0.45 µm filter and then sterile filtered through a 0.22 µm membrane into autoclaved glass bottles. The incomplete medium was stored at 4 °C until further use.

Sodium bicarbonate (5%)

The solution was prepared by dissolving 50 g of $NaHCO_3$ in 1 L of distilled water and sterile filtered through a 0.22 µm membrane into 100 ml autoclaved glass bottles. The solution was stored at 4 °C until further use.

Complete culture medium

Complete culture medium was prepared by adding 8.4 ml of 5% $NaHCO_3$ to 200 ml of incomplete culture medium before use. The complete medium was stored at 4 °C until further use.

Wash medium

Wash medium was prepared in the same way as the complete culture medium but without albumax II.

Washed O^+ human red blood cells (RBCs)

The human blood used in the experiments was obtained from the blood bank (Groote Schuur Hospital). The blood was washed by adding wash medium to whole blood in a 1:1 ratio. The solution was centrifuged at 1200 rcf (relative centrifugal force) for 5 min and the supernatant was aspirated. This process was repeated a second time and the washed blood was stored at 4 °C.

Sorbitol (5%)

A solution of 5% D- Sorbitol was prepared by dissolving 50 g of D-sorbitol in 1 L of distilled water. The solution was sterile filtered through a 0.22 µm membrane into 250 ml autoclaved glass bottles and stored at 4 °C until further use.

Sodium chloride (12%)

A 12% solution of sodium chloride was prepared by dissolving 12 g of NaCl in 100 ml of distilled water. The solution was sterile filtered through a 0.22 µm membrane into a 100 ml autoclaved glass bottle and stored at 4 °C until further use.

Sodium chloride (1.8%)

The solution was prepared by dissolving 1.8 g of NaCl in 100 ml of distilled water. The solution was sterile filtered through a 0.22 µm membrane into a 100 ml autoclaved glass bottle and stored at 4°C until further use.

Sodium chloride (0.9%) with glycerine (0.2%)

The solution was prepared by dissolving 0.9 g of NaCl and 0.2 ml glycerine in 100 ml of distilled water. The solution was sterile filtered through a 0.22 µm membrane into a 100 ml autoclaved glass bottle and stored at 4 °C until further use.

Freezing medium

Freezing medium was prepared by dissolving 1.6 g sodium lactate, 30 mg potassium chloride (KCl), 1.38 g sodium dihydrogen phosphate, 57 g glycerine in 100 ml distilled water. The solution was sterile filtered through a 0.22 µm membrane into a 100 ml autoclaved glass bottle and stored at 4 °C until further use.

PBS

PBS was prepared by dissolving 1 tablet in 200 ml of distilled water. The final preparation yielded a solution containing 0.01 M phosphate buffer, 0.0027 M KCl and 0.14 M NaCl with a pH of 7.4 at 25 °C.

Giemsa stain (10%)

Giemsa stain was prepared before use by diluting the stain 1:10 in PBS.

2.4.2 Antiplasmodial assays

Malstat

Malstat was prepared by dissolving 400 µl TritonX100, 4 g L-lactate and 1.32 g Tris buffer in 150 ml of distilled water. To this, 22 mg of APAD was added and the pH adjusted to 9 with 32% HCl. The final volume was made up to 200 ml with distilled water. The solution was stored at 4 °C.

NBT

A solution of NBT was prepared by dissolving 160 mg of NBT and 8 mg phenazine ethosulphate in distilled water to a final volume of 100 ml. The storage container was covered with foil as NBT is light sensitive and stored at 4 °C.

SYBR Green lysis buffer

The lysis buffer was prepared by dissolving 1.6 g of Triton; 0.16 g of saponin; 0.29 g of EDTA and 1.58 g of Tris in 100 ml water. The lysis buffer was stored at 4 °C until required. Immediately before use 2 µl of SYBR Green 10 000 × was added per ml of lysis buffer.

2.4.3 Detergent mediated assay for β-haematin inhibitors

DMSO: NP-40: water / 10: 20: 70 (v/v)

The solution was prepared by mixing 14 ml of water with 4 ml of NP-40 (305.5 µM) and 2 ml of DMSO and used immediately.

NaOH (5 M)

5 M NaOH was prepared by dissolving 40 g of NaOH pellets in 200 ml of water. The solution was stored at room temperature.

Acetate buffer (1 M)

The acetate buffer was prepared by weighing 4.1 g of sodium acetate and dissolving in approximately 40 ml of water. 2.4 ml of acetic acid was added and the solution was diluted to 50 ml with water. The final pH was adjusted to 4.80 with 5 M NaOH.

Haemin stock solution

A 25 mM haemin stock solution was prepared by weighing 16.30 mg of haemin into a 2 ml Eppendorf tube and dissolved in 1 ml of DMSO. The solution was sonicated for 1 min and 178.80 µl was immediately added to 20 ml of 1 M acetate buffer. The solution was vortexed well and used immediately, ensuring the haem remained uniformly suspended in the buffer during use.

HEPES buffer pH 7.5 (2 M)

A solution of 2 M HEPES buffer was prepared by dissolving 47.66 g of HEPES in 80 ml of distilled water. The pH was adjusted to 7.5 with 5 M NaOH before diluting to a final volume of 100 ml with distilled water. The solution was stored at room temperature.

Pyridine solution in HEPES (50% v/v)

Buffered pyridine was prepared by mixing 10 ml of pyridine with 4 ml of acetone, 4 ml of water and 2 ml of 2 M HEPES (pH 7.5).

2.4.4 Transmission electron microscopy

NaOH (1 M)

A solution of 1 M NaOH was prepared by dissolving 40 g of NaOH pellets in 1000 ml of water. The solution was stored at room temperature.

RPMI-1640 (5×) / sorbitol (25%)

A solution of 5 × RPMI-1640 / 25% sorbitol was prepared by dissolving 1.05 g of RPMI-1640 (with glutamine but without $NaHCO_3$) and 5.0 g of D-sorbitol in 15 ml of distilled water. The pH was adjusted to 7.4 using 1 M NaOH and diluted to 20 ml with distilled water. The solution was sterile filtered through a 0.22 µm membrane and stored at 4 °C until further use.

Percoll® (60%)

A 60% solution of Percoll® was prepared by mixing 6 ml of Percoll® with 2 ml of 5 x RPMI-1640 / 25% sorbitol and 2 ml of complete medium. The solution was stored at 4 °C until further use.

Percoll® (90%)

A 90% solution of Percoll® was prepared by mixing 9 ml of Percoll® with 1 ml of 5 x RPMI-1640 / 25% sorbitol. The solution was stored at 4°C until further use.

Glutaraldehyde (5%)

A stock solution of 50% gluteraldehyde was diluted in a 1:10 ratio with distilled water before use.

Glutaraldehyde (2.5%)

A stock solution 50% gluteraldehyde was diluted in a 1:20 ratio with distilled water before use.

Osmium tetroxide (OsO_4)

A 4% solution of OsO_4 was diluted 1:2 in PBS pH 7.5 immediately before use.

Agarose (4%)

The solution was prepared by dissolving 0.1 g of low melting agarose in 2.5 ml of water with gentle heating.

2.4.5 Pyridine haem fractionation assay (flask method)

Reaction buffer

Reaction buffer was prepared by dissolving 0.5 g magnesium sulphate ($MgSO_4.7H_2O$), 7.4 g KCl, 0.58 g NaCl and 6 g HEPES in 1 L of distilled water. The pH was adjusted to 7.5 using 1 M NaOH. The solution was stored at room temperature.

Saponin (1%)

The solution was prepared by dissolving 0.5 g of saponin in 50 ml of reaction buffer. The solution was stored at 4 °C until further use.

HEPES buffer pH 7.5 (0.2 M)

The buffer was prepared by dissolving 4.76 g of HEPES in 80 ml of distilled water. The pH was adjusted to 7.5 with 5 M NaOH before diluting to a final volume of 100 ml with distilled water. The solution was stored at room temperature.

SDS (4%)

The solution was prepared by dissolving 4 g of SDS in 100 ml of distilled water. The solution was stored at room temperature.

NaCl (0.3 M)

The solution was prepared by dissolving 1.75 g of NaCl in 100 ml of distilled water. The solution was stored at room temperature.

Pyridine in HEPES pH 7.5 (25%)

A buffered solution of pyridine was prepared by mixing 25 ml pyridine with 10 ml of 2 M HEPES pH 7.5 and diluting to 100 ml with distilled water.

NaOH (0.3 M)

The solution was prepared by dissolving 1.2 g of NaOH pellets in 100 ml of water. The solution was stored at room temperature.

HCl (0.3 M)

The solution was prepared by diluting 3 ml of 32% HCl up to 100 ml of water. The solution was stored at room temperature in a dark bottle.

Haematin porcine standard

A haem standard curve was prepared from a 100 µg/ml standard solution of haematin (porcine) in 0.3 M NaOH.

5% SDS

The solution was prepared by dissolving 5 g of SDS in 100 ml of distilled water. The solution was stored at room temperature.

2.4.6 Ferrozine assay

Trichloroacetic acid (11.3%)

The solution was prepared by dissolving 11.3 g of trichloroacetic acid (TCA) in 100 ml of distilled water and stored at room temperature.

Ascorbic acid (2%)

The solution was prepared by diluting 2 g of ascorbic acid and 1.67 ml concentrated HCl to a final volume of 100 ml with distilled water. This solution was prepared fresh before use and stored at 4 °C.

Ammonium acetate (10%)

A solution of ammonium acetate was prepared by dissolving 10 g of ammonium acetate in 100 ml of distilled water. The solution was stored at room temperature.

Ferrozine

A ferrozine solution was prepared by dissolving 75 mg of neocuproine HCl hydrate and 75 mg ferrozine in 20 ml of distilled water. One drop of concentrated sulphuric acid was added and the solution was diluted to 25 ml with distilled water.

Ferrous ammonium sulphate standard (Fe standard)

A standard curve for Fe at a starting concentration of 10 µg/ml iron was prepared by accurately weighing 7.023 mg of ferrous ammonium sulphate ($Fe(NH_4)_2(SO_4)_2.6H_2O$). The solution was dissolved to a final volume of 100 ml with distilled water, acidified with 1 drop of concentrated sulphuric acid. This standard was prepared fresh before use.

2.4.7 Thin layer chromatography of haem and osmium tetroxide fixed haem

Haemin (0.5 mg/ml)

A solution of haemin was prepared by dissolving 1 mg of haemin in 2 ml of 0.3 M NaOH. The solution was prepared fresh before use and stored at room temperature.

2.4.8 Haem fractionation assay (24-well plate method)

Glutaraldehyde (0.125%)

A stock solution of 50 % glutaraldehyde was diluted in a 1:400 ratio with 0.22 µm filtered PBS (pH 7.5) before use.

1 × SYBR® green I

This solution was prepared immediately before and used away from direct light. 1 µl of SYBR Green 10 000 × was added per 10 ml of 0.22 µm filtered PBS (pH 7.5).

2.5 Methods

2.5.1 Tissue culture of Plasmodium falciparum

The chloroquine sensitive (CQS) strains of *Plasmodium falciparum* D10 (derived from FQC-27, Papau New Guinea) and NF54 (derived from a patient near Schiphol, Amsterdam presumed to be of West African origin) obtained from the MR4 were used throughout this study.

Thawing of parasites

Parasites were thawed by slowly adding 1 volume of 12% sodium chloride to 5 volumes of thawed parasites with constant mixing. After 5 min 10 ml of 1.8% NaCl was added and centrifuged for 5 min at 400 rcf. The supernatant was removed; 10 ml of 0.9% NaCl with glucose was added and allowed to stand for 5 min. The solution was centrifuged for 5 min at 400 rcf. After removing the supernatant the pellet was placed into culture.

Cryostorage of parasites

Parasites were prepared for cryostorage in the ring phase by slowly adding 5 volumes of freezing medium to 3 volumes of PRBCs and allowed to stand for 5 min. The solution was transferred into cryotubes and frozen overnight at -80 °C before being transferred into liquid nitrogen for long term storage.

Maintaining parasites in continuous culture

CQS strains of *P. falciparum* (D10 or NF54) were cultured using a modified method of Trager and Jensen.[204] Cultures were maintained under sterile conditions in the prepared washed O+ human RBCs in complete medium at 2% haematocrit. Every day, medium with PRBCs was transferred to sterile 50 ml centrifuge tubes and centrifuged at 750 rcf for 5 min. The supernatant was aspirated and the parasitaemia and predominant phase in the remaining PRBC pellet was determined by viewing a Giemsa stained blood smear under a light microscope. Briefly, a thin blood smear on a glass slide from the culture was fixed to the glass with methanol and stained by covering with a thin layer of freshly prepared 10%

Giemsa stain for 10 min. The slide was rinsed with tap water and allowed to dry before viewing with an oil immersion lens under a light microscope. The parasitaemia was determined by counting the number of parasitised erythrocytes as a percentage of the total number of cells (erythrocytes and parasitised erythrocytes) counted. Trophozoite cultures were diluted to 5% parasitaemia with washed O+ human RBCs. Ring cultures were sorbitol synchronised with 5 x volume of 5% sorbitol at 37 °C for ten min as described by Lambros and Vanderberg.[205] Post synchronisation, cultures were centrifuged at 750 rcf for 5 min and the layer of debris corresponding to lysed cells and the associated haemozoin (Hz) was carefully removed from the culture by aspiration. Finally 40 ml of complete culture medium was added to 1 ml of PRBC pellet in a 200 ml flat bottomed culture flask and gassed with a mixture of 3% O_2, 4% CO_2 and N_2 for 1 min and incubated at 37 °C. The cycle was repeated until sufficient material for experiments was obtained.

2.5.2 Antiplasmodial assays

Parasite lactate dehydrogenase assay

In vitro antiplasmodial activity was determined in CQS strains (NF54 or D10) of *P. falciparum* via the parasite lactate dehydrogenase (pLDH) assay using a modified method described by Makler *et al.*, which indirectly colourimetrically measures *Plasmodium* lactate dehydrogenase. [206] Lactate dehydrogenase (LDH) present in both the parasite and erythrocyte catalyses the conversion of lactate to pyruvate during glycolysis, with nicotinamide adenine dinucleotide (NAD) as a co-enzyme (Figure 2-1). The activity of NAD in the parasite is indistinguishable from the erythrocyte; however the NAD analogue, 3-acetyl pyridine dinucleotide (APAD) is selectively and rapidly used by the malaria parasite as a coenzyme instead of NAD during glycolysis and forms APADH. Erythrocyte LDH converts lactate to pyruvate at a much slower rate in the presence of APAD. During assay development, plates are supplemented with Malstat™ reagent containing both APAD and lactate and the yellow NBT reagent. APADH is rapidly formed by viable parasites as the reaction proceeds and reduces yellow NBT to its purple formazan salt. The formation of this purple formazan product is measured at 620nm and corresponds to parasite viability.

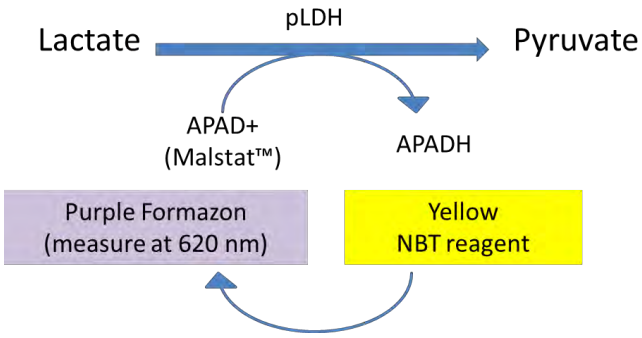

Figure 2-1: The conversion of lactate to pyruvate in the presence of the coenzyme APAD (Malstat™) in the malaria parasite. As APADH is formed yellow NBT is reduced to purple formazan.

The assay was carried out by preparing 2 mg/ml solutions of test samples in 100% DMSO and storing at -20 °C. On the day of use, samples were diluted in medium to a starting concentration of 1000 ng/ml or 100 ng/ml and serially diluted two-fold in medium in 96-well plates. All samples were tested in triplicate at ten concentrations, with the lowest concentration being 0.2 ng/ml. The blank column contained unparasitised erythrocytes at 1% haematocrit. The positive control and the drug testing wells all contained PRBCs at 2% parasitaemia and 1% haematocrit. The plates were covered with a sterile lid and gassed in an airtight chamber with a mixture of 3% O_2, 4% CO_2 and N_2 for 4 min and incubated at 37 °C for 48 h. The highest concentration of DMSO to which the parasites were exposed was 0.5%. Post incubation the plate was frozen at -20 °C. The plate was thawed when required and developed by adding 100 µl of Malstat and 25 µl of NBT to 15 µl of the resuspended PRBC pellet. The absorbance of each well on the plate was measured at 620 nm using a Modulus™ Microplate Multimode Reader (Turner Biosystems). IC_{50} values were obtained using a non-linear dose-response curve fitting analysis via Graph Pad Prism v.4.0 software. [203]

SYBR Green I assay

In vitro antiplasmodial activity was also determined using a modified method of the fluorescent SYBR green assay by Johnson et al. [207] SYBR green I is a nucleic acid intercalating fluorescent dye with preferential binding affinity for double stranded DNA over single stranded DNA or RNA. As mature erythrocytes lack RNA or DNA, i*n vitro* parasite growth is measured as a result of the binding and consequent

fluorescence of SYBR Green to malarial DNA after 72 h of incubation in the presence of an antimalarial agent. The test samples and plates were prepared as described above in section 2.5.2 for the pLDH assay; however the assay was started in ring phase of the lifecycle and incubated at 37 °C for 72 h rather than 48 h. Post incubation the plate was frozen at -20 °C. The plate was thawed when required and developed by transferring 50 µl of resuspended PRBCs to the corresponding wells of a flat bottomed black 96-well plate. To each well, 50 µl of the SYBR Green lysis buffer mix was added and the plate incubated at 37 °C for 2 h. The blue fluorescence in each well was measured using the Modulus™ Microplate Multimode Reader (Turner Biosystems). IC_{50} values were obtained using a non-linear dose-response curve fitting analysis via Graph Pad Prism v.4.0 software. [203]

2.5.3 Detergent mediated β-haematin inhibition assay

The inhibition of the Hz formation pathway, where toxic soluble haem is converted to non-toxic insoluble Hz crystals remains an efficient, favourable drug target and several antimalarials including the quinolines CQ and AQ have been shown to inhibit the formation of βH.[66 69 208 105] The formation of Hz has been shown to be closely associated with neutral lipids in the digestive vacuole of the parasite and Hz associated neutral lipids have been shown to mediate βH formation under physiological conditions at rates analogous to parasite Hz formation. [75 76 107] This process of cellular lipid mediated Hz formation is mimicked synthetically under physiological conditions in a robust detergent mediated assay which substitutes neutral lipids for the low cost, commercially available lipophilic detergent NP-40. [102] Under these assay conditions the efficiency of a compound to inhibit the formation of βH is evaluated. Unreacted haematin is quantified based on the pyridine hemochrome inhibition (Phiβ) method developed by Ncokazi and Egan, where pyridine under neutral or mildly basic conditions complexes with only free haematin in the presence of βH and is quantified as a pyridine-haematin complex at 405 nm. [101] This technique has been applied as a high throughput screening tool and has successfully identified several novel scaffolds capable of inhibiting Hz formation. [105 103] The assay is carried out by preparing stock solutions of the test compounds at known concentration in the range of 5 mM to 20 mM by dissolving accurately weighed amounts in DMSO on the day of use. The test compounds were

transferred to a 96 well plate and serially diluted in a solution of 10% DMSO / 20% NP-40 / 70% water to a final volume of 100 µl. All samples were tested in triplicate at 11 concentrations. The blank column contained no drug. A freshly prepared homogenous suspension of haematin in 1 M acetate buffer pH 4.8 was added to all wells, including the blank column, such that the final concentration of haematin in all wells was 100 µM. The plate was covered and incubated at 37 °C in a water bath for 5 - 6 h. Post incubation, a solution of 50 % pyridine (50% pyridine; 20% water; 20% acetone and 10% 2 M HEPES pH 7.5) was added to all wells such that the final concentration of pyridine per well was approximately 5%. Finally, acetone was added to aid in the dispersion of the haematin. Analysis of the plate was carried out at 405 nm using a SpectraMax plate reader after 5 s of shaking. The 50% βH inhibitory concentration for each test compound was obtained from the blank corrected absorbance values at 405 nm using a sigmoidal dose-response curve fitting analysis via Graph Pad Prism v.4.0 software.[203]

2.5.4 Transmission electron microscopy

TEM with electron energy loss spectroscopy (EELS) by electron spectroscopic imaging (ESI) for Fe was performed using a modification of the method previously described by Egan et al .[30]

Enrichment and gluteraldehyde fixing

Ring stage sorbitol synchronized parasitised red blood cells at 5% parasitemia and 2% haematocrit were inoculated with a known concentration of test compounds and incubated for 24 h at 37 °C. After the incubation period the trophozoite culture was centrifuged at 750 rcf for 5 min and the supernatant removed by aspiration. The remaining PRBC pellet was enriched by Percoll® density gradient centrifugation using a modified version of the method by Ginsburg et al.[86] Briefly, 500 µl of 60% Percoll® was carefully layered on top of 500 µl of 90% Percoll® in a 1.5 ml Eppendorf tube. 300 µl of the PRBC pellet was layered on top of the 90% Percoll®. Samples were centrifuged at 10 000 rpm (revolutions per minute) for 20 min. Post centrifugation the trophozoite infected erythrocytes were seen as a band between the 60% and 90% Percoll® layers and transferred into a 15 ml centrifuge tube. The parasitised erythrocytes were incubated with 10 ml of

complete medium for 10 min at 37 °C then centrifuged at 1200 rpm for 3 min and the supernatant discarded. A 10% Giemsa stained slide was made to confirm the presence of an enriched PRBC pellet (Fig. 2-2). The pellet was then washed twice with 5 ml of medium. Fixation was carried out by resuspending the enriched pellet in an equal volume of 5% glutaraldehyde in PBS pH 7.4 for 10 min at room temperature. Following a wash with 1 ml of PBS (centrifuged at 3000 rpm for 45 s), the cells were re-suspended in 1 ml 2.5% of glutaraldehyde in PBS and left at 4 °C overnight for further fixation.

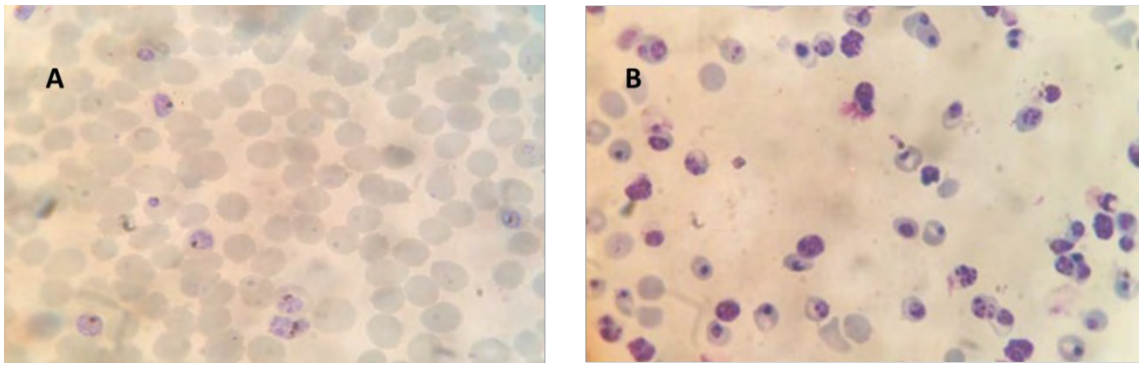

Figure 2-2: Giemsa stained, microscopic images (100× objectification) of trophozoite infected red blood cells before (A) and after Percoll® enrichment (B).

Sample dehydration, resin fixing and trimming

Two washes with 1 ml of PBS were performed before the samples were post-fixed with 1% OsO_4 in PBS for 1 h, washed once with PBS and three times with distilled water and stained with 1% uranyl acetate. Following a further two washes with distilled water samples were suspended in a 1:1 ratio in freshly prepared 4% agarose and allowed to solidify. Samples were then cut into 1 mm cubes under water and dehydrated with aqueous ethanol (30%, 50%, 60%, 70%, 80%, 90%, 95% for 5 min each, 2 × 100% ethanol for 10 min each) and twice with acetone for 10 min each. Acetone was gradually replaced with Spurr's epoxy resin over two days in 2 h incubation periods with 25:75, 50:50 and 75:25. The final infiltration in 100% resin took place overnight. The blocks were transferred into fresh resin, tumbled for the day and allowed to harden for 16 h at 60 °C. Blocks were trimmed and cut into ultrathin sections, suitable for TEM imaging with a Reichert Ultracut S ultratome using diamond knives. Sections were picked up on 200 mesh square copper grids stained with 1% uranyl acetate followed by 1% lead citrate in a

closed container containing NaOH for 10 min each with 5 distilled water washes in between each stain. Samples which underwent ESI for Fe were not subjected to the previous staining procedure.

Extraction of Hz crystals

Hz crystals were extracted from isolated trophozoites as previously.[209] Trophozoites were released from PRBCs by saponin lysis. PRBCs were incubated in 1% saponin for 2 min, followed by centrifugation at 1500 rpm for 10 min. The supernatant was discarded and the pellet washed three times with PBS. A final wash was performed with reaction buffer and the pellet was resuspened in deionised water acidified to pH 4.6. This suspension was triturated ten times with a 26.5 gauge needle to break open the trophozoites, releasing the trophozoite cytosol and DVs into solution. The solution was centrifuged at 1300 rpm for one minute and the supernatant was discarded. The pellet was resuspended in reaction buffer to final volume of 1 ml and 10 µL of DNase I was added to digest any DNA released from the trophozoite cytosol. The solution was incubated for 5 min at 37 °C, followed by centrifugation at 1300 rpm for 1 min. The supernatant was discarded and the pellet washed three times with reaction buffer. The isolated DVs were resuspended in deionised water and frozen at -80 °C. The pellet was thawed to release the Hz from the DV by freeze thaw lysis. The mixture was centrifuged at 1300 rpm for 1 min and the supernatant discarded. Freeze thaw lysis was repeated a minimum of three times to ensure complete lysis of all the DVs. Solutions containing Hz crystals were placed on a glow discharged carbon coated grid and blotted with filter paper to remove excess solution. Crystals were stained with 1% uranyl acetate for 10 min with five distilled water washes in between each stain.

Performing TEM with EELS

TEM has far superior resolving capacity than a light microscope capturing features as small as a tenth of a nanometer. Used in conjunction with EELS with ESI for Fe, the location and distribution of Fe within treated and untreated *P. falciparum* infected cells and also the association of Fe with any identifiable cellular organelles was determined. All measurements were performed using a LEO 912 OMEGA or Tecnai 20 transmission electron microscope for images collected in Chapter 3 and 6 respectively. Images were collected using a slit width of 18 eV on a Tiedtz

charge-coupled-device camera (1024 × 1024 pixels) and processed with analySIS software from Soft Imaging System using a two window difference method to obtain the element-distribution image. Two images were recorded at energies before the Fe L_3 absorption edge, namely at 658 eV and 688 eV respectively and the third was centred around 718 eV. The background image was then predicted by extrapolating the two images collected at 658 eV and 688 eV and then subtracted from the image collected around 718 eV resulting in an elemental map with intensity values proportional to the amount of iron in a particular section.

3 MEASURING HAEMOZOIN FORMATION IN *PLASMODIUM FALCIPARUM* IN THE PRESENCE OF ANTIMALARIALS

3.1 Introduction

As discussed in Chapter 1, in the trophozoite, during the asexual stage of the parasite lifecycle up to 65% of the host RBC Hb is ingested by the parasite and transferred to the acidic DV where it is degraded by a series of proteases. [36 38 29] In the DV, toxic haem derived from Hb digestion is sequestered into innocuous Hz crystals in a parasite-specific pathway essential for survival of the parasite. [24]

A study by Ginsberg et al published in 1998 suggested that only 30% of Hb derived haem is converted into Hz and the majority exits the food vacuole where it is degraded by glutathione. This glutathione driven haem degradation was competitively inhibited by the presence of CQ and AQ outside of parasites and increased resistance to CQ was achieved by increasing cellular levels of glutathione. The study confirmed a relationship between membrane haem levels and the extent of parasite killing in *P. falciparum* infected erythrocytes, showing an increase in toxic membrane associated haem in a time and dose dependent manner in the presence of both CQ and AQ. [86] In contrast, a later study of the chemical analysis of elemental Fe in isolated D10 trophozoites and DVs showed the majority of Fe present in trophozoites was located in the DV (92±6%). Further analysis of Hz isolated from DVs showed that 88±9% of the Fe in the DV corresponds to inert Hz. This finding was confirmed by ^{57}Fe-Mössbauer spectroscopy performed on freeze-dried isolated trophozoites which revealed that more than 95% of the Fe in trophozoites was present as Hz, with the spectra of the freeze dried trophozoites being identical to that of synthetic βH with the exception of larger background scatter in the biological sample. It therefore follows that the majority of Fe located in the DV of the trophozoite is present as Hz. [30] The Hz formation pathway unquestionably represents a vital process in the lifecycle of the malaria parasite and as such the inhibition of this pathway presents a point of susceptibility exploited as a drug target by several clinically relevant antimalarials, including CQ. As discussed in Chapter 1, CQ for many years was considered the gold standard in antimalarial treatment and it is a well-accepted theory that CQ acts by inhibiting the formation of Hz.[72 210] Despite being widely accepted, the theory that CQ and related quinoline antimalarials inhibit Hz formation within the DV has never been

demonstrated in the cell, while the inhibition of the synthetic counterpart of Hz, βH, has been demonstrated many times in cell-free systems. [105 184 211 212 69]

This chapter describes a cellular fractionation assay developed to measure haem species in isolated *P. falciparum* trophozoites. In an attempt to determine the effects of CQ in the parasite, all major haem species were determined in trophozoites isolated from cultures of *P. falciparum* incubated with increasing doses of CQ. The quantification of haem in each fraction was based on the ability of neutral aqueous pyridine to selectively form a low spin Fe(III)haem-pyridine complex with haem in the presence of Hz.[101] This cellular fractionation technique was extended to several well-known antimalarials; ART, AQ, LF, MQ, QN and a sulfadoxine-pyrimethamine (SP) combination at a single concentration corresponding to 2.5 × their IC_{50} as a measurement of their ability to inhibit Hz. With the exception of the antifolate combination of SP, it has been proposed that all other compounds are able to interfere with the formation of βH.[69 106 178 98 110 213]

In the case of LF, the package inserts of several AMN-LF combination tablets indicate that the mechanism of action of LF is through βH inhibition. [214 215] The claim is controversial for ART. Haynes et al in 2003 showed that the AMNs do not inhibit βH.[110] However several studies have implicated the AMNs in βH inhibition, proposing that AMN's inhibit Hz formation and kill through the consequent build-up of toxic haem.[179 178]

In the case of CQ, the findings of the haem fractionation assay was enhanced by TEM with ESI using EELS for Fe on CQ treated parasitised erythrocytes used to demonstrate the differences in the distribution of cellular haem in CQ treated and untreated *P. falciparum* parasites. Previously, TEM with ESI using EELS for Fe performed on untreated trophozoite infected erythrocytes showed the presence of Fe was localised to Hz crystals within the DV, while the rest of the trophozoite was devoid of Fe levels higher than those seen in the erythrocyte.[30] Subsequent studies have shown that CQ disrupts Hz crystal growth, altering Hz crystal morphology resulting in the formation of less uniform crystals in the parasite.[107 209]

The haem fractionation assay described in this chapter provides an approach to determine parasite Hz inhibition in the presence of antimalarials and hence the determination of mechanisms of action of both current and novel antimalarials. The method is especially relevant in light of recent screening studies of substantial compound libraries which yielded several effective potential therapies effective at

the blood stage of *P. falciparum.*[216] The target of several of these drugs could very likely be the Hz formation pathway, and perhaps one of these candidates will be capable of emulating the success demonstrated by CQ during the mid-1900's.[217]

3.2 Materials

All materials used throughout this chapter are listed in chapter 2. Materials were of AR grade or higher and used without further purification.

3.3 Sample Preparation

The preparation of all samples used throughout this chapter is described in Chapter 2. The water used throughout this work was double distilled deionised Millipore® Direct-Q water.

3.4 Methods

3.4.1 Pyridine-Haem fractionation assay

The pyridine-haem fractionation assay described here was based on the method developed by Ncokazi and Egan used to determine the cell free ability of a compound to inhibit βH formation. [101] The method, abbreviated from here onwards as the Phiβ (pyridine hemichrome inhibition of β-haematin) is based on the pyridine hemochrome method published by Partos in 1922, where haem was quantified as a haem pyridine complex.[100] Haematin dissolved in aqueous medium forms aggregates and as a result displays a relatively weak, broad Soret peak, with a maximum absorbance at 389 nm. In contrast the spectrum of the pyridine-haematin (Fe(III)PPIX) complex exhibits a sharper more intense peak, shifting 15 nm to an absorption maximum of 404 nm indicative of the monomeric low-spin state of the Fe(III)PPIX and well separated from haem aggregates. This pyridine-

Fe(III)PPIX complex obeys Beers law, a valuable feature, as it makes quantification of haem species possible with this method. The increased peak intensity enhances the sensitivity of the assay in comparison to the use of the absorbance of aqueous Fe(III)PPIX and ensures linear proportionality of absorbance to concentration. To maintain direct proportionality between absorbance and concentration, it was found that the pyridine solution must be buffered to pH 7.5 for optimal formation of pyridine co-ordinated to the Fe(III) porphyrin center. Under basic conditions, in the presence of aqueous pyridine it has been shown that the μ-oxo dimer of Fe(III)PPIX is induced by pyridine.[218] Additionally, it was determined that neutral or very mildly basic solutions of 5 - 10% (v/v) pyridine do not react with βH but are still able to dissolve and form complexes with haematin. In mixtures of haematin and βH, the absorbance at 405 nm upon addition of a fixed volume of neutral aqueous pyridine (5% v/v, pH 7.5) increased linearly with increasing amount of haematin. The method can therefore be used to selectively quantify haematin in mixtures of both βH and haematin as a complex with pyridine. [101]

Here the method was applied to parasite haem, measuring the ability of a compound to inhibit Hz formation in *P. falciparum* cells. All major haem species; Hb, free haem and Hz in isolated *P. falciparum* trophozoites isolated through a series of fractionation steps were determined spectrophotometrically as a low-spin complex with aqueous pyridine at neutral pH (5% v/v, pH 7.5) (Figure 3-1).[107] "Free" haem was defined as haem in the parasite material which can be solubilised by 2% SDS and 5% (v/v, pH 7.5) pyridine and is most likely membrane or lipid associated haem or weakly and non-specifically associated with SDS solubilisable proteins. All spectra were recorded on a Varian Cary 100 UV-vs spetrophotometer.

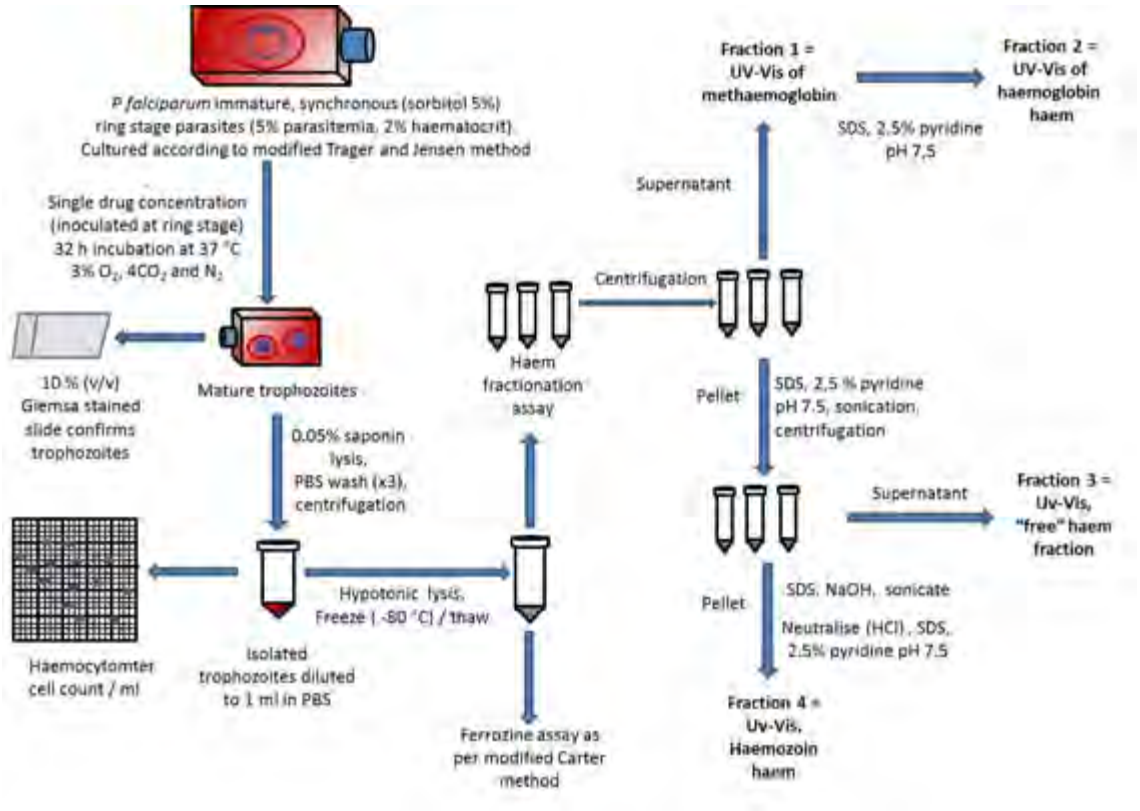

Figure 3-1: A schematic representation of the haem-pyridine fraction assay. A CQS strain of *P. falciparum* was cultured according to a modification of the Trager and Jensen method.[204] Immature ring stage PRBCs were inoculated with several different increasing drug concentrations. After 32 h, mature trophozoites were harvested via saponin lysis of erythrocytes and taken through a series of fractionation steps. Following hypotonic lysis and centrifugation, Hb was measured in the first fraction. The second fraction corresponds to SDS treated soluble Hb measured in the supernatant as a low spin haem-pyridine complex. The pellet was further treated with SDS and pyridine to solubilise "free" haem in the third fraction, measured in the supernatant following centrifugation. The fourth fraction corresponds to Hz, measured after solubilising the pellet in NaOH, neutralising with HCl and treating with pyridine.[107]

Incubation

The phase of highly synchronous ring stage cultures was confirmed by viewing 10% (v/v) Giemsa stained blood smears under a light microscope with an oil immersion lens at 100x magnification. The parasitemia of rings was determined by counting a minimum of 1000 cells and the percentage of ring stage infected cells in the total number of counted cells was calculated. The ring culture was diluted to

5% parasitemia with washed O+ human RBCs and 2% haematocrit with complete medium to a final volume of 50 ml in a 200 ml flat bottomed culture flask. Each prepared flask was inoculated with a specific multiple of the test compounds IC_{50}. No more than 100 µl of the drug stock solution diluted in DMSO was added to each flask, such that the final concentration of DMSO in the flask was less than 0.5% (v/v). No drug was added to the control flask. The flask was gassed with a mixture of 3% O_2, 4% CO_2 and N_2 for 1 min and incubated at 37 °C for 32 h.

Harvesting and isolation of trophozoites

After 32 h of incubation at 37 °C, flasks were removed from the incubator and the contents transferred to 50 ml centrifuge tubes. The cultures were centrifuged at 750 rcf for 5 min and the supernatant as well as any cell debris and associated Hz corresponding to a black layer on top of the PRBC pellet was discarded. A 10% (v/v) Giemsa stained blood smear of each culture was viewed under a light microscope with an oil immersion lens to confirm the presence of trophozoites. Trophozoites were isolated by saponin lysis by adding 46 ml of PBS and 2.5 ml of 1% saponin to a 1 ml pellet of parasitised erythrocytes. The solution was mixed well and left to stand for 2 min at 37 °C, followed by centrifugation at 1500 rcf for 10 min. The supernatant was discarded and the pellet washed 3× with 10 ml of PBS to remove all traces of Hb. In between each wash, the supernatant, cell debris and associated Hz corresponding to a black layer on top of the PRBC pellet was discarded The trophozoite pellet was diluted to a final volume of 1 ml with PBS and mixed well using a vortex. A 1:40 dilution of the trophozoite suspension in PBS was prepared and used to obtain a final cell count/ml using a haemocytometer. The remaining solution was frozen overnight at -80 °C.

Cell counting on a haemocytometer

The number of cells/ml was determined by loading 10 µl of cells from the well mixed 1:40 trophozoite dilution prepared above onto a bright-line haemocytometer and 5 large squares were counted after 10 min of settling. The concentration of cells in each well of the plate was determined using equation 3-1:

$$CH = N \times F \times DF \times 10{,}000 \qquad (3\text{-}1)$$

Where: *CH* = concentration of cells per ml as determined with haemocytometer

N = number of cells counted in five fields

F = number of fields counted = 5

DF = dilution factor = 40

Pyridine-haem fractionation assay

The trophozoite suspension was thawed and 200 µl aliquots dispensed in triplicate into Eppendorf tubes, including a blank of 200 µl PBS. The remaining 400 µl sample was reserved for the determination of total Fe by means of the ferrozine assay described in section 3.4.2. To each aliquot, 100 µl of water was added and sonicated for 5 min. This was followed by 100 µl 0.2 M HEPES buffer pH 7.5 and 100 µl water and the sample was then centrifuged in a minifuge (14000 rpm) for 3 min. The spectrum of the supernatant (fraction 1, Figure 3-1) was recorded from 330 to 800 nm and corresponds to the spectrum of methaemoglobin (Figure 3-2).

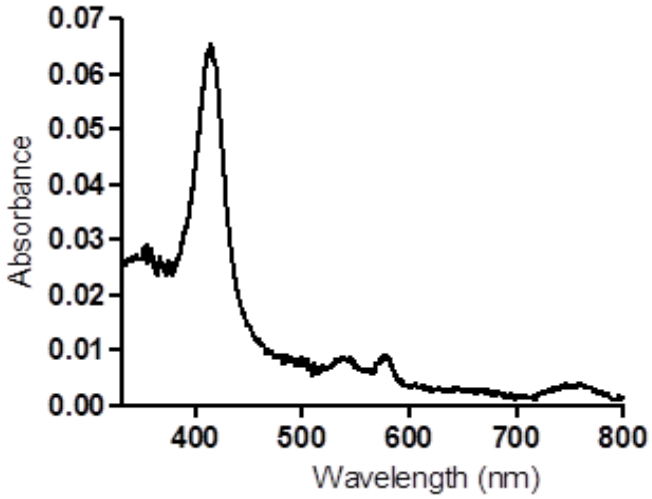

Figure 3-2: Absorption spectrum for fraction 1, corresponding to methaemoglobin (fraction1).

The supernatant was retained for further processing by adding 100 µl 4% SDS, sonicating for 5 min and then incubating at room temperature for 30 min. Finally, 100 µl of 0.3 M NaCl and 100 µl of 25% pyridine (v/v) were added and the solution was diluted to volume in a 1 ml volumetric flask. The spectrum of the resulting Fe(III)haem-pyridine complex (fraction 2, Figure 3-1) was recorded from 330 to 800 nm and used to determine the fraction of haem present as Hb (spectrum not shown).

The pellet was further treated by adding 100 µl of water, followed by 100 µl of 4% SDS. After vortexing well, the solution was sonicated for 5 min and incubated for 30 min at room temperature. To this, 100 µl 0.2 M HEPES pH 7.5, 100 µl 0.3 M NaCl and 100 µl 25% pyridine were added and centrifuged for 5 min. The supernatant was transferred to a 1 ml volumetric flask and diluted to volume with water. The spectrum (fraction 3, Figure 3-1) which is characteristic of the Fe(III)haem-pyridine complex was recorded from 330 to 800 nm to determine the fraction of "free" haem (Figure 3-3).

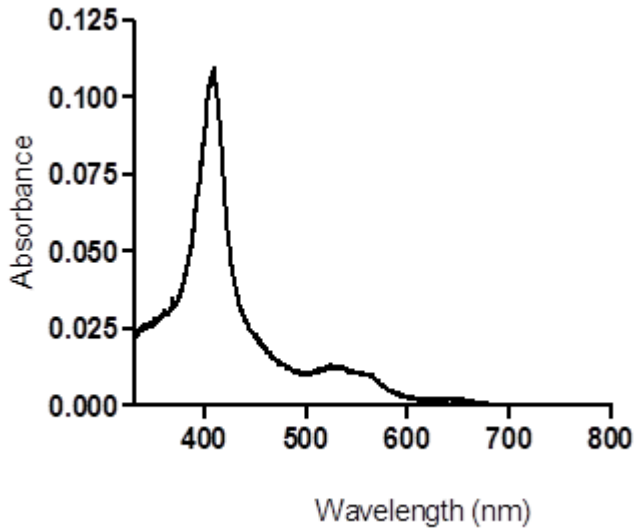

Figure 3-3: Absorption spectrum of the "free" haem-pyridine complex (fraction 3).

The absorbance of the resulting pyridine-Fe(III)PPIX complex at the Soret band of the spectrum shown in Figure 3-3 was recorded at 405 nm. The remaining pellet was treated with 100 µl of water and 100 µl of 0.3 M NaOH. The solution was vortexed well, sonicated for 60 min and incubated for 30 min at room temperature. To the supernatant, 100 µl 0.2 M HEPES pH 7.5, 100 µl 0.3 M HCl and 100 µl 25% pyridine were added and diluted to volume in a 1 ml volumetric flask. The spectrum (fraction 4, Figure 3-1) was recorded from 330 to 800 nm for the determination of the Hz fraction (Figure 3-4). Where required, solutions of fraction 4 were diluted with diluent (1 ml 4% SDS, 1 ml NaCl, 1 ml HEPES and 1 ml 25% pyridine diluted to volume with water in a 10 ml volumetric flask).

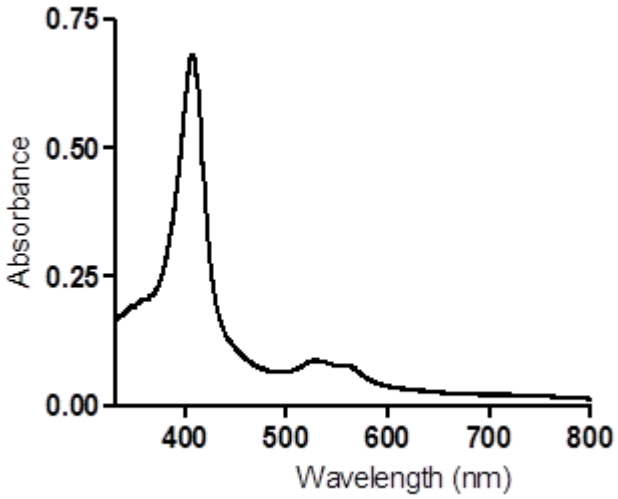

Figure 3-4: Absorption spectrum of Fe(III)haem-pyridine complex for Hz (fraction 4, diluted 3× in diluent).

The percentages of Hb (fraction 2, Figure 3-1), "free" haem (fraction 3, Figure 3-1) and Hz (fraction 4, Figure 3-1) for each sample were calculated from the maximum absorbance reading for each species as follows:

A_{max} for Fe(III)haem-pyridine (fraction 2) = A_{Hb}

A_{max} for Fe(III)haem-pyridine (fraction 3) = $A_{"free" haem}$

$D \times A_{max}$ for Fe(III)haem-pyridine (fraction 4) = A_{Hz} (D = dilution factor, Hz)

$A_{Total} = A_{Hb} + A_{"free" haem} + A_{Hz}$

% Hb = $(A_{Hb}/ A_{Total}) \times 100$

% "free" haem = $(A_{'free" haem}/ A_{Total}) \times 100$

% Hz = $(A_{Hz}/ A_{Total}) \times 100$

Haem standard curve

The total haem in each sample was quantified by constructing a haem standard curve from a 100 µg/ml haem standard solution of haematin (porcine) in 0.3 M NaOH. Dilutions of the standard were carried out in Eppendorf tubes to a final volume of 200 µl in triplicate and 200 µl of 0.15 M NaOH was used as a blank. To the blank and each of the standards, 100 µl of the following solutions were added: 0.2 M HEPES pH 7.5, 4% (w/v) SDS, 0.3 M NaCl, 0.3 M HCl, 25% pyridine in 0.2 M HEPES pH 7.5 and diluted to 1 ml with distilled water. The visible spectra of

haematin as a Fe(III)haem-pyridine complex was recorded. The amount of haem Fe per cell was calculated by dividing the total haem Fe in each fraction by the number of cells determined in each fraction. A representative standard curve of absorbance versus concentration of haematin is shown below in Figure 3-5. The molar extinction coefficient calculated for the assay from a representative calibration curve (Figure 3-5) was determined to be 86480 ± 667 M^{-1} cm^{-1}, similar to the value of 90 800 M^{-1} cm^{-1} determined for haem at 404 nm by Asakura et al. [219]

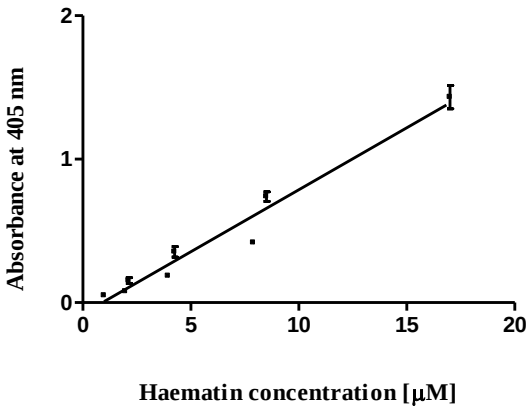

Figure 3-5: Calibration curve of absorbance at 405 nm vs haematin (µM) of the pyridine-Fe(III)PPIX complex. The molar extinction co-efficient was calculated from the slope of the graph to be 86480 ± 667 M^{-1} cm^{-1}. The data represents the mean ± SD of three separate experiments. The linear portion of the graph is shown for which the correlation coefficient, R^2 = 0.962. The graph was plotted using GraphPad Prism 4.0 linear regression function.

3.4.2 Ferrozine Assay for Total Fe

Fixed volumes of isolated trophozoites were assayed for total Fe using a modification of the ferrozine assay by Carter which colourimetrically measures the formation of a ferrozine-Fe(II) complex at 562 nm.[220 221] All glassware used in this assay was washed with 1% nitric acid before use to remove all traces of metals. A 100 µl aliquot of the trophozoite suspension harvested and isolated in section 3.4.1 was accurately diluted to 1 ml with distilled water. Samples were digested using a combination of 250 µl 5% SDS, 100 µl 11.4% TCA and 200 µl 30% H_2O_2, followed

by sonicating. Samples were centrifuged for 5 min in a minifuge (14000 rpm) and 1 ml of the supernatant was transferred into a labelled test tube. To the supernatant, 1 ml of 2% ascorbic acid was added and the samples were incubated for 5 min at room temperature. Post incubation, 800 µl of ammonium acetate and 200 µl of the ferrozine colour reagent were added. The absorbance of each sample was read at 562 nm in a 1 cm quartz cuvette. A blank consisting of 1 ml of distilled water and a series of Fe standards prepared from a stock solution of ferrous ammonium sulphate corresponding to 10 µg/ml of Fe was run alongside the samples according to the method described above. The molar extinction coefficient calculated for the assay from a representative calibration curve shown below in figure 3-6 was determined to be 27247±690 M^{-1} cm^{-1}, which agrees well with the original value of 28000 M^{-1} cm^{-1} quoted by Carter et al. [220] The total Fe present in each cell was calculated by dividing the value obtained for total Fe by the number of cells in each sample as determined by the haemocytometer count in section 3.4.3.3. The fraction of Fe present as haem was calculated by dividing the value obtained for total haem in section 3.4.1 by the total Fe value and converting to a percentage.

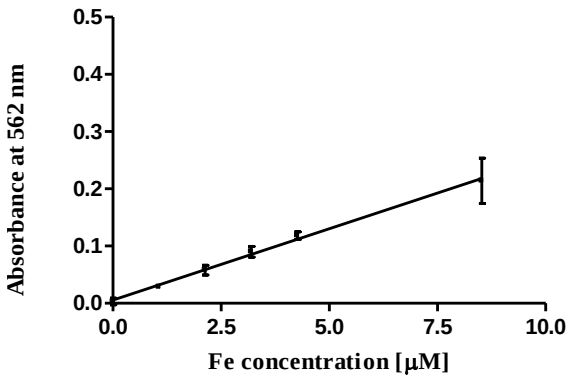

Figure 3-6: Calibration curve of absorbance at 562 nm vs Fe concentration (as the Fe^{+2}-ferrozine complex). The molar extinction co-efficient was calculated from the slope of the graph to be 27247±690 M^{-1} cm^{-1}. The data represents the mean ± SD of four separate experiments. The linear portion of the graph is shown for which the correlation coefficient R^2 = 0.997. The graph was plotted using GraphPad Prism 4.0 linear regression function.

3.4.3 Thin layer chromatography (TLC) of haem and osmium tetroxide fixed haem

A mixture of 0.5 mg/ml haemin (Cl-Fe(III)protoporphyrin IX) and OsO_4, (100 × molar excess) was tumbled for a minimum of 1 h before spotting on a silica gel TLC plate alongside a solution of untreated haemin (0.5 mg/ml). After thorough drying of the spots, the plate was run in a series of solvents mimicking the dehydration procedure used when samples are prepared for TEM: 30% EtOH, 50% EtOH, 70% EOH, 90% EtOH, 100% EtOH and 100% acetone. The retention factor (Rf) values for untreated haemin and OsO_4 treated haemin were calculated in each solvent system.

3.5 Results and Discussion

3.5.1 Determination of the parasitic growth inhibition IC_{50} in *P. falciparum*

The biological IC_{50} of several clinically relevant antimalarials was determined in a CQS strain of *P. falciparum*, D10 using a modification of the method previously published by Makler et al. [206] In the case of PYR the biological IC_{50} was determined using a modification of the SYBR Green assay with a 72 h incubation time. [207] Both methods are described in detail in Chapter 2. The IC_{50} values obtained are summarised below in Table 3-1.

Table 3-1: The IC_{50} values (nM) of several clinically relevant antimalarials in the CQS strain D10 determined using the pLDH assay or in the case of PYR and S, a modification of the SYBR Green assay.[206 207]

Compounds tested	Mean IC_{50} value (nM)	Range at 95% CI (nM)
Chloroquine	15	11 - 25 (n=8)
Amodiaquine	16	14 - 19 (n=8)
Quinine	142	90 - 226 (n=6)
Mefloquine	24	12 - 47 (n=8)
Lumefantrine	27.1	23.6 – 31.0 (n=8)
Artesunate	7.6	5.75 – 9.35 (n=3)
Pyrimethamine	50	14 - 60 (n=4)
Sulfadoxine	ND	ND

ND = not detected.

The parasite survival curves were generated using GraphPad Prism 4.0 non-linear regression function (sigmoidal dose response equation) as shown in Figure 3-7 for AQ in red and PYR in blue.

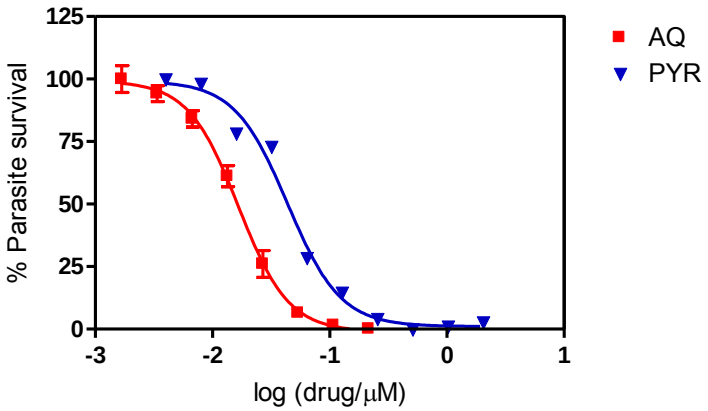

Figure 3-7: Representative graphs of parasite survival curves of the 4-aminoquinoline AQ (red) and the antifolate PYR (blue) in D10 determined using a modification of the parasite lactate dehydrogenase assay previously published by Makler et al and a modification of the SYBR Green assay with a 72 h incubation time respectively.[206 207] The curve was generated using GraphPad Prism 4.0 non-linear regression function (sigmoidal dose response equation).

The measured IC_{50} values summarised in Table 3-1 were used to determine the concentrations at which cultures used for the haem fractionation assay would be inoculated. PYR and S were included as negative controls to be used in the subsequent haem fractionation assay as both have no known effect on the formation of βH.[105] Both drugs share a similar mechanism of action, known to interfere with folate synthesis and both are potent inhibitors of *P. falciparum*. The sulfonamide, S is an analog of p-aminobenzoic acid (PABA) required for the *de novo* synthesis of folate and PYR inhibits dihydrofolate reductase (DHFR), the enzyme responsible for converting dihydrofolate to tetrahydrofolate cofactor. [194] [195]. The antimalarial activities of these drugs have previously been shown to be diminished in the presence of folic acid and PABA in the routinely used culture medium and the determination of an accurate biological activity should ideally be tested in culture medium with reduced concentrations of PABA, folate and hypoxanthine. [194] [222] Normal RPMI used in the culture medium preparation throughout this thesis contains 1 mg/L each PABA and folic acid, a concentration 100 fold greater than the physiological concentration of folic acid. [195] Wein et al, showed that the IC_{50} values for PYR measured using RPMI with low concentrations of PABA and folate were approximately 6 fold lower than when measured in normal RPMI. In addition it was shown that a longer incubation of 72 h, as used in the SYBR green assay was required in the case of both normal RPMI and RPMI with low PABA and folate concentrations to obtain reliable, reproducible results in agreement with microscopically determined biological IC_{50} values of Giemsa stained parasites. [222] The IC_{50} of PYR was therefore determined using the SYBR green assay with a 72 h incubation period and normal RPMI as used in the subsequent pyridine-haem fraction assays. However the biological activity of S was not detected in any of the assays used, most likely due to the high concentration of exogenous PABA competing with S in the normal culture medium used. [223] As a result, a combination of S and PYR (SP) was used in the subsequent haem fractionation assays with a S concentration corresponding to 16 molar equivalents of PYR. This ratio of PYR to S corresponded to the dose normally used in a clinical setting.

3.5.2 Haem fractionation assay

Haem fractionation of CQ in D10

The cell fractionation study described in section 3.4.1 was applied to the 4-aminoquinoline, CQ to determine the effect of CQ on all major haem species in the cell. Briefly, cultures of highly synchronous CQS D10 at 5% parasitemia and 2% haematocrit were inoculated at the immature ring stage with increasing doses of CQ, corresponding to multiples of the parasite growth IC_{50} and incubated for a period of 32 h. The mature trophozoites were harvested by saponin lysis and exposed to a series of cellular fractionation steps where the relative amounts of each haem species in the isolated trophozoites was determined as a Fe(III)PPIX-pyridine complex (Figure 3-1).[107] The results of these experiments are discussed below.

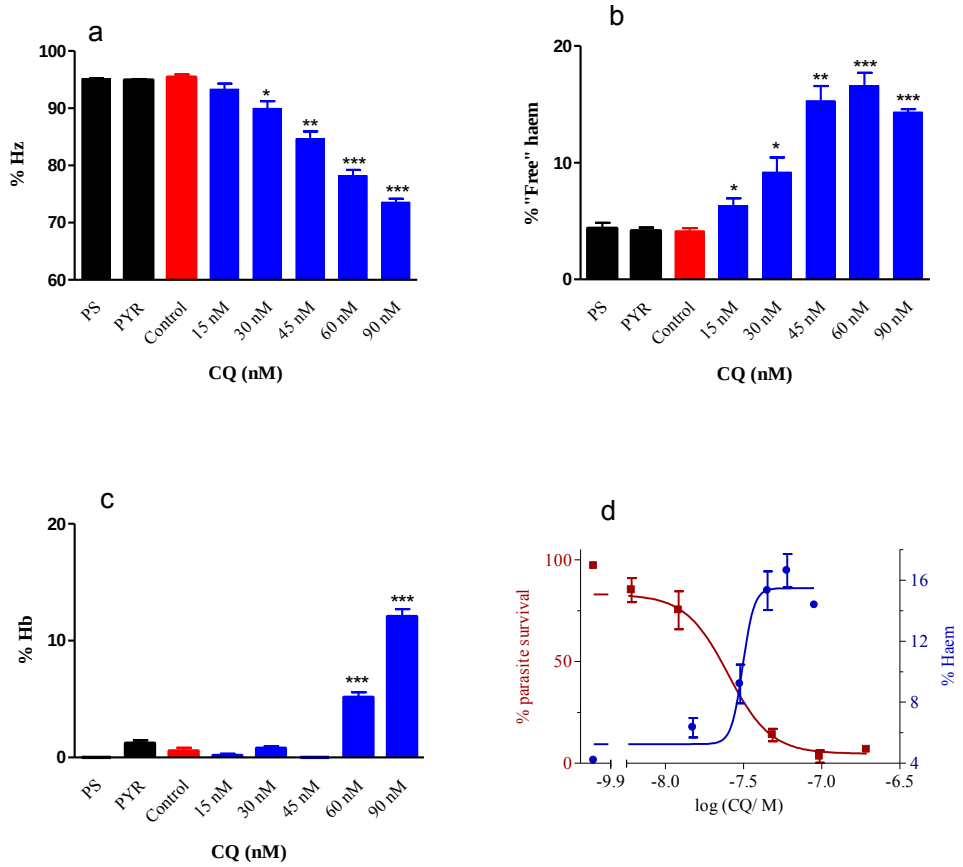

Figure 3-8: The fraction of each haem species present in isolated trophozoites is shown as a function of the CQ concentration (nM) for (a) %Hz, (b) %"free" haem and (c) %Hb. In each case a control with no CQ added is shown in red (0 nM CQ). CQ treated samples are displayed in blue and the negative controls PYR and SP in black. Asterisks displayed on the graph indicate statistical significance relative to the control (95% CI) determined using a two-tailed t-test (* P <0.05; ** P <0.01; *** P <0.001). (d) Parasite survival curve for CQ in D10 (red graph) as determined using method of Makler et al overlaid with the percentage of "free" haem (blue graph) as a function of CQ concentration.[206]

Figure 3-8 above illustrates the effect of increasing concentrations of CQ on the haem species in *P. falciparum*. A reduction in the fraction of total haem present as Hz, with increasing CQ concentration is seen in Figure 3-8a, decreasing from 95% in the control to approximately 74% at 90 nM CQ, the highest concentration of CQ tested. This reduction in Hz, is accompanied by an increase in toxic "free" haem (Figure 3-8b) from a baseline level of 4.2% in the untreated trophozoites to a

maximum of 16.6% in CQ treated cells. Undigested Hb within the CQ treated trophozoites follows suite increasing to a maximum of 12% at 60 nM CQ as shown in Figure 3-8c. Interestingly, a significant rise in Hb occurs only after 45 nM CQ, after a significant increase in free haem which appears from 15 nM CQ upwards. This observation that significant increased levels of free haem appear before undigested Hb suggests that this increase in %Hb is a consequence of higher "free" haem levels in the cell, and has been observed in a previous study examining the effects of quinolines on endocytosis in a CQS strain of *P. falciparum* (3D7). In this study trophozoites inoculated with CQ concentrations corresponding to five times the biological IC_{50} showed an increase of 283% in Hb levels determined by western blotting gel electrophoresis. [125] In contrast to the effect of CQ on the cell, the antifolates PYR and the SP combination had no significant effect on the percentages of Hz, "free" haem or Hb levels in the cell.

A shortcoming of the technique is that reliable results were only obtained up to a maximum concentration of 90 nM CQ as shown in Figure 3-8. Beyond this concentration of CQ, cells were too vulnerable to survive the harvesting process and too few parasites survived to obtain reliable measurements. Despite this limitation, a clear correlation exists between the increase in "free" haem and the parasite survival curve as shown in Figure 3-8d with a decrease in parasite survival accompanied by a corresponding increase in toxic "free" haem. CQ inhibition of haem degradation in a dose and time dependent manner has previously been demonstrated by Ginsburg et al. Although this study confirmed a relationship between membrane haem levels and parasite survival, a consequent decrease in Hz formation was not demonstrated. [86] The results provide direct evidence that Hz inhibition is indeed the mechanism of action of CQ in *P. falciparum* and is likely to be the mechanism for several other quinoline and related antimalarials. This prospect is discussed in the following section.

3.5.3 Haem fractionation of clinically relevant antimalarials in D10

A preliminary study to determine the effect of several other quinoline and related antimalarials on Hz formation was performed by exposing parasites to a single concentration of these antimalarials. The relative quantities of Hz and "free" haem

obtained in *P. falciparum* parasites after 32 h of exposure to ART, AQ, LF, MQ and QN at a single dose of 2.5 × their IC_{50} values was examined.

With the exception of the antifolate combination of SP, all other drugs have in the past been implicated in the interference of the formation of βH. [69 68 178 98 213 110] The βH inhibition dose response curves for LF and S (Figure 3-9d) as determined by the detergent mediated βH inhibition assay in section 2.5.3 shows that LF effectively inhibits βH (IC_{50} = 11 μM) and the antifolate S had no effect. Similarly, with the exception of the antifolate combination of SP all drugs caused a statistically significant decrease in Hz and increase in "free" haem as a percentage of the total haem in treated trophozoites tested at a single concentration of each drug (Figure 3-9a, b) when compared to the untreated control. Hz inhibition by ART has been a widely debated subject. Haynes et al in 2003 showed that contrary to several previously published reports proposing that AMNs inhibit Hz formation and kill through the consequent build-up of toxic haem, the AMNs do not inhibit βH.[179 178 110] However it can be seen in figure 3-9a, b that ART does cause a decrease in percent Hz formation and corresponding increase in percent "free" haem in the D10 strain of *P. falciparum*. With the exception of LF none of the drugs showed an increase in percentage "free" haem and decrease in percentage haemozoin, statistically comparable to CQ.

The time consuming nature of the assay means this preliminary study was limited to testing percentages of each haem species at a single concentration for each antimalarial. Demonstrating that Hz inhibition is a likely mechanism of action for these antimalarials required a full dose response study and is addressed in Chapters 4 and 5. It is worth noting that a percentage change cannot distinguish an absolute from a relative change. Consequently these percentage results are not definitive.

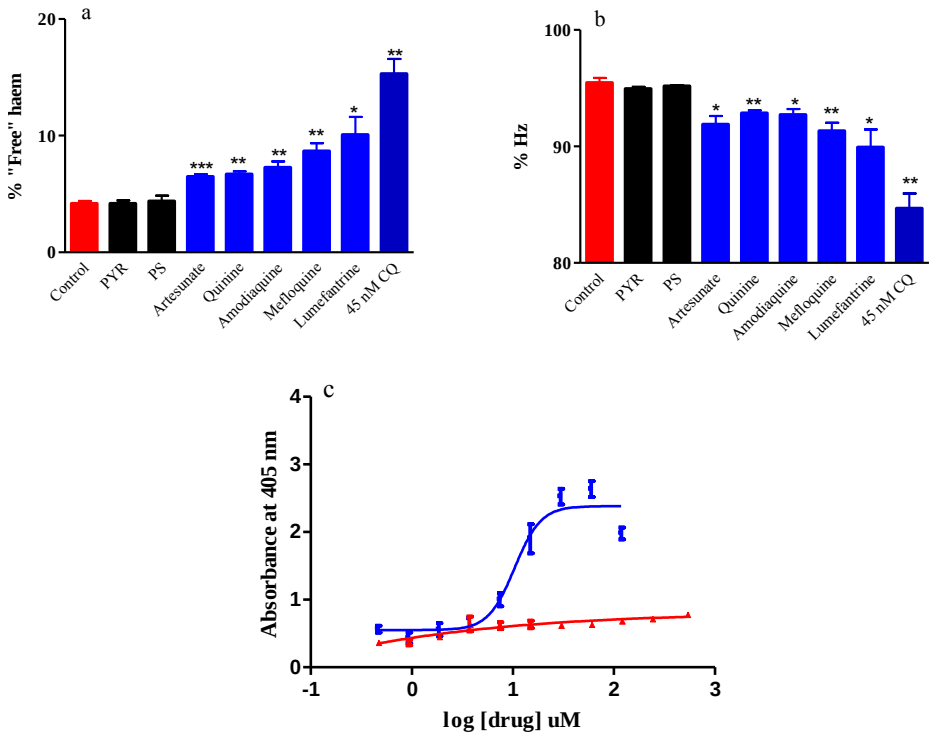

Figure 3-9: % "Free" haem (a) and %Hz (b) profiles in isolated trophozoites for several well-known antimalarials at a single dose corresponding to 2.5 × parasite growth IC_{50} values with the exception of CQ shown at 45 nM and SP at 2.5 × the IC_{50} of PYR and 16 molar equivalents of S relative to PYR. Asterisks displayed on the graph indicate statistical significance relative to the control (95% CI) determined using a two-tailed t-test (* P <0.05; ** P <0.01; *** P <0.001, n = 3 except for ART and MQ (n = 5), SP (n = 5) and PYR (n = 7)). (c) The free haematin inhibition for LF (blue) and S (red) was determined using the method described in section 2.5.3. The inhibition curves clearly indicate that LF inhibits the formation of βH with an IC_{50} value of 11 µM, while S does not.

3.5.4 Ferrozine Assay for Total Fe

The ferrozine assay developed by Carter et al was previously used to determine the total Fe content in isolated CQ-sensitive *P. falciparum* trophozoites. It was found that trophozoites (D10 strain) contain 58 ± 2 fg of Fe per cell, of which 95% is haem Fe in the form of Hz within the DV.[220] [30] The method was used here to determine the total cellular Fe content in isolated trophozoites exposed to

increasing doses of CQ after a 32 h incubation period. Total haem Fe as determined by the pyridine haem fraction assay in untreated and CQ treated cells was compared to the total Fe as determined by the ferrozine assay. In CQ treated cells the average total haem Fe was 57.8 ± 6.6 fg/cell versus 61.4 ± 6.5 fg/cell haem Fe (n = 6, P = 0.38, statistical significance determined using a two-tailed t-test). The total haem Fe was statistically indistinguishable from the total Fe content in both treated and untreated cells, demonstrating that the overwhelming majority of Fe in the parasite is present as haem.

3.5.5 TEM with EELS for Fe in CQ treated D10

The effect of CQ on the distribution of Fe within the parasite was examined by TEM with ESI using EELS (Figure 3-10) according to the technique described in Chapter 2. Previously unpublished images of untreated merozoite and ring stage parasites showed these parasites contained very little Fe in comparison to the host RBC. With exposure to 30 nM CQ there was very little change seen in the Fe distribution in the merozoite and ring stages. This is in stark contrast to the Fe distribution seen in trophozoites (Figure 3-10). Images of untreated trophozoites show a large concentration of Fe inside the DV, while the rest of the cell is virtually devoid of the presence of Fe. With the exception of Hz Fe within the DV, control parasites at the trophozoite stage contain very little Fe relative to the host RBC cytoplasm. In a separate study where Hz crystals extracted from untreated trophozoites were examined using TEM, the crystals were shown to consist of single, ordered crystals having uniform fringes corresponding to the {100} face of the crystal.[107] In contrast images of trophozoites treated with 30 nM CQ show large concentrations of Fe in areas corresponding to Hz crystals within the DV but also outside the DV in the cytosol, concentrated in areas indicated by yellow asterisks in Figure 3-10. This cytosolic Fe can be attributed to haem as virtually all Fe in both treated and untreated parasites was found to present as haem species. Furthermore, because treated parasites contain very little Hb, this haem can most likely be attributed to free haem. TEM images of crystals isolated from CQ treated parasites showed less uniform crystals at 30 nM and at 60 nM TEM images showed evidence of grain

boundaries in the crystals at high magnification, directly signifying that CQ disrupts Hz crystallization in the parasite.[107]

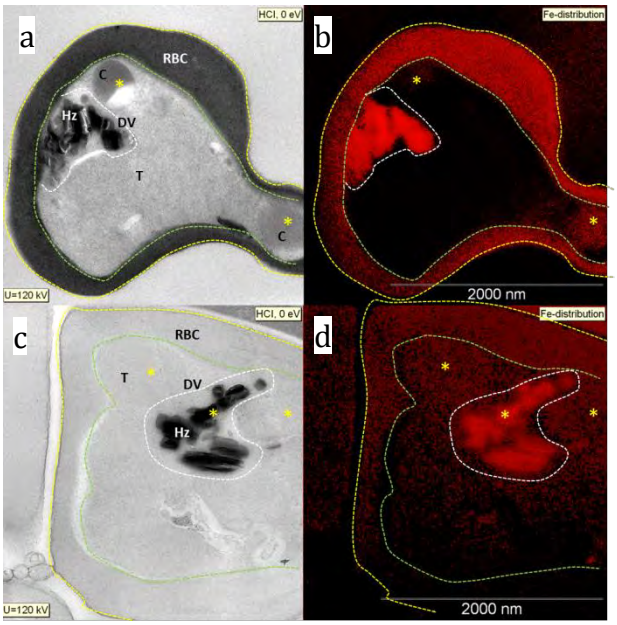

Figure 3-10: TEM images with ESI using EELS for Fe of untreated D10 PRBCs and PRBCs inoculated with 30 nM CQ prepared as described in Chapter 2. In all images RBCs are delineated by a yellow dashed line, parasite by a green dashed line and DV by a white dashed line. The Fe distribution measured by ESI using EELS is shown in red. The Fe signal in untreated parasites (Figure 3-10 a and b) is localized to the Hz crystals in the DV and 2 areas highlighted by yellow asterisks (*) which could be attributed to RBC cytosol containing cytostomes (C). The rest of the untreated parasite is devoid of detectable Fe. In both the untreated and treated PRBC, Fe is readily detected in the RBC cytoplasm. CQ treated parasites show large concentrations of Fe in areas corresponding to Hz crystals within the DV and also outside the DV in the troph cytoplasm, concentrated in areas indicated by yellow asterisks (*). The Fe signal attributed to Hz crystal inside the DV of CQ treated cells is not as strong as in untreated cells. This cytosolic Fe can be attributed to haem, as virtually all Fe in both treated and untreated parasites was found to present as haem species. Additionally, because treated parasites contain very little Hb, this haem can most likely be attributed to free haem.

3.5.6 TLC of haem and OsO4 fixed haem

The TEM images in Figure 3-10 were prepared from cells which underwent a lengthy process of chemical fixation before TEM images with EELS for Fe were captured. Given the significance of the Fe distribution map in these images, the possibility that Fe could have been redistributed during preparation was considered. Cells were treated with OsO_4 which fixes membranes and so haem fixation was also considered. A TLC experiment described in section 3.4.3 was conducted where haemin (Cl-Fe(III)protoporphyrin IX) and OsO_4-treated haemin were spotted alongside each other onto a silica gel TLC plate and after drying were run in a series of solvents mimicking the dehydration procedure used when samples are prepared for TEM (Figure 3-11). The Rf values obtained for untreated haemin in each solvent system are summarised in Table 3.5. As opposed to untreated haemin, haemin treated with OsO_4 remained on the baseline (Rf = 0) in all of the solvent systems. This TLC experiment proves that haemin is immobilized following exposure to OsO_4.

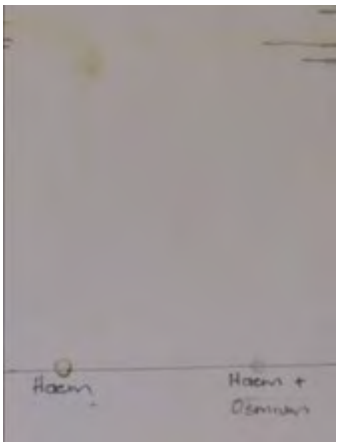

Figure 3-11: Image (unedited) of the thin layer chromatogram of haemin and OsO_4 fixed haem in acetone. The OsO_4 fixed haem remained on the baseline in all solvent sytems.

Table 3-2: Summary of Rf values of haemin in several solvent systems obtained by TLC

Solvent System	**Rf value: Untreated haemin**	**Rf value: OsO_4 – treated haemin**
30% EtOH (aq)	0.85	0.00
50% EtOH (aq)	0.95	0.00
70% EtOH (aq)	0.91	0.00
90% EtOH (aq)	0.98	0.00
100% EtOH	0.98	0.00
100% acetone	0.98	0.00

In addition to the evidence provided by the TLC experiment, further evidence for the OsO_4 fixation of haem can be seen by examining the images of untreated trophozoites (Figure 3-10). The Fe signal originates strongly from the HZ crystals in the DV with no bleeding of Fe into the cytosol which is completely void of Fe. If Fe had diffused out during fixation a uniform distribution of Fe would be seen throughout the cell. Furthermore, there is a sharp boundary between the Fe present in the RBC cytoplasm and the parasite cytosol indicating that Hb Fe does not shift during preparation. Similarly the Fe signal corresponding to the edges of the Hz crystals in the DV remain sharp and well defined, confirming that Hz Fe iron is not redistributed.

3.6 Summary and conclusions:

This study very strongly supports the proposed mechanism of action of CQ as a Hz inhibitor and establishes a standard method to be used for the validation of cellular Hz inhibition for other antimalarial compounds. CQ was shown to cause a dose-dependent decrease in Hz and related increase in toxic “free” haem in a cultured CQS strain of *P. falciparum* that is directly correlated with parasite survival. Statistically relevant increases in Hb appeared only after the appearance of significantly higher levels of free haem suggesting a causative link. Furthermore, TEM with EELS for Fe show that haem is redistributed from the DV to parasite cytosol in CQ treated *P. falciparum* cells where it most likely interacts with

membranous structures such as endoplasmic reticulum in the parasite cytosol. Schmitt et al showed that aggregates of haemin in aqueous solution rapidly enter and accumulate into lipid bilayers, associating with organelles, causing membrane disorder and enhancing permeability leading to eventual cell lysis.[51] The resolution of the TEM images obtained was not high enough to distinguish association with any specific organelles in the parasite cytosol; however as this theory represents a possible way of killing the parasite it necessitates further investigation.

The haem fractionation study was extended to several other antimalarials, ART, AQ, LF, MQ and QN as well as the antifolate PYR and its combination with S (SP) at a single dose of 2.5 × their IC_{50}. With the exception of the antifolates it has been suggested that these antimalarials share the same mechanism of action as CQ. Although controversial for ART, numerous studies have shown that the quinolines interfere with the formation of βH at concentrations that correlate with their biological IC_{50} values, suggesting that like CQ they disrupt the formation of haemozoin. [69 106 178 213 98 179 110] Nonetheless, QN and MQ have been implicated in alternative mechanism of action, targeting cytosolic and membrane targets.[129] Neither QN nor MQ accumulate to the same degree as CQ within the acidic DV and while CQ treatment of *P. berghei* infected mice resulted in decreased Hz production, neither QN nor MQ treatment affected Hz production. [79 127] The measurement of "free" haem and Hz at a fixed single dose for the antimalarials investigated in this chapter provides only an initial screen. A more comprehensive study of each of the compounds tested is required before any definitive conclusions can be made.

The method presented here provides valuable information regarding drug mechanisms of action, enhancing existing information to aid in the rational selection of novel compounds for drug design and development. The single biggest limiting factor of the technique presented in this chapter is the length of time required to complete a profile for a single drug at several different concentrations as carried out for CQ. The full potential of this technique as a basis for assaying parasite Hz inhibition in the presence of antimalarial compounds could only be realised if it was adapted to higher throughput method with shorter lead times.

4 DEVELOPMENT AND OPTIMISATION OF A MULTIWELL COLORIMETRIC ASSAY FOR THE DETERMINATION OF HAEM SPECIES IN *PLASMODIUM FALCIPARUM*

4.1 Introduction

The process of cellular lipid mediated Hz formation is mimicked synthetically in a detergent-mediated assay using the lipophilic detergent NP-40 as a substitute for the neutral lipids. [102] The NP-40 assay has been applied as a high throughput screening tool and identified several novel Hz inhibiting scaffolds. [105 104 224 225] This laboratory based method for the determination of βH inhibition was translated into an equivalent process in laboratory cultured malaria parasites, the "haem fractionation assay".[107] The previous chapter described the results of the haem fractionation assay used to directly determine Hb, "free" haem and Hz in *P. falciparum* inoculated with increasing concentrations of CQ. All haem species were spectroscopically measured as a Fe(III)haem complex with pyridine, based on a previously published method by Ncokazi and Egan in which it was shown that in a mixture of βH and haematin, the latter forms a low-spin complex with aqueous pyridine (5% v/v, pH 7.5) without disturbing βH.[101] As described in Chapter 3, CQ, caused a dose-dependent increase in cellular "free" haem (i.e., labile haem that can be solubilized with detergent), alongside a decrease in Hz correlated to decreased parasite survival in CQS D10 *P. falciparum*. The data were supplemented by TEM images with EELS for Fe of CQ-treated cells and showed a redistribution of Fe from the DV into the parasite cytoplasm. [107] The method successfully demonstrated that CQ is able to inhibit the cellular formation of Hz, however, due to its protracted nature and high demand on parasite starting material, it could not easily be extended to other drugs.

In this chapter a modification of this haem fractionation assay is described. Performed in 24-well plates, this modified technique was primarily developed to increase output as multiple drug concentrations can be evaluated in one session with relatively low amounts of parasite starting material translating to reduced material costs. A significant improvement in output over the previous method was achieved, producing results for two compounds per week in comparison to the original method which produced results for one compound every two months. The method was validated against the original haem fractionation assay performed in flasks using CQ, described in detail in Chapter 3. Several experiments were carried out to assess the robustness of the method with particular reference to the

measurement of each haem species at each fractionation step and the possibility of cross-contamination of haem species between fractionation steps. This increased throughput method was applied to three clinically relevant antimalarials covering a broad spectrum of mechanisms of actions: the 4-aminoquinoline AQ which like CQ has been shown to inhibit βH formation, the non-βH inhibiting antifolate PYR and finally the non-βH inhibiting anti-malarial ATV. [105 184]

Previously cell counts were acquired using a haemocytometer; however the technique was tedious and impractical when applied to a large number of samples. As a result counting was also performed with a novel flow cytometry method using SYBR green I fluorescent staining of isolated cells. [226-228] [229] Based on the fluorescent binding of SYBR green I to double stranded DNA, the SYBR green I fluorescence signal increases over the course of the 48 h lifecycle of the parasite as the amount of DNA increases with maturation from early rings to multi-nucleated schizonts. [230] SYBR green I was specifically chosen due to its low binding affinity for RNA and preference for double stranded DNA over single stranded DNA. [231] Furthermore, this flow cytometry method provided valuable information about morphological changes of cells treated with antimalarials as the stage of the *P. falciparum* cells can be determined from the associated fluorescence of the population.

This chapter describes the development and implementation of this improved throughput, modified version of the assay developed in the previous chapter allowing for the more rapid determination of haem species in isolated *P. falciparum* trophozoites. The assay was then applied to several clinically relevant antimalarials at multiple concentrations.

4.2 Materials

All materials used throughout this chapter are listed in Chapter 2. Materials were of AR grade or higher and used without further purification.

4.3 Sample Preparation

The preparation of all samples used throughout this chapter, are previously described in Chapters 2 and 3. The water used throughout this work was double distilled deionised Millipore® Direct-Q water.

4.4 Methods

4.4.1 Haem fractionation assay

The haem fractionation assay is a cellular fractionation technique based on the ability of neutral aqueous pyridine to selectively form a low spin haem-pyridine complex with "free" haem in the presence of Hz.[101] The original method described in detail in Chapter 3, was performed in 250 ml culture flasks, testing a single drug concentration at a time and performing spectroscopic measurements in a cuvette.[107] The modified method was performed in 24-well plates, testing several drug concentrations, four replicates at a time and using a multiwell plate reader to record absorbance values, resulting in a six-fold increase in throughput. The original method performed in 250 ml culture flasks is compared to the modified 24-well plate method in the flow chart, Figure 4-1 below.

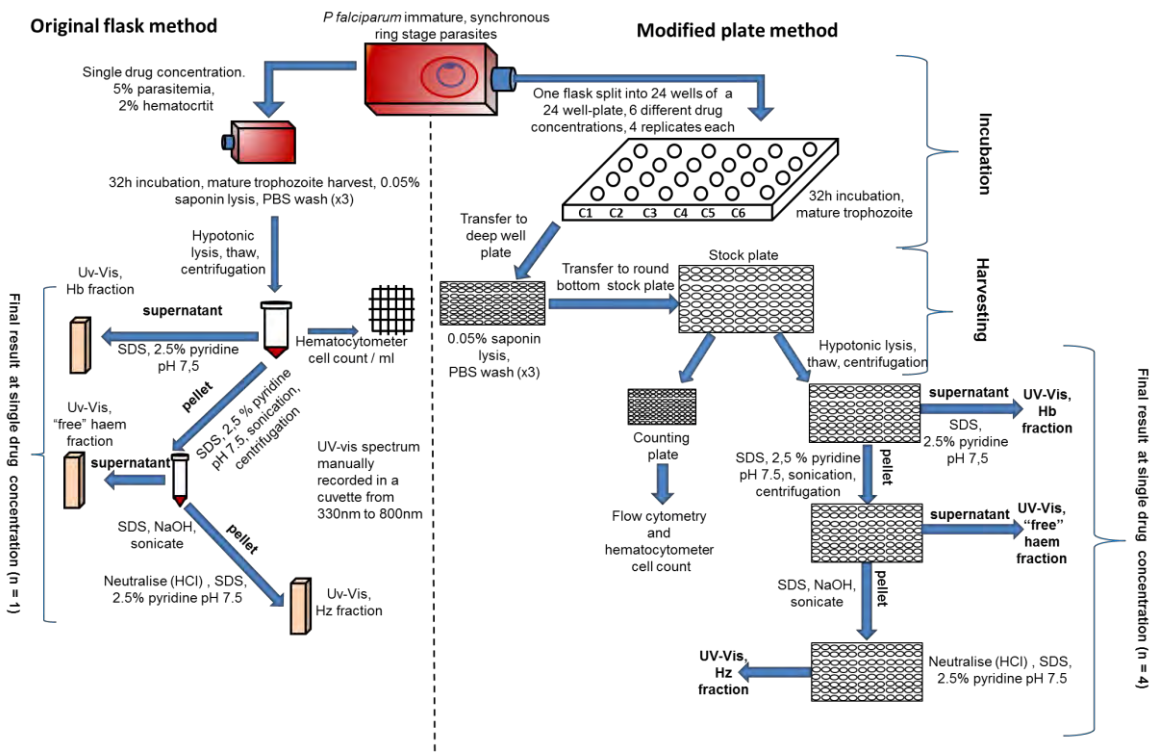

Figure 4-1: Flow diagram showing the haem fractionation assay: original flask method (left) versus increased throughput plate method (right). Immature ring stage PRBCs were inoculated with several different increasing drug concentrations. After 32 h, mature trophozoites were harvested via saponin lysis of erythrocytes. Following hypotonic lysis and centrifugation the supernatant was isolated and the SDS treated soluble Hb was measured in the supernatant as a low spin haem-pyridine complex. The pellet was further treated with SDS and pyridine to solubilize "free" haem, measured in the supernatant following centrifugation. Hz was measured after solubilizing the pellet in NaOH, neutralizing with HCl and treating with pyridine.

Incubation:

The parasitaemia of an early ring-stage sorbitol synchronized culture was determined from a 10% (v/v) Giemsa stained blood smear under a light microscope with an oil immersion lens at 100× magnification. The culture was diluted to 5% parasitaemia with washed O+ human RBCs at a 2% haematocrit with complete medium. Aliquots of 2 ml were added to each well of a 24-well flat-bottom cell culture plate (Figure 4-2). Unless indicated otherwise, all drugs were tested at five different concentrations corresponding to 0.5×, 1.0×, 2.0×, 3.0× and

4.0× their 50% growth inhibition concentration measured in vitro. Drugs were diluted in medium from the previously prepared 2 mg/ml stock solution (Chapter 2, Section 2.5.3) and 20 µl added to each well of the 24-well plate such that the final concentrations in each well corresponded to 0.5×, 1.0×, 2.0×, 3.0× and 4.0× the parasite growth IC_{50} of the test compounds. Each concentration was tested as four replicates and the highest concentration of drug tested was at 4× IC_{50}, since beyond this concentration very few cells remained for harvesting. No drug was added to the 4 control wells on each plate. The plates were gassed in a gas chamber with a mixture of 3% O_2, 4% CO_2 and N_2 for 4 min and incubated at 37 °C for 32 h (Figure 4-1).

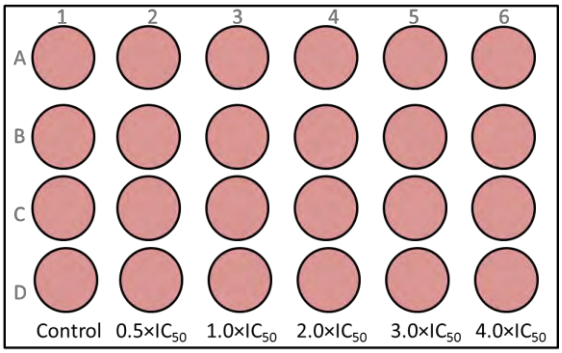

Figure 4-2: Setup for a 24-well flat-bottom cell culture plate. Each well contains 2 ml of PRBCs at 5% parasitaemia and 2% haematocrit. To each well 20 µl of drug was added such that the final concentrations in each well corresponded to 0.5×, 1.0×, 2.0×, 3.0× and 4.0× the biological IC_{50} of the test drug. Cell counts determined using flow cytometry were performed on all 24 wells of the 24-well plate while haemocytometer counts were performed on the 6 wells in row A only.

Harvesting:

After 32 h, excess supernatant as well as any cell debris and associated Hz corresponding to a black layer on top of the PRBC pellet was aspirated. Giemsa-stained thin smears were prepared on glass slides at each concentration tested and viewed under a light microscope with an oil immersion lens to confirm the presence of trophozoites. Each pellet was resuspended in 1.9 ml PBS (pH 7.5) and transferred to a round bottomed deep well 2.2 ml rectangular 96-well plate. These new plates ensured maximum sample recovery in subsequent steps and were essential for further processing. Trophozoites were isolated by lysing erythrocytes

with the addition of 100 µl 1% (w/v) saponin. After 2 min at 37 °C, plates were centrifuged at 750 rcf for 15 min. The supernatant was aspirated and the pellets washed three times with 0.5 ml PBS (pH 7.5) to remove all traces of erythrocyte Hb. The washed pellet, corresponding primarily to isolated trophozoites, was resuspended to a final volume of 100 µl with PBS pH 7.5 and accurately transferred to a round-bottomed, 96-well 0.5 ml plate referred to as the stock plate. The stock plate was used to prepare a second plate for cell counting as described below after which it was frozen at -80 °C (Figure 4-1).

Preparation of the counting plate and cell fixation:

A counting plate was prepared by adding 10 µl of the isolated washed trophozoites to the corresponding wells of a flat-bottomed 96-well plate. The cells were fixed with 0.125% (v/v) glutaraldehyde in PBS pH 7.5 to a final volume of 200 µl and refrigerated at 4 °C overnight (Figure 4-1).

Haemocytometer counting:

Haemocytometer counting was performed on the first row of each plate only, corresponding to 6 samples, a control and one at each of the drug concentrations tested. The haemocytometer determined cell counts for these 6 samples were statistically compared to the cell counts determined by flow cytometry to test for agreement. The number of cells/ml was determined by loading 10 µl of cells from each well onto a bright-line haemocytometer and five large squares were counted after 10 min of settling. The concentration of cells in each well of the plate was determined using equation 4-1:

$$CH = N \times F \times DF \times 10{,}000 \qquad (4\text{-}1)$$

Where: *CH* = concentration of cells per ml as determined by haemocytometer

N = number of cells counted in 5 fields

F = number of fields counted = 5

DF = dilution factor

Flow cytometry counting:

The cell count in each well of the counting plate was determined using fluorescent staining and flow cytometry.[226-228] Samples were prepared by diluting 100 µl of

cells taken from the counting plate with 800 µl of 1 × SYBR® green I in PBS pH 7.5 and incubating for 30 min in the dark at 37 °C. Next, each sample was spiked with 100 µl of Trucount™ beads (Becton Dickinson) such that each sample contained a known fixed amount of fluorescent beads in a final volume of 1 ml. Samples were analysed on a Becton Dickinson FACSCalibur using SSC/FL1 530 nm with CellQuestPro software. All samples were analysed using FloJo software version 10 (Tree Star Inc). The samples were mixed well before use. The concentration of cells in the acquisition tube was calculated according to equation 4-2:

$$CF = (T/B) \times CB \qquad (4\text{-}2)$$

Where: *CF* = concentration of cells per ml as determined with flow cytometry

T = number of trophozoites gated

B = number of fluorescent beads gated

CB = concentration of fluorescent Trucount™ beads in the acquisition tube per ml (calibrated bead count per acquisition is unique to each lot of Trucount™ tubes obtained from the supplier)

Trophozoite gates were established by running isolated trophozoites obtained from a highly synchronous trophozoite culture through the process of harvesting and flow cytometry analysis as described above. A 10% (v/v) Giemsa-stained slide confirmed the presence of trophozoites. The same process was applied to a highly synchronous late stage ring culture; however it was difficult to distinguish rings from the debris accumulated during the isolation and harvesting procedure in the Giemsa-stained slides. The latter population presumed to correspond to rings and associated debris was omitted during gating and only intact trophozoites were gated and used to determine cell counts. Typically 10,000 events were counted for each sample. Initial gating was performed with unstained cells to account for autofluorescence.

Haem fractionation:

The stock plate was thawed at room temperature and 50 µl of water was added to each well. The plate was floated in an ultrasound bath and sonicated for 5 min. Each well was resuspended with 50 µl each of 0.2 M HEPES buffer pH 7.5 and water. The plate was then centrifuged at 3600 rpm for 20 min. The supernatant in each well was transferred to an adjacent set of wells on the same plate with extreme care as to avoid disturbing the pellet. The supernatant was processed

further with 50 µl 4% SDS, sonicated for 5 min and then incubated at 37 °C for 30 min. Finally, 50 µl of 0.3 M NaCl and 50 µl of 25% (v/v) pyridine in 0.2 M HEPES pH 7.5 were added and 200 µl of the solution was transferred to a flat-bottomed UV-Star 96-well plate. This fraction corresponds to the Hb fraction (Figure 4-1).

The remaining pellet containing "free" haem and Hz was resuspended with 50 µl water and 50 µl 4% SDS. The plate was sonicated for 5 min and incubated at 37 °C for 30 min to solubilize "free" haem. This was followed by the addition of 50 µl 0.2 M HEPES pH 7.5, 50 µl 0.3 M NaCl and 50 µl 25% pyridine. The plate was centrifuged at 3 700 rpm for 20 min. Again, very carefully without disturbing the pellet, the supernatant was transferred to an adjacent set of wells on the same plate. The supernatant was diluted to a final volume of 400 µl with water. This fraction corresponds to the "free" haem fraction (Figure 4-1); 200 µl of this solution was transferred to the flat-bottomed UV-Star 96-well plate, the same plate previously used for the Hb fraction.

The remaining pellet containing Hz was solubilized in 50 µl of water and 50 µl 0.3 M NaOH. The plate was sonicated for 15 min and incubated at 37 °C for 30 min. Finally, 50 µl each of 0.2 M HEPES pH 7.5, 0.3 M HCl, 25% pyridine and 150 µl water were added. This fraction corresponds to the Hz fraction (Figure 4-1); 200 µl of this solution was transferred to vacant wells in the flat-bottomed UV-Star 96-well plate containing the Hb and "free" haem fractions. The UV-visible spectra of haem as Fe(III)haem-pyridine complex was recorded using a multi-well plate reader (Spectramax 340PC, Molecular Devices). The absorbance maxima (A_{max}) of the Fe(III)haem pyridine complex in each well was used to calculate the percentage of each haem species in each sample as the final volume for each fraction was identical. The calculation for percentage of each haem species in each sample is described in equation 4-3 below:

$$A_{Total} = A_{Hb} + A_{"free" haem} + A_{Hz} \quad (4\text{-}3.1)$$

$$\% \text{ Hb} = (A_{Hb} / A_{Total}) \times 100 \quad (4\text{-}3.2)$$

$$\% \text{ "free" haem} = (A_{'free" haem} / A_{Total}) \times 100 \quad (4\text{-}3.3)$$

$$\% \text{ Hz} = (A_{Hz} / A_{Total}) \times 100 \quad (4\text{-}3.4)$$

Where: A_{max} for Fe(III)haem-pyridine (Hb fraction) = A_{Hb}

A_{max} for Fe(III)haem-pyridine ("free" haem fraction) = $A_{"free" haem}$

A_{max} for Fe(III)haem-pyridine (Hz fraction) = A_{Hz}

Haem standard curve:

The total amount of haem in each fraction was quantified using a haem standard curve prepared from a 100 µg/ml haem standard solution of haematin (porcine) in 0.3 M NaOH. Serial dilutions of the standard were carried out in a 96-well plate with 100 µl 0.3 M NaOH as a blank. Each haematin standard was diluted with 50 µl of each of the following solutions: 0.2 M HEPES pH 7.5, 4% (w/v) SDS, 0.3 M NaCl, 0.3 M HCl, 25% pyridine in 0.2 M HEPES pH 7.5 and water. All measurements were performed in triplicate. The visible spectra of haem as Fe(III)haem-pyridine complex was recorded in a multi-well plate reader. A calibration curve of was used to determine the amount of haem Fe present in each sample (Figure 4-3). The amount of haem Fe per cell was calculated by dividing the total haem Fe in each fraction by the number of cells determined in each fraction. For ease of comparison with the total cellular Fe reported in Chapter 3, and with a previous study conducted by Egan et al in 2002 where the total amount of Fe in isolated trophozoites present as Hz was reported, all results are expressed as the amount of haem Fe (fg) per cell. [30]

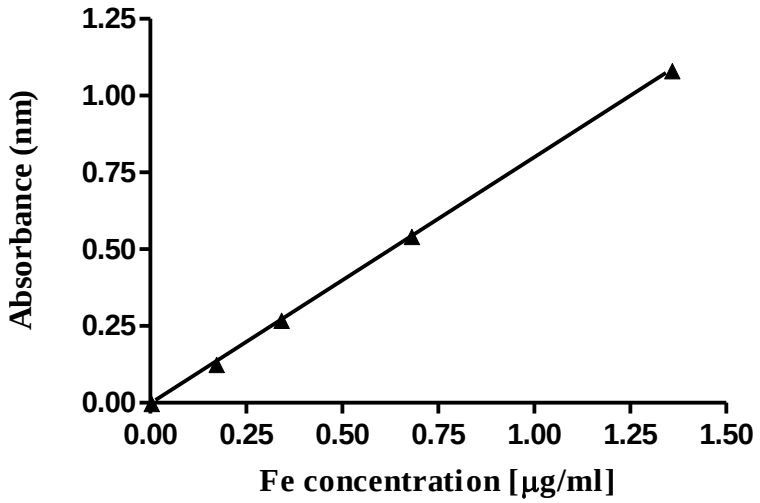

Figure 4-3: Representative calibration curve of haem Fe (as Fe(III)haem-pyridine complex) vs absorbance. The data represents the mean ± SD of 3 repeats. The linear portion of the graph is shown for which the correlation coefficient, R^2 = 0.999. The graph was plotted using GraphPad Prism 4.0 linear regression function.

4.5 Statistical analysis

Bland Altman analysis was used to assess the agreement between the original haem fractionation method and modified plate method.[232] For determination of statistical significance of differences in measurements relative to controls, a two-tailed t-test (95% CI) was used and is displayed on graphs using asterisks (* P <0.05; ** P <0.01; *** P <0.001). In all cases data represent a minimum of three repeats. All analysis was carried out using GraphPad Prism version 4.0 software.[203]

4.6 Results and Discussion

4.6.1 Cell counting: haemocytometer *versus* flow cytometer

Cell concentrations required for the determination of the total amount of haem Fe per cell (reported in fg/cell) in the original haem fractionation assay were determined manually using a haemocytometer. This method was found to be slow and tedious when applied to 24 samples per plate and an alternative, more efficient method for counting cells was set up using flow cytometry (Section 4.4.1). Cell counts using flow cytometry were performed on all wells of each 24-well plate. Haemocytometer counts were routinely done on 6 samples in the first row only of each 24-well plate for comparison and to establish agreement between the methods. In both cases only intact isolated trophozoites were counted. Flow cytometry is a faster, less subjective process than haemocytometer counting but is not without limitations. The first issue relates to the accurate gating of cells. A gate corresponding to trophozoites was established by running isolated trophozoites obtained from a highly synchronous trophozoite culture through the process of harvesting and flow cytometry analysis as described in methods above. Trophozoites were confirmed with a 10% (v/v) Giemsa-stained slide (Figure 4-4A, inset). The resulting dot plot is shown in Figure 4-4A and represents a population corresponding to primarily trophozoites. The same process was applied to a highly

synchronous ring culture and the resulting dot plot of cell material accrued as a consequence of the harvesting process, most likely corresponding to both rings and cell debris, can be seen in Figure 4-4B. Again, a 10% (v/v) Giemsa-stained slide confirmed the presence of accumulated cell debris; however it was difficult to distinguish rings from the debris (Figure 4-4B, inset). The trophozoite population in Figure 4-4A corresponds to cells of a greater side scatter (SSC) and fluorescent intensity (FL1) indicating more complex cells with more nucleic acid in comparison to the population of rings and debris with both lower fluorescent intensity and SSC in Figure 4-4B. The latter population was omitted during gating and only intact trophozoites were gated and used to determine cell counts. Despite having established a gate specifically for trophozoites (Figure 4-4A) which excludes any rings and cell debris collected during the process of harvesting (Figure 4-4B), an overlap exists where cells which appear as larger, more complex and mature rings have the same forward scatter (FSC), SSC and fluorescent intensity as immature or underdeveloped trophozoites. This overlap is demonstrated in Figure 4-4 C, D and E which show the histogram plots of FL1, FSC and SSC of the trophozoite population in Figure 4-4A. The areas of overlap as well as the smaller population corresponding to rings and debris are indicated on each graph. The presence of this overlap can result in an inaccurate trophozoite cell count. The second issue is counting aggregates of cells as a single complex cell resulting in under-counting, however this was largely overcome by mixing samples well during preparation and running the samples at a low flow rate on the flow cytometer.

Despite the limitations associated with both counting methods, it was found there was no statistical difference between the means as determined by each counting method (unpaired two-tailed t-test, 95% CI) for the untreated controls (Figure 4-4F). Furthermore, no significant difference between flow cytometry and haemocytometer determined counts were seen at any concentration of the four drugs tested (Table 4-1).

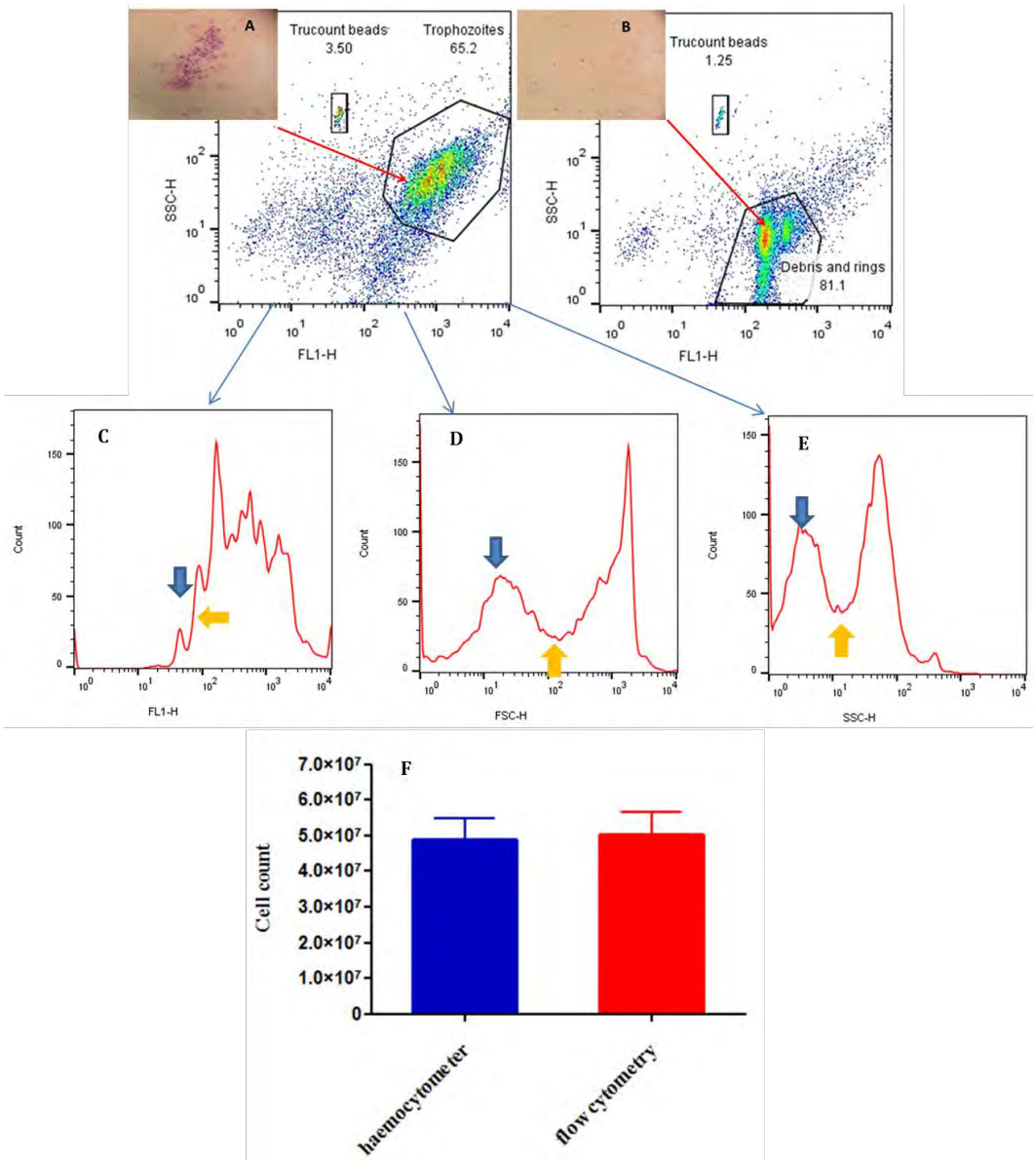

Figure 4-4: Dot plots of SSC vs SYBR green fluorescence (FL1-H) for samples corresponding to populations of primarily isolated trophozoites (A) and isolated rings and associated debris (B). The corresponding 10% Giemsa stained smears of isolated cells as viewed under 100× magnification are shown as insets. Panels C, D and F correspond to FL1, FSC and SSC of the trophozoite population in A. The areas corresponding to rings and debris are indicated by blue arrows and areas of overlap between the trophozoite population and population corresponding to rings and debris are indicated by orange arrows on each graph. Panel F shows the average cell count obtained for control samples using a haemocytometer (blue) vs flow cytometry (red). The mean cell count obtained using the haemocytometer did not differ significantly from the flow cytometry count ($P = 0.88$, $n = 6$, two tailed unpaired t-test at 95% CI).

Table 4-1: The *P*-values obtained when the mean count obtained using the haemocytometer is compared to mean count obtained using flow cytometry for each drug tested at several different concentrations (unpaired, 2 tailed t-test, 95% CI).

CQ (nM)	7.5	15	30	45	90
P-value	0.92	0.68	0.32	0.89	0.96
AQ (nM)	12.5	25	50	75	100
P-value	0.12	0.56	0.056	0.28	0.061
ATV (nM)	1	2	4	8	16
P-value	0.75	0.92	0.69	0.83	0.23
PYR (nM)	25	50	100	150	200
P-value	0.13	0.12	0.087	0.11	0.86

4.6.2 Assessment of the Robustness of the Assay

The robustness of the assay was addressed with particular reference to the specificity of the assay for different haem species in the various fractions. Several opportunities for cross contamination were investigated at each of the fractionation steps.

Contamination by Hz post synchronisation

When cultured parasites are synchronized with sorbitol at the ring stage, trophozoites present in the asynchronous culture are lysed and Hz is released into the culture. To avoid any carry-over of this released Hz into the synchronized culture to be used in the subsequent assay, any visible pigmented cell debris was removed by aspiration immediately following sorbitolization. To confirm that significant quantities of pre-formed Hz did not contaminate the sample a synchronous culture was split into 2. One half was subjected to the process of harvesting, followed by the haem fractionation assay at the ring stage soon after sorbitol treatment. At this stage of the lifecycle early rings would have produced little or no Hz.[233] Consequently; any haem detected in the Hz fraction arises from

either Hz carried over during the previous round of sorbitol synchronization, or from a small fraction of trophozoites that survive sorbitol treatment. The second half of the same culture was harvested 24 h later as trophozoites and taken through the same process of the haem fraction assay. The resulting absorbance spectrum of the Hz haem fraction corresponding to rings (grey) and trophozoites (red) is shown in Figure 4-5A. The absorbance spectrum of Hz haem present in the ring stage fraction was minimal compared to material isolated from the same culture 24 h later at the trophozoite stage. At the maximum, the amount of Hz in the ring culture equates to 4.2 ± 0.4% (n = 4) of the Hz haem in the trophozoite culture and most likely arose from a small proportion of trophozoites that survived sorbitol treatment, still present in the ring culture. Thus, post synchronisation Hz cross-contamination was found to be negligible.

Contamination by host RBC Hb post synchronisation

Host RBC Hb is another potential source of cross-contamination. RBC Hb is the dominant form of haem in the total culture at 5% parasitaemia. Trophozoites isolated by saponin lysis for the haem fractionation assay are accompanied by lysed RBC membranes. The isolated trophozoite pellet could be contaminated with Hb if the washing steps described as part of the harvesting protocol in the haem fractionation assay are not efficient enough. RBC Hb would therefore not be removed and would result in elevated trophozoite Hb readings which could potentially carry over into subsequent fractions and elevate the haem values in those fractions. To test this, 2 ml of PRBC at 2% haematocrit (40 µl RBC) and 5% parasitaemia was spiked with 100 µL of packed RBCs. This mixture was then subjected to the usual harvesting and haem fractionation assay and Hb (Figure 4-5B), "free" haem (Figure 4-5C) and Hz haem (Figure 4-5D) were measured. None of the fractions showed any significant change in haem levels relative to the unspiked control. This demonstrated that cross-contamination by RBC Hb is not significant provided that the washing protocol is followed.

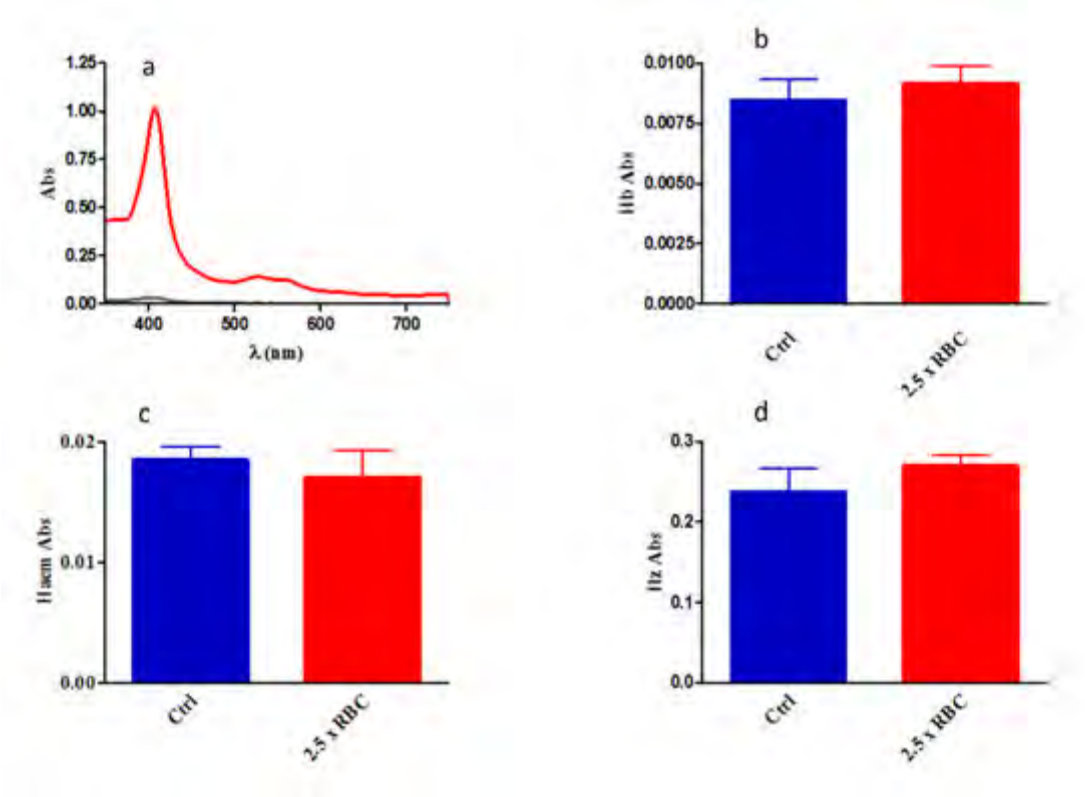

Figure 4-5: (A) The absorbance spectrum for the Hz haem fraction of isolated trophozoites is shown in red and rings in grey. The Soret peak corresponding to the ring culture is minimal compared to the strong signal obtained from the trophozoite culture. The cross contamination carried over from previous synchronisation cycles was determined to be less than 4%. The same culture was used to generate both graphs, with isolations performed 24 h apart using approximately 2.5 × 10^7 cells each time. The Soret band absorbance readings for Hb (B), "free" haem (C) and Hz (D) fractions of a sample spiked with 100 µl of packed RBCs compared to a control sample containing 40 µl of 5% PRBCs. Both the control and spiked sample were from the same culture and contained 10^7 parasites. No significant change was seen in the Hb fraction (P = 0.57), "free" haem fraction (P = 0.52) and Hz fraction (P = 0.33) of the spiked sample containing 2.5× more RBCs compared to the control sample (unpaired two tailed *t*-test, 95% CI, n = 6).

Contamination of "free" haem fraction:

Finally, contamination of the "free" haem fraction by Hz was investigated. The "free" haem fraction could potentially be contaminated as a result of the

breakdown of Hz during ultrasound treatment in the presence of SDS. Two approaches were used to test this. Firstly, the duration of ultrasound treatment was increased 3-fold to 15 min. No significant change in free haem levels was detected (Table 4-2). Secondly, the pellet containing "free" haem and Hz was spiked with isolated Hz prior to addition of SDS and ultrasound treatment. This Hz was obtained from the final pellet of a control experiment isolated prior to addition of NaOH, doubling the quantity of Hz in the sample. Isolation of "free" haem from this spiked sample showed no significant difference relative to an unspiked control (Table 4-2). This confirmed that Hz does not contaminate the "free" haem fraction.

Table 4-2: The mean absorbance of a control sample compared to a sample sonicated for an extra 15 min and a sample spiked with Hz. The P-values indicate that the average absorbances do not differ significantly from the control (unpaired two tailed t-test, 95% CI, n = 6).

Sample Description	Average Absorbance	P-value
Control	0.024 ± 0.003	N/A
Sonicated for 15 min	0.021 ± 0.001	0.08
Spiked with Hz	0.027 ± 0.006	0.26

4.7 Validation of plate method with CQ

The plate method was validated in CQS D10 *P. falciparum* inoculated with CQ. A full dose response profile was previously described for CQ using the flask method at several different concentrations in Chapter 3, allowing for direct comparison of results obtained with the established flask method and modified 24 well plate method. The effect on all three haem species, Hb, "free" haem and Hz was examined and compared to the data obtained with the original flask method (Figure 3-8).

Haem fractionation profiles:

The results achieved with the modified plate method paralleled the results obtained with the original flask method, producing a dose dependent increase in the % "free" haem with corresponding decrease in Hz in CQS *P. falciparum* inoculated with CQ (Figure 4-6). At high concentrations of CQ, corresponding to the highest "free" haem levels very few trophozoites survived after the 32-hour incubation period. Despite the similar trend, the modified plate method showed a more muted response for both the increase in % "free" haem and decrease in % Hz (Figure 4-6b, c, e and f). At 45 nM CQ the mean % "free" haem reached with the flask method was 15.3%, while the mean % "free" haem obtained with the modified plate method was 11.1%, an increase of 11.1% and 7.0% respectively above the untreated control. This muted response can be attributed to several factors. Firstly a decreased absorbance as a result of reduced starting material volumes for each sample, which is in turn associated with larger errors in the plate method. Secondly, small but significant sample losses occurred at each fractionation step during the transfer and separation of the supernatant and pellets. Nonetheless, as in the original flask method, the rise in "free" haem is correlated to the decline in the survival curve of the parasite (Figure 4-6g and h).

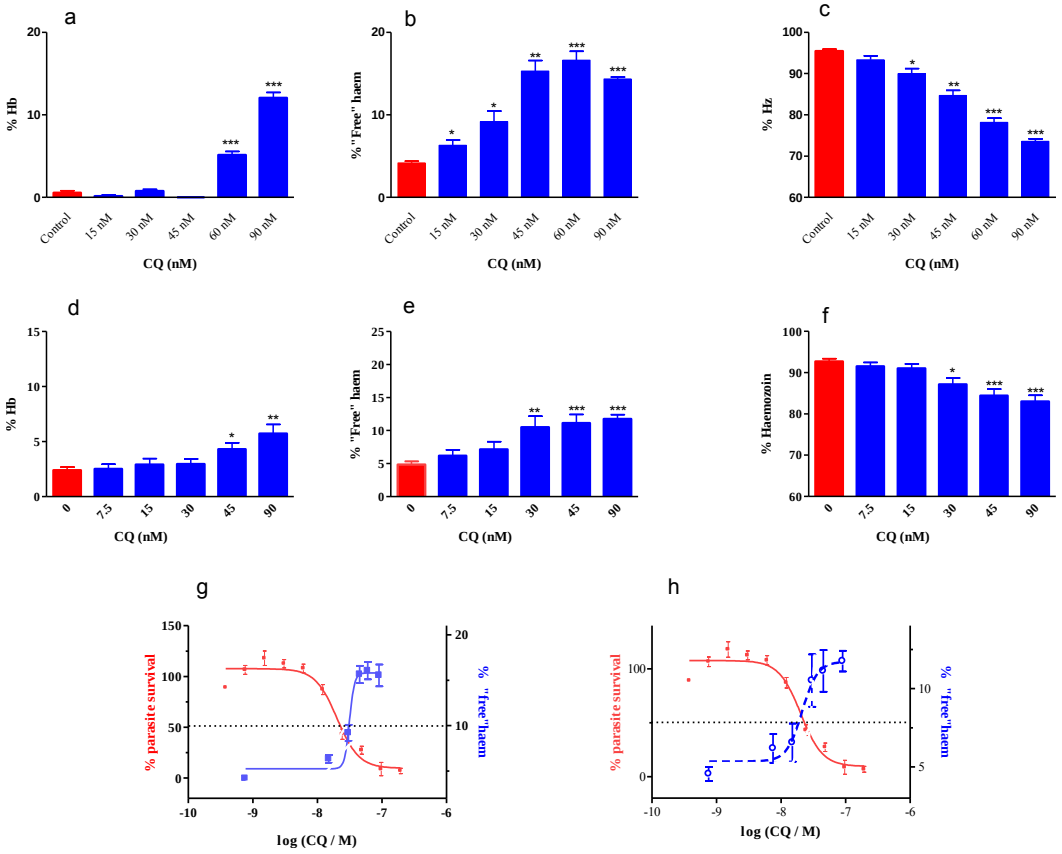

Figure 4-6: Graphs of % Hb (a), % "free" haem (b) and % Hz (c) obtained with the original flask method and % Hb (d), % "free" haem (e) and % Hz (f) obtained with the higher throughput 24-well plate method in isolated trophozoites with increasing concentrations of CQ (nM). Asterisks displayed on the graph indicate statistical significance relative to the control (95% CI) determined using a 2-tailed t-test (* P <0.05; ** P <0.01; *** P <0.001). The parasite survival curve with CQ, determined using a modification of the pLDH assay by Makler et al (red graph, left axis) is overlaid with the % "free" haem obtained using the original flask method (blue graph, right axis) (g) and modified plate method (---- blue graph, right axis) (h).[206] The parasite survival curve intersects each of the "free" haem curves at a point which corresponds closely to both the parasite growth IC_{50} and the halfway point of the increase in each of "free" haem graphs. Both methods show a dose dependent increase in % "free" haem and a decrease in % Hz, correlated to parasite death, although a more muted response is seen with the 24 well plate method. In all cases the scales of the parasite survival graph overlaid with "free" haem levels have been adjusted such that the 50% mark on the parasite survival y-axis coincides with the half way mark on the "free" haem y-axis.

Bland-Altman analysis:

Bland-Altman analysis was used to compare the new 24-well plate method to the established flask method, with respect to the percentage of each haem species determined.[232] The Bland-Altman method has been widely used in evaluating agreement between different methods of measurement and calculates the mean difference between two methods of measurement plotted against the mean and the 95% limits of agreement of the mean differences. [229 230] The criterion for agreement between two methods of measurement is that 95% of the differences between the two measurements should lie within the 95% limits of agreement and results are represented graphically in a Bland-Altman plot. [232 234 235] The Bland-Altman plots for each of % Hb, % "free" haem and % Hz are shown in Figure 4-7, where the difference in the result obtained with the established flask and modified plate method for each haem species is plotted against the mean of the result obtained with each method. The agreement between the two methods for both % "free" haem (Figure 4-7b) and Hz (Figure 4-7c) were good, showing narrow limits of agreement in comparison to the means. Hz however does show evidence of systematic error, bordering on the limits of the upper 95% limits of agreement for the three lowest mean percentages (Figure 4-7c). These borderline data points correspond to cells which were dosed at 90 nM CQ (greater than four times the IC_{50} of CQ) and the results are most likely associated with larger errors due to poor recovery at high drug concentrations. Hb showed much broader limits of agreement between the methods relative to the mean for each set of measurements (Figure 4-7a). In addition to the small sample volume used (2 ml), Hb is present in very small amounts in mature trophozoites resulting in low absorbance values for this haem species. The determination of Hb, specifically in the plate method was very often associated with large errors. In view of the good agreement for Hz and especially 'free' haem, the higher throughput plate method was subsequently used for further investigations and extended to several well know antimalarials.

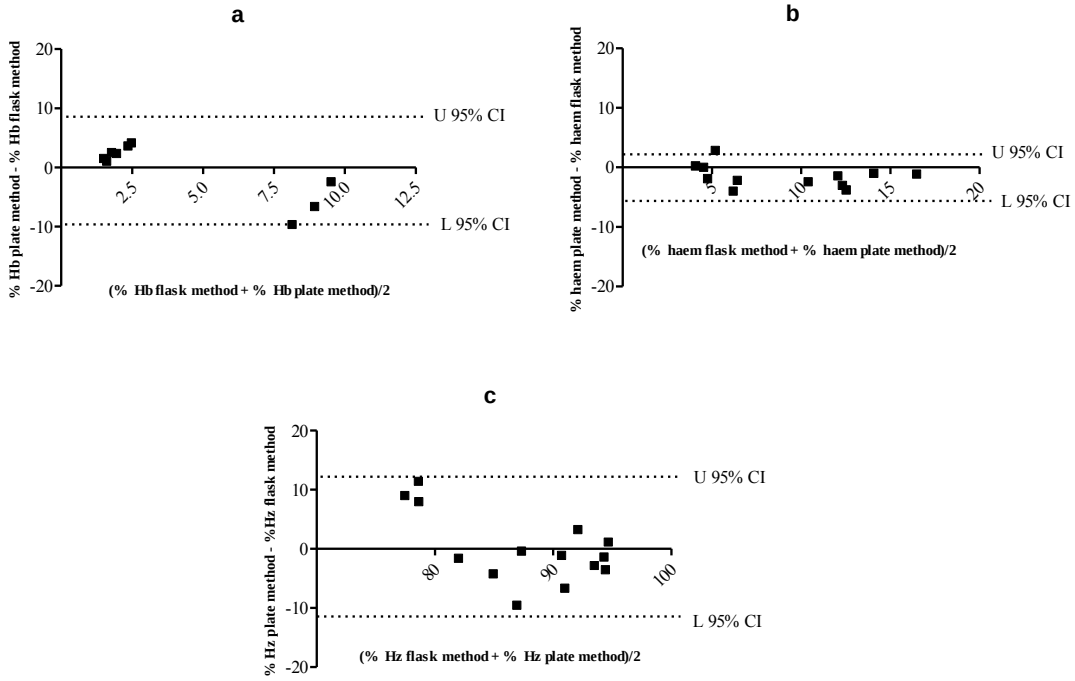

Figure 4-7: Bland-Altman statistical analysis was used to compare the results obtained with the original flask method and the higher throughput plate method. The difference in the result obtained with the flask and modified plate method was plotted against the mean of the result obtained with each method for % Hb (a), % "free" haem (b) and % Hz (c). The dotted lines in each graph represent the upper and lower 95% limits of agreement between the two methods. Before analysis, outliers were removed using the modified Thompson Tau test (n = 3 at each concentration).

Haem Fe per cell:

The amount of haem Fe per trophozoite (fg/cell) at each dose of CQ was determined from flow cytometry derived cell counts (Methods, 4.4.1). Counts of isolated trophozoites determined using flow cytometry did not differ statistically from those determined using a haemocytometer (Figure 4-6 and Table 4-6). In Chapter 3 it was shown that the total amount of haem Fe in CQ-treated isolated trophozoites was not statistically different to control trophozoites, isolated using the established flask method with haemocytometer cell counting. These results were confirmed in the current study where it was found that the total haem Fe in

CQ-treated trophozoite cells was statistically indistinguishable from control cells (Figure 4-8d). The haem fractionation profiles showing the amount of Hb (Figure 4-8a), "free" haem (Figure 4-8b) and Hz (Figure 4-8c) Fe per trophozoite with increasing CQ concentration followed the same trend as the corresponding percentage profiles seen in Figure 4-6d, e and f. Similarly an overlay of the parasite survival curve with the amount of "free" haem Fe per trophozoite shows an increase in the amount of "free" haem per cell correlated to cell death (Figure 4-8e) with both graphs intersecting at a point corresponding to 50% parasite survival.

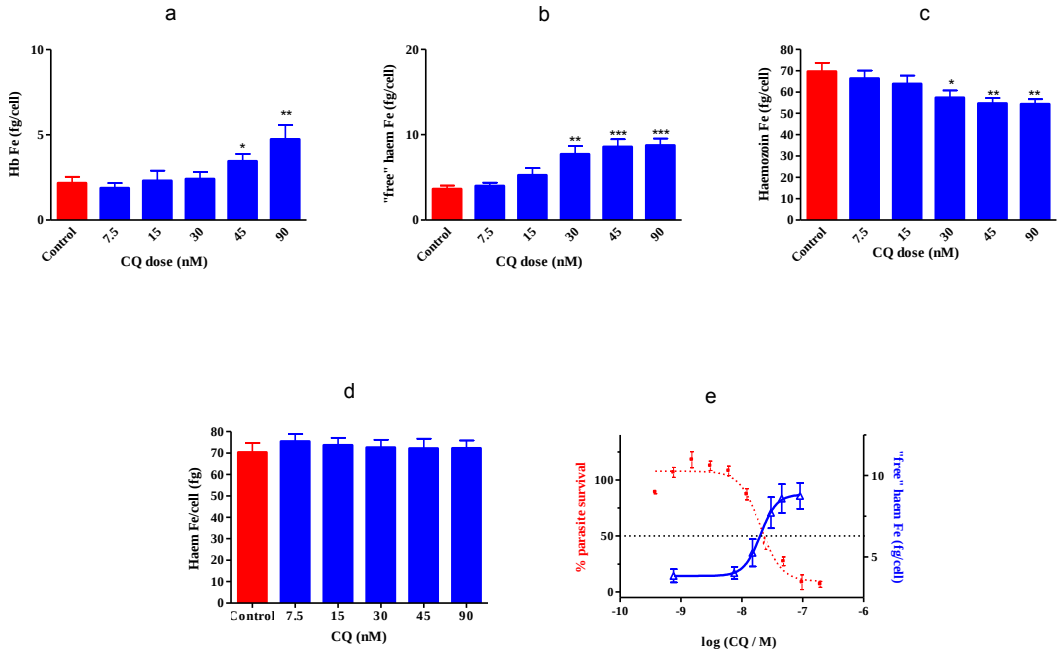

Figure 4-8: Haem fractionation profiles for CQ. The amount of Hb (a), "free" haem (b) and Hz (c) expressed in terms of the amount of haem Fe (fg) per isolated trophozoite with increasing concentrations of CQ (nM). The total haem Fe per cell (fg) for the CQ-treated isolated trophozoites was not statistically different to the control (d). Asterisks displayed on the graph indicate statistical significance relative to the control (shown in red) at the 95% CI, determined using a 2-tailed t-test (* P <0.05; ** P <0.01; *** P <0.001). The parasite survival curve with CQ, determined using a modification of the p-LDH assay by Makler et al (red graph, left axis) is overlaid with the amount of "free" haem Fe (fg) per cell (blue graph, right axis) as a function of CQ concentration (nM).[206] In all cases the scales of the parasite survival graph overlaid with "free" haem have been adjusted such that the 50% mark on the parasite survival y-axis coincides with the half way mark on the "free" haem y-axis.

4.8 Antimalarial testing

4.8.1 Amodiaquine

The haem fractionation assay was previously applied to the 4-aminoquinoline AQ at a single concentration only using the original flask method in Chapter 3. Closely related to CQ, AQ is speculated to share the same the same mechanism of action and has been shown to inhibit βH formation with the NP-40 detergent mediated βH inhibition assay.[105] Preliminary results shown in Chapter 3 for "free" haem performed on parasites treated with AQ at 2.5× the parasite growth inhibition IC_{50} showed an increase in "free" haem significantly different to the control. A full dose response study at several different concentrations of AQ was performed using the modified higher throughput 24 well plate haem fractionation assay. The results of this study confirmed that AQ, like CQ was a Hz inhibitor, causing a dose related increase in "free" haem accompanying parasite death (Figure 4-9a-f). Again as in the case of CQ, no statistical difference was found in total haem Fe/trophozoite (fg/cell) between the control and AQ-treated samples (Figure 4-9g). This result made it possible to use the percentage values of "free" haem (Figure 4-9a) and Hz (Figure 4-9b) as a direct indication of the effect of AQ on each of the haem species, as was the case for CQ (Figure 4-6d, e, f and 4-8a, b, c). The profiles for the amount of "free" haem Fe/trophozoite (fg) and Hz Fe/trophozoite (fg) with increasing AQ concentration (Figure 4-9c and d) mirror the profiles obtained with the percentage values of the corresponding haem species (Figure 4-9a and b).

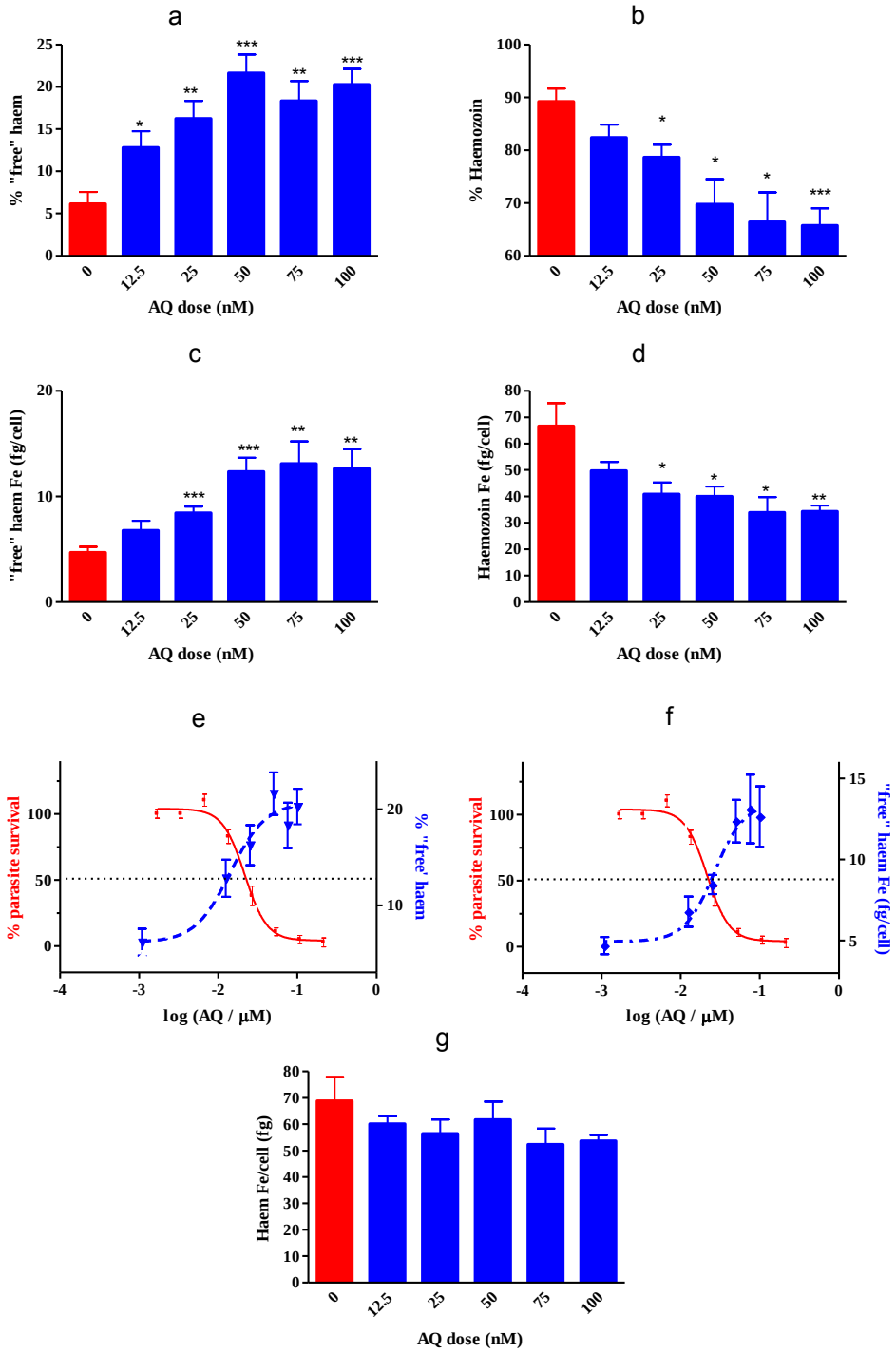

Figure 4-9: Haem fractionation profiles for AQ. The % "free" haem (a) and % Hz profiles (b) with increasing concentrations of AQ (nM) obtained using the modified 24 well plate haem fraction assay. The trend of increasing "free" haem and decreasing Hz with increasing AQ concentrations in isolated trophozoites is mirrored in the profiles for the amount of "free" haem Fe (fg/cell) (c) and amount Hz Fe (fg/cell) (d). Asterisks displayed on the graph indicate statistical significance

relative to the control (shown in red) at the 95% CI, determined using a 2-tailed t-test (* P <0.05; ** P <0.01; *** P <0.001). An overlay of the parasite survival curve determined with AQ using a modified method of Makler et al (red graph, left axis) with the % "free" haem (e) (--- blue graph, right axis) and amount of free haem Fe (fg) per cell (f) (- · - · blue graph, right axis) in both cases show decreased parasite survival is correlated to an increase in "free" haem.[206] In all cases the scales of the parasite survival graph overlaid with "free" haem have been adjusted such that the 50% mark on the parasite survival y-axis coincides with the half way mark on the "free" haem y-axis. The total haem Fe per cell (fg) for the AQ-treated isolated trophozoites was not statistically different to the control (g).

4.8.2 Pyrimethamine

The non βH inhibiting antimalarial PYR, known to interfere with folate synthesis was used as negative control in the modified 24 well plate haem fractionation assay. [184] [105] [194] As discussed in Chapter 3, PYR showed no increase in the % "free" haem or decrease in % Hz when tested at 2.5× its parasite growth inhibition IC_{50}.[107] Here, PYR was tested at 5 different concentrations, from 0.5× up to a maximum of 4× its parasite growth inhibition IC_{50} using the 24 well plate haem fractionation assay. The haem fractionation profiles for the % of "free" haem and % Hz as well the amount of "free" haem and Hz expressed in terms of fg haem Fe per isolated trophozoite are shown in Figure 4-10a-d. At higher concentrations of PYR corresponding to 3× and 4× IC_{50}, the % "free" haem does show a statistically significant increase in % "free" haem compared to the control (Figure 4-10a). This increase in % "free" haem is however not dose related and is not accompanied by a decrease in % Hz (Figure 4-10b) which remains constant at all PYR concentrations. This statistically significant increase in % "free" haem is not replicated in the PYR profile for the amount of "free" haem Fe (fg) per isolated trophozoite, where all PYR treated cells were statistically indistinguishable from the amount of free haem in the untreated control (Figure 4-10c). Furthermore, the increase in the amount of "free" haem is significant only at the highest doses of PYR where the recovery of cells is known to be minimal and associated with a high degree of error. This data is consistent with the fact that that PYR is not a βH inhibitor.

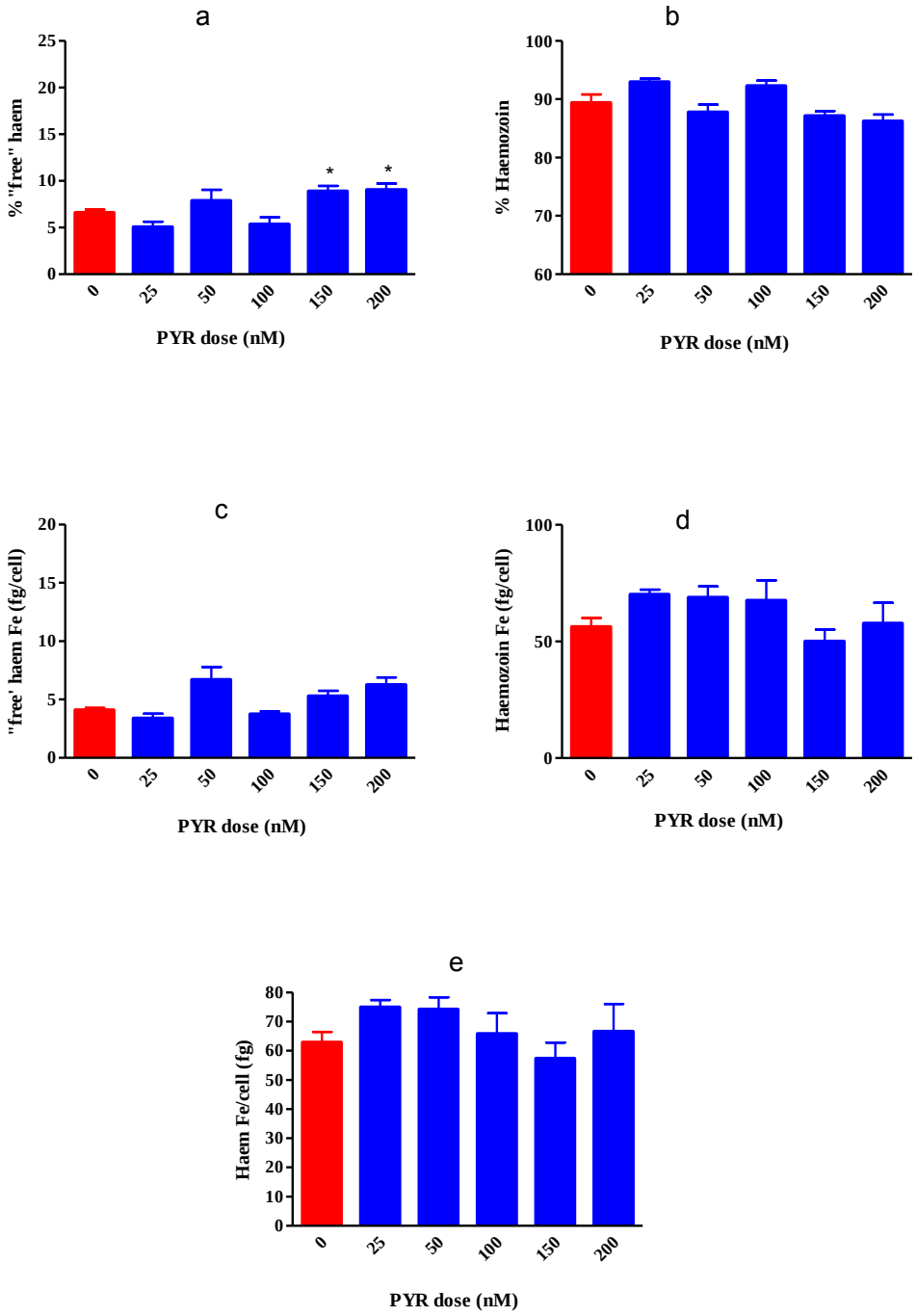

Figure 4-10: Haem fractionation profiles for PYR. The profiles for the % "free" haem (a) and % Hz (b) with increasing concentration of PYR emulates the profiles obtained for the amount of "free" haem Fe (fg) per cell (c) and Hz Fe (fg) per cell (d). Asterisks displayed on the graph indicate statistical significance relative to the control (shown in red) at the 95% CI, determined using a 2-tailed t-test (* P <0.05; ** P <0.01; *** P <0.001). The total haem Fe in untreated isolated trophozoite did not differ significantly from PYR treated isolated trophozoites (e).

4.8.3 Atovaquone

The 24 well plate haem fractionation method was also applied to ATV, an antimalarial which like PYR, has a mechanism of action which does not involve βH inhibition.[98] ATV exerts its antimalarial activity by selectively disrupting mitochondrial electron transport in the parasite by inhibiting the essential respiratory enzyme complex, cytochrome *bc1* without affecting host cell. [198 199] The mechanism of action of ATV is confirmed by the fact that ATV resistance coincides with mutations in the cytochrome *bc1* gene.[200] Surprisingly, unlike PYR, ATV clearly showed a significant dose dependent increase in % "free"' haem and decrease in % Hz (Figure 4-11a, b). Although the increase was less than that seen for both CQ and AQ at the equivalent IC_{50} values, it was nonetheless significant. Further investigation however, revealed statistically significant decreasing total haem Fe per trophozoite in ATV-treated cells, showing that treated cells accumulated less haem than control cells (Figure 4-11e). This is in contrast to results obtained for total haem Fe per trophozoite in CQ (Figure 4-8d), AQ (Figure 4-9g) and PYR (Figure 4-10e) treated cells, where cells treated with drug showed no significant difference to untreated cells. Despite the percentage increase in "free" haem with increasing ATV concentration, when the amount of "free" haem Fe per trophozoite (fg/cell) was calculated, it was found to remain constant with increasing dose, with no significant difference to the control (5.4 ± 1.6 fg Fe/cell), at the 95% CI (Figure 4-11c). The amount of Hz haem Fe per trophozoite (fg/cell) however decreases significantly in comparison to the untreated control (Figure 4-11d). The decrease in Hz is likely as a result of decreased Hb uptake and digestion secondary to treatment of cells with this drug. This result demonstrates the importance of determining the total haem Fe per cell, using cell counts with either a haemocytometer or flow cytometry. In the case of ATV, where the total haem Fe in treated cells was significantly less than the control (Figure 4-11e), the percentage values for each haem species are misleading (Figure 4-11a and b) and the amounts of each haem species per cell (Figure 4-11c and d) must be used. This approach demonstrated that there was no change in "free" haem and no relationship with inhibition of parasite growth in the case of ATV (Figure 4-11f).

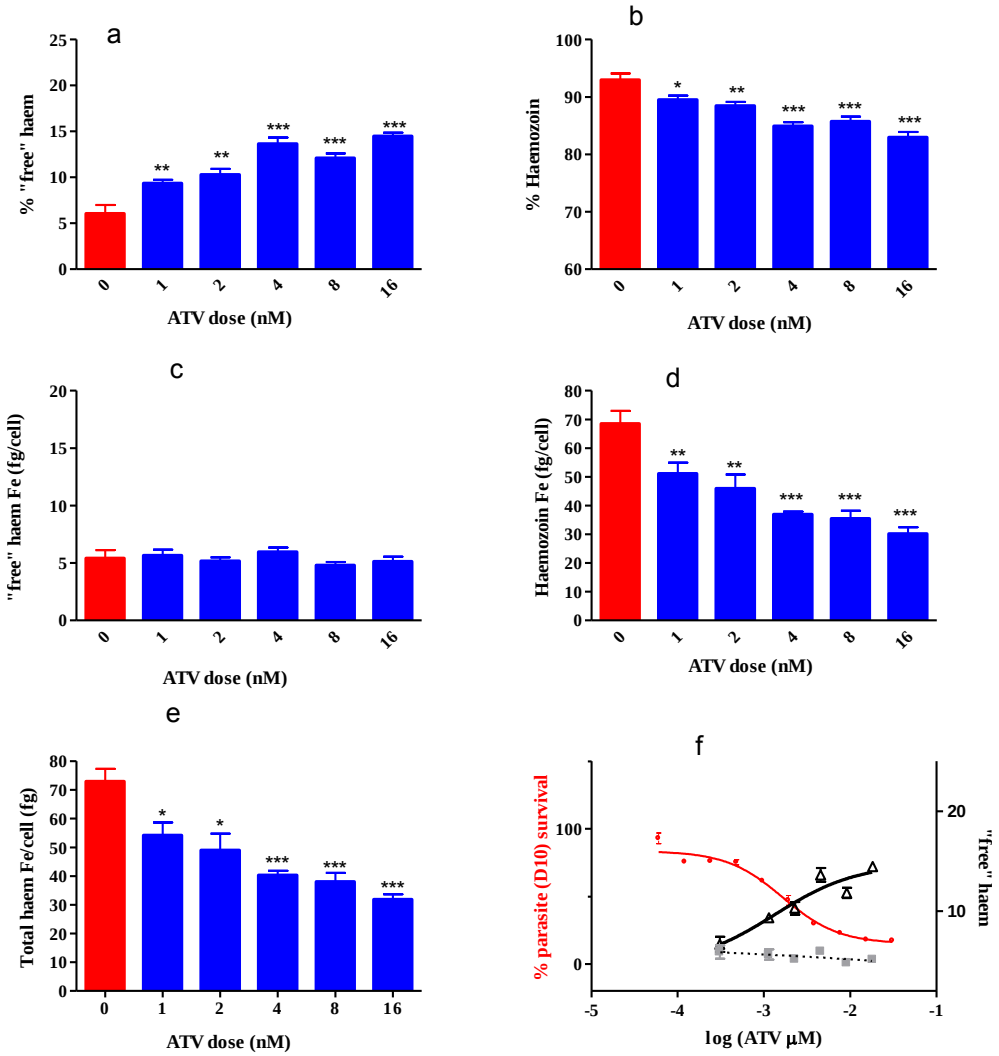

Figure 4-11: Haem fractionation profiles for ATV. The % "free" haem (a) and Hz (b) profiles show a statistically significant dose dependent response to increasing ATV concentrations. The amount of "free" haem Fe (fg) per cell shows no dose related increase in "free" haem (c) while the amount of Hz Fe (fg) per cell (d) again shows a significant dose related decrease in Hz with increasing ATV concentration in isolated trophozoites. The total amounts of haem Fe (fg) per cell decreases significantly with increasing ATV. An overlay of the parasite survival curve (red plot, left axis) with the % "free" haem (black plot, right axis) shows an apparent correlation between decreased parasite survival and increased free haem while no relationship in fact exists between the amount of "free" haem per trophozoite (grey plot, right axis) and parasite survival (f). The biological IC_{50} of ATV in CQS *P. falciparum*, D10 was determined to be 2.0 ± 0.8 nM using a modified version of the pLDH assay by Makler et al. [206]

4.8.4 Flow cytometry histograms

Flow cytometry histogram overlays (Figure 4-12) corresponding to trophozoites isolated after treatment with CQ (blue dotted line), PYR (purple solid line), AQ (orange solid line) and ATV (green solid line) at the 2× the parasite growth IC_{50} of each drug were overlaid to compare changes in cell morphology with drug treatment, to an untreated control (solid red line).The cells were compared using three parameters, forward scatter (FSC) to evaluate change in size (Figure 4-12a), side scatter (SSC) to evaluate change in complexity (Figure 4-12b) and SYBR green fluorescence (FL1) to evaluate the change in DNA (Figure 4-12c). Cells treated with PYR showed very little change in FSC and SSC, but did show a reduction in the amount of DNA compared to the control. Cells treated with CQ, AQ and ATV showed a similar reduction in all three parameters indicating that cells were less complex, smaller and contained less DNA than cells treated with PYR and the untreated control.

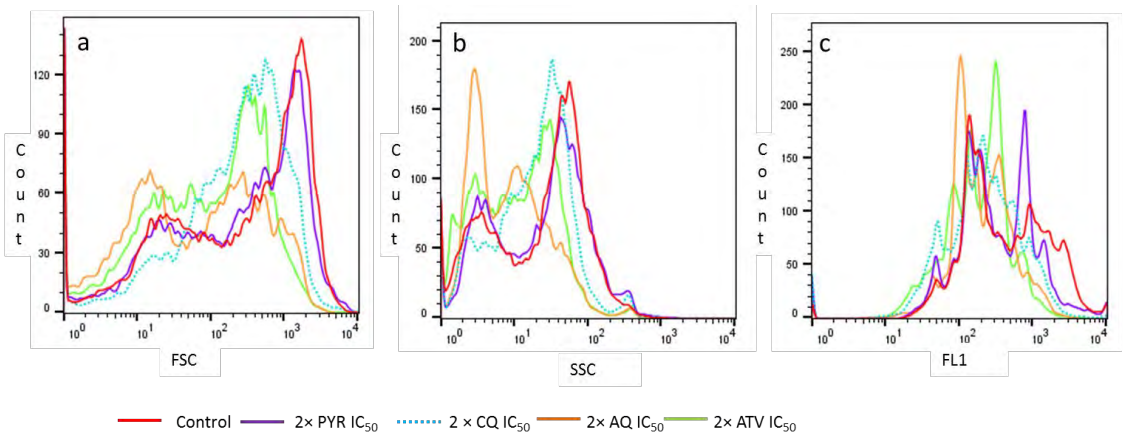

Figure 4-12: Change in morphology of PYR, CQ, AQ and ATV treated isolated, *P. falciparum* trophozoites. Trophozoites were isolated 32 h post inoculation at the ring stage with 2× the parasite growth IC_{50} of each drug. Flow cytometry histogram overlays displaying the change in FSC (a), SSC (b) and FL1 (c) for isolated untreated control trophozoites (solid red line), PYR treated isolated trophozoites (purple solid line), CQ treated isolated trophozoites (blue dotted line), AQ treated isolated trophozoites (orange solid line) and ATV treated isolated trophozoites (green solid line).

4.9 Summary and conclusions

The successful adaptation of the haem fractionation assay from a very low throughput method performed in 250 ml flasks with high demand on valuable parasite starting material to a more efficient process was achieved and validated using CQ as a model. This higher throughput haem fractionation assay performed in 24 well plates, using at most ten million trophozoites was validated against the original method using CQ and its robustness was confirmed. [107] Although the improved throughput plate method produced more muted sample responses than the established flask method, it is capable of reproducing the results obtained with the flask method using 24 times less starting material and increasing output by at least six-fold. A fluorescent flow cytometry-based technique for the determination of cell counts of isolated trophozoites was also developed. This new method of determining cell counts produced cell counts which were not statistically different to haemocytometer determined cell counts and provided a faster alternative to traditional manual methods of cell counting. Flow cytometry histograms allowed changes in cell morphology to be compared in terms of size, complexity and the amount of DNA present in cells.

The plate method was subsequently applied to three other established antimalarials, AQ, PYR and ATV, providing rapid and valuable insight into the mechanistic action of antimalarials and has highlighted the important role which haem plays in the action of several drugs. AQ was shown to inhibit Hz formation, while the antifolate PYR and the mitochondrial electron transporter inhibitor ATV demonstrated no increase in toxic cellular free haem. Results with ATV emphasize the crucial importance of measuring haem levels per cell, a calculation which requires the determination of the cell count in each well of the 24-well plate, rather than just percentages of haem species in order to interpret the effects of drugs on parasite haem concentrations. This approach is essential in those cases where the total haem Fe per cell changes with drug dose. While initial results for ATV showed an unanticipated increase in the percentage of “free” haem with increasing ATV concentration, the total amount of haem iron per cell was found to be significantly less in cells treated with ATV. This corresponds to unchanged free haem per cell with increasing ATV concentration.

This higher throughput cellular haem fractionation assay can easily be applied to novel antimalarials with a significantly decreased lead time, providing a valuable tool with which to probe the mechanisms of action of both new and established antimalarials. Applied to novel compounds, this method will provide an important cellular complement to the existing detergent-mediated βH inhibition assay in improving understanding of mechanism of action and in exploring structure activity relationships and prospects for rational drug design.

5 THE HAEM FRACTIONATION PROFILES OF SEVERAL CLINICALLY RELEVANT ANTIMALARIALS

5.1 Introduction

The relationship between haem and several well-known antimalarials is explored in detail in this chapter. In Chapter 3, as an initial investigation the percentage of haem species in isolated CQS *P. falciparum* trophozoites inoculated at a single drug concentration of each of QN, MQ, LF and ART was determined. All showed an increase in the percentage "free" haem and decrease in percentage Hz significantly different to the untreated control. However, with the exception of LF, none showed an increase in percentage "free" haem or decrease in percentage Hz statistically comparable to CQ at the equivalent dose relative to their respective parasite growth IC_{50} values. This investigation was preliminary and to ascertain whether Hz inhibition is essential to the mechanism of action, a full dose response study at several concentrations of each drug is required.

In Chapter 4 the importance of determining the amount of each haem species per cell was demonstrated using ATV (Figure 4-11). Cells treated with ATV showed a significant dose related decrease in the total haem Fe per cell (Figure 4-11e). Therefore, while the percentage of each haem species suggested that ATV acted as Hz inhibitor, taking into account the decrease in total haem Fe it was demonstrated that ATV has no effect on free haem levels and therefore is unlikely to be a direct Hz inhibitor. Classifying a compound as a Hz inhibitor therefore requires determination of the amount of each haem species per cell. Throughout this chapter a compound is defined as a direct Hz inhibitor when a decrease in the amount of Hz per cell is accompanied by an increase in the amount toxic "free" haem per cell which can be correlated to the survival of the parasite. All compounds which showed evidence of putative Hz inhibition in Chapter 3 were assayed using the higher throughput haem fractionation method described in detail in Chapter 4.

This chapter describes in detail the full haem fractionation profiles for 6 well known antimalarials: QN, QD, MQ, LF, PQ and ART. The AMN derivative, 10-dO-AMN was also tested. The amount of each haem species in drug treated isolated trophozoites was determined and is supplemented with images of Giemsa stained slides and flow cytometry profiles of isolated treated trophozoites highlighting

differences in cell morphology. The results provide valuable insights, confirming or excluding Hz inhibition as the likely mechanism of action of these antimalarials.

5.2 Materials

All materials used throughout this chapter are listed in Chapter 2. Materials were of AR grade or higher and used without further purification.

5.3 Sample Preparation

The preparation of all samples used throughout this chapter, are previously described in Chapters 2 and 3. The water used throughout this work was double distilled deionised Millipore® Direct-Q water.

5.4 Methods

The methods used in this chapter, are previously described in Chapters 2, 3 and 4.

5.5 Results and Discussion

5.5.1 Determination of the parasitic growth inhibition IC_{50} in *P. falciparum*

The parasite growth IC_{50} values of the clinically relevant antimalarials investigated in this chapter were determined in a CQS strain of *P. falciparum*, D10 or NF54. The D10 strain was used for all initial investigations while the NF54 strain was used for subsequent studies after being adopted as the standard CQS strain in the Division of Pharmacology. The similarity between the two CQS strains was verified by determining parasite growth IC_{50} values in NF54 for CQ and AQ and comparing it to values obtained in D10. The parasite growth IC_{50} values for CQ and AQ were

determined in NF54 to be 11.7 ± 2.7 nM and 18 ±0 .4 nM respectively. These values fall into the range of parasite growth IC_{50} values determined in D10 for CQ and AQ to be 11 – 25 nM and 14 – 19 nM (95% CI) respectively (Table 3-1). All parasite growth IC_{50} values were determined using a modification of the pLDH assay described in detail in Chapter 2, previously published by Makler et al.[206] The parasite survival curves were generated using GraphPad Prism 4.0 non-linear regression function (sigmoidal dose response equation). [203]

Table 5-1: The parasite growth IC_{50} values (nM) of several clinically relevant antimalarials were determined in a CQS strain (D10 or NF54) of *P. falciparum*. The *P. falciparum* strain used is indicated in brackets next to each compound tested. All values were determined using the pLDH assay.[206] Results are expressed as the mean with the associated standard deviation of several repeat experiments.

Compounds tested	**Mean IC_{50} value with SD (nM)**
Artesunate (D10)	7.6± 1.8 (n=3)
10-deoxoartemisinin (NF54)	8.6 ± 2.3 (n=11)
Lumefantrine (D10)	27.1 ± 3.3 (n=8)
Quinine (D10)	142 ± 18.8 (n=8)
Quinidine (D10)	40.8 ± 3.9 (n=6)
Mefloquine (NF54)	10.43 ± 1.95 (n=4)
Primaquine (NF54)	3120 ± 890 (n=4)

The measured parasite growth IC_{50} values summarised in Table 5-1 were used to determine the concentrations at which to inoculate cultures for the haem fractionation assay. The *P. falciparum* strain in which the parasite growth IC_{50} was determined (indicated in brackets next to each compound tested in Table 5-1) was used in the subsequent haem fractionation assay.

5.5.2 Arylmethanols

It is widely assumed that QN, QD, MQ and LF investigated here target Hz formation, resulting in increased levels of toxic haematin eventually leading to cell death through oxidative stress and membrane damage. [51 57] Both the 4-aminoquinolines,

CQ and AQ tested in Chapters 3 and 4 unequivocally showed concentration dependent increased "free" haem levels and decreased Hz formation correlated to cell death and can be classed as Hz inhibitors. Like CQ and AQ; QN, QD, MQ and LF all act on the intraerythrocytic asexual stage of the *P. falciparum* lifecycle and several studies have demonstrated a strong relationship between their ability to inhibit βH formation and parasite growth inhibition in a CQS strain of *P. falciparum.* [106 107 52 69 101 184] However, unlike the 4-aminoquinolines it is not certain that the above mentioned antimalarials primarily target the haem detoxification pathway and drug targets other than Hz inhibition have been implicated in the mechanism of action of several arylmethanols.[58 79]

5.5.2.1 Quinine

The least active arylmethanol tested, QN, was shown to have a parasite growth IC_{50} of 142 ± 18.8 nM in a CQS strain of *P. falciparum* (Table 5-1). In Figure 3-9 QN was shown to cause a significant increase in the percentage "free" haem and decrease in percentage Hz in isolated trophozoites treated with 2.5× the parasite growth IC_{50} of QN in comparison to an untreated control. This increase in percentage "free" haem of QN treated cells was significantly less than in cells treated with CQ (Figure 3-9). The structures of the Fe(III)PPIX complexes formed with both QN and QD have been elucidated using single crystal X-ray diffraction. It is proposed that the formation of Fe(III)PPIX-QN prevents detoxification of Fe(III)PPIX by inhibiting its incorporation into inert Hz crystals within the malaria parasite.[118] The biologically active stereoisomer of QN, QD (IC_{50} value of 40.8±3.9 in CQS D10) efficiently inhibits βH formation while the stereoisomers 9-epiquinine (9-EQN) and 9-epiquinidine (9-EQD), found to be 100 fold less active than QN and QD in a CQS strain of *P. falciparum* have been shown to be very weak inhibitors of βH formation. The correlation between biological IC_{50} and βH formation in this set of compounds differing only in their stereochemistry further strengthens the argument that Hz inhibition is the mechanism of action of both QN and QD. [66 69 118 236]

Images of Giemsa stained slides of a control population of trophozoites (Figure 5-1a) compared to QN treated cells (Figure 5-1b) show that QN treated cells had

matured to trophozoites smaller than the control population. Flow cytometry histogram overlays (Figure 5-1c - e) corresponding to trophozoites isolated after treatment with QN (solid green line) or CQ (blue dotted line) at the highest concentration tested for each drug showed a larger population of smaller (FSC), less complex (SSC) cells present in cultures treated with QN at 5× the parasite growth IC_{50} compared to cells treated at 6× the parasite growth IC_{50} of CQ (Figure 5-1d, e). The SYBR Green profiles (FL1, Figure 5-1c) representing the populations of CQ and QN treated cells show that QN treated cells contained slightly more DNA than CQ treated cells, indicating that decreased complexity cannot be attributed to a decrease in the amount of DNA in QN treated cells. Despite the fact that the flow cytometry profiles for QN correspond to cells which were treated at a lower relative dosage (5× the parasite growth IC_{50}), the change in the morphology of QN treated cells, specifically the reduced complexity is more pronounced than CQ treated cells at a higher relative dose (6× the parasite growth IC_{50}). The differences in cell morphology between CQ and QN treated cells therefore suggest the effects of the drug within the cell are somewhat different.

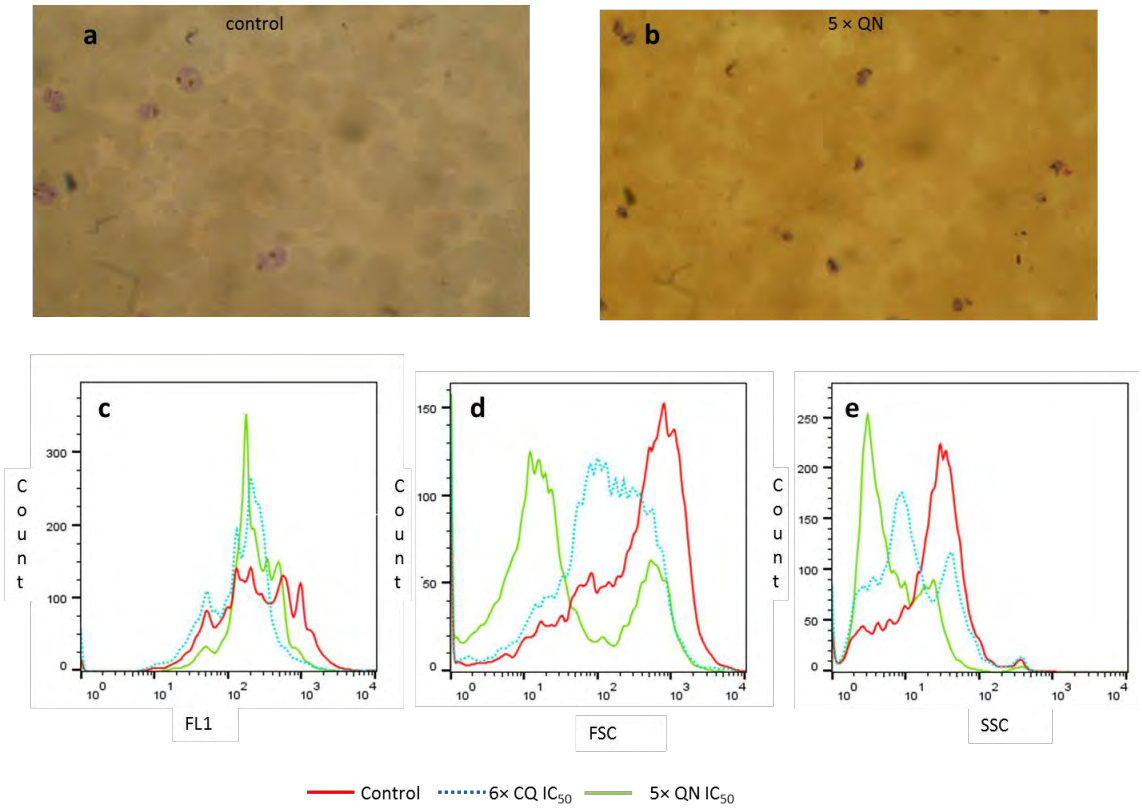

Figure 5-1: Change in morphology of QN treated isolated D10, *P. falciparum* trophozoites. Trophozoites were isolated 32 h post inoculation at the ring stage with 5× and 6× the parasite growth IC_{50} of QN and CQ respectively, corresponding to the highest concentration at which both QN and CQ were tested. The image of the Giemsa stained slide of the control culture (a) shows the presence of large, mature trophozoites, while the image of the QN treated culture (b) shows trophozoites which appear smaller than the control (100× objectification). This result is confirmed upon examination of the flow cytometry histogram overlays displaying the change in fluorescence intensity (FL1) (c), change in FSC (d) and change in SSC (e) for isolated untreated control trophozoites (solid red line), CQ treated isolated trophozoites (blue dotted line) and QN treated isolated trophozoites (green solid line). A clear shift towards cells containing less DNA (FL1, c), less complex (SSC, e) and smaller (FSC, d) cells can clearly be seen in QN and CQ treated cells compared to untreated control cultures. While plots corresponding to the amount of DNA present in CQ and QN treated cells are very similar, QN treated cells are smaller (d) and show a greater decrease in cell complexity (e) compared to CQ treated cells.

Unlike CQ treated *P. falciparum*, where a significant increase in the amount of "free" haem Fe (fg) per cell was seen at 2× the parasite growth IC_{50} of CQ (Figure 4-8b), QN produces a statistically significant ($P < 0.05$) increase in the amount of "free" haem and decrease in the amount of Hz Fe in isolated trophozoites only at 5× the parasite growth IC_{50} of QN (Figure 5-2b, c). The amount of Hb Fe (fg) per cell (Figure 5-2a) shows no significant change with increasing QN concentration, however a relatively large amount of scatter in the data makes evaluation difficult. Figure 5-2d shows the total haem Fe (fg) per cell decreases systematically, with increasing QN concentrations greater than 2.5× the parasite growth IC_{50}, however the decrease in the total Haem Fe (fg) per cell is only statistically significant relative to the control at the highest concentration of QN tested. An overlay of the amount of "free" haem Fe (fg) per cell with the parasite survival curve for QN (Figure 5-2e) shows that although the increase in the amount of "free" haem is small and not statistically significant relative to the control at lower concentrations of QN, the increase in "free" haem does appear to be systematically correlated with parasite survival. Therefore while QN does appear to cause Hz inhibition the effect is not as pronounced as seen in both CQ and AQ (Figure 4-8, 4-9). The amount of "free" haem starts to increase more rapidly at a point where parasite survival is low, at approximately 15% parasite survival. It has been speculated that unlike the 4-aminoquinolines, the quinoline methanols have a drug target other than Hz inhibition. [58] [79] Treatment of *P. berghei* infected mice with a range of antimalarials showed that while CQ and 4-aminoquinoline derivatives caused a decrease in the amount of Hz produced, QN, MQ and PQ showed no effect. [127] In comparison to CQ, both QN and MQ have been shown to have a different effect on the endocytic pathway.[58] CQ was found by Hoppe and co-workers to inhibit trafficking of Hb-laden transport vesicles resulting in increased Hb accumulation of 283% and the TEM images showed an accumulation of Hb transport vesicles in the cell. In comparison MQ and QN were shown to inhibit endocytosis resulting in reduced Hb accumulation of 83% and 64% respectively. [124] [125] In Chapter 4, CQ treated cells at 3× the parasite growth IC_{50} showed an increase in Hb levels of 60%. While previous studies have shown reduction in the amount of Hb in QN treated cells, Figure 5-2a showed no evidence of this, although the scatter in the Hb data for QN makes establishment of a firm trend difficult. [124] [125] The accumulation of transport vesicles in cells treated with high doses of CQ can explain why the flow cytometry

histograms of CQ treated cells are greater in both complexity and size compared to cells treated with QN (Figure 5-1d, e). QN has been shown to be highly lipophilic, binding tightly to serum components and has been shown to bind to phospholipids possibly affecting membrane formation and the consequent formation of transport vesicles resulting in reduced Hb uptake, while CQ has been shown to have a low affinity for phospholipids.[237 238 239 57] Despite evidence of βH inhibition and the formation of a QN-Fe(III)PPIX complex speculated to be capable of inhibiting Hz formation, the results show that classifying QN as a Hz inhibitor is not as definitive as is the case for the 4-aminoquinolines CQ (Figure 4-6 and 4-8) and AQ (Figure 4-9). It is probable that in addition to inhibiting Hz formation accompanied by a small dose related increase in "free" haem in the parasite, QN may either have other drug targets or the complex is exceptionally active against the parasite, possibly accounting for the reported inhibition of endocytosis.

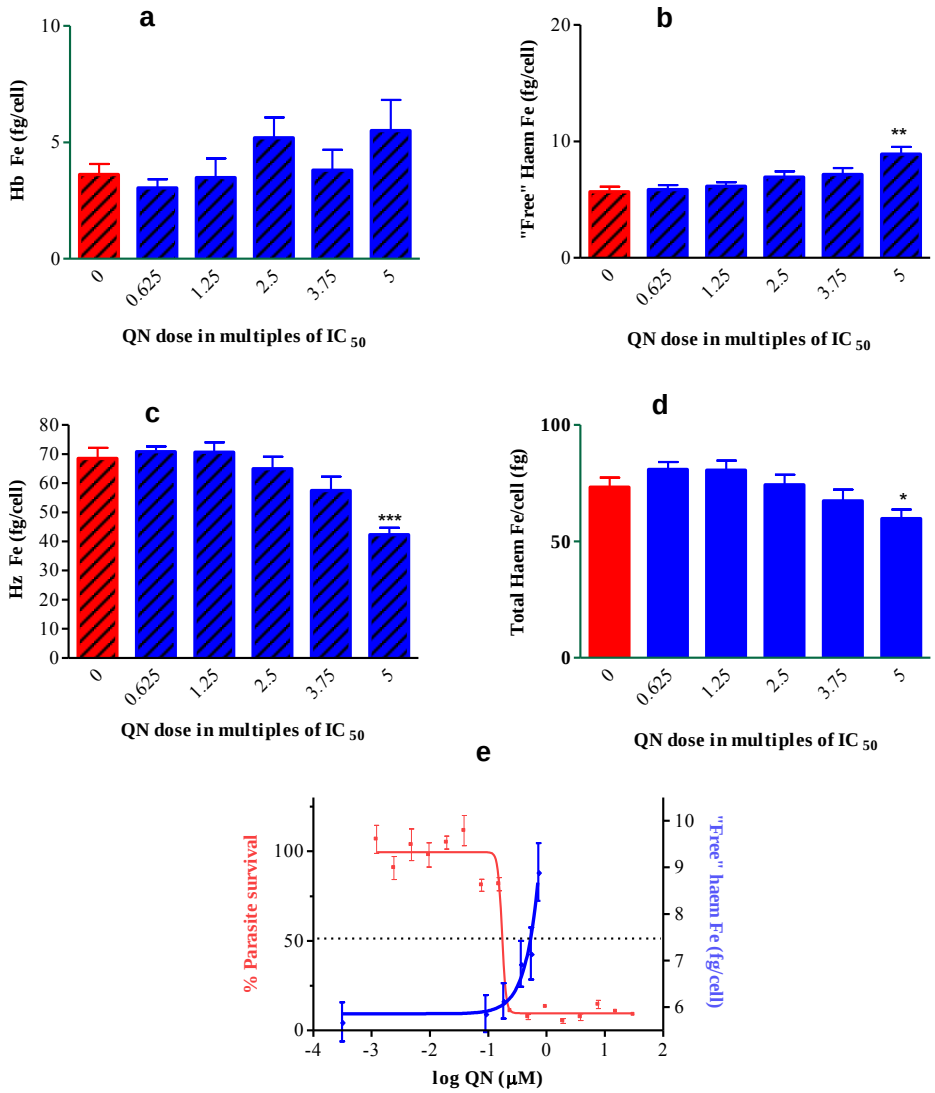

Figure 5-2: Haem fractionation profiles for QN in D10, CQS *P. falciparum*. The profiles obtained for the amount of Hb Fe (fg) per cell (a), "free" haem Fe (fg) per cell (b) and Hz Fe (fg) per cell (c) are shown as a function of increasing multiples of the parasite growth IC_{50} of QN. The total haem Fe in untreated isolated trophs did not differ significantly from QN treated isolated trophozoites, except at the highest concentration (d). An overlay of the parasite survival curve (red plot, left axis) with the amount of free haem (fg) per cell (blue plot, right axis) representing the amount of "free" haem per cell (fg) shows that "free" haem Fe (fg/cell) increases at a point corresponding to low parasite survival (e).

5.5.2.2 Quinidine

A stereoisomer of QN, QD, is a more potent inhibitor of *P. falciparum* growth with a parasite growth IC_{50} value of 40.8 ± 3.9 nM, compared to 142 ± 18.8 nM for QN in CQS D10 (Table 5-1). However, its cardiotoxicity makes it a less desirable antimalarial. [78] QD was selected since like QN, it has also been assumed to share a similar mechanism of action to CQ and AQ. [54 202] Although the effect of QD on haem species in CQS isolated trophozoites was not investigated at a single concentration in Chapter 3, it has been shown to inhibit the formation of βH on several occasions. [52 240 208 69] Like QN, QD has been shown to form a complex with Fe(III)PPIX through a three point interaction involving co-ordination, π-stacking and intramolecular hydrogen bonding making the haem propionate group of Fe(III)PPIX unavailable and consequently preventing the incorporation of Fe(III)PPIX into Hz. Molecular modelling of Fe(III)PPIX complexes with QN, QD and their inactive stereoisomers 9-EQN and 9-EQD showed a correlation between the ease of formation of the intramolecular hydrogen bond in these complexes and both the biological and βH inhibition activities in this group of stereoisomers. [117]

Flow cytometry histograms (Figure 5-3) corresponding to populations of isolated trophozoites inoculated with 4.0× the parasite growth IC_{50} of QD (solid green line) and 3.75 × the parasite growth IC_{50} of QN (solid orange line) show the profiles for the amount of DNA present in cells (Figure 5-3a), the size (Figure 5-3b) and complexity (Figure 5-3c) of cells are almost identical. The changes in cell morphology of QN and QD treated populations are therefore very similar to each other and also differ in the same manner from CQ treated cells (blue dotted line). Flow cytometry histogram plots of cells treated with QD at 4.0× the parasite growth IC_{50} compared to cells treated 6.0× the parasite growth IC_{50} of CQ showed that QD treated cells are smaller (Figure 5-3b) and less complex (Figure 5-3c) but contain more DNA (Figure 5-3a) than CQ treated cells. As suggested for QN versus CQ the increased cell complexity in CQ treated cells compared to QD treated cells, can probably be attributed to the accumulation of Hb transport vesicles correlated to increased Hb levels in the case of CQ treatment. [124]

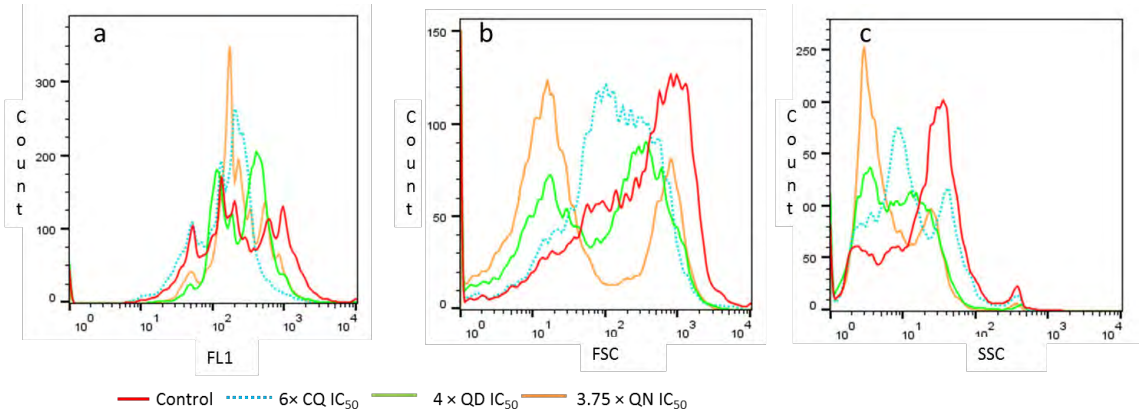

Figure 5-3: Change in morphology of QD treated isolated D10, *P. falciparum* trophozoites. Trophozoites were isolated 32 h post inoculation at the ring stage with 4× and 6× the parasite growth IC_{50} of QD and CQ respectively, corresponding to the highest concentration at which both QD and CQ were tested. Flow cytometry histogram overlays displaying the change in fluorescence intensity (FL1) (a), FSC (b) and SSC (c) for isolated untreated control trophozoites (solid red line), CQ treated isolated trophozoites (blue dashed line) and QD treated isolated trophozoites (green solid line). QN treated isolated trophozoites inoculated at 3.75× the parasite growth IC_{50} of QN is shown for comparison (solid orange line). A clear shift towards cells containing less DNA (FL1, c), less complex (SSC, e) and smaller (FSC, d) cells can clearly be seen in QD and CQ treated cells compared to untreated control cultures.

QD treatment results in a significant decrease of Hb levels from 3× the parasite growth IC_{50} (Figure 5-4a) and a significant dose related decrease in the amount of Hz and the total haem Fe (fg) per cell from as low as 0.5× the parasite growth IC_{50} of QD (Figure 5-4c, d). A significant increase in the amount of "free" haem from 1.0× the parasite growth IC_{50} of QD is seen in Figure 5-4b to a maximum of 35% relative to the control. As in the case of QN, direct Hz inhibition in QD is not as obvious as for both CQ and AQ (Figure 4-8, 4-9). An overlay of the parasite survival curve for QD (red plot, right axis) with the amount of "free" haem Fe (fg) per cell (blue plot, left axis) in Figure 5-4e shows that despite a small increase in "free" haem levels in QD treated cells, a dose responsive relationship exists between parasite survival and "free" haem levels. QD therefore does appear to behave as a Hz inhibitor. However, it is likely that Hz inhibition is not the only effect of QD and

given their similar physiochemical properties and similar morphological changes after treatment (Figure 5-3), it can be assumed that QD shares the mechanism of endocytosis inhibition with its stereoisomer QN, but also has an effect on the formation of Hz resulting in significantly higher levels of "free" haem correlated to parasite survival. As in the case of QN, the increase in "free" haem is not as pronounced as for the 4-aminoquinolines CQ and AQ. Inhibition of endocytosis results in decreased Hb accumulation, which in turn reduces the amount of haem available for conversion to Hz. Therefore although inhibition of Hz formation and the consequent build-up of "free" haem takes place in QD treated cells the manifestation appears to be diminished due to reduced Hb uptake.

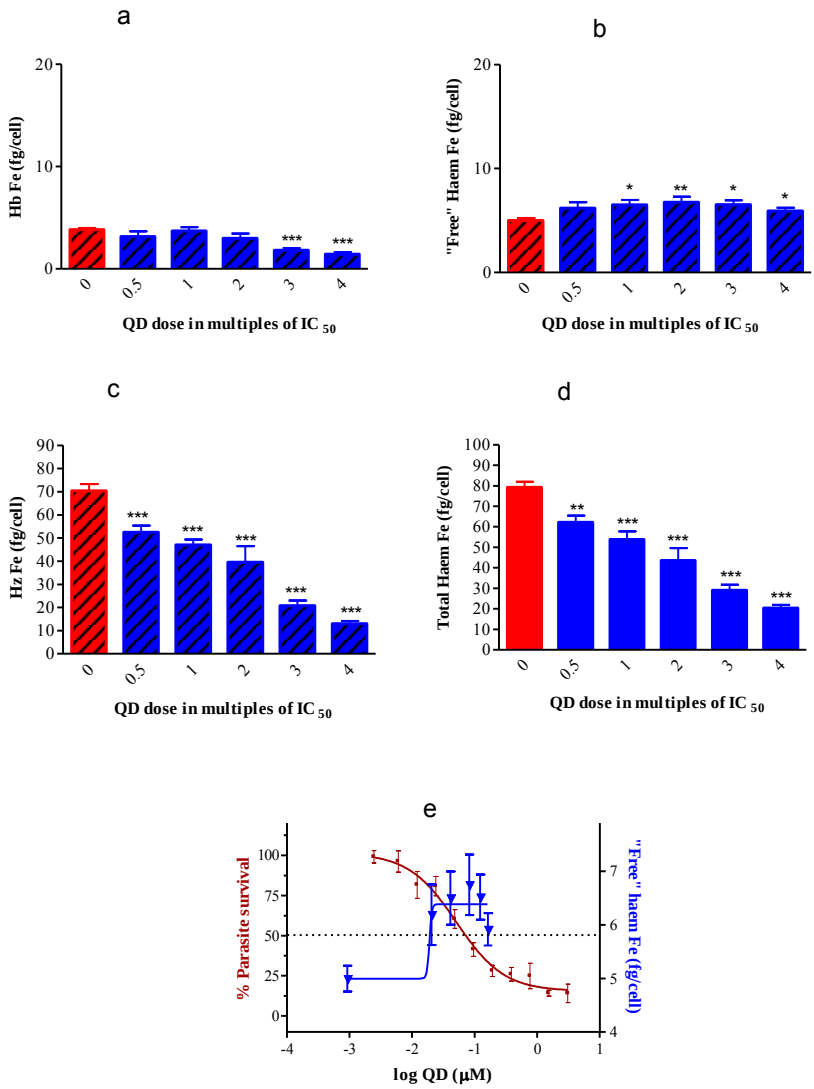

Figure 5-4: Haem fractionation profiles for QD in D10, CQS *P. falciparum*. The profiles for the amount of Hb Fe (fg) per cell (a), "free" haem Fe (fg) per cell (b) and Hz Fe (fg) per cell (c) are shown as a function of increasing multiples of the parasite growth IC_{50} of QD. The total haem Fe in QD treated isolated trophs differed significantly from untreated isolated trophozoites, decreasing with increasing concentration of QD (d). An overlay of the parasite survival curve determined with QD using a modified method of Makler et al (red plot, right axis) with the amount of "free" haem Fe (fg) per cell (blue plot, left axis) shows parasite survival decreases with increasing "free" haem in a dose responsive manner (e) [206]. The left axis displaying the amount of "free" haem Fe (fg) per cell is scaled such that the point corresponding to 50% survival (red plot, right axis) on the parasite survival curve corresponds to the halfway point in the graph of the amount of "free" haem Fe (fg) per cell (blue plot, left axis).

5.5.2.3 Mefloquine

MQ was the final quinoline methanol investigated, with a parasite growth IC_{50} of 10.43 ± 1.95 nM in NF54 CQS *P. falciparum,* it is both better tolerated and more effective than either QD and QN. In Figure 3-9 MQ was shown to cause a significant increase in the percentage "free" haem and decrease in percentage Hz in isolated trophozoites treated with 2.5× the parasite growth IC_{50} in comparison to an untreated control. As is the case for the quinoline methanols previously discussed, where several studies have demonstrated a strong relationship between βH inhibition and parasite growth inhibition, MQ has been shown to efficiently inhibit the formation of βH. [101] [99] The chemical similarity of MQ to both QN and QD indicates that MQ is able to form a complex with Fe(III)PPIX in a manner similar to QN and QD through a three point interaction involving co-ordination, π-stacking and intramolecular hydrogen bonding, consequently preventing the conversion of Fe(III)PPIX to Hz.[118] Evidence thus seems to be in favour of classifying MQ as a Hz inhibitor. The effect of MQ on the formation of Hz within the parasite is explored here.

Images of Giemsa stained slides of parasites treated with MQ at a concentration corresponding to 3.0× the parasite growth IC_{50} (Figure 5-5b) show that cells inoculated with MQ at the ring stage matured to trophozoites, although much smaller than the control (Figure 5-5a). Histogram overlays of CQ and MQ treated cells at 3.0× the parasite growth IC_{50} show that cells treated with MQ contained less DNA (Figure 5-5c), were much smaller (Figure 5-5d) and less complex (Figure 5-5e) than CQ treated cells. While treatment of cells with both QN and QD resulted in smaller, less complex cells compared to CQ treated cells, neither caused as large a reduction in the amount of DNA in cells as seen in MQ treated cells. The dramatic changes in the morphology of MQ treated cells indicates that growth of parasites treated with MQ is inhibited earlier in the parasite lifecycle and suggests that the effect of MQ within the cell is different not only to CQ, but also to QN or QD.

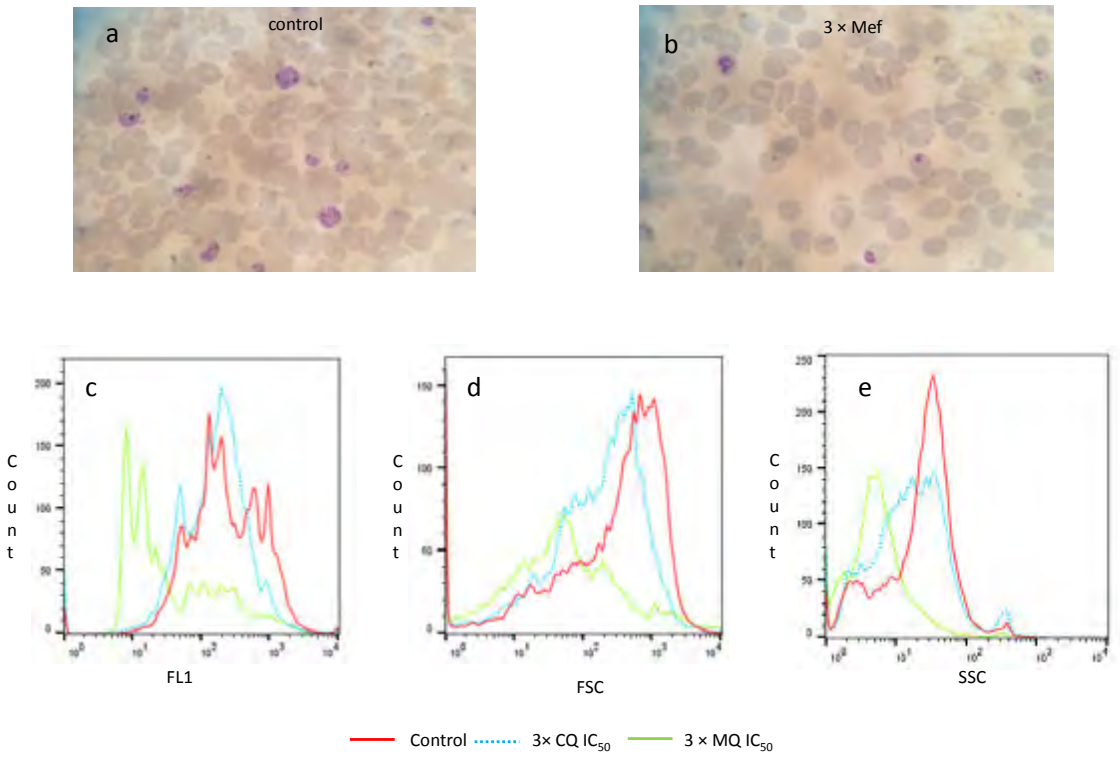

Figure 5-5: Change in morphology of MQ treated isolated NF54, *P. falciparum* trophozoites. Trophozoites were isolated 32 h post inoculation at the ring stage with 3× the parasite growth IC_{50} of MQ and CQ. The image of the Giemsa stained slides of the control culture (a) shows the presence of large, mature trophs, while the image of the MQ treated culture (b) show smaller trophozoites (100× objectification). This result was confirmed upon examination of the flow cytometry histogram overlays displaying the change in (FL1) (c), FSC (d) and SSC (e) for isolated untreated control trophozoites (solid red line), CQ treated isolated trophozoites (blue dashed line) and MQ treated isolated trophozoites (green solid line). A clear shift towards cells containing less DNA (FL1, c), less complex (SSC, e) and smaller (FSC, d) cells can clearly be seen in MQ and CQ treated cells compared to untreated control cultures.

The haem fractionation profiles of MQ treated cells in Figure 5-6 show the amount of Hb per cell did not change significantly with MQ treatment (Figure 5-6a). Similarly the amount of "free" haem per cell showed no significant change compared to the control, except for a significant decrease in "free" haem at 3× parasite growth IC_{50} of MQ (Figure 5-6b). The amount of Hz Fe per cell decreases in a dose related manner by 44.8 ± 6.1% compared to the control (Figure 5-6c). An

overlay of the parasite survival curve for MQ with the amount of "free" haem (fg) per MQ treated trophozoite in Figure 5-6e shows no relationship exists between the amount of "free" haem Fe (fg/cell) per trophozoite (blue diamonds, right axis) and parasite survival (red plot, left axis). MQ therefore does not appear to behave as Hz inhibitor, since despite a dose related decrease in Hz, there is no concomitant increase in "free" haem correlated to parasite survival. As for QD, MQ causes a dose related immediate decrease in total haem Fe in treated cells (Figure 5-6d) most likely attributed to decreased Hb uptake by MQ treated parasites. The lipophilicity of MQ could contribute towards its ability to inhibit endocytosis by binding strongly to lipids and membranes, interfering with vesicle formation and Hb uptake.[238] [57] Cells treated with MQ also show a reduction in the amount of DNA compared to CQ treated cells. Both QN and QD treated cells contained more DNA than CQ treated cells suggesting that growth of MQ treated cells is inhibited earlier in the parasite lifecycle than QN and QD treated cells (Figure 5-5c). Inhibition of endocytosis was similarly identified as possible mechanism for QD and QN, however in the case of QN and QD this was accompanied an increase in "free" haem not seen in MQ treated cells. The differences in cell morphology and haem species profiles between CQ, QN and QD compared to MQ treated cells indicate that the intracellular targets and the effects of the drugs are different and MQ most likely does not directly inhibit Hz formation.

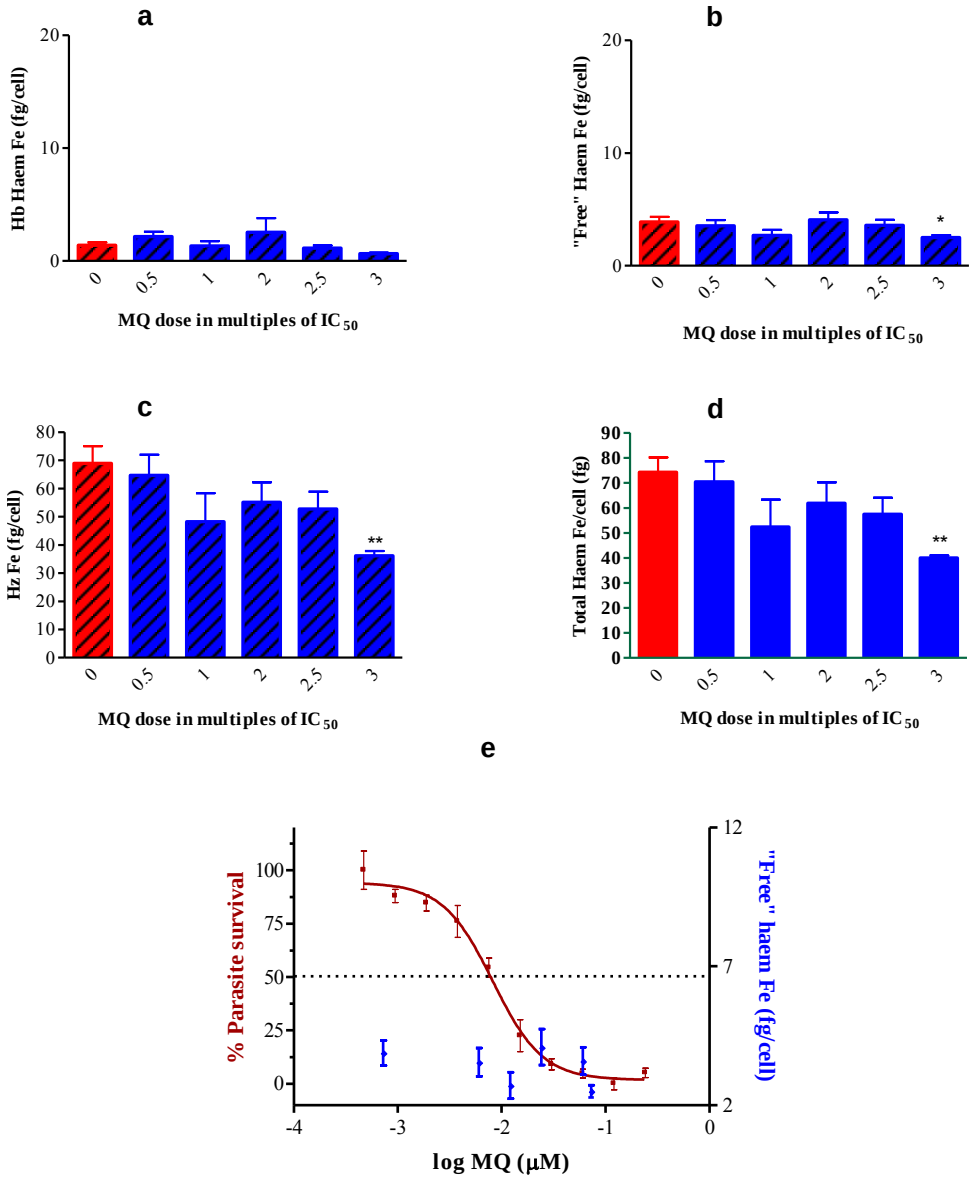

Figure 5-6: Haem fractionation profiles for MQ in NF54, CQS *P. falciparum*. The profiles for the amount of Hb Fe (fg) per cell (a), "free" haem Fe (fg) per cell (b) and Hz Fe (fg) per cell (c) as a function of increasing multiples of the parasite growth IC_{50} of MQ. The total haem Fe in untreated isolated trophs shows a dose related decrease (significant at 3× parasite growth IC_{50} of MQ) per cell (d). An overlay of the parasite survival curve for MQ (red plot, left axis) with the data points (blue diamonds, right axis) representing the amount of "free" haem per MQ treated trophozoite (fg) shows no relationship exists between the amount of "free" haem Fe (fg/cell) per trophozoite and parasite survival (e).

5.5.2.4 Lumefantrine

Of all the antimalarials tested in Chapter 3 in a D10, CQS *P. falciparum* at a concentration corresponding to 2.5× the parasite growth IC_{50}, LF was the only drug which caused an increase in the percentage "free" haem and decrease in percentage Hz comparable to that of CQ (Figure 3.9a, b). LF was shown to produce a dose dependent inhibition of the formation of βH using the NP40 mediated βH inhibition assay with a βHIC_{50} value of 11 μM (Figure 3.9d) comparable to AQ with an IC_{50} value of 21 μM. [105] The package inserts of several LF-AMN combination therapies including COARTEM and ARCEVA indicate Hz inhibition as the mechanism of action of LF. [215] [214] The experimental evidence listed above thus suggests Hz inhibition as the mechanism of action of LF.

Flow cytometry histogram plots of cells treated with 1× the parasite growth IC_{50} of LF (solid green line) display an immediate dramatic decrease in the amount of DNA present in LF treated cells, cell size and cell complexity compared to cells treated with CQ (dotted blue line) at the equivalent IC_{50} (Figure 5-7a, b, c). The flow cytometry histograms of LF treated isolated trophozoites are very similar to the flow cytometry histograms obtained for MQ treated trophozoites (solid orange line) at the equivalent IC_{50} indicating a similar effect on the morphology of cells after treatment with LF or MQ. A Giemsa stained slide of CQ treated cells at 1× IC_{50} shows cultures inoculated with CQ at the ring stage, matured to trophozoites (Figure 5-7f) smaller than trophozoites in untreated cultures (Figure 5-7d). LF dosed cultures in comparison had very few trophozoites and consisted of mostly rings and a large amount of debris (Figure 5-7e). At 4× the parasite growth IC_{50} cultures inoculated with LF consisted predominantly of rings and debris (Figure 5-7g), while CQ treated cultures were comprised of trophozoites (Figure 5-7h). Similar to MQ, growth in LF treated cultures therefore seems to have been inhibited much earlier in the parasite lifecycle compared to CQ treated cells.

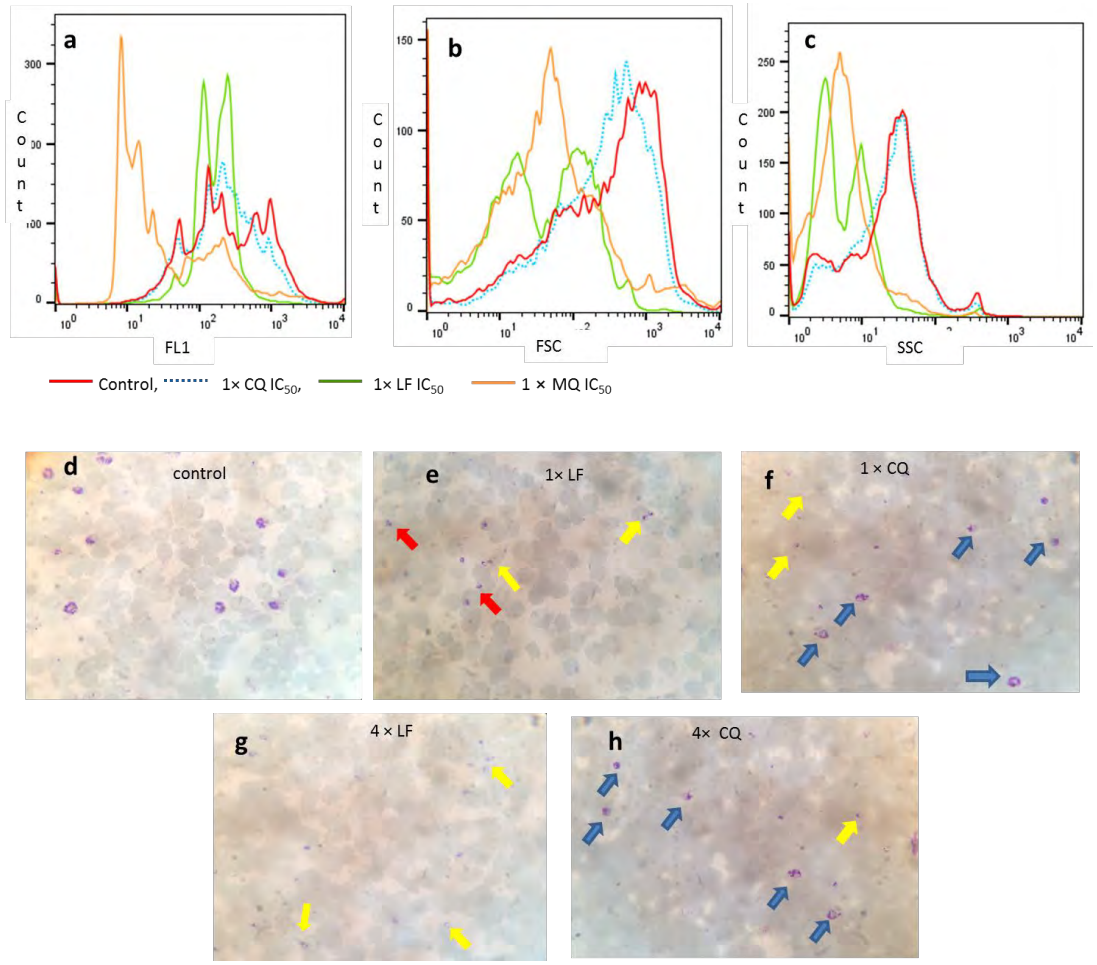

Figure 5-7: Changes in morphology of LF and CQ treated D10, *P. falciparum* shown using flow cytometry histogram plots (a - c) and images from Giemsa stained slides (d - h) prepared 32 h after inoculation with the drug at the ring stage (100× objectification). CQ treated cells are shown for comparison. The histogram plots show the change in SYBR green fluorescence intensity (FL1) (a), FSC (b) and SSC (c) for isolated untreated control trophozoites (solid red line), 1× IC_{50} CQ treated isolated trophozoites (blue dashed line), 1× IC_{50} LF treated isolated trophozoites (solid green line) and 1× IC_{50} MQ treated isolated trophozoites (solid orange line) shown for comparison. Cells treated with LF even at 1× the parasite growth IC_{50} show a dramatic decrease in cell size (FSC), cell complexity (SSC) and the amount of DNA present in the cells (FL1) compared to cells treated with CQ at the equivalent multiple of the IC_{50} (a - c). Images taken from Giemsa stained slides of cultures treated at the equivalent multiple of the IC_{50} of both LF and CQ show that CQ treated cells (f, h) mature to larger trophs (blue arrows) while LF treated cells (e, g) show the presence of very small stunted trophs (red arrows) and rings (yellow arrows).

Initial experiments described in Chapter 3 (Figure 3.9) showed the percentage increase in "free" haem in LF treated cells differed significantly from the untreated control. In Figure 5-8 the haem fractionation profiles for LF are expressed as the amount of each haem species per cell at several multiples of the parasite growth IC_{50} of LF. The amount of Hb Fe (fg) per cell (Figure 5-8a) and the amount of "free" haem Fe (fg) per cell (Figure 5-8b) do not differ significantly from the control and do not increase with increasing concentration of LF. As observed for MQ, the amount of Hz Fe (fg) per cell (Figure 5-8c) shows a dose related significant decrease in comparison to the control with increasing concentration of LF. This is mirrored in the total amount of haem Fe per isolated trophozoite (fg) which decreases significantly in comparison to the control from 1.1× the parasite growth IC_{50} of LF. The initial results in Chapter 3 which suggested LF may be a Hz inhibitor are therefore evidently invalidated by the results summarised here. Despite decreasing Hz formation with increasing LF concentration there is no associated increase in toxic "free" haem and direct Hz inhibition does not appear to the mechanism of action of LF. Figure 5-8a shows that Hb Fe levels per cell (fg) do not increase significantly in comparison to control cells and although Hz levels decrease, it continues to be formed in LF treated cells indicating that Hb metabolism and the conversion of "free" haem to Hz is not inhibited with LF treatment. Decreased total haem Fe (fg) levels in LF treated cells (Figure 5-8d) as well as evidence of inhibited cell growth displayed in flow cytometry histogram overlays indicate that growth in LF treated cells is inhibited early in the lifecycle, possibly at a stage where Hb uptake is not prolific. An overlay of the parasite survival curve for LF with the amount of "free" haem Fe per cell shows no relationship exists between the two parameters (Figure 5-8e). Therefore, although LF efficiently inhibits the formation of βH, it appears to have an alternative mechanism of action, unrelated to haemozoin inhibition in the parasite which halts parasite growth earlier in the lifecycle and causes a reduction in total haem Fe most likely due to reduced uptake of Hb. This example with LF reiterates the importance of determining the per cell profiles for each of the haem species and not only the percentages of each.

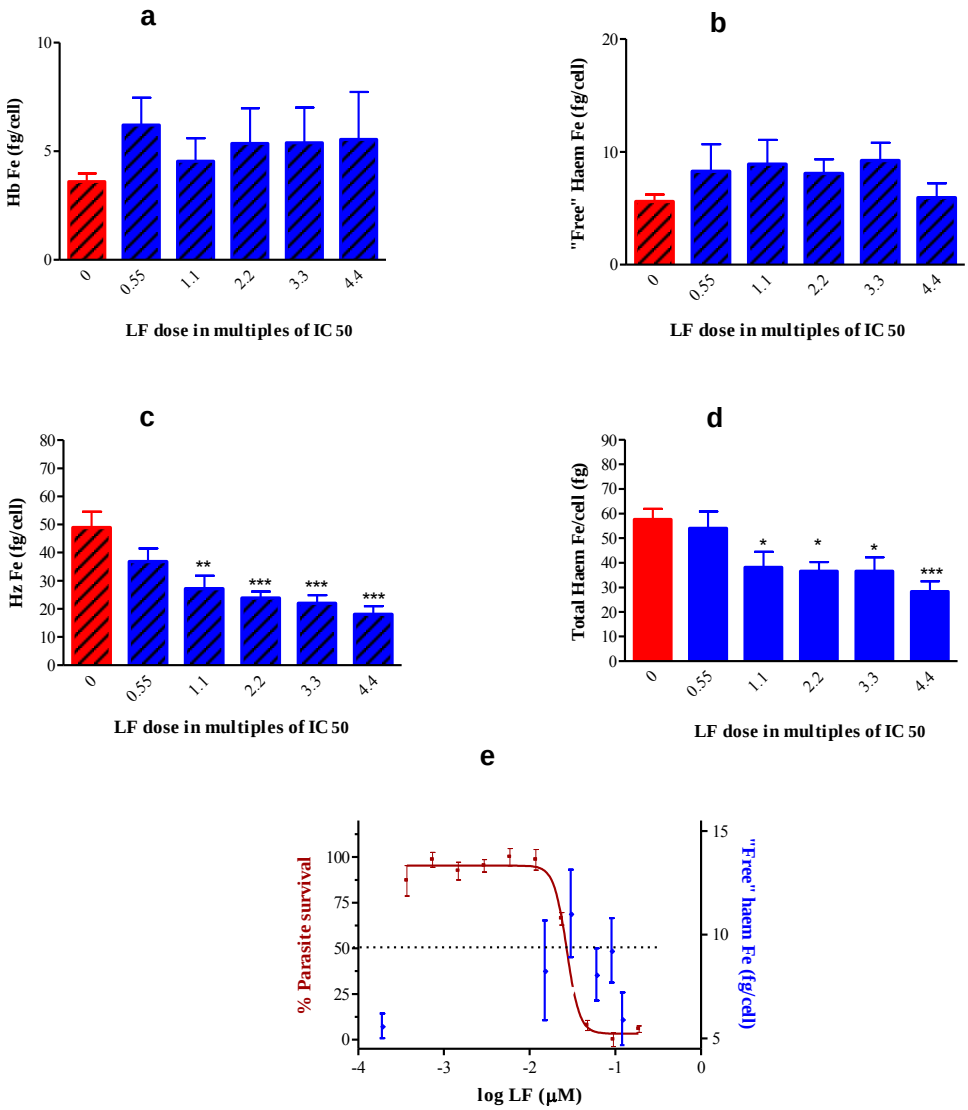

Figure 5-8: Haem fractionation profiles for LF treated isolated trophozoites in D10, CQS *P. falciparum*. The amount of Hb (a) and "free" haem (b) Fe (fg) per cell shows no dose related increase in Hb or "free" haem while the amount of Hz Fe (fg) per cell (c) does show a significant dose related decrease with increasing LF concentration in isolated trophozoites. The total amount of haem Fe (fg) per cell decreases significantly with increasing LF from 1.1× parasite growth IC_{50} of LF (d). An overlay of the parasite survival curve (red plot, left axis) with the data points (blue diamonds, right axis) representing the amount of "free" haem per cell (fg) shows no relationship exists between the amount of "free" haem Fe (fg/cell) per trophozoite and parasite survival (e).

5.5.3 8-Aminoquinolines

5.5.3.1 Primaquine

PQ was the only 8-aminoquinline screened using the cellular haem fractionation assay. Unlike the previous antimalarials screened, which were all active against the intra-erythrocytic stages, PQ is primarily active against the liver stages, and has potent gametocidal activity, preventing transmission of malaria. [70] [241] [242] Nonetheless, PQ does show inhibition of intra-erythrocytic parasite growth, albeit with an IC_{50} value determined to be 3120 ± 890 nM in NF54, CQS *P. falciparum* determined using a modification of the pLDH assay.[206] PQ and other related 8-amino quinolines have been shown to form relatively weak interactions with "free" haem and PQ is incapable of inhibiting the formation of βH. [99] [178]

Flow cytometry histogram plots describing the change in morphology of PQ treated cells show a reduction in cellular DNA (FL1, Figure 5-9a) and are smaller (Figure 5-9b) and have a larger population of less complex cells (Figure 5-9c). However, the change in morphology of PQ treated cells is not nearly as pronounced as the changes seen in CQ treated parasites at the equivalent parasite growth IC_{50} multiple (Figure 5-9a - c).

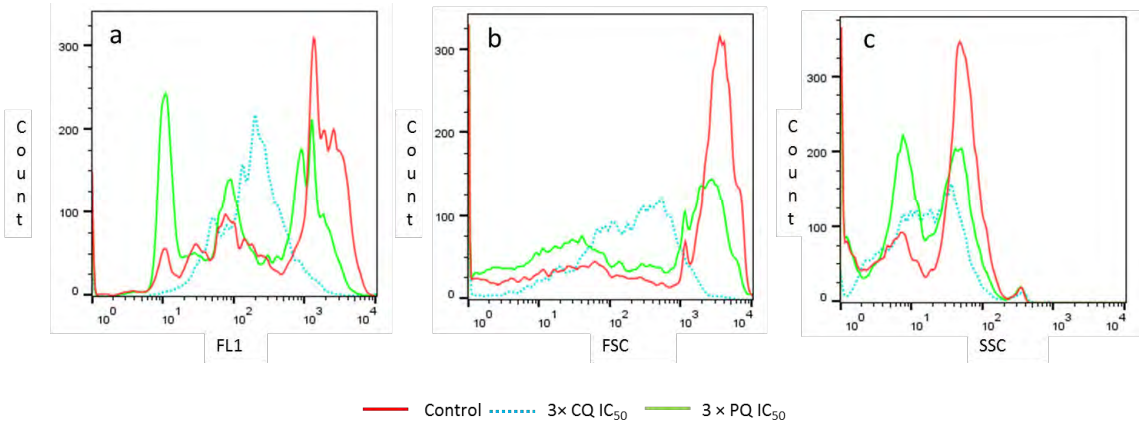

Figure 5-9: Change in morphology of PQ treated NF54, *P. falciparum* trophozoites; isolated 32 h post inoculation at the ring stage with 3× the parasite growth IC_{50} of PQ and CQ. Examination of the flow cytometry histogram overlays displaying the change in (FL1) (a), change in FSC (b) and change in SSC (c) for isolated untreated control trophozoites (solid red line), CQ treated isolated trophozoites (blue dashed line) and PQ treated isolated trophozoites (green solid line) shows a clear shift towards cells containing less DNA (FL1, a), less complex (SSC, b) and smaller (FSC, c) cells in PQ and CQ treated cells compared to untreated control cultures.

The haem fractionation profiles for PQ treated cells show that with the exception of a slight reduction in the amount of Hz Fe (fg) per trophozoite (Figure 5-10c) and the total haem Fe (fg) per trophozoite (Figure 5-10d) at the highest concentration of PQ, there is no dose related increase in "free" haem (Figure 5-10b) or decrease in Hz. Hb levels in PQ treated cells remained relatively unchanged (Figure 5-10a). Furthermore, an overlay of the parasite survival curve for PQ with the amount of "free" haem determined in PQ treated cells in Figure 5-10e shows no relationship exists between the amount of "free" haem Fe (fg/cell) per trophozoite (data points shown as blue diamonds, right axis) and parasite survival (red plot, left axis) in PQ treated cells (h). PQ therefore does not inhibit Hz formation within the parasite. This finding is in line with expectation given its inability to inhibit βH inhibition.

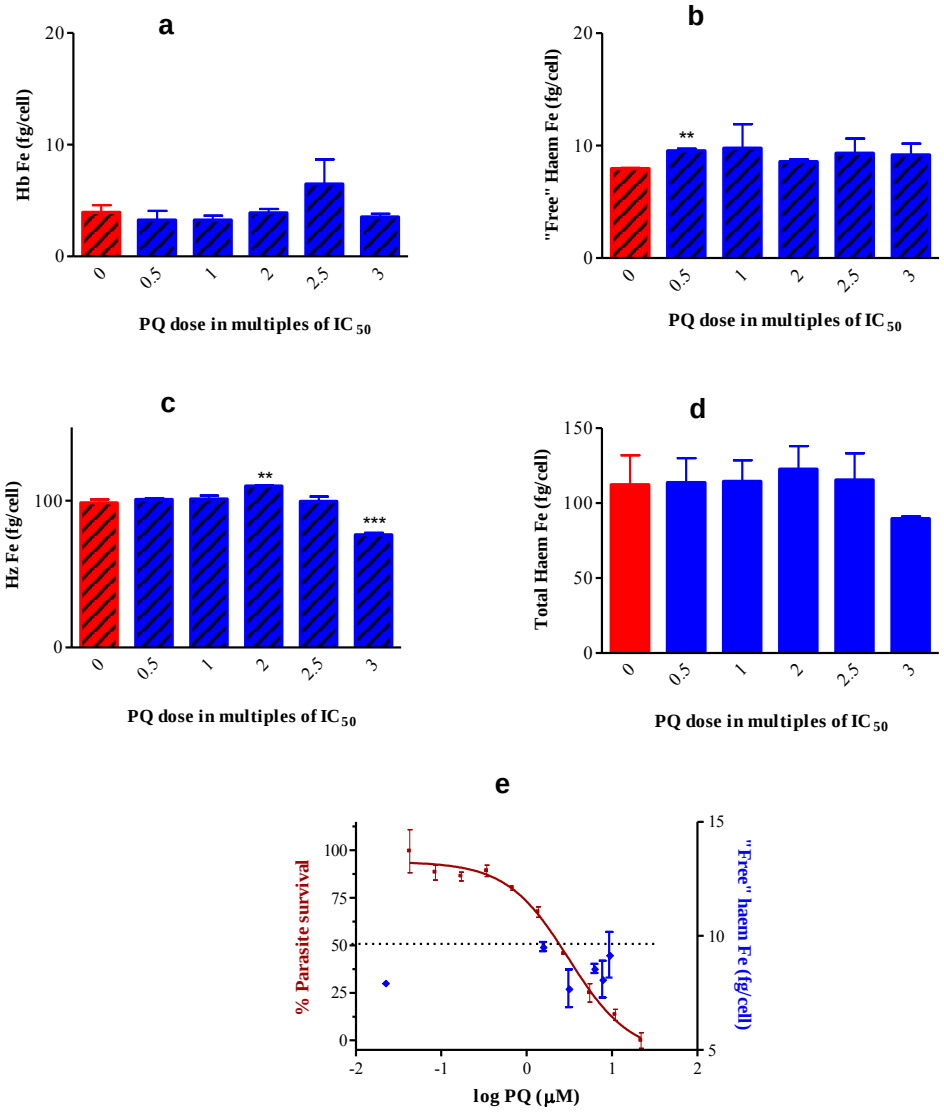

Figure 5-10: Haem fractionation profiles for PQ in NF54 *P. falciparum* isolated trophozoites. The profiles for the amount of Hb Fe (fg) per cell (a), "free" haem Fe (fg) per cell (b) and Hz Fe (fg) per cell (c) as a function of increasing multiples of the parasite growth IC_{50} of PQ. The total haem Fe in untreated isolated trophs did not differ significantly from PQ treated isolated trophozoites (d). No relationship exists between the amount of "free" haem Fe (fg/cell) per trophozoite (data points shown as blue diamonds, right axis) and parasite survival (red plot, left axis) in PQ treated cells (e).

5.5.4 The Artemisinins

The capacity of a compound to inhibit Hz formation within the parasite is surmised from its ability to inhibit the formation of βH from haemin or haematin under laboratory conditions which normally favour βH formation. Several studies have shown that both ART and 10-dO-AMN do not to interfere with the formation of βH. However, the mechanism of action and the role of haem in the mechanism of action of this drug class remains a widely debated topic. [2 110 98] Here, the effect of ART and 10-dO-AMN on the formation of Hz within the *P. falciparum* parasite is investigated.

5.5.4.1 Artesunate

Loup et al showed that ART was not capable of inhibiting the formation of βH from haemin in the presence of acetate at pH 5 (18 h incubation, 37 °C).[178] However, a preliminary study described in Chapter 3 to determine the effect of several clinically relevant antimalarials on Hz formation at a single drug concentration, corresponding to 2.5× the parasite growth IC_{50} showed ART caused an increase in the percentage "free" haem and a decrease in percentage Hz significantly different to the control (Figure 3-9a, b). A full dose response profile performed at several concentrations of ART was carried out to investigate the preliminary findings in Chapter 3.

Examination of images of Giemsa stained glass slides of infected PRBCs at 3× parasite growth IC_{50} of ART show that cells matured to the trophozoite stage (Figure 5-11b). The trophozoites appear smaller and less mature than the corresponding control (Figure 5-11a); however they contain the same amount of haem Fe as the control cells (Figure 5-12d). Parasite viability measured using the pLDH assay showed that treatment with ART is effective at killing the parasite, resulting in 10.2% survival at 3× parasite growth IC_{50} after a period of 48 h. The appearance of smaller trophozoites on the Giemsa stained slide images was confirmed by flow cytometry histogram plots. In the case of ART, the most reduced shift in treated cells was in SSC (Figure 5-11e), followed by the FL1 signal corresponding to SYBR green fluorescence (Figure 5-1c) and a small reduction in

FSC (Figure 5-11d). This indicates cells were less complex, appeared to contain less DNA and were slightly smaller in comparison to the control. A histogram overlay of trophozoites treated with 3× the parasite growth IC_{50} of CQ showed, CQ treated cells contained less DNA, were smaller and less complex than cells treated with 3× the parasite growth IC_{50} of ART (Figure 5-11c - e). The findings above are interesting considering that AMNs are distinguished by their ability to act on all stages of the *P. falciparum* lifecycle, from recently formed rings to schizonts. [159 160] In a recent study determining the speed of action and stage specificity of a number of established antimalarials both CQ and ART were classed as fast acting antimalarials, displaying activity against both ring and schizont stages. Interestingly inoculation for a period of 24 h with either CQ or ART showed that CQ was more effective at inhibiting parasite growth at concentrations ≤ 3× the parasite growth IC_{50}.[120] The uptake of the AMN derivative, artemisone was shown to be highest at the immature ring stage, agreeing with several other studies which have shown that in the *P. falciparum* lifecycle, the ring stage is most susceptible to the effects of AMNs. [243 244 245] More recently, Klonis et al showed that AMNs are less active against mid ring stages of infection and most effective in young rings (2 – 4 h post invasion).[171] The effects or ART suggest that inoculation was performed at a stage where rings were more mature (older than 4 h) and the effect of the drug was attenuated, resulting in maturation to trophozoites. The timing of the inoculation in the haem fractionation assay could therefore be important in determining whether any trophozoites are obtained in order to measure haem species and also on the effectiveness and action of the drug. Indeed, inoculation earlier in the lifecycle could result in a more dramatic change in parasite growth or even complete inhibition at the ring stage.

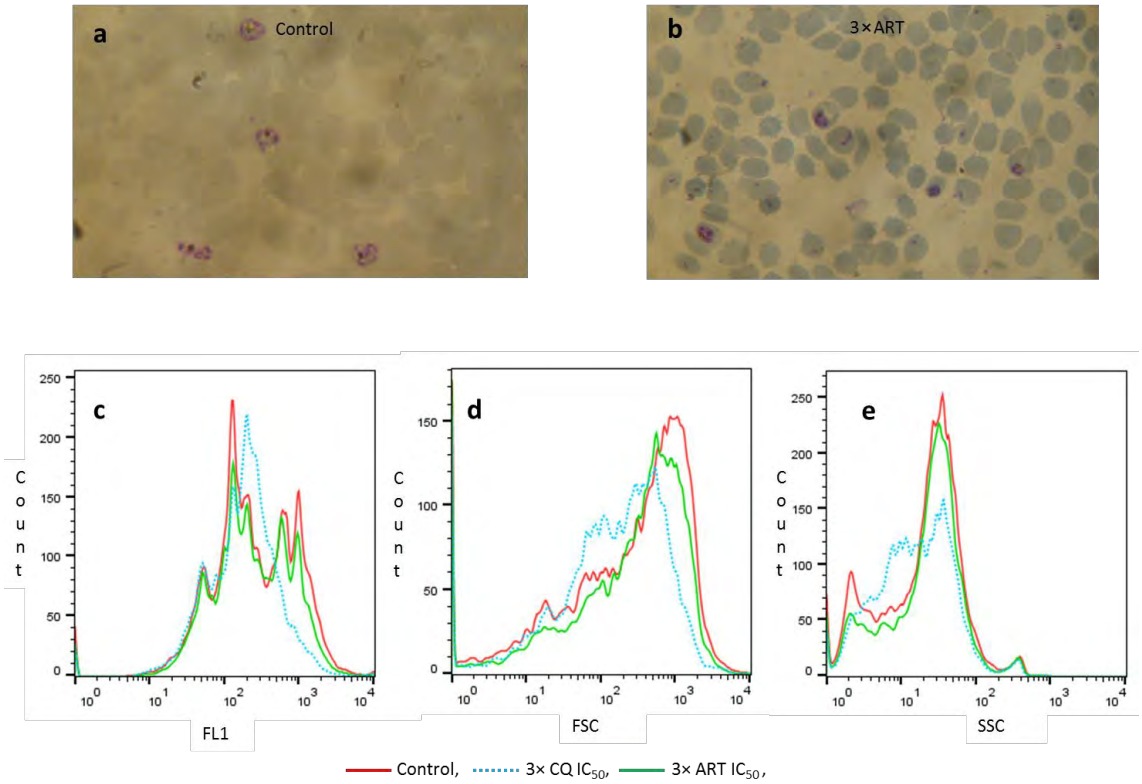

Figure 5-11: Changes in morphology of D10 *P. falciparum* trophozoites treated with ART. Images of control trophozoites and trophozoites isolated 32 h post inoculation at the ring stage with ART at 3× the parasite growth IC_{50} are shown using Giemsa stained slides (100× objectification). The image of the Giemsa stained slide of the control culture (a) shows the presence of mature trophs and some schizonts, while the image of the ART treated culture (b) shows trophozoites, the majority of which appear smaller than the control. This result was confirmed upon examination of the flow cytometry histogram overlays displaying the change in fluorescence intensity (FL1) (c), change in FSC (d) and change in SSC (e) for isolated untreated control trophozoites (solid red line), CQ treated isolated trophozoites (blue dashed line) and ART treated isolated trophozoites (green solid line). Interestingly, cells treated with CQ at the equivalent parasite inhibitory concentration show a more pronounced decrease in all 3 measured parameters (FL1, FSC and SSC) compared to ART treated cells, most notably the FL1 and SSC parameters. In the case of ART, only the size appears to be smaller while, FL1 and SSC appear almost identical to the control.

In Chapter 3, Figure 3-9, a significant increase in the percentage "free" haem and decrease in percentage Hz was seen in isolated trophozoites treated with a single

concentration of ART corresponding to 2.5× the parasite growth IC_{50}. The current study conducted at several multiples of the parasite growth IC_{50} of ART and expressed as the amount of each haem species per cell (fg) shows that ART does not inhibit Hz. No significant increases in Hb (Figure 5-12a), "free" haem (Figure 5-12b) or decrease in Hz (Figure 5-12c) was observed at any ART concentration and the total haem Fe (fg) per cell (Figure 5-12d) remains constant at all concentration of ART tested. Additionally an overlay of the amount of haem Fe (fg) per cell with the parasite survival curve for ART (Figure 5-12e) shows no relationship between the parasite survival and the change in "free" haem levels. ART therefore does not appear to inhibit Hz formation in the parasite, producing no increase in toxic "free" haem that can be correlated to parasite survival in the presence of ART. The result is not surprising given that studies have shown that several AMNs, including ART do not inhibit βH formation. [110 178]

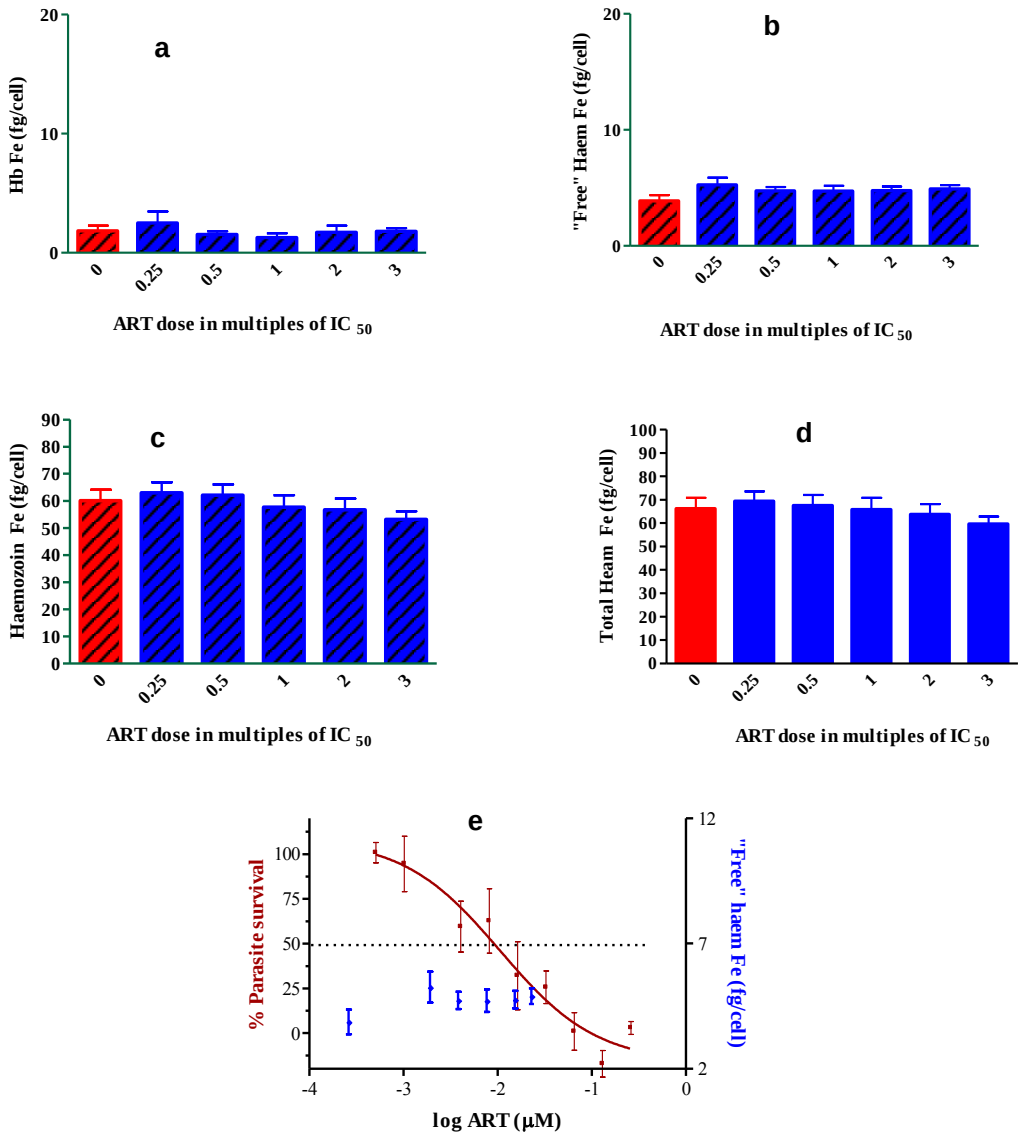

Figure 5-12: Haem fractionation profiles for ART in D10, CQS *P. falciparum*. The profiles for the amount of Hb Fe (fg) per cell (a), "free" haem Fe (fg) per cell (b) and Hz Fe (fg) per cell (c) are shown as a function of increasing concentration of ART. The total haem Fe in untreated isolated trophs did not differ significantly from ART treated isolated trophozoites, despite a slight decrease in total haem Fe per cell at higher ART concentrations (d). An overlay of the parasite survival curve (red plot, left axis) with the data points (blue diamonds, right axis) representing the amount of "free" haem per cell (fg) shows no dose response relationship between the amount of "free" haem Fe (fg/cell) per ART treated trophozoite and parasite survival (e).

5.5.4.2 10-Deoxoartemisinin

10-DO-AMN was specifically chosen for investigation because despite being a highly effective antimalarial it has been previously shown to have no chemical interaction with haem. 10-dO-AMN was negative for βH inhibition when screened with both the so called "haem polymerisation inhibitory activity" assay (HPIA, acetic acid at pH 2.7 for 18 h at 37 °C) and the β-haematin inhibitory activity assay (βHIA, DMSO-acetate buffer at pH 5.0 for 18 h at 37 °C).[110] Despite lack of activity in both the HPIA and βHIA and the inability to bind to Fe(III)PPIX, 10-dO-AMN remains a potent antimalarial.

Giemsa stained slides of 10-dO-AMN treated parasites (Figure 5-13b) show that despite the presence 10-dO-AMN at 3× the parasite growth IC_{50}, cells mature to the trophozoite stage. Once more, as in the case of ART the trophozoites appear smaller and less mature than the corresponding control but contain the same amount of haem Fe as the control cells (Figure 5-13a). As explained in the case of ART, this could be as a result of the time point at which the inoculation was performed in the parasite lifecycle.

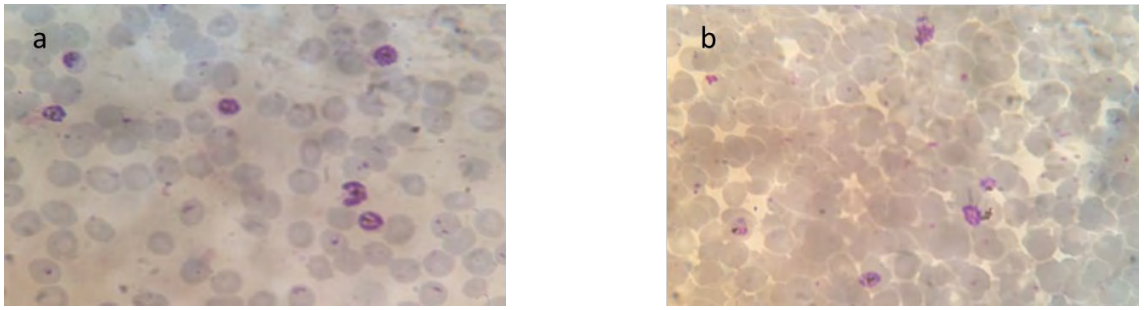

Figure 5-13: Changes in morphology in NF54, *P. falciparum* trophozoites treated with 10-dO-AMN. Trophozoites isolated 32 h post inoculation at the ring stage with 10-dO-AMN at 3× the parasite growth IC_{50} are shown using Giemsa stained slides with an untreated control shown for comparison (100× objectification). The image of the Giemsa stained slide of the 10-dO-AMN treated culture image (b) shows smaller trophozoites in comparison to the control (a).

The haem fractionation profiles (Figure 5-14), show that Hz formation in the parasite was not inhibited in the presence of 10-dO-AMN. No significant increase in

Hb (Figure 5-14a) or decrease in Hz (Figure 5-14c) was seen with increasing drug concentration and with the exception of a significant change in "free" haem at 3× the parasite growth IC_{50}, no dose related increase in "free" haem per cell was seen (Figure 5-14b). The total amount of haem Fe (fg) per cell remained relatively unchanged with increasing 10-dO-AMN concentration, exhibiting a single significant increase at 2× the parasite growth IC_{50} of 10-dO-AMN, (Figure 5-14d). Furthermore no dose dependent relationship was seen between "free" haem levels and parasite survival (Figure 5-14e). The results presented here show that 10-dO-AMN does not appear to inhibit Hz formation in the parasite.

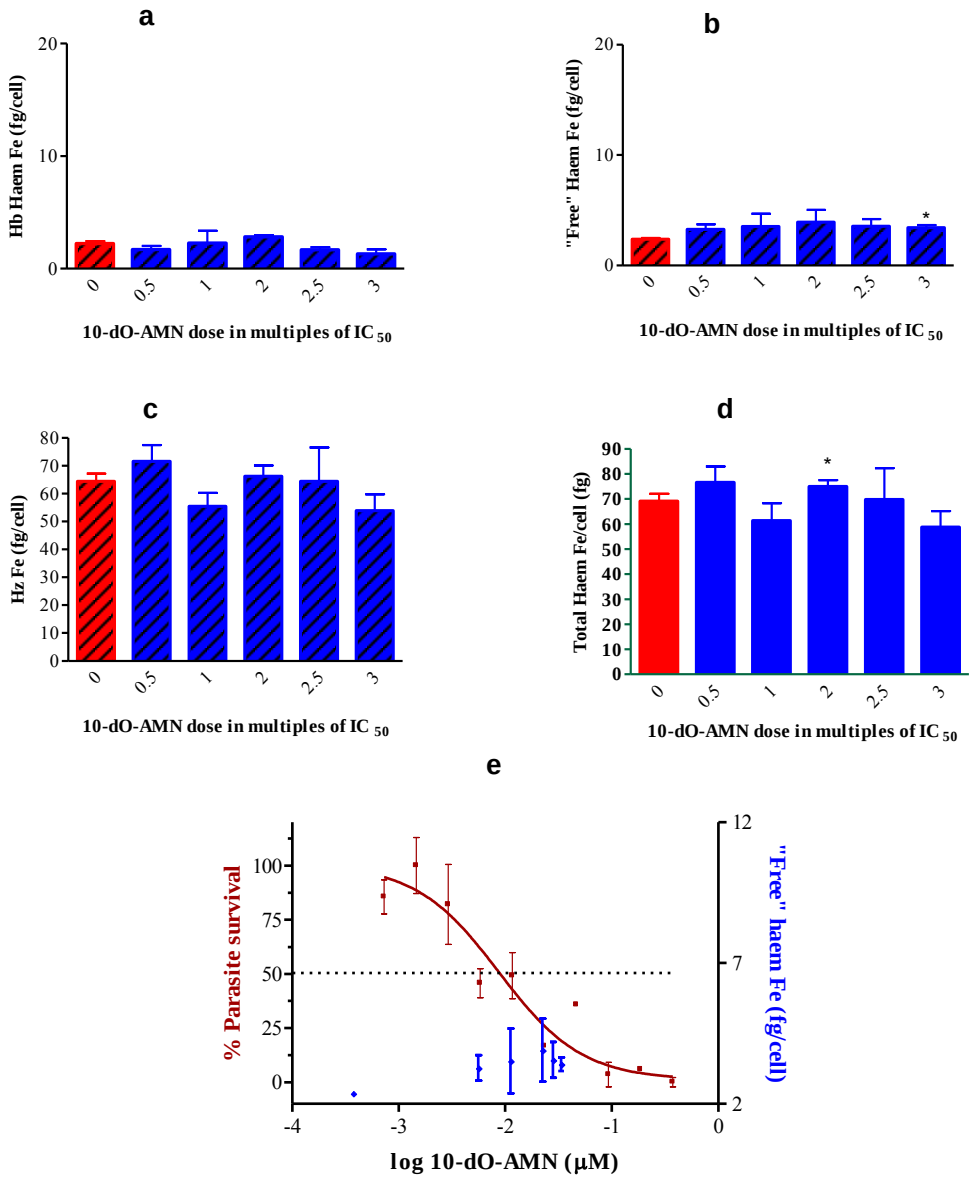

Figure 5-14: Haem fractionation profiles for 10-dO-AMN in NF54, CQS *P falciparum*. The profiles for the amount of Hb Fe (fg) per cell (a), "free" haem Fe (fg) per cell (b) and Hz Fe (fg) per cell (c) are shown as a function of increasing concentration of 10-dO-AMN. The total haem Fe per cell (fg) in untreated isolated trophs did not differ significantly from 10-dO-AMN treated isolated trophozoites (d). An overlay of the parasite survival curve and the amount of "free" haem Fe per cell shows that no relationship exists between the amount of "free" haem Fe (fg/cell) (data points shown as blue diamonds, right axis) and parasite survival (red plot, left axis) in 10-dO-AMN treated cells (e).

5.6 Summary and Conclusion

Seven antimalarials were investigated in this chapter using the modified higher throughput haem fractionation assay to determine if they inhibited Hz as a mechanism of action. The results have been supplemented with flow cytometry profiles and images of Giemsa stained slides which provided additional information detailing the change in morphology of treated parasites.

The aryl methanols, QN, QD, MQ and LF have all been shown to inhibit the formation of βH in a manner which some studies suggest correlates with the parasite survival IC_{50} implicating Hz inhibition as the mechanism of action of these drugs. [106 105 107 52 69 72 101 108] Treatment of parasites at the ring stage with each of the aryl methanols resulted in much smaller and less complex cells in comparison to CQ treated cells at the equivalent multiple of the parasite growth IC_{50}. This suggests that the effects of these drugs within the parasite are different to CQ, especially in the case of LF and MQ. Cells treated with LF and MQ, in addition to being smaller and less complex also showed a reduction in the amount of DNA present in cells suggesting that growth was inhibited earlier in the lifecycle than in CQ, QN or QD treated cells.

Cells treated with the quinoline methanols, QN and QD shared similar effects to each other. Isolated trophozoites showed a dose related increase in "free" haem levels which could be correlated to parasite survival. However, the increase in "free" haem levels was not nearly as pronounced as the levels seen in cells inoculated with the 4-aminoquinolines CQ and AQ discussed in Chapter 4. The increased levels of "free" haem in QN and QD treated cells were accompanied by a decrease in Hz and a decrease in the total amount of haem Fe. This was more pronounced in the case of QD, where an immediate dose related significant decrease in the total haem Fe per cell was seen. The latter effect was also produced in the final 2 compounds, MQ and LF, where in both cases an immediate reduction in both the amount of Hz and total haem Fe per cell occurred. However unlike QN and QD, neither MQ nor LF induced a measurable increase in "free" haem in treated cells correlated to parasite survival. Both LF and MQ showed a reduction in the amount of DNA present in cells suggesting that growth was inhibited much earlier in the parasite lifecycle compared to QN or QD treated cells. Previous

studies have shown that while CQ treatment of *P. falciparum* results in increased levels of Hb accompanied by accumulation of Hb laden transport vesicles, QN and MQ treatment inhibited endocytosis reducing the amount of Hb taken up by treated cells. [124 125] Therefore, while QN and QD appear to exert some degree of Hz inhibition, all four aryl methanols evaluated appear to have an alternative mechanism of action possibly involving the inhibition endocytosis, resulting in reduced Hb uptake.

The 8-amino-quinoline, PQ and the two AMNs, ART and 10-dO-AMN can be grouped together as the outcomes for these three compounds were very similar. Flow cytometry histogram plots and images of Giemsa stained slides showed that the morphology of the cells treated with these compounds changed in comparison to untreated cells but not to the degree which cells treated with CQ changed. In general CQ treated cells were smaller, less complex and contained less DNA. Application of the haem fractionation assay to all three compounds showed that none of the compounds inhibited the formation of Hz in treated parasites. No dose related change in the levels of Hb, "free" haem or Hz in comparison to the control was seen and the total amount of haem Fe per cell remained unchanged at all concentrations of drug tested. An overlay of the parasite survival curve for each of PQ, ART and 10-dO-AMN with the amount of "free" haem produced in treated cells shows no relationship exists between the two parameters. The results are not surprising given that all 3 compounds did not inhibit the formation of βH and while the exact mechanism of action of the AMNs remains unknown, PQ is known to possess activity against the liver stage and against mature gametocytes. [99 110 178] Direct Hz inhibition does not therefore appear to be the mechanism of action for these antimalarials. However the assay cannot disprove the presence of small quantities of highly toxic haem-ART complexes which some authors have proposed play a role in the mechanism of action of the AMNs. [51 176 175 177] The haem fractionation assay on its own, therefore cannot totally exclude the role of haem in the mechanism of action in the AMNs.

The application of the haem fractionation assay to six clinical and one experimentally effective antimalarial in this chapter demonstrates the insight the technique can provide as a valuable contribution in understanding the mechanism in existing and novel antimalarials focussing on Hz inhibition as target. In the next

chapter the assay will be applied to several novel βH inhibiting compounds possessing favourable antimalarial properties.

6 NOVEL NON-QUINOLINE HZ INHIBITING ANTIMALARIALS

6.1 Introduction

In this chapter the haem fractionation assay was applied to six novel compounds shown to have favourable antimalarial properties. The compounds were derived from scaffolds identified in a high-throughput screening (HTS) campaign conducted on a library of 144 330 compounds belonging to the Vanderbilt University Institute of Chemical Biology (VUICB) chemical library to identify novel βH inhibiting scaffolds using the NP-40 mediated assay. The results of this HTS found 530 βH inhibiting "hits" of which 73 showed activity below 5 μM in a CQS strain of *P. falciparum*. Compounds belonging to the quinoline scaffold comprised the majority of "hits" in the screen. Having been extensively investigated in the previous chapters, no compounds belonging to the quinoline scaffold were selected for investigation. Of the 14 scaffolds identified in the HTS, the benzamide chemotype had the second highest βH inhibiting hit rate, surpassed only by the quinolines and made up 10% of the hits. Three of the novel compounds investigated in this chapter belong to this scaffold. The final three compounds selected for investigation were chosen from the triarylimidazole (TAI) scaffold. This scaffold displayed favourable βH inhibiting activity and most of the βH inhibiting "hits" also displayed favourable parasite inhibitory activity. [104 246 247] All six compounds selected were biologically active against a CQS strain of *P. falciparum* and five of the six compounds selected were potent inhibitors of βH formation. The cellular haem fractionation assay was performed to validate that inhibition of βH seen in the majority of the selected compounds translates to the inhibition of Hz formation within the *P. falciparum* infected RBC resulting in parasite death. Whereas previously the relationship between the inhibition of βH, biological activity and the inhibition of Hz formation in the parasite using the haem fractionation assay has been limited to the study of βH inhibiting quinolines, the extension of the study to these novel βH inhibiting antimalarials provides the opportunity to gain insight into the mechanism of βH inhibition and its translation into Hz formation within a non-quinoline system.

6.2 Materials

All materials used throughout this chapter are listed in Chapter 2. Materials were of AR grade or higher and used without further purification. The novel compounds tested in this chapter were synthesised and characterised by Dr Katherine Wicht and reported elsewhere. [246]

Table 6-1: A list of compounds tested in the pyridine haem fractionation study.

Compound	Scaffold	Molecular formula	*Percentage purity
KW2	Benzamide	$C_{12}H_7N_4O_5$	99.3%
KW15	Benzamide	$C_{24}H_{23}N_2O_2$	99.3%
KW17	Benzamide	$C_{22}H_{21}N_4O_2$	99.4%
TSI_3	Triarylimidazole	$C_{23}H_{21}N_2O_2$	98.5%
TSI_6	Triarylimidazole	$C_{21}H_{16}N_3O_2$	98.8%
TSI_12	Triarylimidazole	$C_{25}H_{25}N_2O_4$	98.0%

*Percentage purity determined by HPLC.

6.3 Sample Preparation

The preparation of all samples used throughout this chapter, are previously described in Chapters 2 and 3. The water used throughout this work was double distilled deionised Millipore® Direct-Q water.

6.4 Methods

The methods used in this chapter, are previously described in Chapters 2, 3 and 4.

6.5 Results and Discussion

6.5.1 Selection of novel antimalarials for the cellular haem fractionation assay

Three compounds from the benzamide scaffold and three from the TAI scaffold were selected for testing using the haem fractionation assay (Figure 6-1). Both scaffolds have previously been investigated for antimalarial activity.[103] [104] Phenylbenzamides have shown antimalarial activity against CQS 3D7 and one monobenzamide has been identified as a kinase inhibitor and subsequently optimised for solubility and parasite selectivity. [211] [248] The TAI scaffold has previously been identified as a "hit" in a HTS campaign of several thousand compounds, screened specifically for antiprotozoal activity as haem detoxification protein (HDP) inhibitors.[249] More recently several TAIs were identified as promising antimalarial leads in a HTS of almost two million compounds in the Glaxo Smith Kline chemical library for activity against CQS 3D7.[216] TAI's capable of βH inhibition have also been shown to have early stage gametocyte activity.[103] The structures of the compounds selected for the cellular haem fractionation assay along with the 50% parasite inhibitory concentrations determined in the CQS NF54 strain and the 50% βH inhibitory concentrations are shown in Figure 6-1. The compounds selected covered a broad range of parasite inhibitory concentrations ranging from 0.6 μM to 14.8 μM. The range of parasite growth IC_{50} values in the sample set could provide insight as to how differences in "free" haem levels affect parasite activity. With the exception of one benzamide, KW15 which showed no βH inhibitory activity, all had similar βH IC_{50} values ranging from 13.0 μM to 18.7 μM, more active than the βH IC_{50} of CQ of 31.5 ± 0.5 μM. The single non βH inhibiting antimalarial, KW15, served as a negative control in this study.

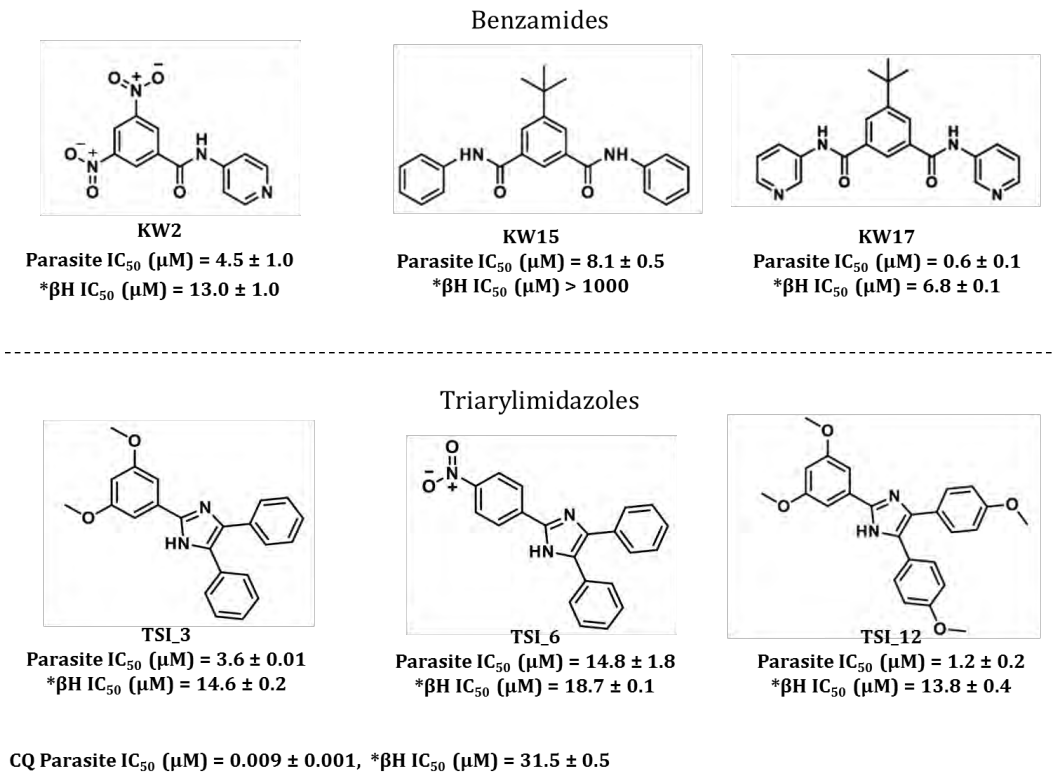

Figure 6-1: The six compounds chosen for assessment of Hz parasite inhibitory activity derived from the benzamide and TAI scaffolds are shown above. The parasite growth IC_{50} values (μM) were determined in a CQS strain of *P. falciparum,* NF54 using a modification of the pLDH assay described in Section 2.5.2. The βH IC_{50} value (μM) for each compound was determined using the NP-40 detergent mediated βH inhibition assay described in Section 2.4.3. The parasite growth IC_{50} value (μM) and βH IC_{50} value (μM) for CQ is listed for comparison. *All βH inhibition values listed in Figure 6-1 were determined by Katherine Wicht.[246]

A significant correlation between the inverse of parasite activity and the inverse of βH inhibition activity in compounds selected from the benzamide and TAI scaffolds is shown in Figure 6-2. This significant correlation suggests the mechanism of action of these compounds can be attributed to Hz inhibition in the parasite. A similar relationship was demonstrated by Wicht et al between the inverse of the βH inhibition IC_{50} and the inverse of the parasite growth IC_{50} for several benzamide analogues showing a positive correlation ($r^2 = 0.68$, $P < 0.0001$); again suggesting that Hz inhibition is the expected mechanism of action. [247]

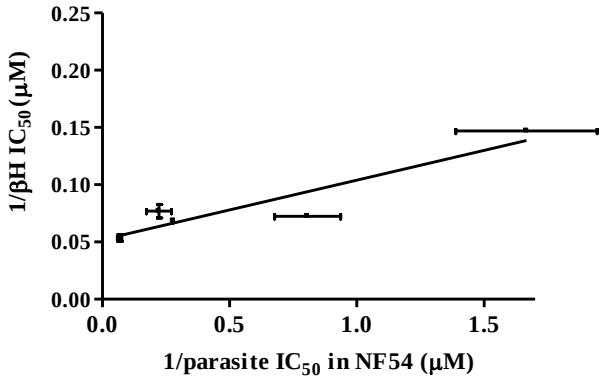

Figure 6-2: A plot of the inverse of the βH IC_{50} vs the inverse of the parasite growth IC_{50} shows a significant linear relationship exists between the parasite growth IC_{50} and βH IC_{50} for the TAIs and benzamides selected for testing (r^2 =0.86, P = 0.022). Data are displayed as the mean with the associated SEM of 3 repeat measurements. The benzamide, KW15 was omitted from the plot as it did not exhibit any βH inhibition activity.

6.5.2 The haem fractionation profiles of benzamide and triarylimidazoles

The haem fractionation assay was performed to confirm that Hz inhibition was the mechanism of action for all compounds which tested positive for βH inhibition using the NP-40 mediated assay. The novel compounds derived from the benzamide and TAI scaffolds are structurally distinct from the quinolines previously studied and provide a unique opportunity to gain insight into the Hz inhibition pathway in an alternative scaffold.

6.5.2.1 The Benzamide scaffold

By contrast to KW15 which had no βH inhibitory activity, both KW2 and KW17 showed dramatic increases in "free" haem levels accompanied by decreased levels of Hz correlated to parasite survival (Figure 6-3). Compound KW15 served as a negative control. Biologically active, with an parasite growth IC_{50} value of 8.1 ± 0.5 μM, KW15 showed no inhibition of βH (βH IC_{50} > 1000 μM) and also no inhibition of Hz or build-up of "free" haem in the parasite. Therefore despite being

biologically active against *P. falciparum*, KW15 most likely exerts activity via a mechanism other than Hz inhibition within the *Plasmodium* infected RBC. The antiplasmodial activity of a monobenzamide has previously been linked to kinase inhibition and it is possible that KW15 shares a similar mechanism of action.[248] KW2 and KW17 produced maximum "free" haem levels of 48.3 ± 1.8 and 39.1 ± 5 fg haem Fe per cell respectively, higher than any of the Hz inhibiting antimalarials previously tested, including the highly effective Hz inhibiting antimalarial CQ which reached at most 8.8 ± 0.8 fg of "free" haem Fe per cell (Figure 4-8). An overlay of the parasite survival curve for KW2 and KW17 with the amount of "free" haem produced in the presence of each drug (Figure 6-3 c and i) showed that decreased parasite survival corresponds to an increase in "free" haem. In the case of both KW2 and KW17 the graphs intersect at or close to the 50% parasite inhibitory concentration reinforcing the relevance of the relationship between decreasing parasite survival and increasing "free" haem levels. Conversely, the negative control KW15 showed no relationship between parasite survival and free haem levels (Figure 6-3f).

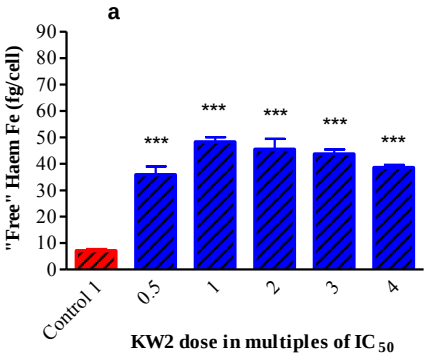

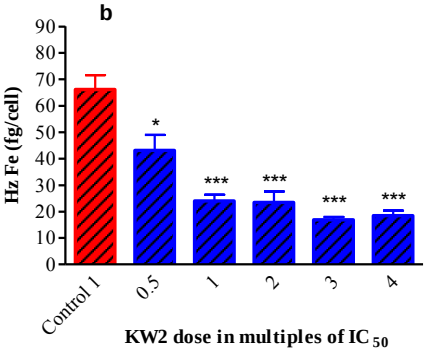

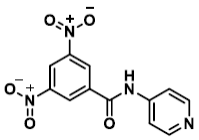

KW_2
NF54 parasite IC_{50} (µM) = 4.5 ± 1.0
ßH IC_{50} (µM) = 13.0 ± 1.0

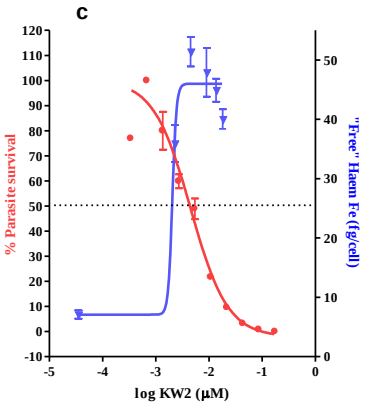

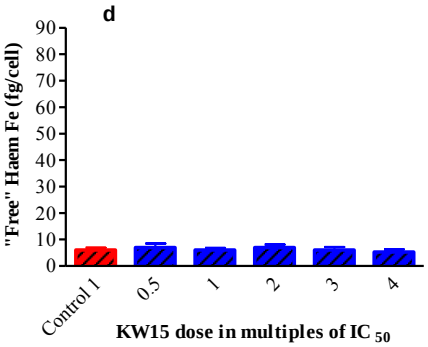

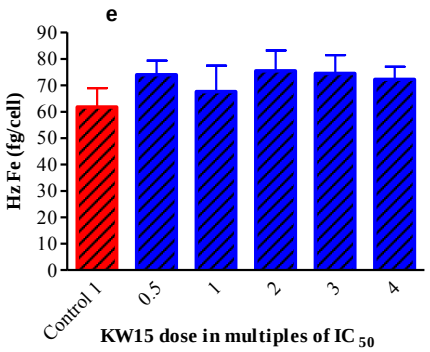

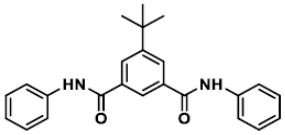

KW_15
NF54 parasite IC_{50} (µM) = 8.1 ± 0.5
ßH IC_{50} (µM) > 1000

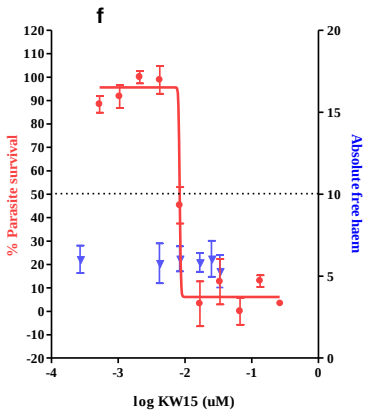

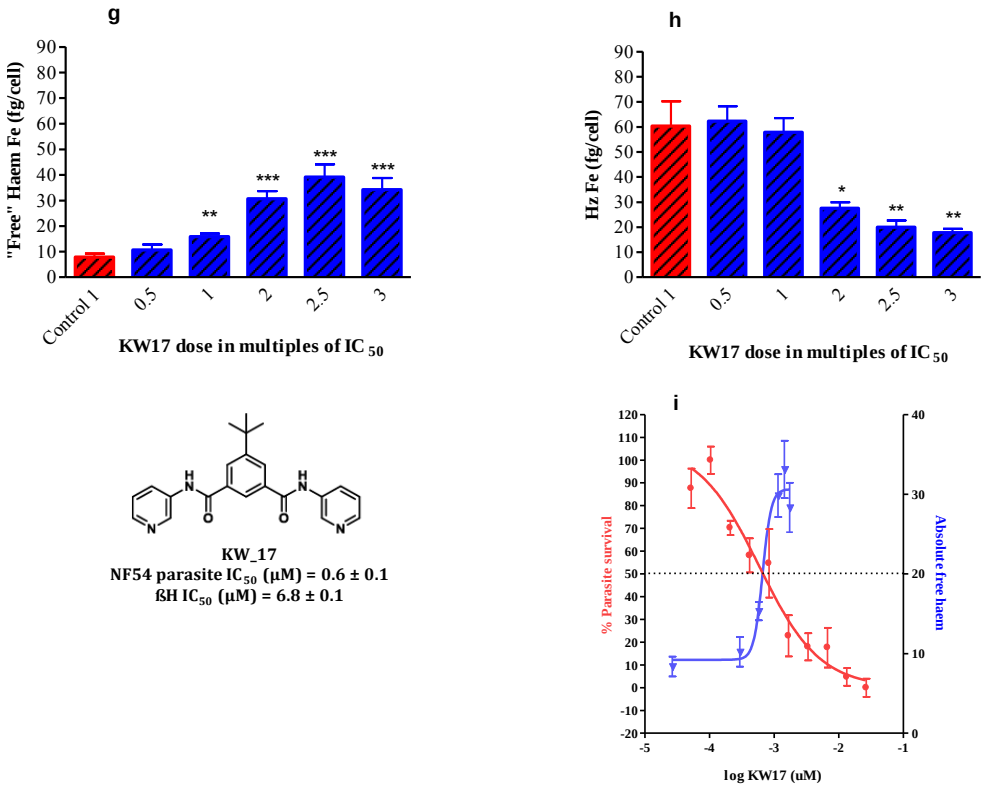

Figure 6-3: The haem fractionation profiles of the benzamide derivatives KW2 (a, b, c), KW15 (d, e, f) and KW17 (g, h, i) showing the amount of "free" haem Fe per cell (a, d, g) and Hz Fe per cell (b, e, h) with increasing drug concentration. An overlay of the parasite survival curve with the amount of "free" haem is shown in c, f and i for each of KW2, KW15 and KW17 respectively. In the case of KW2 (c) and KW17 (i) the scales of the parasite survival curve overlaid with "free" haem levels have been adjusted such that the 50% mark on the parasite survival y-axis coincides with the half way mark on the "free" haem y-axis. A dose related increase in "free" haem and decrease in Hz related to parasite survival is seen for KW2 and KW17. Asterisks displayed on the graph indicate statistical significance relative to the control (shown in red) at the 95% CI, determined using a 2-tailed t-test (* P <0.05; ** P <0.01; *** P <0.001).

The change in morphology of cells after treatment with 3× the parasite growth IC_{50} of CQ, KW2, KW15 and KW17 is represented in the flow cytometry histogram overlays in Figure 6-4. Cells treated with the benzamide KW15 (solid dark purple line), which exhibited no evidence of Hz inhibition (Figure 6-3d – f) showed no change in the amount of DNA (Figure 6-4a), size (Figure 6-4b) or complexity

(Figure 6-4c) compared to the control (solid red line). The benzamides KW2 (solid green line) and KW17 (solid purple line) which produced high "free" haem Fe levels of 43.7 ± 1.7 and 34.3 ± 4.5 fg per cell at 3× parasite growth IC_{50} showed a reduction in the amount of DNA (Figure 6-4a) and the complexity of the cells (Figure 6-4c) but very little change in the size of the cells compared to the control. In comparison to CQ, the flow cytometry profiles of KW2 and KW17 were almost identical with the exception of the FSC parameter which showed that cells treated with CQ had a larger population of smaller cells. Treatment with the benzamides KW2 and KW17 which produced "free" haem levels of up to 5.5× more than in CQ treated cells therefore resulted in a larger proportion of bigger cells and cells which were very similar in complexity and amount of DNA as cells treated with CQ. The results obtained here differ from flow cytometry histogram plots of cells treated with the aryl methanols in Chapter 5 which showed treated cells were less complex and in most cases smaller than cells treated with CQ.

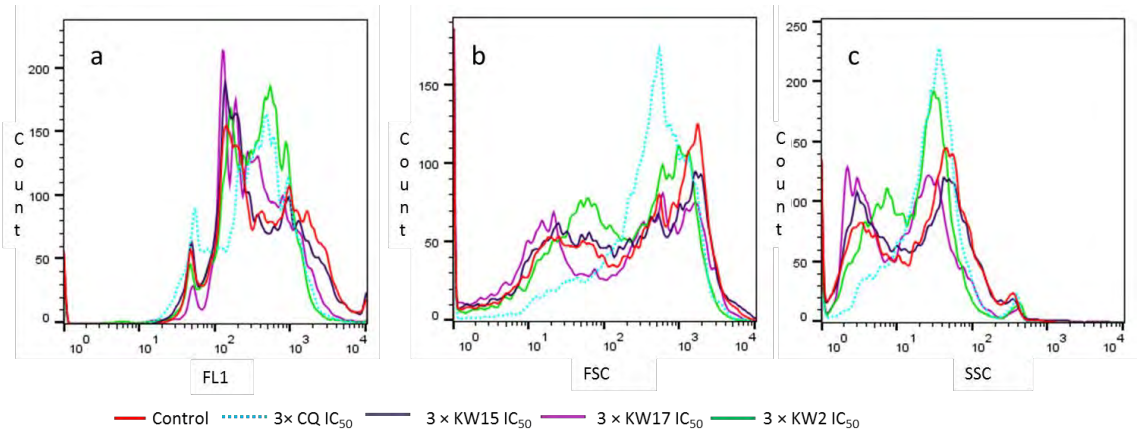

Figure 6-4: Change in morphology of isolated *P. falciparum* trophozoites treated with 3× the parasite growth IC_{50} of KW15, KW17, KW2 and CQ. Flow cytometry histogram overlays displaying the change in FL1 (a), FSC (b) and SSC (c) for isolated untreated control trophozoites (solid red line), CQ (blue dotted line), KW15 (solid dark purple line), KW17 (solid purple line) and KW2 (solid green line) treated isolated trophozoites. While very little shift in any of parameters was seen between the control and KW15, the profiles of KW2, KW17 and CQ treated cells are very similar.

6.5.2.2 The Triarylimidazole scaffold

All three TAIs tested showed evidence of Hz inhibition (Figure 6-4). As seen in the benzamides, TSI_3 and TSI_12 produced unusually high levels of "free" haem corresponding to maximum levels of 36.9 ± 6.0 and 46.4 ± 3.0 fg of "free" haem Fe per cell respectively. By contrast, TSI_6 produced at most 17.4 ± 1.4 fg of "free" haem Fe per cell. Although higher, this result is comparable to AQ which produced at most 13.1 ± 2.1 fg of "free" haem Fe per cell. The increase in "free" haem in each case is accompanied by a decrease in Hz. In all three cases an overlay of the parasite survival curves with the amount of "free" haem (Figure 6-4c, f and i) showed that decreased parasite survival corresponds to an increase in "free" haem levels.

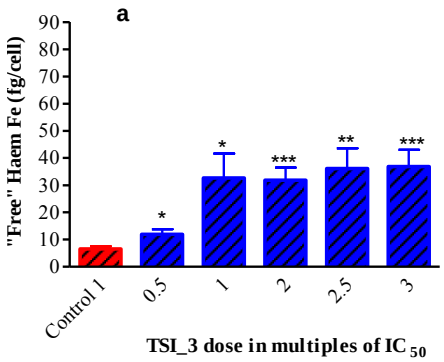

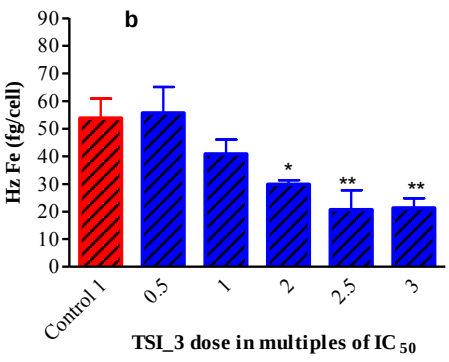

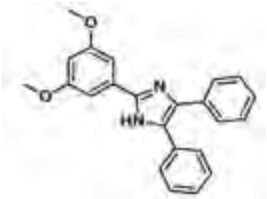

TSI_3
NF54 parasite IC_{50} (µM) = 3.6 ± 0.01
ßH IC_{50} (µM) = 14.6 ± 0.2

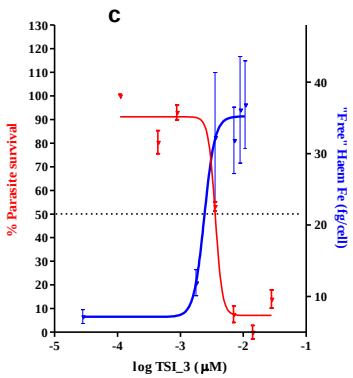

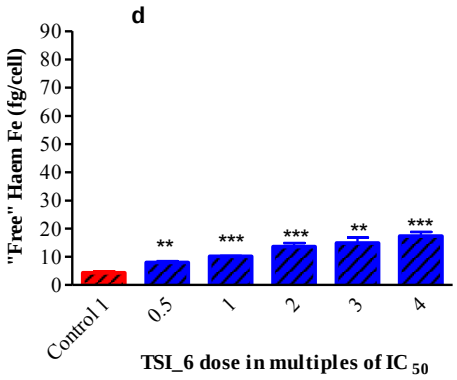

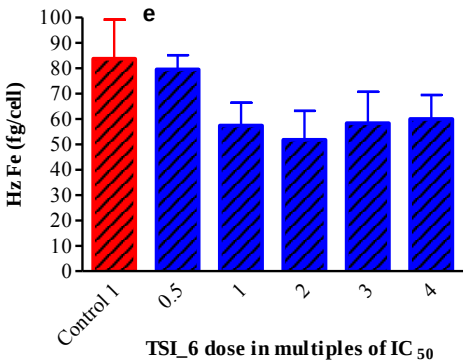

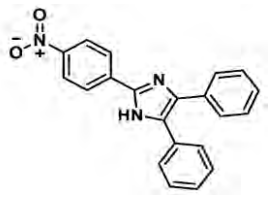

TSI_6
NF54 parasite IC_{50} (µM) = 14.8 ± 1.8
ßH IC_{50} (µM) = 18.7 ± 0.1

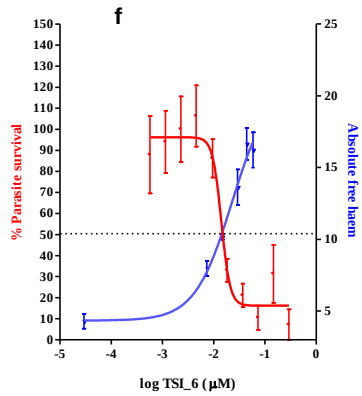

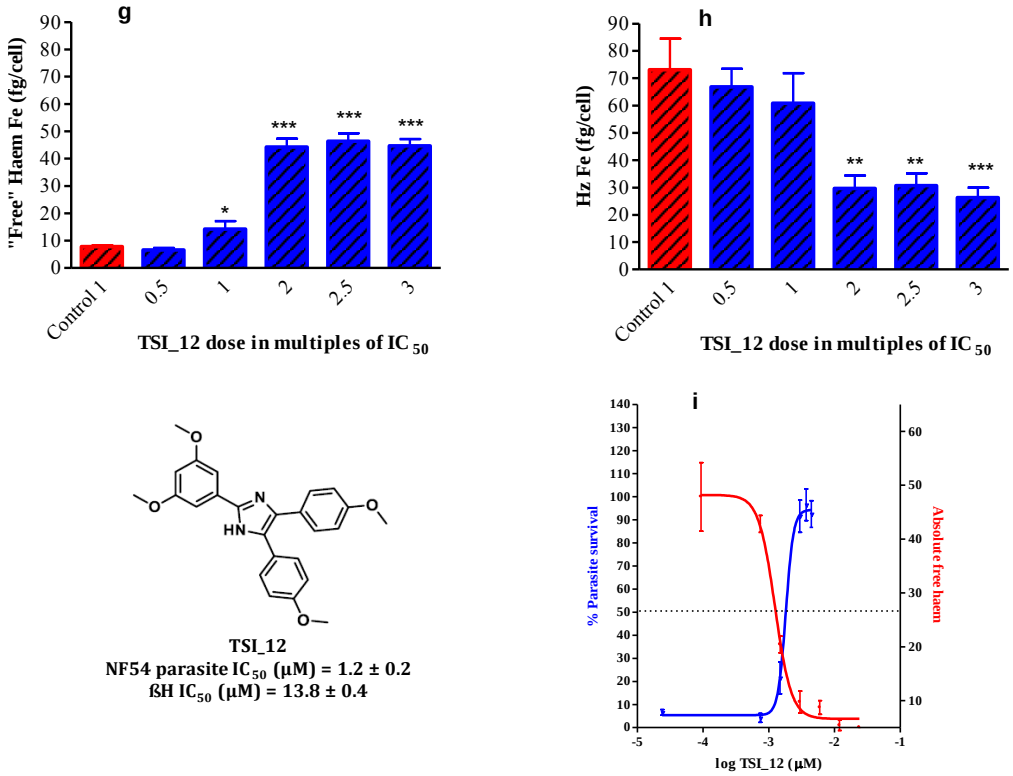

Figure 6-5: The haem fraction profiles of the TAI derivatives TSI_3 (a, b, c), TSI_6 (d, e, f) and TSI_12 (g, h, i) showing the amount of "free" haem Fe per cell (a, d, g) and Hz Fe per cell (b, e, h) with increasing drug concentration. An overlay of the parasite survival curve with the amount of free haem is shown in c, f and i for TSI_3, TSI_6 and TSI_12 respectively. In all cases the scales of the parasite survival curve overlaid with "free" haem levels has been adjusted such that the 50% mark on the parasite survival y axis coincides with the half way mark on the "free" haem y-axis. A dose related increase in "free" haem and decrease in Hz related to parasite survival is seen in all of the TAI derivatives. Asterisks displayed on the graph indicate statistical significance relative to the control (shown in red) at the 95% CI, determined using a 2-tailed t-test (* P <0.05; ** P <0.01; *** P <0.001).

Flow cytometry histogram profiles of CQ and TAI treated cells in Figure 6-6 show a reduction in all three parameters evaluated (FL1, FSC and SSC) in comparison to the untreated control. Unlike the flow cytometry profiles of benzamide treated cells (Figure 6-4), where a definite trend of larger cells as complex as CQ treated cells could easily be identified, the effect of the TAIs on cell morphology differ with each derivative tested and no single trend could be established with the TAI treated cells. Cells treated with TSI_6 showed a marked reduction in DNA in

comparison to cells treated with CQ at the equivalent parasite growth IC_{50}. Both TSI_3 and TSI_6 showed a marked reduction in cell size as well as a decrease in the fraction of complex cells in the population. As seen in the benzamides (Figure 6-4), the flow cytometry profiles of TSI_12 were very similar to CQ at the equivalent parasite growth IC_{50} in all parameters evaluated. Although Hz inhibition along with increased levels of free haem was established as the likely mechanism of action for all TAIs, the effect of each TAI evaluated on the morphology of the parasite appears to be different.

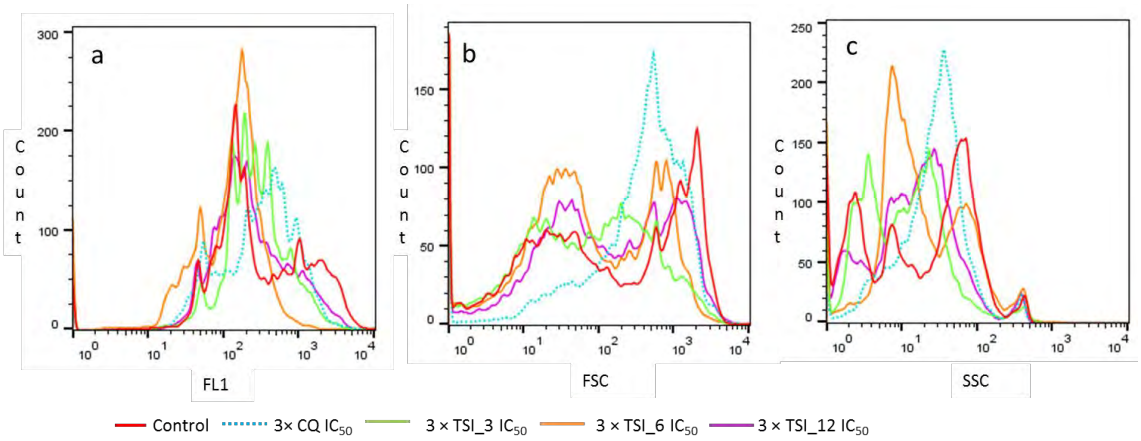

Figure 6-6: Change in morphology of isolated *P. falciparum* trophozoites treated with each of 3× the parasite growth IC_{50} of TSI_3, TSI_6, TSI_12 and CQ. Flow cytometry histogram overlays displaying the change in fluorescence intensity (FL1) (a), change in FSC (b) and change in SSC (c) are shown for isolated untreated control trophozoites (solid red line), CQ treated isolated trophozoites (blue dotted line) TSI_3 (solid green line), TSI_6 (solid orange line) and TSI_12 (solid purple line).

6.5.3 Towards understanding high "free" haem levels

A compound was considered to be a Hz inhibitor when the following three criteria were met: an increase in "free" haem, an accompanying decrease in Hz and a decrease in parasite survival that could be correlated to the increase in "free" haem and decrease in Hz. All five compounds which tested positive for βH inhibition (KW2, KW17, TSI_3, TSI_6 and TSI_12) were found to inhibit Hz formation within

the *P. falciparum* infected RBC, confirming the biological relevance of the NP-40 βH inhibition assay. Interestingly all five compounds produced higher levels of "free" haem (Figure 6-7a and b) and lower levels of Hz than seen in any of the Hz inhibiting antimalarials previously tested. In the case of KW2 the amount of "free" haem Fe reached within the parasite was ~35 - 40 fg higher than the highest amount of "free" haem reached within CQ and AQ treated cells. The vastly different levels of "free" haem Fe between the Hz inhibiting 4-aminoquinolines and specifically KW2, KW17, TSI_3 and TSI_12 suggests that Hz inhibition in these non-quinoline antimalarials follows a different mechanism. The ability of the parasite to reach high levels of "free" haem Fe while still exhibiting reasonable parasite survival suggests the toxicity of the "free" haem produced is lower than that produced in CQ and AQ treated cells. Compounds belonging to the quinoline scaffold require only a small increase in "free" haem to induce parasite death signifying that the ultimate effect of the quinolines is more effective at killing the parasite. The relationship between parasite growth IC_{50} and βH IC_{50} with change in "free" haem levels is shown in Figure 6-7c and d respectively. A significant correlation exists between the parasite growth IC_{50} and the change in "free" haem levels. Thus high levels of "free" haem are produced by compounds with high parasite growth IC_{50} values. The highly effective Hz inhibiting antimalarial CQ shown in Figure 6-7c for comparison produces the smallest increase in "free" haem but is the most biologically active antimalarial. The relationship is counterintuitive, as less biologically effective compounds produce higher levels of "free" haem known to be toxic to the parasite resulting in cell death. One explanation could be that the resulting complex formed between "free" haem and these novel compounds is less toxic than "free" haem alone or "free" haem-CQ complex. This concept requires further investigation and can only be firmly established with the inclusion of more data acquired from Hz inhibiting compounds. It must be noted that the positive relationship between the change in "free" haem levels and the parasite growth IC_{50} only exists with the exclusion of TSI_6 as this TAI had a high parasite growth IC_{50} value of 14.8 μM but a small change in "free" haem of 5.9 fg haem Fe at 1× the 50% parasite inhibitory concentration. TSI_6 therefore does not conform to the relationship of less biologically effective compounds producing higher levels of "free" haem. Interestingly TSI_6 was the only compound which caused a significant reduction in the amount of DNA per cell suggesting that aside

from Hz inhibition this compound has an additional, possibly nonspecific cytotoxic effect on the cell. No significant relationship was observed between the 50% βH inhibition concentrations and the change in "free" haem at 1× 50% parasite inhibitory concentration (Figure 6-7d). Therefore although the NP-40 assay successfully identified all Hz inhibitors in the sample set it did not predict the level of Hz inhibition observed in each sample.

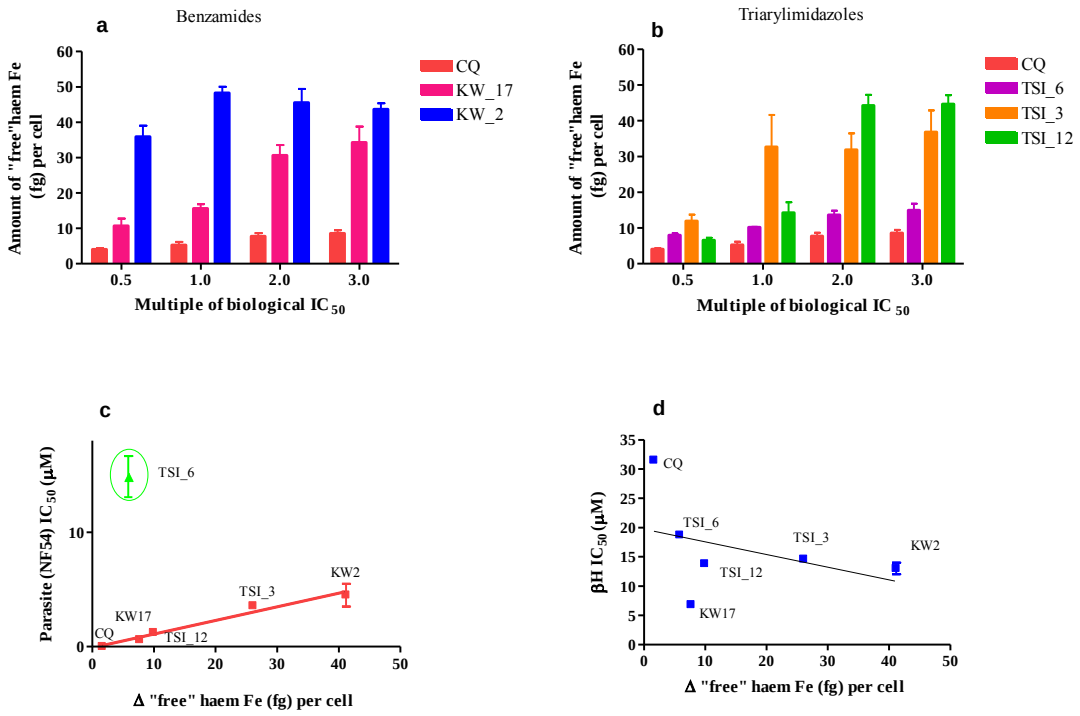

Figure 6-7: The amount of "free" haem produced in cells inoculated with 0.5×, 1.0×, 2× and 3× the parasite 50% inhibitory concentration of CQ, KW2 and KW17(a) and CQ, TSI_3, TSI_6 and TSI_12 (b). The Hz inhibiting quinoline, CQ is shown for comparison. The amount of "free" haem produced in the presence of the benzamide and TAI derivatives are considerably higher than in CQ treated cells at the equivalent parasite inhibitory concentration with KW2 producing the highest amount of free haem Fe (fg) per cell. The benzamide, KW15 was omitted from the plot as it did not exhibit βH inhibition activity. Graph c shows that a significant relationship exists between the 50% parasite inhibitory concentration and the change in "free" haem at 1× parasite inhibitory concentration (r^2 = 0.97, P =0.002). Both KW15 and TSI_6 (data point shown in green) were omitted from the plot. KW15 was omitted as it showed no Hz inhibition and TSI_6 as it had a high parasite growth IC_{50} value of 14.8 µM and small change in "free" haem of 5.9 fg at 1× the 50% parasite inhibitory concentration. The inclusion of TSI_6 eliminates the significant correlation (P= 0.997). No significant correlation was seen between the 50% βH inhibition concentration (d) with the change in "free" haem at 1× 50% parasite inhibitory concentration (r^2 = 0.15, P = 0.44). Again KW15 was omitted from the plot.

To further investigate the phenomenon of unusually high levels of "free" haem, one compound was selected for further investigation. The benzamide KW17 was chosen on account of its high levels of "free" haem and because it exhibited the most potent biological activity amongst the compounds chosen in either scaffold with a parasite growth IC_{50} of 0.6 ± 0.1 μM in the NF54 strain. TEM with EELS for Fe was performed on cells treated with 2× the parasite growth IC_{50} of KW17 and highlighted the morphological changes in KW17 treated cells compared to untreated cells and cells treated with CQ at 2× the parasite growth IC_{50} of CQ (Figures 6-8 and 6-9). Samples were prepared as previously described in Section 2.4.4 from NF54 cultures inoculated with 2× the parasite growth IC_{50} of KW17 or CQ at the ring stage. The amount of "free" haem in isolated trophozoites derived from these cultures corresponded to 30.6 ± 3.0 fg haem Fe, 3.5 fold higher than CQ treated trophozoites at the equivalent parasite growth IC_{50} (Figure 6-8a). Several morphological changes between the control cell (Figure 6-8b), the CQ treated cell (Figure 6-8c) and the KW17 treated cells (Figures 6-8d, e and 6-9a) were observed. The first was the presence of an enlarged DV in KW17 treated cells, most evident in Figures 6-8e and 6-9a. The second was that Hz formation within the DV was disrupted. The TEM images of KW17 treated cells clearly show the presence of apparently "non-crystalline" Hz, possibly corresponding to aggregated haem confined to the DV. Unlike the tightly packed Hz crystals in DV of the untreated control (Figure 6-8b) and CQ (Figure 6-8c) treated cells, the Hz crystals in the DV of KW17 treated cells were loosely distributed within the DV, mostly at the periphery of the enlarged DV (Figures 6-8d, e). A distinct shadow could be seen surrounding each crystal in KW17 treated cells, not observed in untreated cells (Figure 6-8b) and very slightly in CQ treated cells (Figure 6-8c). In comparison, Hz crystals in the DV of the untreated PRBC (Figure 6-8b) were uniform in shape, ordered, sharp crystals. Previous studies have showed that treatment with 30 nM CQ (corresponding to 2× the 50% parasite inhibitory concentration) produced less ordered crystals and at 60 nM CQ. TEM of extracted Hz clearly shows disruption of Hz formation with obvious grain boundaries visible between multiple small crystals making up Hz [107]. TEM images of extracted Hz crystals treated with 2× the 50% parasite inhibitory concentration of CQ (Figure 6-9c) and KW17 (Figure 6-9d) respectively are shown with insets magnifying a portion of the crystal. While the crystals of the CQ treated cell are not as regularly shaped as the untreated control,

the extracted CQ treated Hz crystals in Figure 6-9c exhibit a repetitive pattern with areas of non-uniform interaction at points where two crystals overlap. The inset corresponding to a magnified portion of extracted CQ treated Hz (Figure 6-9c) shows lattice fringes are clearly visible, indicative of a crystal structure. KW17 treated extracted material in Figure 6-9d appears to be amorphous with no distinct order. The inset in Figure 6-9d showing a magnified portion of the material corresponding to Hz extracted from KW17 treated cells appears amorphous and shows no evidence of lattice fringes as seen in Hz of CQ treated cells. Finally a large number of vesicles, highlighted by yellow and orange asterisks (*,*) were observed in KW17 treated PRBC images (Figure 6-9a, b). The vesicles were primarily seen in the DV, some of which contained Fe (*) concentrations greater than Fe levels in the RBC and parasite cytosol. Similar transport vesicles are seen in much smaller numbers in the image of the untreated PRBC (Figure 6-8b) and have also been identified in large numbers in the TEM of CQ treated PRBCs, attributed to the accumulation of Hb containing transport vesicles. However in both cases these transport vesicles were found outside of the DV [124]. Further work is required to elucidate the role of these vesicles in KW17 treated cells and whether they play a role in the extraordinary high levels of "free" haem obtained with this compound.

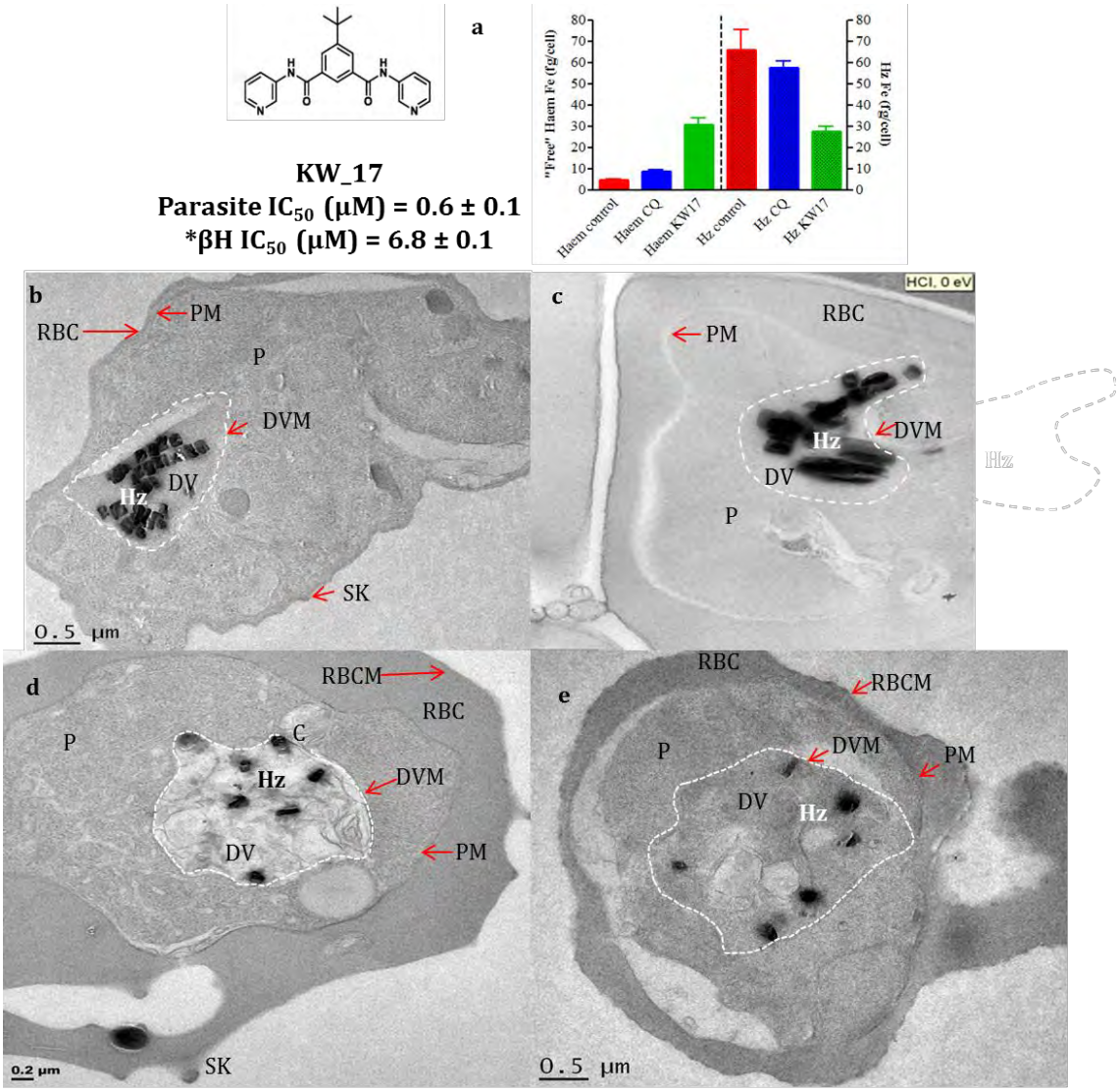

Figure 6-8: TEM of PRBCs treated with KW17. Graph (a) shows the increase in "free" haem (left y-axis) and decrease in Hz (right y-axis, dotted bar graphs) in KW17 treated cells (green bar graphs), and CQ treated cells (blue bar graphs) at 2× the 50% parasite growth inhibition dose compared to an untreated control (red bar graphs). TEM images of untreated (b) and CQ treated PRBCs (c) shown for comparison with KW17 treated PRBCs. TEM images of KW17 treated PRBCs (d, e) display an enlarged DV and "non-crystalline" loosely distributed amorphous electron dense material. C = cytostome; RBC = red bool cell; RBCM = red blood cell membrane; P = parasite cytosol; PM = parasite membrane; DV = digestive vacuole; DVM = digestive vacuole membrane; Hz = Haemozoin; SK = surface knobs.

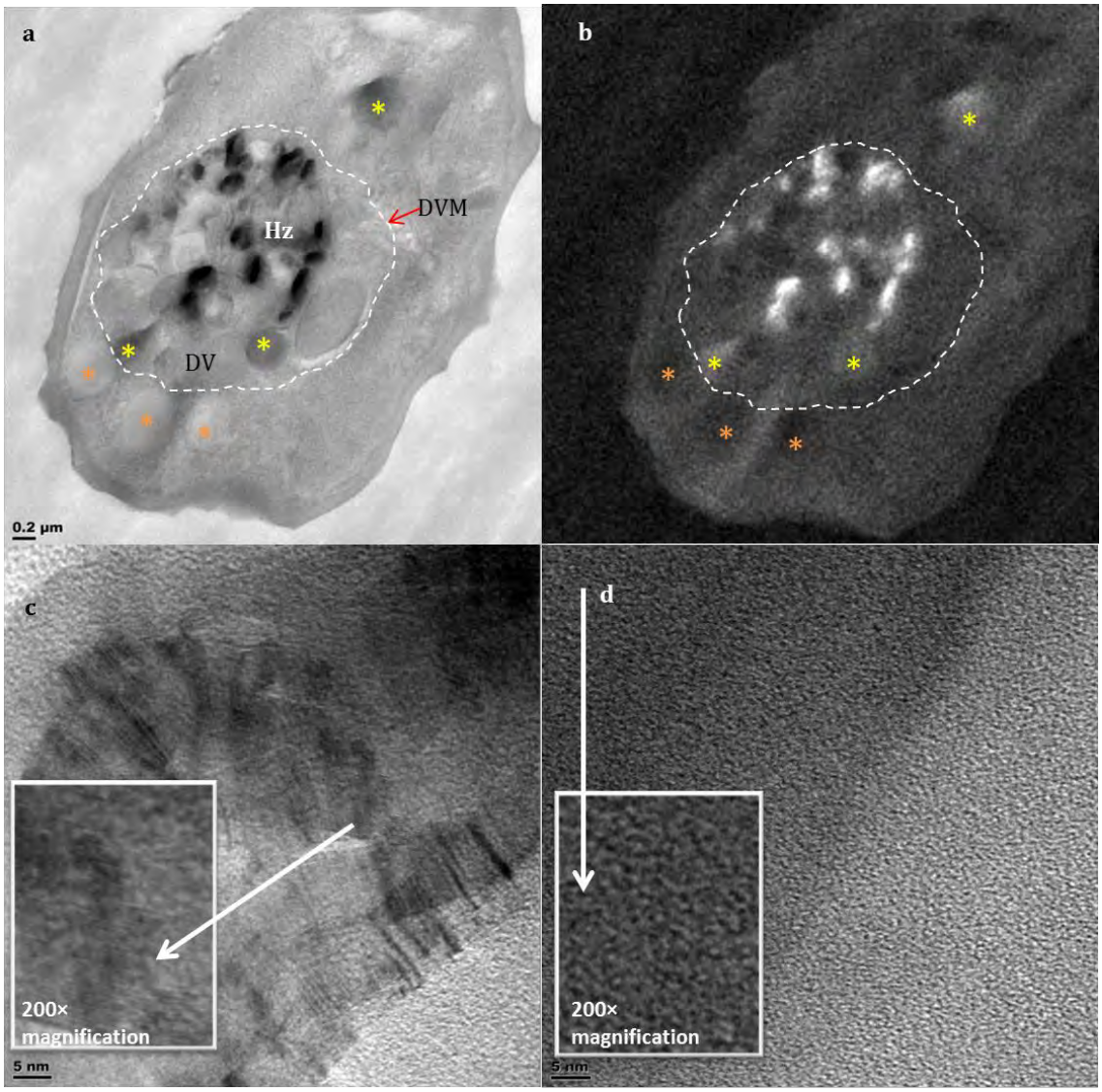

Figure 6-9: TEM images of KW17 treated PRBCs (a) display an enlarged DV, "non crystalline" loosely distributed amorphous electron dense material and a large number of vesicles throughout the parasite. The Fe distribution measured by ESI using EELS for Fe is shown in white (b). The Fe signal in vesicles is highlighted by yellow asterisks (*) while vesicles devoid of Fe are highlighted by an orange asterisks (*). In all images the DVM is delineated by a white dashed line. Hz crystals extracted from CQ treated PRBCs (c) with inset of magnified crystals displaying lattice fringes. Hz crystals extracted from KW17 treated PRBCs (d) with inset of magnified extracted Hz crystals. DV = digestive vacuole; DVM = digestive vacuole membrane; Hz = Haemozoin.

6.6 Summary and Conclusion

In this chapter, six derivatives of two non-quinoline scaffolds; the benzamide and TAI scaffolds identified by HTS as having promising βH inhibiting and parasite inhibitory activity were tested using the haem cellular fractionation assay. The relationship between βH inhibition, parasite inhibitory activity and Hz inhibition in the *P. falciparum* parasite has been explored in relation to these two scaffolds. βH inhibition does not always translate into Hz inhibition as the primary mechanism of action of the drug. In Chapter 5, the βH inhibiting antimalarial LF determined to have a βH IC_{50} value of 11 μM (Figure 3.9d) did not inhibit Hz formation in CQS *P. falciparum.* Although Hz inhibition may still theoretically be able to occur, LF most likely also has an alternative more effective mechanism of action occurring at a stage in the lifecycle where Hz inhibition is not possible. Of the six novel compounds selected for investigation, five tested positive for βH inhibition with βH IC_{50} values approximately half those of CQ. All five of these compounds subsequently tested positive as inhibitors of Hz formation within the *P. falciparum* infected RBC, confirming the biological relevance of the NP-40 assay with reference to the benzamide and TAI scaffolds. This relationship was strengthened by the inclusion of the negative control, KW15. This non βH inhibiting antimalarial (βH IC_{50} > 1000 μM) showed no inhibition of Hz formation within the parasite. The results of this investigation indicate that βH inhibition for the benzamides and TAIs translates into Hz inhibition. However no correlation exists between the βH IC_{50} value and the amount of free haem produced (Figure 6-5d). The βH inhibition NP-40 assay therefore accurately predicts whether a compound will inhibit haemozoin but does not predict the degree of Hz inhibition seen within the parasite.

The most notable effect of the benzamide and TAI analogues was the exaggerated levels of “free” haem produced in *P. falciparum* infected RBCs. High levels of “free” haem have previously been reported for the benzamide and TAI scaffolds. In separate studies performed using the haem fractionation assay described in Chapter 3, Sandlin et al identified three different benzamides and one TAI from the VUICB chemical library which produced levels of “free” haem 51% above the control. These “free” haem levels were the highest amongst all other βH inhibiting

scaffolds identified, including several quinolines. The quinolines represented the largest percentage of βH inhibiting hits in the HTS and produced very small but significant increases in "free" haem correlated to parasite death.[104] Similarly, Fong et al in another HTS campaign of active antimalarial compounds in the Medicines for Malaria Venture (MMV) Malaria Box identified ten βH inhibiting hits of which two were benzamides and three were TAIs. Again it was shown that treatment with these compounds resulted in the highest "free" haem levels amongst all scaffolds identified [103]. Findings presented in this chapter as well as previous studies have therefore shown that the amount of "free" haem required to achieve the equivalent level of toxicity and associated parasite survival was much higher in the TAI and benzamide scaffolds than in βH inhibiting quinolines.

TEM with EELS for Fe of KW17 treated parasites was undertaken to provide morphological clues to explain the high levels of "free" haem. A significantly enlarged DV containing a large number of vesicles as well as disrupted Hz formation was observed. The presence of these vesicles as well as the enlarged DV could account for the flow cytometry profiles of KW17 treated cells which were as complex as and larger than cells treated with CQ. Most significant was the appearance of the Hz in KW17 treated cells compared to control and CQ treated cells. Structured, sharp Hz crystals were seen in both the control and CQ treated cells compared to the "non-crystalline" amorphous material which has been attributed to aggregated haem confined to the DV.

High levels of free haem and distinct morphological differences in treated cells indicate that the benzamides and TAIs clearly have a different toxicity to the parasite compared to quinolines. Although the exact mechanism of Hz formation and inhibition is not known, recent evidence indicates that CQ inhibits Hz formation through interaction with growing Hz crystals resulting in termination of growth and increased levels of toxic "free" haem. Haem cellular fractionation studies with CQ and other Hz inhibiting quinolines have shown that very small but significant increases in "free" haem are required to cause parasite death. CQ, with a 50% parasite inhibitory concentration of 11.0 nM in NF54 causes an approximate two fold maximum increase in "free" haem above the untreated control. The graph of parasite growth IC_{50} vs the change in "free" haem in Figure 6-5c shows that the higher the parasite growth IC_{50}, the more "free" haem produced in the presence of

the drug within the parasite. Therefore the highly effective Hz inhibiting antimalarial CQ produces the smallest increase in "free" haem whereas the less biologically effective benzamides and TAIs produce high amounts of "free" haem while still exhibiting reasonable parasite survival. This phenomenon suggests that the toxic effect of the "free" haem produced in the presence of these novel compounds is attenuated possibly through the formation of haem-drug complexes which are less harmful to the parasite than "free" haem itself, possibly because of low solubility. Therefore in addition to inhibiting Hz crystal growth through interaction with Hz crystals, the TAI and benzamide derivatives could also form complexes with Fe(III)PPIX, diminishing the effect of the toxic "free" haem and allowing extraordinarily high levels of "free" haem to be reached within the parasite. All benzamide and TAI compounds investigated here had βH inhibition values 2 - 3 fold more effective than CQ. The ability to inhibit βH therefore does not translate directly into parasite activity or biological effectiveness, but rather possibly into the ability to favourably form complexes with Fe(III)PPIX which could be less toxic than "free" haem thereby reducing the biological effectiveness of the compounds. Future work is certainly required to provide more insight into the formation of these high "free" haem levels, beginning with identifying the composition of the "non-crystalline" electron dense material seen in the DV as well as the role played by the vesicles identified in the DV of KW17 treated PRBCs.

7 CONCLUSION AND FURTHER STUDIES

7.1 Conclusion

CQ is no longer routinely administered as the standard treatment for *P. falciparum* malaria, having been replaced by WHO recommended AMN combination therapies. The rapid acting AMNs are administered with a partner drug of alternate, longer acting mechanism of action and in several cases this partner is a quinoline.[2] The emerging threat of resistance to the AMNs, which manifests as reduced clearance rates places extra pressure on the partner drug, eventually resulting in the emergence of multidrug resistance. In keeping with the most recent WHO "Global Technical Strategy for Malaria 2016 – 2030" which aims to curb and eventually eliminate the global spread of malaria, the need for the development of new drugs remains necessary.[2] Even though CQ is no longer recommended for malaria treatment due to the emergence of CQ resistance, the long running success of CQ means it remains a drug to emulate. CQ resistance has been attributed primarily to mutations in the parasite transmembrane protein PfCRT, resulting in reduced CQ accumulation and therefore does not directly affect Hz formation in the parasite.[129] Recently it was found that administering a double dose of CQ in children younger than 5 years infected with CQR *P. falciparum* strains resulted in an approximate five-fold increase in CQ efficacy. [250] Furthermore, CQ analogues continue to be effective against CQ resistant strains of *P. falciparum.*[251] The Hz formation pathway therefore remains a desirable target for the development of new antimalarials. Being unique to the parasite this vital pathway represents a point of vulnerability in the parasite lifecycle. Monitoring the inhibition of βH production in the presence of drugs has provided an abiotic means of measuring inhibition of the Hz formation pathway. The recently developed NP-40 assay, which uses a synthetic neutral lipid blend to mimic the lipid environment assumed to be the conditions under which Hz is formed in the parasite, showed a strong correlation between parasite growth inhibition and the ability of a compound to inhibit the formation of βH. [102 105] Although biologically relevant, this assay nonetheless does not always unequivocally show that Hz inhibition occurs within the cell.

In this project, a cellular haem fractionation assay was developed to directly determine the amounts of Hb, "free'" haem and Hz in drug treated isolated trophozoites. Aqueous soluble Hb, "free" haem corresponding to haem that is

labile, most likely membrane bound and soluble in the presence of SDS, and finally Hz soluble in base, was determined through a series of fractionation steps in isolated trophozoites. Based on a method developed by Ncokazi and Egan, each haem species was spectrophotometrically quantified as a Fe(III)haem complex with aqueous pyridine at near neutral pH (5% v/v, pH 7.5).[101] The method was originally applied to CQ treated cells and performed in 250 ml culture flasks. The determination of each haem species in isolated trophozoites, inoculated 32 h earlier with different concentrations of CQ, showed a decrease in the percentage of Hz and increase in the percentage of "free" haem with increasing CQ concentration. CQ was therefore classed as a Hz inhibitor as it demonstrated a dose related direct inhibition of Hz and a build-up of toxic "free" haem resulting in the death of CQ treated *P. falciparum* parasites. An increase in the percentage Hb, most likely corresponding to undigested RBC cytosol in transport vesicles was observed following a significant increase in the percentage "free" haem. The appearance of statistically higher levels of Hb after significant increases in the percentage "free" haem suggests a causative link, a result of the downstream effects of increased "free" haem (or haem-CQ complex) levels in the parasite. The observation agrees with previous studies which showed a build-up of undigested Hb and the accumulation of Hb transport vesicles at high CQ concentrations, possibly attributed to the disruption of Hb metabolism by proteases and the failure to deliver Hb in transport vesicles to the parasite DV for digestion. [121] [122] [124] [125] The results were supplemented by TEM images of CQ treated PRBCs in conjunction with EELS for Fe. In comparison to the control, haem Fe had been redistributed outside the DV into the parasite cytosol, where due to its lipophilic nature, haem most likely interacts with lipid rich membranes and organelles causing eventual cell death. [51] [57]

Having established the cellular haem fractionation assay in 250 ml flasks, it was applied to several other clinically relevant antimalarials. The percentage of each haem species at a single drug concentration corresponding to 2.5× the parasite growth IC_{50} was determined for each of LF, MQ, AQ, QN, ART, PYR and SP. With the exception of the antifolates PYR and the SP combination, all species showed some degree of Hz inhibition. However, with the exception of LF, none showed inhibition comparable to CQ. The study, conducted at a single concentration of each drug, provided only a glimpse into the full effect of haem on the parasite with drug

treatment. A comprehensive dose response investigation was required to explore the results obtained as part of this initial investigation. This was important in light of the fact that in addition to Hz inhibition, several other mechanisms of action have been proposed for the antimalarials investigated. The quinoline methanols have been associated with reduced DV accumulation, reduced Hz formation and inhibition of endocytosis calling into question Hz inhibition as the major mechanism of action. [79 127 124 125] While haem association with AMNs has been demonstrated in several studies, Hz inhibition as the mechanism of action of AMNs remains a widely debated topic with several conflicting opinions. [178 252 98]

High demands on parasite starting material and the length of time required to complete a full dose response study on a single compound were the biggest limiting factors of the original assay performed in 250 ml flasks as described in Chapter 3. It was therefore adapted to a higher throughput method performed in 24-well plates, containing at most ten million trophozoites per well, significantly improving the output and reducing the amount of parasite starting material required. Whereas previously results for a single compound were obtained after 2 months the newer method shortened output time to 2 compounds per week. Although the new higher throughput cellular haem fractionation assay was associated with a loss in sensitivity, the results obtained with CQ in the original flask method was successfully reproduced in the higher throughput 24-well plate method. The new method was validated using CQ and was found to be robust. In addition to CQ the method was also applied to AQ, ATV and PYR. An extra facet of the newer higher throughput 24-well plate cellular haem fractionation assay was the inclusion of flow cytometry-based cell counting. In addition to determining the concentration of cells assayed, flow cytometry provided information about changes in morphology of drug treated cells. Cell counting enabled results to be expressed as the amount of each haem species per cell rather than in percentage terms. The importance of this step became apparent when it was determined that treatment of cells with the mitochondrial electron transport inhibitor ATV, caused a dose dependent reduction in the total amount of haem Fe per cell. Initial results expressed as a percentage gave the appearance that ATV was a Hz inhibitor, resulting in an unexpected increase in the percentage “free” haem and decrease in percentage Hz. However, taking into account the dose related reduction in total haem Fe levels it was found that the “free” haem levels per cell remained

unchanged with increasing concentration of ATV. ATV almost certainly does not inhibit Hz formation within the parasite since it does not inhibit βH formation. In cases where the total haem Fe per cell changes with drug dose it was essential to express each haem species as the amount of Hb, "free" haem and Hz Fe per cell to accurately interpret the effects on parasite haem concentrations. Similar to CQ, AQ was shown to inhibit Hz formation with a dose related increase in "free" haem correlated to decreased parasite survival. The antifolate PYR showed no evidence of Hz inhibition, demonstrating no increase in the amount of toxic cellular "free" haem or decrease in the amount of Hz Fe per cell.

Having successfully adapted the haem fractionation assay to a higher throughput technique, the method could then be applied to six additional clinically relevant antimalarials: QN, QD, MQ, LF, PQ and ART as well as the novel AMN 10-dO-AMN. Based on the results of this comprehensive investigation as well as results previously obtained for CQ, AQ, ATV and PYR, compounds can be classified into three groups (with several subdivisions within each group) according to the degree of Hz inhibition exhibited within the parasite (Table 7-1). Group A can be defined as compounds which exhibit direct Hz inhibition and can be further subdivided by defining three subgroups of Hz inhibition. The 4-aminoquinolines, CQ and AQ are classified under group A-1, as compounds which exhibit typical direct Hz inhibition. CQ and AQ both showed a dose related increase in "free" haem levels, correlated closely to decreased parasite survival, accompanied by a dose related decrease in Hz. The aryl methanols investigated have all been shown to inhibit of βH formation and several studies have correlated this βH inhibition with parasite growth IC_{50} suggesting a causative link.[69 106 52 101 105] However inhibition of βH did not translate into Hz inhibition in all cases. While both QN and QD exhibited Hz inhibition with an accompanying increase in "free" haem which could be correlated to parasite survival, the effect was not nearly as pronounced as in cells inoculated with CQ and AQ. The increased levels of "free" haem in QN and QD treated cells were accompanied by a decrease in Hz and a decrease in the total amount of haem Fe, the latter effect being more pronounced in the case of QD. Both QN and QD can be grouped under class A-2 as compounds which show reduced levels of Hz inhibition in comparison to CQ accompanied by a dose related reduction in total haem Fe. Neither MQ nor LF caused an increase in "free" haem levels, however, both drugs caused an immediate reduction in both the amount of

Hz and total haem Fe per cell. Hz inhibition did not therefore appear to be the mechanism of action for MQ or LF and both compounds can be classified under group B as compounds which do not directly inhibit Hz formation but cause a dose related decrease in total haem Fe. Comparison of the cell morphology of CQ treated cells, with cells treated with QN, QD, MQ and LF showed CQ treated cells were generally larger and more complex. Cells treated with LF and MQ also showed a reduction in the amount of DNA, suggesting cell growth was inhibited earlier in the lifecycle than CQ, QN and QD treated cells. The results suggest that the effect of QN, QD, MQ and LF are different to the effects of CQ in the cell. While QN and QD appear to exert some degree of Hz inhibition, all four aryl methanols evaluated appear to have an alternative mechanism of action possibly involving the inhibition of endocytosis, resulting in reduced Hb uptake. The findings agree with previous studies which have shown that QN and MQ treatment inhibited endocytosis reducing the amount of Hb taken up by treated cells. [121] [124] [125] Similar to PYR, the non-βH inhibiting antimalarials PQ, ART and 10-dO-AMN had no effect on the Hz inhibition pathway. All four compounds can be classified under group C-1, as non βH inhibiting antimalarials which show no dose related change in the levels of Hb, "free" haem or Hz in comparison to the control. The total amount of haem Fe per cell remained unchanged at all drug concentrations in all four compounds. The morphology of the cells treated with PYR, PQ, ART and 10-dO-AMN changed in comparison to untreated cells but in general were larger, more complex and contained more DNA than cells treated with CQ. ATV can be classified under group C-2. Similar to the non-βH inhibiting antimalarials previously mentioned, ATV did not appear to inhibit Hz formation, however treatment of cells with increasing concentrations of ATV did cause a dose responsive decrease in levels of Hz and total haem Fe. Furthermore in comparison to CQ treated cells, the morphology of ATV treated cells showed a slight reduction in cell size and complexity and the amount of DNA present. The result that compounds in group C do not inhibit Hz formation is not surprising. PQ is known to possess potent activity against mature gametocytes in *P. falciparum* and to eliminate hypnozoites in *P. vivax*, PYR is a known antifolate and ATV is known to disrupt mitochondrial electron transport in parasites. However the exact mechanism of action of the AMNs is not fully understood. The presence of small quantities of highly toxic haem-AMN adducts which some authors have proposed play a role in the

mechanism of action of the AMNs cannot be either verified or excluded within the tolerance of the assay. Although the AMNs did not exhibit Hz inhibition, the cellular haem fractionation assay on its own, cannot unequivocally exclude the role of haem adducts in the mechanism of action of the AMNs. [99 110 178 51 176 177 175]

The cellular haem fractionation assay was also applied to six novel antimalarials belonging to the benzamide (KW2, KW15 and KW17) and Triarylimidazole or TAI (TSI_3, TSI_6 and TSI_12) non-quinoline chemotypes. Five of the six novel compounds selected inhibited βH formation with a βH IC_{50} twice as active as CQ. All five βH inhibiting compounds tested positive as inhibitors of Hz formation within the *P. falciparum* infected RBC, confirming the biological relevance of the NP-40 assay with reference to the benzamide and TAI scaffolds. The single non βH inhibiting antimalarial (βH IC_{50} > 1000 μM), KW15, showed no inhibition of Hz formation within the parasite and was classified accordingly under group C-1 in Table 7-1. The most notable effect of the benzamide and TAI analogues was the exaggerated levels of "free" haem produced in *P. falciparum* infected RBCs. TEM with EELS for Fe of KW17 treated parasites showed a significantly enlarged DV containing a large number of vesicles and evidence of disrupted Hz formation was observed. Structured, well-defined Hz crystals were seen in both the control and CQ treated cells, compared to "non-crystalline" material with amorphous appearance which was attributed to aggregated amorphous haem confined to the DV. Haem cellular fractionation studies with CQ and other Hz inhibiting quinolines have shown that small but significant increases in "free" haem are required to cause parasite death. CQ, with a 50% parasite inhibitory concentration of 11.0 nM in NF54 causes an approximate two fold maximum increase in "free" haem above the untreated control. High levels of "free" haem and distinct morphological differences in benzamide and TAI treated cells indicate they have a different toxicity to the parasite compared to the quinolines. The amount of "free" haem required to reach the equivalent level of toxicity and associated parasite survival was much higher in the TAI and benzamide scaffolds than in βH inhibiting quinolines. Surprisingly, a positive relationship was observed between the parasite growth IC_{50} and the change in "free" haem. The higher the parasite growth IC_{50}, the more "free" haem produced in the presence of the drug within the parasite. Therefore the highly effective Hz inhibiting antimalarial CQ produces the smallest increase in "free" haem whereas the less biologically effective benzamides and

TAIs produce high amounts of "free" haem. This phenomenon suggests that the toxic effect of the "free" haem produced in the presence of these novel compounds is attenuated, possibly through the formation of haem-drug complexes which are less harmful to the parasite than "free" haem itself or haem-CQ complexes. Therefore in addition to inhibiting Hz crystal growth through interaction with Hz crystals, the TAI and benzamide derivatives could also form complexes with Fe(III)PPIX, diminishing the effect of the toxic "free" haem and allowing extraordinarily high levels of "free" haem to be reached within the parasite. All benzamide and TAI compounds investigated here had βH inhibition values 2 - 3 fold more effective than CQ. The ability to inhibit βH therefore does not translate directly into parasite activity or biological effectiveness, but rather into the ability to favourably form complexes with Fe(III)PPIX which could be less toxic than "free" haem thereby reducing the biological effectiveness of the compounds. All five βH inhibiting novel compounds can be classified under a group A-3 as compounds which exhibited Hz inhibition with unusually high levels of "free" haem attained within the parasite.

Table 7-7-1: Summary of the outcomes of the cellular haem fractionation assay performed on clinically relevant and novel antimalarials with a proposed classification system. All compounds classified under Group A exhibited varying degrees of Hz inhibition. Compounds classified under Group B have been shown to inhibit βH formation but do not directly inhibit Hz formation. Compounds classified under Group C have no impact on βH formation or Hz inhibition. In all cases, comparisons are made with respect to the results obtained with the archetypical Hz inhibitor CQ.

Group		Compounds	Evidence of βH inhibition	Direct Hz inhibition showing an increase in "free" haem	Change in cell morphology	Reduction in total haem Fe(fg) per cell
A	A1	CQ, AQ	Yes	Yes	Slight decrease in cell size, complexity and amount of DNA	No
	A2	QN, QD	Yes	Yes. Very small increase in level of "free" haem in comparison to CQ.	Decreased cell size and complexity	Yes, most likely attributed to reduced Hb uptake
	A3	KW2, KW17	Yes	Yes. Very large increase in level of "free" haem in comparison to CQ	Bigger population of larger cells.	No
		TSI_3, TSI_6, TSI_12	Yes	Yes. Very large increase in level of "free" haem in comparison to CQ	No specific trend	No
B		MQ, LF,	Yes	No	Decreased cell size, complexity and amount of DNA	Yes, most likely attributed reduced Hb uptake
C	C1	PQ, ART, 10-dO-AMN, KW15, PYR,	No	No	Larger, more complex and contains more DNA.	No
	C2	ATV	No	No	Slight Decrease in cell size, complexity and amount of DNA	Yes.

In this project a cellular fractionation assay for the determination of Hb, "free" haem and Hz in a CQS strain of *Plasmodium falciparum* was developed and applied to a diverse group of sixteen clinically relevant antimalarials and novel compounds active against *Plasmodium falciparum.* The method provided direct evidence which

confirmed or excluded Hz inhibition as a likely mechanism of action for all compounds investigated. While CQ and AQ were classified as archetypical Hz inhibitors that caused a significant build-up of "free" haem, it was found that several compounds investigated increased "free" haem levels to varying degrees. In comparison to CQ, QN and its stereoisomer QD caused increased "free" haem to a lesser degree. This was accompanied by a reduction in total haem Fe, exhibiting an alternative mechanism in addition to haemozoin inhibition, possibly as a downstream effect of haemozoin inhibition or as a direct effect of the drug itself. Five novel compounds belonging to the benzamide and TAI series were found to cause exaggerated levels of "free" haem correlated to decreased parasite survival suggesting that the "free" haem produced was of diminished toxicity. Several non-βH inhibiting compounds including two AMNs, ATV, PYR, ART and PQ did not inhibit Hz formation. However LF and MQ, both of which inhibit the formation of βH, surprisingly also did not appear to inhibit Hz formation since they caused no increase in "free" haem. Similar to QN and QD they showed a reduction in total haem Fe, attributed reduced uptake of Hb. Therefore, while the haem fractionation assay was developed initially as a means to directly identify haemozoin inhibitors, the outcomes have provided valuable insights into the nuances of Hz inhibition, a process which is still being studied in an attempt to design new drugs capable of mimicking the past success of Hz inhibiting antimalarials such as CQ.

7.2 Further studies

The direct in-cell demonstration of CQ as a Hz inhibitor was a major milestone in this study. The relationship between increased levels of toxic "free" haem and decreased parasite survival in conjunction with TEM imaging techniques showing redistribution of haem out of the DV into the parasite cytosol provided evidence of Hz inhibition. However, the direct downstream consequences of increased "free" haem levels resulting in cell death were not identified. Interestingly, baseline levels of "free" haem were found to be present in untreated cells at approximately 4 fg of haem Fe per cell. In a PRBC corresponding to a volume of 90 fL this equates to a concentration of 796 μM of "free" haem. This concentration is far above that which has been shown to have adverse effects on the cell and therefore to maintain this

high concentration of "free" haem in the cell it is likely to be present mainly as an insoluble precipitate within the DV rather than soluble toxic "free" haem.[55] Presumably, treatment with Hz inhibitors leads to a small increase in soluble haem leading to parasite death.

Schmitt et al, have demonstrated that aggregates of haemin in aqueous solution rapidly enter and accumulate into lipid bilayers, associating with organelles and enhancing permeability leading to eventual cell lysis. Fe(III)PPIX identified in the parasite cytosol, most likely present as the anionic form of haematin would behave in a manner similar to haemin as described by Schmitt et al. It was anticipated that evidence of "free" haem association with membranes and organelles in the cytosol would be obtained from the TEM EELS images collected, however the image resolution was not sufficient to distinguish association with any specific organelles in the parasite cytosol. The determination of possible association with specific organelles is a rational next step in concluding the investigation of the effects of CQ induced "free" haem within the cell and requires further investigation. In this regard, the use of more powerful imaging techniques with superior resolving capabilities is required. While studies using TEM have proved useful in demonstrating the location of haem in drug treated cells and changes in cell morphology, lengthy fixation of isolated cells in resin and the high cost of image processing limits the application of the technique. The use of Cryo-TEM would eliminate several fixation steps and could be expected to produce better resolved images. An alternative to TEM imaging would be the introduction of a haem fluorescent marker. Used in conjunction with commercially available fluorescent sensors known to associate with specific organelles, a haem fluorescent marker could track the pathway of labile haem microscopically in cells. While this type of fluorescent sensor is not yet available, several studies have made use of GFP based haem fluorescent sensors to investigate the dynamics of haem in live cells. [253] [254] [255] Encoding *P. falciparum* with a haem fluorescent sensor such as recently developed and applied to yeast cells by Hanna et al may prove useful in a wide variety of applications relating to Hz inhibition. However this requires the modification of the genome of a CQS strain of *P. falciparum* to express the haem fluorescent protein in specific compartments within the parasite. Used in conjunction with confocal microscopy, flow cytometry and the wide variety of commercial available fluorescent trackers for organelles within *P. falciparum* this application may be

able to quantify haem levels as in the cellular haem fraction assay and additionally identify possible specific associations with organelles in individual cells.

Hz inhibition has been implicated as the mechanism of action of LF and MQ, both of which strongly inhibit the formation of βH. Despite such evidence that MQ and LF could act as Hz inhibitors, neither caused increased "free" haem levels in the malaria parasite. Both compounds displayed reduced levels of total haem Fe, attributed to reduced uptake of Hb. The findings agree with several studies which have shown that MQ treated cells inhibit endocytosis reducing the amount of Hb taken up by treated cells. [121] [124] [125] Furthermore flow cytometry profiles of SYBR green stained trophozoites treated with LF and MQ showed reduced levels of DNA suggesting growth was inhibited earlier in the parasite lifecycle than each of CQ, AQ, QN and QD treated cells. Inoculation of cells with LF or MQ at the ring stage therefore appears to kill cells by a mechanism other than Hz inhibition. However evidence suggests that Hz inhibition could still be a possible mechanism of action. Inoculating parasites with LF or MQ, later in the lifecycle at the trophozoite stage rather than early ring stage would determine if more than one stage specific mechanism of action or different effects from the same drug are possible. This type of experiment might prove useful in cases where Hz inhibition was expected and not seen, perhaps due to alternative or secondary mechanisms of action of the drugs involved.

Finally, further work is required to elucidate the mechanism behind exaggerated levels of "free" haem seen with the five novel benzamide and TAI compounds tested in Chapter 6. The amount of "free" haem required to reach equivalent levels of toxicity was much higher in cells treated with the benzamide and TAI derivatives than CQ treated cells. Furthermore TEM images of cells treated with the benzamide KW17, showed an enlarged DV containing "non-crystalline" material corresponding to Hz. A large number of vesicles were observed throughout the parasite some of which were shown to contain Fe. The ability to reach high levels of "free" haem was attributed to the formation of a Fe(III)PPIX-drug complex between haem and the novel compounds tested, attenuating the effect of toxic "free" haem. The identification of these Fe(III)PPIX-drug complexes in the parasite, possibly associated with the large number of vesicles seen in TEM images of cells treated with the benzamide KW17 is required to validate this explanation. Furthermore, the extraction and identification of the "non-crystalline"

material corresponding to Hz seen in TEM images within the DV might provide more insight into the mechanism of Hz inhibition observed with these novel compounds.

Even in the face of successful AMN combination therapies studying the mechanism of action behind the quinolines, especially CQ remains relevant. To emulate the success of CQ which was both clinically effective and cost effective would go a long way in curbing the spread malaria which is of greatest concern in countries which do not have access to costly medical interventions.

8 REFERENCES

[1] Ridley, R. G. (2002) Medical need, scientific opportunity and the drive for antimalarial drugs, *Nature 415*, 686.

[2] WHO (2015) *World malaria report 2015*, World Health Organization.

[3] Greenwood, B. M., Fidock, D. A., Kyle, D. E., Kappe, S. H., Alonso, P. L., Collins, F. H., and Duffy, P. E. (2008) Malaria: progress, perils, and prospects for eradication, *J. Clin. Invest. 118*, 1266.

[4] Francis, S. E., Sullivan Jr, D. J., and Goldberg, D. E. (1997) Hemoglobin metabolism in the malaria parasite *Plasmodium falciparum*, *Annu. Rev. Microbiol. 51*, 97.

[5] U.N.O. (2009) *The millennium development goals report 2009*, United Nations Publications.

[6] Tilley, L., Dixon, M. W., and Kirk, K. (2011) The *Plasmodium falciparum*-infected red blood cell, *Int. J. Biochem. Cell. Biol. 43*, 839.

[7] Hempelmann, E., and Krafts, K. (2013) Bad air, amulets and mosquitoes: 2,000 years of changing perspectives on malaria, *Malar. J. 12*, 232.

[8] Baton, L. A., and Ranford-Cartwright, L. C. (2005) Spreading the seeds of million-murdering death: metamorphoses of malaria in the mosquito, *Trends Parasitol. 21*, 573.

[9] Ross, R. (1923) *Memoirs: with a full account of the great malaria problem and its solution*, London J. Murray.

[10] Manson, P. (1900) Experimental proof of the mosquito-malaria theory. , *Br. Med. J. 2*, 949.

[11] Cox-Singh, J., Davis, T. M., Lee, K.-S., Shamsul, S. S., Matusop, A., Ratnam, S., Rahman, H. A., Conway, D. J., and Singh, B. (2008) *Plasmodium knowlesi* malaria in humans is widely distributed and potentially life threatening, *Clin. Infect. Dis. 46*, 165.

[12] Rowe, J. A., Claessens, A., Corrigan, R. A., and Arman, M. (2009) Adhesion of *Plasmodium falciparum*-infected erythrocytes to human cells: molecular mechanisms and therapeutic implications, *Expert Rev. Mol. Med. 11*, e16.

[13] Millar, S. B., and Cox-Singh, J. (2015) Human infections with *Plasmodium knowlesi*—zoonotic malaria, *Clin. Microbiol. Infect. 21*, 640.

[14] Fidock, D. A., Rosenthal, P. J., Croft, S. L., Brun, R., and Nwaka, S. (2004) Antimalarial drug discovery: efficacy models for compound screening, *Nat. Rev. Drug Discovery 3*, 509.

[15] Köhler, S., Delwiche, C. F., Denny, P. W., Tilney, L. G., Webster, P., Wilson, R., Palmer, J. D., and Roos, D. S. (1997) A Plastid of Probable Green Algal Origin in Apicomplexan Parasites, *Science 275*, 1485.

[16] Lucantoni, L., Silvestrini, F., Signore, M., Siciliano, G., Eldering, M., Dechering, K. J., Avery, V. M., and Alano, P. (2015) A simple and predictive phenotypic High Content Imaging assay for *Plasmodium falciparum* mature gametocytes to identify malaria transmission blocking compounds, *Sci. Rep. 5*.

[17] Tanaka, T. Q., Dehdashti, S. J., Nguyen, D.-T., McKew, J. C., Zheng, W., and Williamson, K. C. (2013) A quantitative high throughput assay for identifying gametocytocidal compounds, *Mol. Biochem. Parasitol. 188*, 20.

[18] Sun, W., Tanaka, T. Q., Magle, C. T., Huang, W., Southall, N., Huang, R., Dehdashti, S. J., McKew, J. C., Williamson, K. C., and Zheng, W. (2014) Chemical signatures and new drug targets for gametocytocidal drug development, *Sci. Rep. 4*, 3743.

[19] Bannister, L., and Mitchell, G. (2009) The malaria merozoite, forty years on, *Parasitology 136*, 1435.

[20] Mikolajczak, S. A., and Kappe, S. H. (2006) A clash to conquer: the malaria parasite liver infection, *Mol. Microbiol. 62*, 1499.

[21] Bannister, L., Hopkins, J., Fowler, R., Krishna, S., and Mitchell, G. (2000) A brief illustrated guide to the ultrastructure of *Plasmodium falciparum* asexual blood stages, *Parasitol. Today 16*, 427.

[22] Rosenthal, P. J., and Meshnick, S. R. (1996) Hemoglobin catabolism and iron utilization by malaria parasites, *Mol. Biochem. Parasitol. 83*, 131.

[23] Ginsburg, H. (1989) Some reflections concerning host erythrocyte-malarial parasite interrelationships, *Blood Cells 16*, 225.

[24] Pagola, S., Stephens, P. W., Bohle, D. S., Kosar, A. D., and Madsen, S. K. (2000) The structure of malaria pigment β-haematin, *Nature 404*, 307.

[25] Atkinson, C., and Aikawa, M. (1989) Ultrastructure of malaria-infected erythrocytes, *Blood Cells 16*, 351.

[26] Lingelbach, K., and Joiner, K. A. (1998) The parasitophorous vacuole membrane surrounding *Plasmodium* and *Toxoplasma*: an unusual compartment in infected cells, *J. Cell Sci. 111*, 1467.

[27] Goldberg, D. E., and Cowman, A. F. (2010) Moving in and renovating: exporting proteins from *Plasmodium* into host erythrocytes, *Nat. Rev. Microbiol. 8*, 617.

[28] Kirk, K., and Saliba, K. J. (2007) Targeting nutrient uptake mechanisms in *Plasmodium*, *Curr. Drug Targets 8*, 75.

[29] Krugliak, M., Zhang, J., and Ginsburg, H. (2002) Intraerythrocytic *Plasmodium falciparum* utilizes only a fraction of the amino acids derived from the digestion of host cell cytosol for the biosynthesis of its proteins, *Mol. Biochem. Parasitol. 119*, 249.

[30] Egan, T. J., Combrinck, J. M., Egan, J., Hearne, G. R., Marques, H. M., Ntenteni, S., Sewell, B. T., Smith, P. J., Taylor, D., and van Schalkwyk, D. A. (2002) Fate of haem iron in the malaria parasite *Plasmodium falciparum*, *Biochem. J. 365*, 343.

[31] Loria, P., Miller, S., Foley, M., and Tilley, L. (1999) Inhibition of the peroxidative degradation of haem as the basis of action of chloroquine and other quinoline antimalarials, *Biochem. J. 339*, 363.

[32] Slomianny, C., and Prensier, G. (1990) A cytochemical ultrastructural study of the lysosomal system of different species of malaria parasites, *J. Protozool. 37*, 465.

[33] Hanssen, E., McMillan, P. J., and Tilley, L. (2010) Cellular architecture of *Plasmodium falciparum*-infected erythrocytes, *Int. J. Parasitol. 40*, 1127.

[34] Gligorijevic, B., Purdy, K., Elliott, D., Cooper, R. A., and Roepe, P. D. (2008) Stage independent chloroquine resistance and chloroquine toxicity revealed via spinning disk confocal microscopy, *Mol. Biochem. Parasitol. 159*, 7.

[35] Aikawa, M., Hepler, P. K., Huff, C. G., and Sprinz, H. (1966) The feeding mechanism of avian malarial parasites, *J. Cell Biol. 28*, 355.

[36] Bakar, N. A., Klonis, N., Hanssen, E., Chan, C., and Tilley, L. (2010) Digestive-vacuole genesis and endocytic processes in the early intraerythrocytic stages of Plasmodium falciparum, *J. Cell Sci. 123*, 441.

[37] Dluzewski, A. R., Ling, I. T., Hopkins, J. M., Grainger, M., Margos, G., Mitchell, G. H., Holder, A. A., and Bannister, L. H. (2008) Formation of the food vacuole in *Plasmodium falciparum*: a potential role for the 19 kDa fragment of merozoite surface protein 1 (MSP1 19), *PLoS One 3*, e3085.

[38] Goldberg, D. (2005) Hemoglobin degradation, In *Malaria: Drugs, Disease and Post-genomic Biology*, pp 275, Springer.

[39] Francis, S. E., Gluzman, I. Y., Oksman, A., Banerjee, D., and Goldberg, D. E. (1996) Characterization of native falcipain, an enzyme involved in *Plasmodium falciparum* hemoglobin degradation, *Mol. Biochem. Parasitol. 83*, 189.

[40] Gluzman, I. Y., Francis, S. E., Oksman, A., Smith, C. E., Duffin, K. L., and Goldberg, D. E. (1994) Order and specificity of the *Plasmodium falciparum* hemoglobin degradation pathway, *J. Clin. Invest. 93*, 1602.

[41] Banerjee, R., Liu, J., Beatty, W., Pelosof, L., Klemba, M., and Goldberg, D. E. (2002) Four plasmepsins are active in the *Plasmodium falciparum* food vacuole, including a protease with an active-site histidine, *Proc. Natl. Acad. Sci. 99*, 990.

[42] Rosenthal, P. J. (2004) Cysteine proteases of malaria parasites, *Int. J. Parasitol. 34*, 1489.

[43] Klemba, M., Gluzman, I., and Goldberg, D. E. (2004) A *Plasmodium falciparum* dipeptidyl aminopeptidase I participates in vacuolar hemoglobin degradation, *J. Biol. Chem. 279*, 43000.

[44] Coronado, L. M., Nadovich, C. T., and Spadafora, C. (2014) Malarial hemozoin: from target to tool, *Biochim. Biophys. Acta, Gen. Subj. 1840*, 2032.

[45] Zarchin, S., Krugliak, M., and Ginsburg, H. (1986) Digestion of the host erythrocyte by malaria parasites is the primary target for quinoline containing antimalarials, *Biochem. Pharmacol. 35*, 2435.

[46] Francis, S. E., Gluzman, I., Oksman, A., Knickerbocker, A., Mueller, R., Bryant, M., Sherman, D., Russell, D., and Goldberg, D. (1994) Molecular characterization and inhibition of a *Plasmodium falciparum* aspartic hemoglobinase, *EMBO J. 13*, 306.

[47] Rosenthal, P. J., McKerrow, J. H., Rasnick, D., and Leech, J. H. (1989) *Plasmodium falciparum*: inhibitors of lysosomal cysteine proteinases inhibit a trophozoite proteinase and block parasite development, *Mol. Biochem. Parasitol. 35*, 177.

[48] Rosenthal, P. J. (1995) *Plasmodium falciparum*: effects of proteinase inhibitors on globin hydrolysis by cultured malaria parasites, *Exp. Parasitol. 80*, 272.

[49] Lew, V. L., Tiffert, T., and Ginsburg, H. (2003) Excess hemoglobin digestion and the osmotic stability of P*lasmodium falciparum*–infected red blood cells, *Blood 101*, 4189.

[50] Atamna, H., and Ginsburg, H. (1993) Origin of reactive oxygen species in erythrocytes infected with *Plasmodium falciparum*, *Mol. Biochem. Parasitol. 61*, 231.

[51] Schmitt, T. H., Frezzatti, W. A., and Schreier, S. (1993) Hemin-induced lipid membrane disorder and increased permeability: a molecular model for the mechanism of cell lysis, *Arch. Biochem. Biophys. 307*, 96.

[52] Egan, T. J., and Ncokazi, K. K. (2005) Quinoline antimalarials decrease the rate of β-hematin formation, *J. Inorg. Biochem. 99*, 1532.

[53] Radfar, A., Diez, A., and Bautista, J. M. (2008) Chloroquine mediates specific proteome oxidative damage across the erythrocytic cycle of resistant *Plasmodium falciparum*, *Free Radic. Biol. Med. 44*, 2034.

[54] Sullivan, D. J., Gluzman, I. Y., Russell, D. G., and Goldberg, D. E. (1996) On the molecular mechanism of chloroquine's antimalarial action, *Proc. Natl. Acad. Sci. 93*, 11865.

[55] Orjih, A. U., Banyal, H., Chevli, R., and Fitch, C. D. (1981) Hemin lyses malaria parasites, *Science 214*, 667.

[56] Rose, M. Y., Thompson, R. A., Light, W. R., and Olson, J. S. (1985) Heme transfer between phospholipid membranes and uptake by apohemoglobin, *J. Biol. Chem. 260*, 6632.

[57] Ginsburg, H., and Demel, R. A. (1984) Interactions of hemin, antimalarial drugs and hemin-antimalarial complexes with phospholipid monolayers, *Chem. Phys. Lipids 35*, 331.

[58] Fitch, C. D. (2004) Ferriprotoporphyrin IX, phospholipids, and the antimalarial actions of quinoline drugs, *Life Sci. 74*, 1957.

[59] Becker, K., Tilley, L., Vennerstrom, J. L., Roberts, D., Rogerson, S., and Ginsburg, H. (2004) Oxidative stress in malaria parasite-infected erythrocytes: host–parasite interactions, *Int. J. Parasitol. 34*, 163.

[60] Muller, S. (2004) Redox and antioxidant systems of the malaria parasite *Plasmodium falciparum*, *Mol. Microbiol. 53*, 1291.

[61] Liochev, S. I., and Fridovich, I. (1999) Superoxide and iron: partners in crime, *IUBMB Life 48*, 157.

[62] Hempelmann, E. (2007) Hemozoin biocrystallization in *Plasmodium falciparum* and the antimalarial activity of crystallization inhibitors, *Parasitol. Res. 100*, 671.

[63] Brown, W. (1911) Malarial pigment (so-called melanin): its nature and mode of production, *J. Exp. Med. 13*, 290.

[64] Slater, A. F., Swiggard, W. J., Orton, B. R., Flitter, W. D., Goldberg, D. E., Cerami, A., and Henderson, G. B. (1991) An iron-carboxylate bond links the heme units of malaria pigment, *Proc. Natl. Acad. Sci. 88*, 325.

[65] Bohle, D. S., Dinnebier, R. E., Madsen, S. K., and Stephens, P. W. (1997) Characterization of the products of the heme detoxification pathway in malarial late trophozoites by X-ray diffraction, *J. Biol. Chem. 272*, 713.

[66] Slater, A., and Cerami, A. (1992) Inhibition by chloroquine of a novel haem polymerase enzyme activity in malaria trophozoites, *Nature 355*, 167.

[67] Dorn, A., Stoffel, R., Matile, H., Bubendorf, A., and Ridley, R. G. (1995) Malarial haemozoin/β-haematin supports haem polymerization in the absence of protein, *Nature 374*, 269.

[68] Dorn, A., Vippagunta, S. R., Matile, H., Bubendorf, A., Vennerstrom, J. L., and Ridley, R. G. (1998) A comparison and analysis of several ways to promote haematin (haem) polymerisation and an assessment of its initiation in vitro, *Biochem. Pharmacol. 55*, 737.

[69] Egan, T. J., Ross, D. C., and Adams, P. A. (1994) Quinoline anti-malarial drugs inhibit spontaneous formation of β-haematin (malaria pigment), *FEBS Lett. 352*, 54.

[70] White, N. J. (2013) Primaquine to prevent transmission of *falciparum* malaria, *Lancet Inf. Dis. 13*, 175.

[71] Sullivan, D. J., Gluzman, I. Y., and Goldberg, D. E. (1996) *Plasmodium* hemozoin formation mediated by histidine-rich proteins, *Science 271*, 219.

[72] Sullivan, D. J. (2002) Theories on malarial pigment formation and quinoline action, *Int J. Parasitol. 32*, 1645.

[73] Jani, D., Nagarkatti, R., Beatty, W., Angel, R., Slebodnick, C., Andersen, J., Kumar, S., and Rathore, D. (2008) HDP—a novel heme detoxification protein from the malaria parasite, *PLoS Pathog. 4*, e1000053.

[74] Fitch, C. D., Cai, G.-z., Chen, Y.-F., and Shoemaker, J. D. (1999) Involvement of lipids in ferriprotoporphyrin IX polymerization in malaria, *Biochem. Biophys. Acta, Mol. Basis Dis. 1454*, 31.

[75] Pisciotta, J. M., Coppens, I., Tripathi, A. K., Scholl, P. F., Shuman, J., Bajad, S., Shulaev, V., and Sullivan, D. J. (2007) The role of neutral lipid nanospheres in *Plasmodium falciparum* haem crystallization, *Biochem. J. 402*, 197.

[76] Ambele, M. A., and Egan, T. J. (2012) Neutral lipids associated with haemozoin mediate efficient and rapid β-haematin formation at physiological pH, temperature and ionic composition, *Malar. J. 11*, 1.

[77] Meshnick, S. R., and Dobson, M. J. (2001) The history of antimalarial drugs, In *Antimalarial Chemotherapy: Mechanisms of Action, Resistance, and New Directions in Drug Discovery* (Rosenthal, P. J., Ed.), pp 15, Humana Press.

[78] Hofheinz, W., and Merkli, B. (1984) Quinine and quinine analogues, In *Antimalarial Drug II*, pp 61, Springer Berlin Heidelberg.

[79] Foley, M., and Tilley, L. (1998) Quinoline antimalarials: mechanisms of action and resistance and prospects for new agents, *Pharmacol. Ther. 79*, 55.

[80] Loeb, F., Clark, W. M., Coatney, G. R., Coggeshall, L. T., Dieuaide, F. R., Dochez, A. R., Hakansson, E. G., Marshall, E. K., Marvel, C. S., and McCoy, O. R. (1946) Activity of a New Antimalarial Agent, Chloroquine (SN 7618). *J. Am. Med. Assoc. 130*, 1069.

[81] Greenwood, D. (1995) Conflicts of interest: the genesis of synthetic antimalarial agents in peace and war, *J. Antimicrobial. Chemother. 36*, 857.

[82] Payne, D. (1987) Spread of chloroquine resistance in *Plasmodium falciparum*, *Parasitol. Today 3*, 241.

[83] Peters, W. (1987) *Chemotherapy and drug resistance in malaria.*, Academic Press Ltd.

[84] Peters, W. (1970) The chemotherapy of rodent malaria. X. Dynamics of drug resistance. II. Acquisition and loss of chloroquine resistance in *Plasmodium berghei* observed by continuous bioassay, *Ann. Trop. Med. Parasitol. 64*, 25.

[85] Warhurst, D., and Hockley, D. (1967) Mode of action of chloroquine on *Plasmodium berghei* and *P. cynomolgi*, *Nature 214*, 935.

[86] Ginsburg, H., Famin, O., Zhang, J., and Krugliak, M. (1998) Inhibition of glutathione-dependent degradation of heme by chloroquine and amodiaquine as a possible basis for their antimalarial mode of action, *Biochem. Pharmacol. 56*, 1305.

[87] Fitch, C. D., Yunis, N. G., Chevli, R., and Gonzalez, Y. (1974) High-affinity accumulation of chloroquine by mouse erythrocytes infected with *Plasmodium berghei*, *J. Clin. Invest. 54*, 24.

[88] Yayon, A., Cabantchik, Z., and Ginsburg, H. (1984) Identification of the acidic compartment of *Plasmodium falciparum*-infected human erythrocytes as the target of the antimalarial drug chloroquine, *EMBO J. 3*, 2695.

[89] Geary, T. G., Jensen, J. B., and Ginsburg, H. (1986) Uptake of [^{3}H] chloroquine by drug-sensitive and-resistant strains of the human malaria parasite *Plasmodium falciparum*, *Biochem. Pharmacol. 35*, 3805.

[90] Ginsburg, H., Nissani, E., and Krugliak, M. (1989) Alkalinization of the food vacuole of malaria parasites by quinoline drugs and alkylamines is not correlated with their antimalarial activity, *Biochem. Pharmacol. 38*, 2645.

[91] Bennett, T. N., Kosar, A. D., Ursos, L. M., Dzekunov, S., Sidhu, A. B. S., Fidock, D. A., and Roepe, P. D. (2004) Drug resistance-associated pfCRT mutations confer decreased *Plasmodium falciparum* digestive vacuolar pH, *Mol. Biochem. Parasitol. 133*, 99.

[92] Dzekunov, S. M., Ursos, L. M. B., and Roepe, P. D. (2000) Digestive vacuolar pH of intact intraerythrocytic *P. falciparum* either sensitive or resistant to chloroquine, *Mol. Biochem. Parasitol. 110*, 107.

[93] Bray, P. G., Saliba, K. J., Davies, J. D., Spiller, D. G., White, M. R., Kirk, K., and Ward, S. A. (2002) Distribution of acridine orange fluorescence in *Plasmodium falciparum*-infected erythrocytes and its implications for the evaluation of digestive vacuole pH, *Mol. Biochem. Parasitol. 119*, 301.

[94] Spiller, D. G., Bray, P. G., Hughes, R. H., Ward, S. A., and White, M. R. (2002) The pH of the Plasmodium falciparum digestive vacuole: holy grail or dead-end trail?, *Trends in Parasitol. 18*, 441.

[95] Klonis, N., Tan, O., Jackson, K., Goldberg, D., Klemba, M., and Tilley, L. (2007) Evaluation of pH during cytostomal endocytosis and vacuolar catabolism of haemoglobin in *Plasmodium falciparum*, *Biochem. J. 407*, 343.

[96] Chou, A. (1980) Ferriprotoporphyrin IX fulfills the criteria for identification as the chloroquine receptor of malaria parasites. , *Biochemistry 19*, 1543.

[97] Basilico, N., Monti, D., Olliaro, P., and Taramelli, D. (1997) Non-iron porphyrins inhibit β-haematin (malaria pigment) polymerisation, *FEBS Lett. 409*, 297.

[98] Basilico, N., Pagani, E., Monti, D., Olliaro, P., and Taramelli, D. (1998) A microtitre-based method for measuring the haem polymerization inhibitory activity (HPIA) of antimalarial drugs, *J. Antimicrobial. Chemother. 42*, 55.

[99] Parapini, S., Basilico, N., Pasini, E., Egan, T. J., Olliaro, P., Taramelli, D., and Monti, D. (2000) Standardization of the physicochemical parameters to assess in vitro the β-hematin inhibitory activity of antimalarial drugs, *Exp. Parasitol. 96*, 249.

[100] Partos, S. (1922) The hemochrome of Herzfeld and Klinger, *Biochem Zeit 129*, 89.

[101] Ncokazi, K. K., and Egan, T. J. (2005) A colorimetric high-throughput β-hematin inhibition screening assay for use in the search for antimalarial compounds, *Anal. Biochem. 338*, 306.

[102] Carter, M. D., Phelan, V. V., Sandlin, R. D., Bachmann, B. O., and Wright, D. W. (2010) Lipophilic mediated assays for β-hematin inhibitors, *Comb. Chem. High Throughput Screening 13*, 285.

[103] Fong, K. Y., Sandlin, R. D., and Wright, D. W. (2015) Identification of beta-hematin inhibitors in the MMV Malaria Box, *Int. J. Parasitol: Drugs Drug Resist. 5*, 84.

[104] Sandlin, R. D., Fong, K. Y., Wicht, K. J., Carrell, H. M., Egan, T. J., and Wright, D. W. (2014) Identification of beta-hematin inhibitors in a high-throughput screening effort reveals scaffolds with in vitro antimalarial activity, *Int. J. Parasitol.: Drugs Drug Resist. 4*, 316.

[105] Sandlin, R. D., Carter, M. D., Lee, P. J., Auschwitz, J. M., Leed, S. E., Johnson, J. D., and Wright, D. W. (2011) Use of the NP-40 detergent-mediated assay in discovery of inhibitors of β-hematin crystallization, *Antimicrob. Agents Chemother. 55*, 3363.

[106] Dorn, A., Vippagunta, S. R., Matile, H., Jaquet, C., Vennerstrom, J. L., and Ridley, R. G. (1998) An assessment of drug-haematin binding as a mechanism for inhibition of haematin polymerisation by quinoline antimalarials, *Biochem. Pharmacol. 55*, 727.

[107] Combrinck, J. M., Mabotha, T. E., Ncokazi, K. K., Ambele, M. A., Taylor, D., Smith, P. J., Hoppe, H. C., and Egan, T. J. (2012) Insights into the role of heme in the mechanism of action of antimalarials, *ACS Chem. Biol. 8*, 133.

[108] O'Neill, P. M., Bray, P. G., Hawley, S. R., Ward, S. A., and Park, B. K. (1998) 4-Aminoquinolines—Past, present, and future; A chemical perspective., *Pharmacol. Ther. 77*, 29.

[109] Ezzet, F., Van Vugt, M., Nosten, F., Looareesuwan, S., and White, N. J. (2000) Pharmacokinetics and pharmacodynamics of lumefantrine (benflumetol) in acute *falciparum* malaria, *Antimicrob. Agents Chemother. 44*, 697.

[110] Haynes, R. K., Monti, D., Taramelli, D., Basilico, N., Parapini, S., and Olliaro, P. (2003) Artemisinin antimalarials do not inhibit hemozoin formation, *Antimicrob. Agents Chemother. 47*, 1175.

[111] Asawamabasakda, W., Ittarat, I., Chang, C.-C., McElroy, P., and Meshnick, S. R. (1994) Effects of antimalarials and protease inhibitors on plasmodial hemozoin production, *Mol. Biochem. Parasitol. 67*, 183.

[112] Burgess, S. J., Kelly, J. X., Shomloo, S., Wittlin, S., Brun, R., Liebmann, K., and Peyton, D. H. (2010) Synthesis, Structure− Activity Relationship, and Mode-of-Action Studies of Antimalarial Reversed Chloroquine Compounds, *J. Med. Chem. 53*, 6477.

[113] Burgess, S. J., Selzer, A., Kelly, J. X., Smilkstein, M. J., Riscoe, M. K., and Peyton, D. H. (2006) A chloroquine-like molecule designed to reverse resistance in *Plasmodium falciparum*, *J. Med. Chem. 49*, 5623.

[114] Ginsburg, H., and Krugliak, M. (1992) Quinoline-containing antimalarials—mode of action, drug resistance and its reversal an update with unresolved puzzles, *Biochem. Pharmacol. 43*, 63.

[115] Rosenthal, P. J., McKerrow, J. H., Aikawa, M., Nagasawa, H., and Leech, J. H. (1988) A malarial cysteine proteinase is necessary for hemoglobin degradation by *Plasmodium falciparum*, *J. Clin. Invest. 82*, 1560.

[116] Egan, T. J., Hunter, R., Kaschula, C. H., Marques, H. M., Misplon, A., and Walden, J. (2000) Structure-function relationships in aminoquinolines: effect of amino and chloro groups on quinoline-hematin complex formation, inhibition of β-hematin formation, and antiplasmodial activity, *J. Med. Chem. 43*, 283.

[117] de Villiers, K. A., Marques, H. M., and Egan, T. J. (2008) The crystal structure of halofantrine–ferriprotoporphyrin IX and the mechanism of action of arylmethanol antimalarials, *J. Inorg. Biochem. 102*, 1660.

[118] de Villiers, K. A., Gildenhuys, J., and le Roex, T. (2012) Iron (III) protoporphyrin IX complexes of the antimalarial cinchona alkaloids quinine and quinidine, *ACS Chem. Biol. 7*, 666.

[119] Gildenhuys, J., Roex, T. l., Egan, T. J., and de Villiers, K. A. (2013) The single crystal X-ray structure of β-hematin DMSO solvate grown in the presence of chloroquine, a β-hematin growth-rate inhibitor, *J. Am. Chem. Soc. 135*, 1037.

[120] Le Manach, C., Scheurer, C., Sax, S., Schleiferbock, S., Cabrera, D. G., Younis, Y., Paquet, T., Street, L., Smith, P., and Ding, X. C. (2013) Fast in vitro methods to determine the speed of action and the stage-specificity of anti-malarials in *Plasmodium falciparum*, *Malar. J 16*, 424.

[121] Famin, O., and Ginsburg, H. (2002) Differential effects of 4-aminoquinoline-containing antimalarial drugs on hemoglobin digestion in *Plasmodium falciparum*-infected erythrocytes, *Biochem. Pharmacol. 63*, 393.

[122] Fitch, C. D., Cai, G.-z., Chen, Y.-f., and Ryerse, J. S. (2003) Relationship of chloroquine-induced redistribution of a neutral aminopeptidase to hemoglobin accumulation in malaria parasites, *Arch. Biochem. Biophys. 410*, 296.

[123] YAYON, A., TIMBERG, R., FRIEDMAN, S., and GINSBURG, H. (1984) Effects of chloroquine on the feeding mechanism of the intraerythrocytic human malarial parasite *Plasmodium falciparum*, *J. Protozool. 31*, 367.

[124] Hoppe, H. C., van Schalkwyk, D. A., Wiehart, U. I., Meredith, S. A., Egan, J., and Weber, B. W. (2004) Antimalarial quinolines and artemisinin inhibit endocytosis in *Plasmodium falciparum*, *Antimicrob. Agents Chemother. 48*, 2370.

[125] Roberts, L., Egan, T. J., Joiner, K. A., and Hoppe, H. C. (2008) Differential effects of quinoline antimalarials on endocytosis in *Plasmodium falciparum*, *Antimicrob. Agents Chemother. 52*, 1840.

[126] Mungthin, M., Bray, P. G., Ridley, R. G., and Ward, S. A. (1998) Central role of hemoglobin degradation in mechanisms of action of 4-aminoquinolines, quinoline methanols, and phenanthrene methanols, *Antimicrob. Agents Chemother. 42*, 2973.

[127] Chou, A., and Fitch, C. (1993) Control of heme polymerase by chloroquine and other quinoline derivatives, *Biochem. Biophys. Res. Commun. 195*, 422.

[128] Findlay, G. M. (1951) *Recent advances in chemotherapy*, J. And A. Churchill Ltd.

[129] Summers, R. L., Nash, M. N., and Martin, R. E. (2012) Know your enemy: understanding the role of PfCRT in drug resistance could lead to new antimalarial tactics, *Cell Mol. Life Sci. 69*, 1967.

[130] Fidock, D. A., Nomura, T., Talley, A. K., Cooper, R. A., Dzekunov, S. M., Ferdig, M. T., Ursos, L. M., Naudé, B., Deitsch, K. W., and Su, X.-z. (2000) Mutations in the *P. falciparum* digestive vacuole transmembrane protein PfCRT and evidence for their role in chloroquine resistance, *Mol. Cell 6*, 861.

[131] Krogstad, D. J., Gluzman, I. Y., Kyle, D. E., Oduola, A., Martin, S. K., Milhous, W. K., and Schlesinger, P. H. (1987) Efflux of chloroquine from Plasmodium falciparum: mechanism of chloroquine resistance, *Science 238*, 1283.

[132] Martin, R. E., and Kirk, K. (2004) The malaria parasite's chloroquine resistance transporter is a member of the drug/metabolite transporter superfamily, *Mol. Biol. Evol. 21*, 1938.

[133] Bray, P. G., Mungthin, M., Hastings, I. M., Biagini, G. A., Saidu, D. K., Lakshmanan, V., Johnson, D. J., Hughes, R. H., Stocks, P. A., O'Neill, P. M., Fidock, D. A., Warhurst, D. C., and Ward, S. A. (2006) PfCRT and the trans-vacuolar proton electrochemical gradient: regulating the access of chloroquine to ferriprotoporphyrin IX, *Mol. Microbiol. 62*, 238.

[134] Ursing, J., Kofoed, P.-E., Rodrigues, A., Blessborn, D., Thoft-Nielsen, R., Björkman, A., and Rombo, L. (2011) Similar efficacy and tolerability of double-dose chloroquine and artemether-lumefantrine for treatment of *Plasmodium falciparum* infection in Guinea-Bissau: a randomized trial, *J. Inf. Dis. 203*, 109.

[135] Warhurst, D. C., Craig, J. C., and Adagu, I. S. (2002) Lysosomes and drug resistance in malaria, *Lancet 360*, 1527.

[136] Martin, S. K., Oduola, A. M., and Milhous, W. K. (1987) Reversal of chloroquine resistance in *Plasmodium falciparum* by verapamil, *Science 235*, 899.

[137] Watt, G., Long, G. W., Grogl, M., and Martin, S. K. (1990) Reversal of drug-resistant *falciparum* malaria by calcium antagonists: potential for host cell toxicity, *Trans. R. Soc. Trop. Med. Hyg. 84*, 187.

[138] Lehane, A. M., and Kirk, K. (2010) Efflux of a range of antimalarial drugs and 'chloroquine resistance reversers' from the digestive vacuole in malaria parasites with mutant PfCRT, *Mol. Microbiol. 77*, 1039.

[139] Rubio, J., Thompson, J., and Cowman, A. (1996) The var genes of *Plasmodium falciparum* are located in the subtelomeric region of most chromosomes, *EMBO J. 15*, 4069.

[140] Sanchez, C. P., Rotmann, A., Stein, W. D., and Lanzer, M. (2008) Polymorphisms within PfMDR1 alter the substrate specificity for anti-malarial drugs in *Plasmodium falciparum*, *Mol. Microbiol. 70*, 786.

[141] Van Es, H., Karcz, S., Chu, F., Cowman, A. F., Vidal, S., Gros, P., and Schurr, E. (1994) Expression of the plasmodial pfmdr1 gene in mammalian cells is associated with increased susceptibility to chloroquine, *Mol. Cell Biol. 14*, 2419.

[142] Price, R. N., Uhlemann, A.-C., Brockman, A., McGready, R., Ashley, E., Phaipun, L., Patel, R., Laing, K., Looareesuwan, S., and White, N. J. (2004) Mefloquine resistance in *Plasmodium falciparum* and increased pfmdr1 gene copy number, *Lancet 364*, 438.

[143] Cowman, A. F., Galatis, D., and Thompson, J. K. (1994) Selection for mefloquine resistance in *Plasmodium falciparum* is linked to amplification of the pfmdr1 gene and cross-resistance to halofantrine and quinine, *Proc. Natl. Acad. Sci. 91*, 1143.

[144] Barnes, D., Foote, S., Galatis, D., Kemp, D., and Cowman, A. (1992) Selection for high-level chloroquine resistance results in deamplification of the pfmdr1 gene and increased sensitivity to mefloquine in *Plasmodium falciparum*, *EMBO J. 11*, 3067.

[145] Pickard, A. L., Wongsrichanalai, C., Purfield, A., Kamwendo, D., Emery, K., Zalewski, C., Kawamoto, F., Miller, R. S., and Meshnick, S. R. (2003) Resistance to antimalarials in Southeast Asia and genetic polymorphisms in pfmdr1, *Antimicrob. Agents Chemother. 47*, 2418.

[146] Reed, M. B., Saliba, K. J., Caruana, S. R., Kirk, K., and Cowman, A. F. (2000) Pgh1 modulates sensitivity and resistance to multiple antimalarials in *Plasmodium falciparum*, *Nature 403*, 906.

[147] Sidhu, A. B. S., Uhlemann, A.-C., Valderramos, S. G., Valderramos, J.-C., Krishna, S., and Fidock, D. A. (2006) Decreasing pfmdr1 copy number in Plasmodium falciparum malaria heightens susceptibility to mefloquine, lumefantrine, halofantrine, quinine, and artemisinin, *J. Inf. Dis. 194*, 528.

[148] Price, R., Cassar, C., Brockman, A., Duraisingh, M., Van Vugt, M., White, N., Nosten, F., and Krishna, S. (1999) The pfmdr1 gene is associated with a multidrug-resistant phenotype in Plasmodium falciparumfrom the western border of Thailand, *Antimicrob. Agents Chemother. 43*, 2943.

[149] Bray, P. G., Martin, R. E., Tilley, L., Ward, S. A., Kirk, K., and Fidock, D. A. (2005) Defining the role of PfCRT in *Plasmodium falciparum* chloroquine resistance, *Mol. Microbiol. 56*, 323.

[150] Cooper, R. A., Ferdig, M. T., Su, X.-Z., Ursos, L. M., Mu, J., Nomura, T., Fujioka, H., Fidock, D. A., Roepe, P. D., and Wellems, T. E. (2002) Alternative Mutations at Position 76 of the Vacuolar Transmembrane Protein PfCRT Are Associated with Chloroquine Resistance and Unique Stereospecific Quinine and Quinidine Responses inPlasmodium falciparum, *Mol. Pharmacol. 61*, 35.

[151] Nsobya, S. L., Kiggundu, M., Nanyunja, S., Joloba, M., Greenhouse, B., and Rosenthal, P. J. (2010) In vitro sensitivities of *Plasmodium falciparum* to different antimalarial drugs in Uganda, *Antimicrob. Agents Chemother. 54*, 1200.

[152] Sanchez, C. P., Stein, W. D., and Lanzer, M. (2008) Dissecting the components of quinine accumulation in *Plasmodium falciparum*, *Mol. Microbiol. 67*, 1081.

[153] Sidhu, A. B. S., Verdier-Pinard, D., and Fidock, D. A. (2002) Chloroquine resistance in *Plasmodium falciparum* malaria parasites conferred by pfcrt mutations, *Science 298*, 210.

[154] Humphreys, G., Merinopoulos, I., Ahmed, J., Whitty, C., Mutabingwa, T., Sutherland, C., and Hallett, R. (2007) Amodiaquine and artemether-lumefantrine select distinct alleles of the Plasmodium falciparum mdr1 gene in Tanzanian children treated for uncomplicated malaria, *Antimicrob. Agents Chemother. 51*, 991.

[155] Bray, P. G., Hawley, S. R., Mungthin, M., and Ward, S. A. (1996) Physicochemical properties correlated with drug resistance and the reversal of drug resistance in *Plasmodium falciparum*, *Mol. Pharmacol. 50*, 1559.

[156] Warhurst, D. C., Craig, J. C., Adagu, I. S., Guy, R. K., Madrid, P. B., and Fivelman, Q. L. (2007) Activity of piperaquine and other 4-aminoquinoline antiplasmodial drugs against chloroquine-sensitive and resistant blood-stages of *Plasmodium falciparum*: role of β-haematin inhibition and drug concentration in vacuolar water-and lipid-phases, *Biochem. Pharmacol. 73*, 1910.

[157] Sá, J. M., Twu, O., Hayton, K., Reyes, S., Fay, M. P., Ringwald, P., and Wellems, T. E. (2009) Geographic patterns of *Plasmodium falciparum* drug resistance distinguished by differential responses to amodiaquine and chloroquine, *Proc. Natl. Acad. Sci. 106*, 18883.

[158] WHO (2006) *Guidelines for the treatment of malaria*, World Health Organization.

[159] Tu, Y. (2011) The discovery of artemisinin (qinghaosu) and gifts from Chinese medicine, *Nat. Med. 17*, 1217.

[160] Krishna, S., Uhlemann, A.-C., and Haynes, R. K. (2004) Artemisinins: mechanisms of action and potential for resistance, *Drug Resist. Updates 7*, 233.

[161] Noedl, H., Se, Y., Schaecher, K., Smith, B. L., Socheat, D., and Fukuda, M. M. (2008) Evidence of artemisinin-resistant malaria in western Cambodia, *N. Engl. J. Med. 359*, 2619.

[162] Dondorp, A. M., Nosten, F., Yi, P., Das, D., Phyo, A. P., Tarning, J., Lwin, K. M., Ariey, F., Hanpithakpong, W., and Lee, S. J. (2009) Artemisinin resistance in *Plasmodium falciparum* malaria, *N. Engl. J. Med. 361*, 455.

[163] Ashley, E. A., Dhorda, M., Fairhurst, R. M., Amaratunga, C., Lim, P., Suon, S., Sreng, S., Anderson, J. M., Mao, S., and Sam, B. (2014) Spread of artemisinin resistance in *Plasmodium falciparum* malaria, *N. Engl. J. Med. 371*, 411.

[164] Li, J., and Zhou, B. (2010) Biological actions of artemisinin: insights from medicinal chemistry studies, *Molecules 15*, 1378.

[165] O'neill, P. M., Barton, V. E., and Ward, S. A. (2010) The molecular mechanism of action of artemisinin—the debate continues, *Molecules 15*, 1705.

[166] Posner, G. H., and Oh, C. H. (1992) Regiospecifically oxygen-18 labeled 1, 2, 4-trioxane: a simple chemical model system to probe the mechanism (s) for the antimalarial activity of artemisinin (qinghaosu), *J. Am. Chem. Soc. 114*, 8328.

[167] Posner, G. H., Wang, D., Cumming, J. N., Oh, C. H., French, A. N., Bodley, A. L., and Shapiro, T. A. (1995) Further evidence supporting the importance of and the restrictions on a carbon-centered radical for high antimalarial activity of 1, 2, 4-trioxanes like artemisinin, *J. Med. Chem. 38*, 2273.

[168] Jefford, C. W., Vicente, M. G., Jacquier, Y., Favarger, F., Mareda, J., Millasson-Schmidt, P., Brunner, G., and Burger, U. (1996) The deoxygenation and isomerization of artemisinin and artemether and their relevance to antimalarial action, *Helv. Chim. Acta 79*, 1475.

[169] Stocks, P. A., Bray, P. G., Barton, V. E., Al-Helal, M., Jones, M., Araujo, N. C., Gibbons, P., Ward, S. A., Hughes, R. H., and Biagini, G. A. (2007) Evidence for a Common Non-Heme Chelatable-Iron-Dependent Activation Mechanism for Semisynthetic and Synthetic Endoperoxide Antimalarial Drugs, *Angew. Chem., Int. Ed. 46*, 6278.

[170] Xie, S. C., Dogovski, C., Hanssen, E., Chiu, F., Yang, T., Crespo, M. P., Stafford, C., Batinovic, S., Teguh, S., and Charman, S. (2016) Haemoglobin degradation underpins the sensitivity of early ring stage *Plasmodium falciparum* to artemisinins, *J. Cell Sci. 129*, 406.

[171] Klonis, N., Xie, S. C., McCaw, J. M., Crespo-Ortiz, M. P., Zaloumis, S. G., Simpson, J. A., and Tilley, L. (2013) Altered temporal response of malaria parasites determines differential sensitivity to artemisinin, *Proc. Natl. Acad. Sci. 110*, 5157.

[172] Robert, A., Benoit-Vical, F., Claparols, C., and Meunier, B. (2005) The antimalarial drug artemisinin alkylates heme in infected mice, *Proc. Natl. Acad. Sci. 102*, 13676.

[173] Meshnick, S. R., Thomas, A., Ranz, A., Xu, C.-M., and Pan, H.-Z. (1991) Artemisinin (qinghaosu): the role of intracellular hemin in its mechanism of antimalarial action, *Mol. Biochem. Parasitol. 49*, 181.

[174] Bhisutthibhan, J., Pan, X.-Q., Hossler, P. A., Walker, D. J., Yowell, C. A., Carlton, J., Dame, J. B., and Meshnick, S. R. (1998) The *Plasmodium falciparum* translationally controlled tumor protein homolog and its reaction with the antimalarial drug artemisinin, *J. Biol. Chem. 273*, 16192.

[175] Robert, A., Cazelles, J., and Meunier, B. (2001) Characterization of the alkylation product of heme by the antimalarial drug artemisinin, *Angew. Chem., Int. Ed. 40*, 1954.

[176] Robert, A., and Meunier, B. (1997) Characterization of the first covalent adduct between artemisinin and a heme model, *J. Am. Chem. Soc. 119*, 5968.

[177] Robert, A., and Meunier, B. (1998) Is alkylation the main mechanism of action of the antimalarial drug artemisinin?, *Chem. Soc. Rev. 27*, 273.

[178] Loup, C., Lelièvre, J., Benoit-Vical, F., and Meunier, B. (2007) Trioxaquines and heme-artemisinin adducts inhibit the in vitro formation of hemozoin better than chloroquine, *Antimicrob. Agents Chemother. 51*, 3768.

[179] Eckstein-Ludwig, U., Webb, R., Van Goethem, I., East, J., Lee, A., Kimura, M., O'Neill, P., Bray, P., Ward, S., and Krishna, S. (2003) Artemisinins target the SERCA of *Plasmodium falciparum*, *Nature 424*, 957.

[180] Goo, Y.-K., Terkawi, M. A., Jia, H., Aboge, G. O., Ooka, H., Nelson, B., Kim, S., Sunaga, F., Namikawa, K., and Igarashi, I. (2010) Artesunate, a potential drug for treatment of Babesia infection, *Parasitol. Int. 59*, 481.

[181] Dunay, I. R., Chan, W. C., Haynes, R. K., and Sibley, L. D. (2009) Artemisone and artemiside control acute and reactivated toxoplasmosis in a murine model, *Antimicrob. Agents Chemother. 53*, 4450.

[182] Matsuu, A., Yamasaki, M., Xuan, X., Ikadai, H., and Hikasa, Y. (2008) In vitro evaluation of the growth inhibitory activities of 15 drugs against Babesia gibsoni (Aomori strain), *Vet. Parasitol. 157*, 1.

[183] Pandey, A. V., Tekwani, B. L., Singh, R. L., and Chauhan, V. S. (1999) Artemisinin, an endoperoxide antimalarial, disrupts the hemoglobin catabolism and heme detoxification systems in malarial parasite, *J. Biol. Chem. 274*, 19383.

[184] Rush, M. A., Baniecki, M. L., Mazitschek, R., Cortese, J. F., Wiegand, R., Clardy, J., and Wirth, D. F. (2009) Colorimetric high-throughput screen for detection of heme crystallization inhibitors, *Antimicrob. Agents Chemother. 53*, 2564.

[185] Ying-Zi, Y., Asawamahasakda, W., and Meshnick, S. R. (1993) Alkylation of human albumin by the antimalarial artemisinin, *Biochem. Pharmacol. 46*, 336.

[186] Ying-Zi, Y., Little, B., and Meshnick, S. R. (1994) Alkylation of proteins by artemisinin: Effects of heme, pH, and drug structure, *Biochem. Pharmacol. 48*, 569.

[187] Hartwig, C. L., Rosenthal, A. S., D'Angelo, J., Griffin, C. E., Posner, G. H., and Cooper, R. A. (2009) Accumulation of artemisinin trioxane derivatives within neutral lipids of *Plasmodium falciparum* malaria parasites is endoperoxide-dependent, *Biochem. Pharmacol. 77*, 322.

[188] Li, W., Mo, W., Shen, D., Sun, L., Wang, J., Lu, S., Gitschier, J. M., and Zhou, B. (2005) Yeast model uncovers dual roles of mitochondria in the action of artemisinin, *PLoS Genet. 1*, e36.

[189] Wang, J., Huang, L., Li, J., Fan, Q., Long, Y., Li, Y., and Zhou, B. (2010) Artemisinin directly targets malarial mitochondria through its specific mitochondrial activation, *PLoS One 5*, e9582.

[190] Mayorga, P., Puisieux, F., and Couarraze, G. (1996) Formulation study of a transdermal delivery system of primaquine, *Int. J. Pharm. 132*, 71.

[191] Graves, P. M., Gelband, H., and Garner, P. (2014) Primaquine or other 8-aminoquinoline for reducing *Plasmodium falciparum* transmission, *Cochrane Database Syst. Rev. 6*.

[192] Guttmann, P., and Ehrlich, P. (1891) Ueber die wirkung des methylenblau bei malaria, *Klin. Wochenschr. 28*, 953.

[193] Sugioka, Y., and Suzuki, M. (1991) The chemical basis for the ferriprotoporphyrin IX-chloroquine complex induced lipid peroxidation, *Biochim. Biophys. Acta, Gen. Subj. 1074*, 19.

[194] Milhous, W. K., Weatherly, N., Bowdre, J., and Desjardins, R. (1985) In vitro activities of and mechanisms of resistance to antifol antimalarial drugs, *Antimicrob. Agents Chemother. 27*, 525.

[195] Chulay, J. D., Watkins, W. M., and Sixsmith, D. G. (1984) Synergistic antimalarial activity of pyrimethamine and sulfadoxine against *Plasmodium falciparum* in vitro, *Am. J. Trop. Med. Hyg. 33*, 325.

[196] Takechi, M., Matsuo, M., Ziba, C., Macheso, A., Butao, D., Zungu, I. L., Chakanika, I., Bustos, M., and Dorina, G. (2001) Therapeutic efficacy of sulphadoxine/pyrimethamine and susceptibility in vitro of *P. falciparum* isolates to sulphadoxine-pyremethamine and other antimalarial drugs in Malawian children, *Trop. Med. Int. Health 6*, 429.

[197] White, N. (1998) Drug resistance in malaria, *Br. Med. Bull. 54*, 703.

[198] Baggish, A. L., and Hill, D. R. (2002) Antiparasitic agent atovaquone, *Antimicrob. Agents Chemother. 46*, 1163.

[199] Srivastava, I. K., Morrisey, J. M., Darrouzet, E., Daldal, F., and Vaidya, A. B. (1999) Resistance mutations reveal the atovaquone-binding domain of cytochrome b in malaria parasites, *Mol. Microbiol. 33*, 704.

[200] Kessl, J. J., Lange, B. B., Merbitz-Zahradnik, T., Zwicker, K., Hill, P., Meunier, B., Pálsdóttir, H., Hunte, C., Meshnick, S., and Trumpower, B. L. (2003) Molecular basis for atovaquone binding to the cytochrome bc1 complex, *J. Biol. Chem. 278*, 31312.

[201] Vander Jagt, D. L., Hunsaker, L. A., and Campos, N. M. (1987) Comparison of proteases from chloroquine-sensitive and chloroquine-resistant strains of *Plasmodium falciparum*, *Biochem. Pharmacol. 36*, 3285.

[202] Slater, A. F. (1993) Chloroquine: mechanism of drug action and resistance in Plasmodium falciparum, *Pharmacol. Ther. 57*, 203.

[203] Prism, G., GraphPad Software Inc., Sorrento Valley Rd., San Diego. CA 92121.

[204] Trager, W., and Jensen, J. B. (1976) Human malaria parasites in continuous culture, *Science 193*, 673.

[205] Lambros, C., and Vanderberg, J. P. (1979) Synchronization of *Plasmodium falciparum* erythrocytic stages in culture, *J. Parasitol. 65*, 418.

[206] Makler, M. T., and Hinrichs, D. J. (1993) Measurement of the lactate dehydrogenase activity of *Plasmodium falciparum* as an assessment of parasitemia, *Am. J. Trop. Med. Hyg. 48*, 205.

[207] Johnson, J. D., Dennull, R. A., Gerena, L., Lopez-Sanchez, M., Roncal, N. E., and Waters, N. C. (2007) Assessment and continued validation of the malaria SYBR green I-based fluorescence assay for use in malaria drug screening, *Antimicrob. Agents Chemother. 51*, 1926.

[208] Huy, N. T., Uyen, D. T., Maeda, A., Oida, T., Harada, S., and Kamei, K. (2007) Simple colorimetric inhibition assay of heme crystallization for high-throughput screening of antimalarial compounds, *Antimicrob. Agents Chemother. 51*, 350.

[209] Ambele, M. A., Sewell, B. T., Cummings, F. R., Smith, P. J., and Egan, T. J. (2013) Synthetic Hemozoin (β-Hematin) Crystals Nucleate at the Surface of Neutral Lipid Droplets that Control Their Sizes, *Cryst. Growth Des. 13*, 4442.

[210] Ziegler, J., Linck, R., and Wright, D. W. (2001) Heme aggregation inhibitors: antimalarial drugs targeting an essential biomineralization process, *Stud. Nat. Prod. Chem. 25*, 327.

[211] Guiguemde, W. A., Shelat, A. A., Bouck, D., Duffy, S., Crowther, G. J., Davis, P. H., Smithson, D. C., Connelly, M., Clark, J., and Zhu, F. (2010) Chemical genetics of Plasmodium falciparum, *Nature 465*, 311.

[212] Kurosawa, Y., Dorn, A., Kitsuji-Shirane, M., Shimada, H., Satoh, T., Matile, H., Hofheinz, W., Masciadri, R., Kansy, M., and Ridley, R. G. (2000) Hematin polymerization assay as a high-throughput screen for identification of new antimalarial pharmacophores, *Antimicrob. Agents Chemother. 44*, 2638.

[213] Xue, J., Jiang, B., Liu, C., Sun, J., and Xiao, S. (2013) Comparative observation on inhibition of hemozoin formation and their in vitro and in vivo anti-schistosome activity displayed by 7 antimalarial drugs, *Chin. J. Parasitol. Parasitic Dis. 31*, 161.

[214] LTD., S. P. P. ARCEVA Tablets / dry suspension.

[215] Highlights of prescibing information COARTEM® (artemether/lumefantrine) Tablets, (Novartis, Ed.).

[216] Gamo, F.-J., Sanz, L. M., Vidal, J., de Cozar, C., Alvarez, E., Lavandera, J.-L., Vanderwall, D. E., Green, D. V., Kumar, V., and Hasan, S. (2010) Thousands of chemical starting points for antimalarial lead identification, *Nature 465*, 305.

[217] Carter, R., and Mendis, K. N. (2003) Evolutionary and Historical Aspects of the Burden of Malaria, *Clin. Microbiol. Rev. 16*, 173.

[218] O'Keeffe, D. H., Barlow, C. H., Smythe, G. A., Fuchsman, W. H., Moss, T. H., Lilienthal, H. R., and Caughey, W. S. (1975) Magnetic and spectroscopic probes for FeOFe linkages in hemin systems, *Bioinorgan. Chem. 5*, 125.

[219] Asakura, T., Minakata, K., Adachi, K., Russell, M., and Schwartz, E. (1977) Denatured hemoglobin in sickle erythrocytes, *J. Clin. Invest. 59*, 633.

[220] Carter, P. (1971) Spectrophotometric determination of serum iron at the submicrogram level with a new reagent (ferrozine), *Anal. Biochem. 40*, 450.

[221] Gibbs, C. R. (1976) Characterization and application of ferrozine iron reagent as a ferrous iron indicator, *Anal. Chem. 48*, 1197.

[222] Wein, S., Maynadier, M., Van Ba, C. T., Cerdan, R., Peyrottes, S., Fraisse, L., and Vial, H. (2010) Reliability of antimalarial sensitivity tests depends on drug mechanisms of action, *J. Clin. Microbiol. 48*, 1651.

[223] Brockelman, C. R., and Tan-ariya, P. (1982) *Plasmodium falciparum* in continuous culture: a new medium for the in vitro test for sulfadoxine sensitivity, *Bull. World Health Organ. 60*, 423.

[224] Joshi, M. C., Wicht, K. J., Taylor, D., Hunter, R., Smith, P. J., and Egan, T. J. (2013) In vitro antimalarial activity, β-haematin inhibition and structure–activity relationships in a series of quinoline triazoles, *Eur. J. Med. Chem. 69*, 338.

[225] Chellan, P., Land, K. M., Shokar, A., Au, A., An, S. H., Taylor, D., Smith, P. J., Riedel, T., Dyson, P. J., and Chibale, K. (2014) Synthesis and evaluation of new polynuclear organometallic Ru (II), Rh (III) and Ir (III) pyridyl ester complexes as in vitro antiparasitic and antitumor agents, *Dalton Trans. 43*, 513.

[226] Bei, A. K., DeSimone, T. M., Badiane, A. S., Ahouidi, A. D., Dieye, T., Ndiaye, D., Sarr, O., Ndir, O., Mboup, S., and Duraisingh, M. T. (2010) A flow cytometry-based assay for measuring invasion of red blood cells by *Plasmodium falciparum*, *Am. J. Hematol. 85*, 234.

[227] Jun, G., Lee, J.-S., Jung, Y.-J., and Park, J.-W. (2012) Quantitative determination of Plasmodium parasitemia by flow cytometry and microscopy, *J. Korean Med. Sci. 27*, 1137.

[228] Jiménez-Díaz, M. B., Mulet, T., Gómez, V., Viera, S., Alvarez, A., Garuti, H., Vázquez, Y., Fernández, A., Ibáñez, J., and Jiménez, M. (2009) Quantitative measurement of *Plasmodium*-infected erythrocytes in murine models of malaria by flow cytometry using bidimensional assessment of SYTO-16 fluorescence, *Cytometry Part A 75*, 225.

[229] Jogdand, P. S., Singh, S. K., Christiansen, M., Dziegiel, M. H., Singh, S., and Theisen, M. (2012) Flow cytometric readout based on Mitotracker Red CMXRos staining of live

asexual blood stage malarial parasites reliably assesses antibody dependent cellular inhibition, *Malar. J. 11*, 235.

[230] Karl, S., Wong, R. P., St Pierre, T. G., and Davis, T. M. (2009) A comparative study of a flow-cytometry-based assessment of in vitro *Plasmodium falciparum* drug sensitivity, *Malar. J. 8*, 1.

[231] Zipper, H., Brunner, H., Bernhagen, J., and Vitzthum, F. (2004) Investigations on DNA intercalation and surface binding by SYBR Green I, its structure determination and methodological implications, *Nucleic acids research 32*, e103.

[232] Altman, D. G., and Bland, J. M. (1983) Measurement in medicine: the analysis of method comparison studies, *Statistician 32*, 307.

[233] Orjih, A. U., and Fitch, C. D. (1993) Hemozoin production by *Plasmodium falciparum*: variation with strain and exposure to chloroquine, *Biochim. Biophys. Acta., Gen. Subj. 1157*, 270.

[234] Dewitte, K., Fierens, C., Stöckl, D., and Thienpont, L. M. (2002) Application of the Bland–Altman plot for interpretation of method-comparison studies: a critical investigation of its practice, *Clin. Chem. 48*, 799.

[235] Myles, P., and Cui, J. (2007) Using the Bland–Altman method to measure agreement with repeated measures, *Br. J. Anaesth. 99*, 309.

[236] Karle, J., Karle, I., Gerena, L., and Milhous, W. (1992) Stereochemical evaluation of the relative activities of the cinchona alkaloids against *Plasmodium falciparum*, *Antimicrob. Agents Chemother. 36*, 1538.

[237] Fitch, C. D., Chevli, R., Banyal, H. S., Phillips, G., Pfaller, M. A., and Krogstad, D. J. (1982) Lysis of *Plasmodium falciparum* by ferriprotoporphyrin IX and a chloroquine-ferriprotoporphyrin IX complex, *Antimicrob. Agents. Chemother. 21*, 819.

[238] Desneves, J., Thorn, G., Berman, A., Galatis, D., La Greca, N., Sinding, J., Foley, M., Deady, L. W., Cowman, A. F., and Tilley, L. (1996) Photoaffinity labeling of mefloquine-binding proteins in human serum, uninfected erythrocytes and Plasmodium falciparum-infected erythrocytes, *Mol. Biochem. Parasitol. 82*, 181.

[239] San George, R. C., Nagel, R. L., and Fabry, M. E. (1984) On the mechanism for the red-cell accumulation of mefloquine, an antimalarial drug, *Biochim. Biophys. Acta, Mol. Cell. Res. 803*, 174.

[240] Warhurst, D. C., Craig, J. C., Adagu, I. S., Meyer, D. J., and Lee, S. Y. (2003) The relationship of physico-chemical properties and structure to the differential antiplasmodial activity of the cinchona alkaloids, *Malar. J. 2*, 26.

[241] Eziefula, A. C., Bousema, T., Yeung, S., Kamya, M., Owaraganise, A., Gabagaya, G., Bradley, J., Grignard, L., Lanke, K. H., and Wanzira, H. (2014) Single dose

primaquine for clearance of *Plasmodium falciparum* gametocytes in children with uncomplicated malaria in Uganda: a randomised, controlled, double-blind, dose-ranging trial, *Lancet Inf. Dis. 14*, 130.

[242] Dicko, A., Brown, J. M., Diawara, H., Baber, I., Mahamar, A., Soumare, H. M., Sanogo, K., Koita, F., Keita, S., and Traore, S. F. (2016) Primaquine to reduce transmission of *Plasmodium falciparum* malaria in Mali: a single-blind, dose-ranging, adaptive randomised phase 2 trial, *Lancet Inf. Dis. 16*, 623.

[243] Terkuile, F., White, N., Holloway, P., Pasvol, G., and Krishna, S. (1993) *Plasmodium falciparum*: in vitro studies of the pharmacodynamic properties of drugs used for the treatment of severe malaria, *Exp. Parasitol. 76*, 85.

[244] Pooley, S., Fatih, F. A., Krishna, S., Gerisch, M., Haynes, R. K., Wong, H.-N., and Staines, H. M. (2011) Artemisone uptake in *Plasmodium falciparum*-infected erythrocytes, *Antimicrob. Agents Chemother. 55*, 550.

[245] Angus, B. J., Chotivanich, K., Udomsangpetch, R., and White, N. J. (1997) In vivo removal of malaria parasites from red blood cells without their destruction in acute *falciparum* malaria, *Blood 90*, 2037.

[246] Wicht, K. J. (2015) Discovery of benzamides and triarylimidazoles active against Plasmodium falciparum via haemozoin inhibition: high throughput screening, synthesis and structure-activity relationships, University of Cape Town.

[247] Wicht, K. J., Combrinck, J. M., Smith, P. J., Hunter, R., and Egan, T. J. (2016) Identification and SAR evaluation of hemozoin-inhibiting benzamides active against *Plasmodium falciparum*, *J. Med. Chem. 59*, 6512.

[248] Wu, T., Nagle, A., Sakata, T., Henson, K., Borboa, R., Chen, Z., Kuhen, K., Plouffe, D., Winzeler, E., and Adrian, F. (2009) Cell-based optimization of novel benzamides as potential antimalarial leads, *Bioorg. Med. Chem. Lett. 19*, 6970.

[249] Rathore, D., Jani, D., and Nagarkatti, R. (2006) Novel therapeutic target for protozoal diseases.

[250] Ursing, J., Rombo, L., Bergqvist, Y., Rodrigues, A., and Kofoed, P.-E. (2015) High-Dose Chloroquine for Treatment of Chloroquine-Resistant *Plasmodium falciparum* Malaria, *J. Inf. Dis. 213*, 1315.

[251] De, D., Krogstad, F. M., Cogswell, F. B., and Krogstad, D. J. (1996) Aminoquinolines that circumvent resistance in *Plasmodium falciparum* in vitro, *Am. J. Trop. Med. Hyg. 55*, 579.

[252] Haynes, R. K., Chan, W. C., Lung, C. M., Uhlemann, A. C., Eckstein, U., Taramelli, D., Parapini, S., Monti, D., and Krishna, S. (2007) The Fe2+-Mediated Decomposition, PfATP6 Binding, and Antimalarial Activities of Artemisone and Other Artemisinins:

The Unlikelihood of C-Centered Radicals as Bioactive Intermediates, *ChemMedChem 2*, 1480.

[253] Takeda, S., Kamiya, N., and Nagamune, T. (2003) A novel protein-based heme sensor consisting of green fluorescent protein and apocytochrome b 562, *Anal. Biochem. 317*, 116.

[254] Hanna, D. A., Harvey, R. M., Martinez-Guzman, O., Yuan, X., Chandrasekharan, B., Raju, G., Outten, F. W., Hamza, I., and Reddi, A. R. (2016) Heme dynamics and trafficking factors revealed by genetically encoded fluorescent heme sensors, *Proc. Natl. Acad. Sci. 113*, 7539.

[255] Carpenter, M. C., and Palmer, A. E. (2016) Unraveling the mystery of the ring: Tracking heme dynamics in living cells, *Proc. Natl. Acad. Sci. 113*, 7296.